ELECTRIC POWER
RESEARCH INSTITUTE

Program on Technology Innovation: Validation of CLASSI and SASSI Codes to Treat Seismic Wave Incoherence in Soil-Structure Interaction (SSI) Analysis of Nuclear Power Plant Structures

Program on Technology Innovation: Validation of CLASSI and SASSI Codes to Treat Seismic Wave Incoherence in Soil-Structure Interaction (SSI) Analysis of Nuclear Power Plant Structures

1015111

Final Report, November 2007

EPRI Project Manager
R. Kassawara

ELECTRIC POWER RESEARCH INSTITUTE
3420 Hillview Avenue, Palo Alto, California 94304-1338 • PO Box 10412, Palo Alto, California 94303-0813 • USA
800.313.3774 • 650.855.2121 • askepri@epri.com • www.epri.com

DISCLAIMER OF WARRANTIES AND LIMITATION OF LIABILITIES

THIS DOCUMENT WAS PREPARED BY THE ORGANIZATION(S) NAMED BELOW AS AN ACCOUNT OF WORK SPONSORED OR COSPONSORED BY THE ELECTRIC POWER RESEARCH INSTITUTE, INC. (EPRI). NEITHER EPRI, ANY MEMBER OF EPRI, ANY COSPONSOR, THE ORGANIZATION(S) BELOW, NOR ANY PERSON ACTING ON BEHALF OF ANY OF THEM:

(A) MAKES ANY WARRANTY OR REPRESENTATION WHATSOEVER, EXPRESS OR IMPLIED, (I) WITH RESPECT TO THE USE OF ANY INFORMATION, APPARATUS, METHOD, PROCESS, OR SIMILAR ITEM DISCLOSED IN THIS DOCUMENT, INCLUDING MERCHANTABILITY AND FITNESS FOR A PARTICULAR PURPOSE, OR (II) THAT SUCH USE DOES NOT INFRINGE ON OR INTERFERE WITH PRIVATELY OWNED RIGHTS, INCLUDING ANY PARTY'S INTELLECTUAL PROPERTY, OR (III) THAT THIS DOCUMENT IS SUITABLE TO ANY PARTICULAR USER'S CIRCUMSTANCE; OR

(B) ASSUMES RESPONSIBILITY FOR ANY DAMAGES OR OTHER LIABILITY WHATSOEVER (INCLUDING ANY CONSEQUENTIAL DAMAGES, EVEN IF EPRI OR ANY EPRI REPRESENTATIVE HAS BEEN ADVISED OF THE POSSIBILITY OF SUCH DAMAGES) RESULTING FROM YOUR SELECTION OR USE OF THIS DOCUMENT OR ANY INFORMATION, APPARATUS, METHOD, PROCESS, OR SIMILAR ITEM DISCLOSED IN THIS DOCUMENT.

ORGANIZATION(S) THAT PREPARED THIS DOCUMENT

ARES Corporation, Inc.

James J. Johnson and Associates

NOTE

For further information about EPRI, call the EPRI Customer Assistance Center at 800.313.3774 or e-mail askepri@epri.com.

Electric Power Research Institute, EPRI, and TOGETHER…SHAPING THE FUTURE OF ELECTRICITY are registered service marks of the Electric Power Research Institute, Inc.

Copyright © 2007 Electric Power Research Institute, Inc. All rights reserved.

CITATIONS

This report was prepared by

ARES Corporation, Inc.
5 Hutton Centre Drive
Suite 610
Santa Ana, CA 92707

Principal Investigators
S. Short
G. Hardy
K. Merz

James J. Johnson and Associates
7 Essex Court
Alamo, CA 94507

Principal Investigator
J. Johnson

This report describes research sponsored by the Electric Power Research Institute (EPRI).

The report is a corporate document that should be cited in the literature in the following manner:

Program on Technology Innovation: Validation of CLASSI and SASSI Codes to Treat Seismic Wave Incoherence in Soil-Structure Interaction (SSI) Analysis of Nuclear Power Plant Structures. EPRI, Palo Alto, CA: 2007. 1015111.

PRODUCT DESCRIPTION

The New Plant Seismic Issues Resolution Program was initiated to address emerging seismic issues as they relate to the design of new nuclear power plants. Task S2.1 of the program is a multi-phase research project to assess the effects of seismic wave incoherence on the response of foundations and structures similar to those being considered for advanced reactor designs. The initial phases of this task focused on the objective of systematically studying seismic wave incoherence effects on structures/foundations. These phases were completed in November 2006 and reported in EPRI 1013504, *Effect of Seismic Wave Incoherence on Foundation and Building Response*.

The final phase of Task S2.1 is documented in this report. This phase entails the validation of analytical methods and their implementation in the soil-structure interaction (SSI) computer programs, CLASSI and SASSI. The objective of this final phase is to demonstrate that the CLASSI and SASSI codes, as modified, correctly calculate the seismic response of foundations and structures when subjected to seismic wave fields, including incoherence effects.

Results & Findings

Three distinct SSI analysis programs (CLASSIinco-SRSS, SASSI-SRSS, and SASSI-Simulation) have been fully validated to treat the phenomena of incoherency for nuclear power plant structures, when applied in the seismic design/qualification process. In addition, the SSI analysis program, SASSI-AS, may be used to treat incoherency for certain situations.

Challenges & Objective(s)

The incoherent seismic responses computed by the CLASSI and SASSI codes were compared and shown to be in good agreement in the first phases of the S2.1 program. However, the example rock/structure model considered in those benchmark analyses did not produce significant incoherency-induced torsion and rocking response, which was deemed essential to the validation efforts of this study. The example rock/structure model used for benchmark comparisons in this final phase has offsets of mass centers from the shear centers and significant "outriggers" (nodes extended from the mass center to simulate the response at the perimeter of the building) to overemphasize seismic response from incoherency-induced rotations. It is judged that the example rock/structure model utilized in this phase provides an extreme (conservative) level of torsion and rocking response induced by seismic wave incoherence, which validates the use of selected versions of the CLASSI and SASSI codes for seismic analysis. Incoherency-induced rotations are a random phenomena resulting from the horizontal spatial variation of ground motion over the foundation area. For response quantities where several components of foundation motion contribute significantly, the phasing of those components must be adequately represented in order to produce reasonable seismic response.

Applications, Values & Use

Validated computer programs that implement the methods and procedures to incorporate incoherence effects are available for evaluation of the site-specific seismic response to support a utility's Early Site Permit (ESP) or Combined Operating License (COL) applications. The primary value of these programs is that they enable a more realistic quantification of the seismic response of structures and equipment in the high-frequency portion of the response spectrum.

EPRI Perspective

EPRI has an industrywide perspective and mandate to address technical issues related to the safe design and efficient operation of nuclear facilities. Methods and procedures described in this report contribute to stabilizing seismic safety reviews for new nuclear power units and to providing a more accurate approach for treatment of the seismic ground motion incoherency phenomena.

Approach

Enhancements to the CLASSI and SASSI approaches have been made to capture the random nature of multi-component seismic response. These enhancements have led to several CLASSI and SASSI methods for evaluating seismic response, including seismic wave incoherence. These approaches include the following:

- CLASSIinco-SRSS—Square root of the sum of the squares (SRSS) combination of structural response computed from random phasing of foundation component response
- SASSI-SRSS—SRSS combination of modal transfer functions to represent random phasing of spatial modes
- SASSI Simulation Mean—Monte Carlo simulations to represent random phasing of spatial modes
- SASSI-AS—Algebraic summation of spatial modes with assumed deterministic phasing

Validation is determined by agreement of results computed using these CLASSI and SASSI methods compared to those available from published literature. It is also determined by agreement within engineering accuracy of CLASSI computed incoherent seismic response with SASSI computed incoherent seismic response for an example rock/structure model.

Keywords

High-Frequency Effects
Seismic Wave Incoherence
Soil-Structure Interactions
Ground Motion Incoherence
CLASSI Code
SASSI Code

ABSTRACT

The New Plant Seismic Issues Resolution Program was initiated to address emerging seismic issues as they relate to the design of new nuclear power plants. Task S2.1 of the program is a multi-phase research project to assess the effects of seismic wave incoherence on the response of foundations and structures similar to those being considered for advanced reactor designs. The initial phases of this task focused on the objective of systematically studying seismic wave incoherence effects on structures/foundations. These phases were completed in November, 2006 and reported elsewhere.

The final phase of Task S2.1 is documented herein. This final phase entails the validation of analytical methods and their implementation in the soil-structure interaction (SSI) computer programs CLASSI and SASSI. The objective of this final phase is to demonstrate that CLASSI and SASSI, as modified, adequately calculate the seismic response of foundations and structures when subjected to seismic wave fields including incoherence effects.

Seismic wave incoherence consists of spatial variation of horizontal and vertical ground motion. Two sources of incoherence or horizontal spatial variation of ground motion are:

a. Local wave scattering: Spatial variation from scattering of waves due to the heterogeneous nature of the soil or rock along the propagation paths of the incident wave fields.
b. Wave passage effects: Systematic spatial variation due to difference in arrival times of seismic waves across a foundation due to inclined waves.

The focus of all phases of Task S2.1 is on local wave scattering.

The effect of seismic wave incoherence is that motions recorded on foundations of structures differ from those measured in the adjacent free-field. Generally, the motion measured on the foundation is less than the motion recorded in the free-field, especially at high-frequencies. Two aspects of soil-structure interaction contribute to the observations of foundation motion being less than the free-field: kinematic and inertial interaction. Kinematic interaction is due to the spatial variation of the free-field ground motion over the portion of the foundation/structure system abutting the soil or rock. Generally, the motion measured on the foundation is less than the motion recorded in the free-field, especially at high frequencies. Johnson [6] and Chang et al. [7] summarize many of the efforts to document these phenomena. Kim and Stewart [8] investigate the isolation of the effects of seismic wave incoherence from other aspects of kinematic interaction based on recorded data. The study was very successful in evaluating the effects of incoherence on foundation translational response; for foundation rotations, a much more difficult problem is encountered due to the lack of appropriate recorded data. For nuclear power plant structures, which have large and stiff foundation mats, the amplitudes of high-frequency seismic response of the foundation mat are expected to be significantly less than those in the free-field due to horizontal spatial variation of ground motion including incoherence.

Validation of CLASSI and SASSI to treat seismic wave incoherence in SSI analyses is accomplished by:

a. Comparison of results computed using CLASSI and SASSI to those available from published literature.

b. Comparison of CLASSI computed incoherent seismic response with SASSI computed incoherent seismic response for an example rock/structure model.

CLASSI and SASSI computed incoherent seismic response were compared and shown to be in good agreement in the first phases of the Program. However, the example rock/structure model considered in those benchmark analyses did not produce significant incoherency-induced torsion and rocking response. The example rock/structure model used for benchmark comparisons in this final phase has offsets of mass centers from the shear centers and significant "outriggers" (nodes extended from the mass center to simulate the response at the perimeter of the building) to overemphasize seismic response from incoherency-induced rotations. It is judged that the example rock/structure model utilized in this phase provides an extreme (conservative) level of torsion and rocking response induced by seismic wave incoherence that validates the use of selected versions of CLASSI and SASSI for seismic analysis.

Incoherency induced rotations are a random phenomena resulting from the horizontal spatial variation of ground motion over the foundation area. For response quantities where several components of foundation motion contribute significantly, the phasing of those components must be adequately represented in order to produce reasonable seismic response. As a result, enhancements to the CLASSI and SASSI approaches as described herein are required to capture the random nature of multi-component seismic response. These enhancements have led to the review and recognition of two CLASSI methods and three SASSI methods for evaluating seismic response including seismic wave incoherence. These approaches include:

- CLASSIinco – deterministic phasing of foundation component response
- CLASSIinco-SRSS – SRSS combination of structural response computed from random phasing of foundation component response
- SASSI-SRSS – SRSS combination of modal transfer functions to represent random phasing of spatial modes
- SASSI Simulation Mean – Monte Carlo simulations to represent random phasing of spatial modes
- SASSI-AS – Algebraic summation of spatial modes with assumed deterministic phasing

The conclusions of this validation effort are:

1. Soil-structure interaction (SSI) analysis is important to calculating seismic response to structures mounted on rock sites and subjected to high-frequency ground motion. SSI produces significant reductions in high-frequency response for these conditions.
2. CLASSIinco and CLASSIinco-SRSS are computationally efficient methods for conducting SSI analyses including incoherency, but are limited to rigid surface foundations. For structures with foundations for which the combined behavior of foundation/structure is deemed flexible and for embedded foundations/partial structure, a version of SASSI is required to accurately capture seismic response.

3. Utilization of SASSI-AS to compute the response for incoherent input requires computational effort comparable to standard SASSI analysis for coherent input. SASSI-SRSS and SASSI Simulation require significantly greater computational effort to analyze the incoherent response for complex structural models.
4. The SSI analysis programs CLASSIinco-SRSS, SASSI-SRSS, and SASSI-Simulation have been fully validated to treat the phenomenon of incoherency for nuclear power plant structures when applied in the seismic design/qualification process. The bases of the validation are:
   - Agreement of results computed using CLASSI and SASSI to those available from published literature (Chapter 3 and Appendix C).
   - Comparison of CLASSI computed incoherent seismic response with SASSI computed incoherent seismic response for an example rock/structure model with agreement within engineering accuracy (Chapter 5 and Appendix A).
5. CLASSIinco-SRSS, SASSI-SRSS, and SASSI-Simulation are the most theoretically correct techniques since they recognize and treat the random nature of the phase of the incoherent SSI response. The results of the analyses where the three input directions are treated independently (Appendix A) demonstrate that the agreement among these three is excellent.
6. The more simplified approach of SASSI-AS has been shown to agree with other methods for response to combined excitations (i.e., Chapter 5 and Appendix C of Short, et.al., 2006). SASSI-AS results deviate from other methods for some instances where single excitation directions are considered (i.e., Appendix A). As a result, SASSI-AS may be used to treat the phenomenon of incoherency for nuclear power plant structures with the following restrictions:
   - SASSI-AS is acceptable for foundation/structural systems demonstrated to have minimal incoherency-induced rotation effects. SASSI-AS may be used for structure configurations where it can be demonstrated that induced rotation effects are adequately treated with this methodology, (e.g., for large plan dimension/low height structures).
   - SASSI-AS may be used if its applicability is demonstrated by sensitivity studies
7. Even though CLASSIinco results were in close agreement with the other approaches that computed incoherent seismic response for the example rock/structure model (Chapter 5), it is recommended that the CLASSIinco-SRSS approach be used for incoherent analysis by CLASSI. CLASSIinco would require the same sensitivity studies as SASSI-AS in order to be used. However, CLASSIinco-SRSS is very computationally efficient, which precludes the need for the simpler version, CLASSIinco.

This report contains an evaluation of the impact on in-structure response spectra of changes to the ground motion coherency functions. Generally, the effect of rock coherency functions on SSI response compared to soil coherency functions is to reduce the reduction in response by about one-half.

ACKNOWLEDGMENTS

EPRI wishes to acknowledge the members of the Technical Review and Advisory Group (TRAG) for their support of this research project:

Robert Kennedy (Chair)	RPK Structural Consulting
Orhan Gurbuz	Consultant
Don Moore	Southern Nuclear
John Richards	Duke Power
Carl Stepp	Earthquake Hazards Solutions

EPRI wishes to acknowledge Dr. Dan Ghiocel at GP Technologies, Inc. and Dr. Farhang Ostadan at Bechtel Engineering for their support of this project. Dr. Ghiocel provided SASSI Simulation Mean results and Dr. Ostadan provided SASSI SRSS results for the benchmark problem in Chapter 5 and Appendix A of this report. Dr. Ghiocel provided the descriptions of SASSI-Simulation and SASSI-AS included as Appendix C. Dr. Ostadan provided the description of SASSI-SRSS under separate cover.

CONTENTS

1 INTRODUCTION AND BACKGROUND 1-1

Background on Seismic Wave Incoherence 1-1

Summary – Effect of Seismic Wave Incoherence on Foundation and Building Response (Short et al., 2006) 1-2

Scope of Current Research Effort 1-3

Contents of the Report 1-4

2 STUDY INPUT PARAMETERS 2-1

Coherency Function 2-1

Site Parameters and Input Ground Motion 2-3

Foundation Parameters 2-7

Structure Properties 2-8

3 CLASSI TECHNICAL APPROACH 3-1

General 3-1

Incorporation of the Coherency Function into CLASSI Procedures 3-1

General CLASSI Approach: Rigid Massless Foundation 3-2

CLASSI Random Vibration Approach: Rigid Massless Foundation 3-3

CLASSI Random Vibration Approach: Foundation and Structure Response 3-4

Procedure to Evaluate the Incoherency Transfer Function (ITF) 3-5

Procedure to Evaluate the Foundation and Structure Incoherent Response Spectra by CLASSI 3-6

Validation of Rigid, Massless Foundation Response 3-10

Objective and Scope 3-10

Ground Motion Coherence Function 3-10

Circular Disk 3-12

Square Foundation 3-17

Conclusions 3-19

4 SASSI TECHNICAL APPROACH 4-1
General 4-1
Coherency Matrix 4-1
SASSI Approach 4-2
Approaches to Solve for SSI Response of Foundation and Structure 4-3
Stochastic Approach or Randomization (SASSI – Simulation Mean) 4-3
Square Root of the Sum of the Squares (SASSI-SRSS) 4-7
SRSS Transfer Functions 4-7
SRSS – SSI Response 4-8
Linear Algebraic Summation (SASSI – AS) 4-8

5 CLASSI AND SASSI IN-STRUCTURE RESPONSE SPECTRA COMPARISONS 5-1
General 5-1
CLASSI-SASSI Comparisons of In-Structure Response Spectra 5-4
Foundation Response 5-4
Auxiliary and Shield Building (ASB) 5-8
Containment Internal Structure (CIS) 5-11
Steel Containment Vessel (SCV) 5-16
Summary of CLASSI-SASSI Comparisons 5-20

6 GUIDELINES FOR APPLICATION OF CLASSI AND SASSI 6-1
General 6-1
CLASSI 6-1
CLASSIinco 6-3
CLASSIiinco-SRSS 6-6
SASSI 6-7
SASSI Simulations 6-10
SASSI-AS 6-17
SASSI-SRSS 6-20

7 CONCLUSIONS AND RECOMMENDATIONS 7-1

8 REFERENCES 8-1

A CLASSI-SASSI IN-STRUCTURE RESPONSE SPECTRA COMPARISONS FOR INDIVIDUAL INPUT DIRECTION COMPONENTS A-1

X-Direction Input Ground Motion A-3
Y-Direction Input Ground Motion A-16
Z-Direction Input Ground Motion A-30

***B* EFFECT OF ABRAHAMSON HARD ROCK COHERENCY FUNCTIONS B-1**
General B-1
SSI and Structure Response B-1
SSI and Incoherence B-4
General Observations B-5
Foundation Response B-5
Auxiliary and Shield Building (ASB) B-5
Steel Containment Vessel (SCV) B-6
Containment Internal Structure (CIS) B-7
Conclusions B-7
References B-26

***C* SASSI SIMULATION & SASSI-AS APPROACHES FOR SSI ANALYSIS WITH INCOHERENT GROUND MOTIONS C-1**
Brief Introduction to Stochastic Modeling Terminology C-1
Coherence Function C-2
Factorization of Coherency Kernels C-3
Incoherent Seismic SSI Analysis Methodology C-3
Incoherent SSI Analysis Implementation C-5
Stochastic Approach or Randomization (SASSI-Simulation Mean) C-6
Deterministic Approach or Linear Algebraic Summation (SASSI-AS) C-7
Specific Numerical Techniques Implemented for Incoherent SSI Analyses C-7
Improved Interpolation Scheme for Incoherent Transfer Function (ITF) Calculations C-8
Phase Adjustment for Incoherent Transfer Functions (ITF) C-9
Illustrative Example C-12
Summary and Conclusions C-14
Selected References C-15

LIST OF FIGURES

Figure 2-1 Coherency Function for Horizontal Ground Motion 2-2
Figure 2-2 Coherency Function for Vertical Ground Motion 2-2
Figure 2-3 Rock Site Profile Shear Wave Velocities vs. Depth 2-4
Figure 2-4 Site-Specific Response Spectra for Rock Site at Ground Surface (Depth 0-ft) 2-6
Figure 2-5 Computed and Target Response Spectra for Rock Site 2-7
Figure 2-6 Advanced Reactor Structure Stick Model With Outriggers and Offset Mass Centers 2-9
Figure 3-1 Elements of the Substructure Approach to SSI Analysis as Implemented in CLASSI 3-7
Figure 3-2 Comparison of Coherency Ground Motion Functions, Horizontal Direction – Abrahamson (2005, 2006) and Luco and Mita (1987) for $\gamma = 0.5$ 3-11
Figure 3-3 Foundation Model, Circular Disk, CLASSIinco 3-13
Figure 3-4 Circular Foundation, Comparison of CLASSIinco Results With Luco and Mita (1987), Horizontal Transfer Function S11 3-14
Figure 3-5 Circular Foundation, Comparison of CLASSIinco Results With Luco and Mita (1987), Torsional Transfer Function S61 3-14
Figure 3-6 Circular Foundation, Comparison of CLASSIinco Results With Luco and Mita (1987), Vertical Transfer Function S33 3-15
Figure 3-7 Circular Foundation, Comparison of CLASSIinco Results With Luco and Mita (1987), Rocking Transfer Function S43 3-15
Figure 3-8 Circular Foundation, Comparison of CLASSIinco Results With Veletsos and Prasad (1989), Horizontal Transfer Function S11 3-16
Figure 3-9 Circular Foundation, Comparison of CLASSIinco Results With Veletsos and Prasad (1989), Torsional Transfer Function S61 3-16
Figure 3-10 Square Foundation Model, CLASSIinco 3-17
Figure 3-11 Square Foundation, Comparison of CLASSIinco Results With Luco and Wong (1986), Horizontal Transfer Function S11 3-18
Figure 3-12 Square Foundation, Comparison of CLASSIinco Results With Luco and Wong (1986), Torsional Transfer Function S61 3-18
Figure 3-13 Square Foundation, Comparison of CLASSIinco Results With Luco and Wong (1986), Vertical Transfer Function S33 3-19
Figure 3-14 Square Foundation, Comparison of CLASSIinco Results With Luco and Wong (1986), Rocking Transfer Function S43 3-19
Figure 4-1 SASSI Simulation Calculated Foundation Vertical Response Spectra for Vertical Input Motion by 20 Simulations 4-4

Figure 4-2 SASSI Simulation Calculated Node 229 CIS Outrigger Vertical Response Spectra for Vertical Input Motion by 20 Simulations 4-5

Figure 4-3 SASSI Simulation Calculated Foundation Vertical Response Spectra for Vertical Input Motion – Mean Spectra by 5, 10, 15, and 20 Simulations 4-6

Figure 4-4 SASSI Simulation Calculated Node 229 CIS Outrigger Vertical Response Spectra for Vertical Input Motion – Mean Spectra by 5, 10, 15 and 20 Simulations 4-6

Figure 5-1 Locations on the AP1000-Based Stick Model With Offsets and Outriggers where In-Structure Response Spectra are Computed 5-2

Figure 5-2 Center of Foundation Response Spectra – X Direction – CLASSlinco, CLASSlinco-SRSS, SASSI-SRSS, SASSI Simulation Mean, SASSI-AS (Node 1) 5-5

Figure 5-3 Center of Foundation Response Spectra – Y Direction – CLASSlinco, CLASSlinco-SRSS, SASSI-SRSS, SASSI Simulation Mean, SASSI-AS (Node 1) 5-5

Figure 5-4 Center of Foundation Response Spectra – Z Direction – CLASSlinco, CLASSlinco-SRSS, SASSI-SRSS, SASSI Simulation Mean, SASSI-AS (Node 1) 5-6

Figure 5-5 Edge of Foundation Response Spectra –XX Rotation – CLASSlinco, CLASSlinco-SRSS, SASSI-SRSS, SASSI Simulation Mean, SASSI-AS (Node 1) 5-6

Figure 5-6 Edge of Foundation Response Spectra –YY Rotation – CLASSlinco, CLASSlinco-SRSS, SASSI-SRSS, SASSI Simulation Mean, SASSI-AS (Node 1) 5-7

Figure 5-7 Edge of Foundation Response Spectra –ZZ Rotation – CLASSlinco, CLASSlinco-SRSS, SASSI-SRSS, SASSI Simulation Mean, SASSI-AS (Node 1) 5-7

Figure 5-8 Top of ASB Response Spectra – X Direction – CLASSlinco, CLASSlinco-SRSS, SASSI-SRSS, SASSI Simulation Mean, SASSI-AS (Node 18) 5-8

Figure 5-9 Top of ASB Response Spectra – Y Direction - CLASSlinco, CLASSlinco-SRSS, SASSI-SRSS, SASSI Simulation Mean, SASSI-AS (Node 18) 5-9

Figure 5-10 Top of ASB Response Spectra – Z Direction – CLASSlinco, CLASSlinco-SRSS, SASSI-SRSS, SASSI Simulation Mean, SASSI-AS (Node 18) 5-9

Figure 5-11 ASB Outrigger Response Spectra – X Direction – CLASSlinco, CLASSlinco-SRSS, SASSI-SRSS, SASSI Simulation Mean, SASSI-AS (Node 118) 5-10

Figure 5-12 ASB Outrigger Response Spectra – Y Direction Due – CLASSlinco, CLASSlinco-SRSS, SASSI-SRSS, SASSI Simulation Mean, SASSI-AS (Node 118) 5-10

Figure 5-13 ASB Outrigger Response Spectra – Z Direction – CLASSlinco, CLASSlinco-SRSS, SASSI-SRSS, SASSI Simulation Mean, SASSI-AS (Node 118) 5-11

Figure 5-14 Top of CIS Shear Center Response Spectra – X Direction – CLASSlinco, CLASSlinco-SRSS, SASSI-SRSS, SASSI Simulation Mean, SASSI-AS (Node 29) 5-12

Figure 5-15 Top of CIS Shear Center Response Spectra – Y Direction – CLASSlinco, CLASSlinco-SRSS, SASSI-SRSS, SASSI Simulation Mean, SASSI-AS (Node 29) 5-12

Figure 5-16 Top of CIS Shear Center Response Spectra – Z Direction – CLASSlinco, CLASSlinco-SRSS, SASSI-SRSS, SASSI Simulation Mean, SASSI-AS (Node 29) 5-13

Figure 5-17 Top of CIS Horizontal Mass Center Response Spectra – X Direction – CLASSlinco, CLASSlinco-SRSS, SASSI-SRSS, SASSI Simulation Mean, SASSI-AS (Node 129) 5-13

Figure 5-18 Top of CIS Horizontal Mass Center Response Spectra – Y Direction – CLASSlinco, CLASSlinco-SRSS, SASSI-SRSS, SASSI Simulation Mean, SASSI-AS (Node 129) 5-14

Figure 5-19 Top of CIS Horizontal Mass Center Response Spectra – Z Direction – CLASSIinco, CLASSIinco-SRSS, SASSI-SRSS, SASSI Simulation Mean, SASSI-AS (Node 129) 5-14

Figure 5-20 CIS Outrigger Response Spectra – X Direction – CLASSIinco, CLASSIinco-SRSS, SASSI-SRSS, SASSI Simulation Mean, SASSI-AS (Node 229) 5-15

Figure 5-21 CIS Outrigger Response Spectra – Y Direction – CLASSIinco, CLASSIinco-SRSS, SASSI-SRSS, SASSI Simulation Mean, SASSI-AS (Node 229) 5-15

Figure 5-22 CIS Outrigger Response Spectra – Z Direction – CLASSIinco, CLASSIinco-SRSS, SASSI-SRSS, SASSI Simulation Mean, SASSI-AS (Node 229) 5-16

Figure 5-23 Top of SCV Response Spectra – X Direction – CLASSIinco, CLASSIinco-SRSS, SASSI-SRSS, SASSI Simulation Mean, SASSI-AS (Node 45) 5-17

Figure 5-24 Top of SCV Response Spectra – Y Direction – CLASSIinco, CLASSIinco-SRSS, SASSI-SRSS, SASSI Simulation Mean, SASSI-AS (Node 45) 5-17

Figure 5-25 Top of SCV Response Spectra – Z Direction – CLASSIinco, CLASSIinco-SRSS, SASSI-SRSS, SASSI Simulation Mean, SASSI-AS (Node 45) 5-18

Figure 5-26 SCV Outrigger Response Spectra – X Direction – CLASSIinco, CLASSIinco-SRSS, SASSI-SRSS, SASSI Simulation Mean, SASSI-AS (Node 145) 5-18

Figure 5-27 SCV Outrigger Response Spectra – Y Direction – CLASSIinco, CLASSIinco-SRSS, SASSI-SRSS, SASSI Simulation Mean, SASSI-AS (Node 145) 5-19

Figure 5-28 SCV Outrigger Response Spectra – Z Direction – CLASSIinco, CLASSIinco-SRSS, SASSI-SRSS, SASSI Simulation Mean, SASSI-AS (Node 145) 5-19

Figure 6-1 Foundation Transfer Function – Z Direction Due to Z Input– (Node 1) 6-14

Figure 6-2 Top of CIS Outrigger Transfer Function – Z Direction Due to Z Input– (Node 229) 6-15

Figure A-1 Locations on the AP1000-Based Stick Model where In-Structure Response Spectra are Computed A-2

Figure A-2 Center of Foundation Response Spectra – X Direction Due to X Input – CLASSIinco, CLASSIinco-SRSS, SASSI-SRSS, SASSI Simulation Mean, SASSI-AS (Node 1) A-3

Figure A-3 Center of Foundation Response Spectra – Y Direction Due to X Input – CLASSIinco, CLASSIinco-SRSS, SASSI-SRSS, SASSI Simulation Mean, SASSI-AS (Node 1) A-3

Figure A-4 Center of Foundation Response Spectra – Z Direction Due to X Input – CLASSIinco, CLASSIinco-SRSS, SASSI-SRSS, SASSI Simulation Mean, SASSI-AS (Node 1) A-4

Figure A-5 Edge of Foundation Response Spectra –XX Rotation Due to X Input – CLASSIinco, CLASSIinco-SRSS, SASSI-SRSS, SASSI Simulation Mean, SASSI-AS (Node 1) A-4

Figure A-6 Edge of Foundation Response Spectra –YY Rotation Due to X Input – CLASSIinco, CLASSIinco-SRSS, SASSI-SRSS, SASSI Simulation Mean, SASSI-AS (Node 1) A-5

Figure A-7 Edge of Foundation Response Spectra –ZZ Rotation Due to X Input – CLASSIinco, CLASSIinco-SRSS, SASSI-SRSS, SASSI Simulation Mean, SASSI-AS (Node 1) A-5

Figure A-8 Top of ASB Response Spectra – X Direction Due to X Input – CLASSIinco, CLASSIinco-SRSS, SASSI-SRSS, SASSI Simulation Mean, SASSI-AS (Node 18) A-6

Figure A-9 Top of ASB Response Spectra – Y Direction Due to X Input – CLASSIinco, CLASSIinco-SRSS, SASSI-SRSS, SASSI Simulation Mean, SASSI-AS (Node 18) A-6

Figure A-10 Top of ASB Response Spectra – Z Direction Due to X Input – CLASSIinco, CLASSIinco-SRSS, SASSI-SRSS, SASSI Simulation Mean, SASSI-AS (Node 18) A-7

Figure A-11 ASB Outrigger Response Spectra – X Direction Due to X Input – CLASSIinco, CLASSIinco-SRSS, SASSI-SRSS, SASSI Simulation Mean, SASSI-AS (Node 118) A-7

Figure A-12 ASB Outrigger Response Spectra – Y Direction Due to X Input – CLASSIinco, CLASSIinco-SRSS, SASSI-SRSS, SASSI Simulation Mean, SASSI-AS (Node 118) A-8

Figure A-13 ASB Outrigger Response Spectra – Z Direction Due to X Input – CLASSIinco, CLASSIinco-SRSS, SASSI-SRSS, SASSI Simulation Mean, SASSI-AS (Node 118) A-8

Figure A-14 Top of CIS Shear Center Response Spectra – X Direction Due to X Input – CLASSIinco, CLASSIinco-SRSS, SASSI-SRSS, SASSI Simulation Mean, SASSI-AS (Node 29) A-9

Figure A-15 Top of CIS Shear Center Response Spectra – Y Direction Due to X Input – CLASSIinco, CLASSIinco-SRSS, SASSI-SRSS, SASSI Simulation Mean, SASSI-AS (Node 29) A-9

Figure A-16 Top of CIS Shear Center Response Spectra – Z Direction Due to X Input – CLASSIinco, CLASSIinco-SRSS, SASSI-SRSS, SASSI Simulation Mean, SASSI-AS (Node 29) A-10

Figure A-17 Top of CIS Horizontal Mass Center Response Spectra – X Direction Due to X Input – CLASSIinco, CLASSIinco-SRSS, SASSI-SRSS, SASSI Simulation Mean, SASSI-AS (Node 129)..... A-10

Figure A-18 Top of CIS Horizontal Mass Center Response Spectra – Y Direction Due to X Input – CLASSIinco, CLASSIinco-SRSS, SASSI-SRSS, SASSI Simulation Mean, SASSI-AS (Node 129)..... A-11

Figure A-19 Top of CIS Horizontal Mass Center Response Spectra – Z Direction Due to X Input – CLASSIinco, CLASSIinco-SRSS, SASSI-SRSS, SASSI Simulation Mean, SASSI-AS (Node 129)..... A-11

Figure A-20 CIS Outrigger Response Spectra – X Direction Due to X Input – CLASSIinco, CLASSIinco-SRSS, SASSI-SRSS, SASSI Simulation Mean, SASSI-AS (Node 229) A-12

Figure A-21 CIS Outrigger Response Spectra – Y Direction Due to X Input – CLASSIinco, CLASSIinco-SRSS, SASSI-SRSS, SASSI Simulation Mean, SASSI-AS (Node 229) A-12

Figure A-22 CIS Outrigger Response Spectra – Z Direction Due to X Input – CLASSIinco, CLASSIinco-SRSS, SASSI-SRSS, SASSI Simulation Mean, SASSI-AS (Node 229) A-13

Figure A-23 Top of SCV Response Spectra – X Direction Due to X Input – CLASSIinco, CLASSIinco-SRSS, SASSI-SRSS, SASSI Simulation Mean, SASSI-AS (Node 45) A-13

Figure A-24 Top of SCV Response Spectra – Y Direction Due to X Input – CLASSIinco, CLASSIinco-SRSS, SASSI-SRSS, SASSI Simulation Mean, SASSI-AS (Node 45) A-14

Figure A-25 Top of SCV Response Spectra – Z Direction Due to X Input – CLASSIinco, CLASSIinco-SRSS, SASSI-SRSS, SASSI Simulation Mean, SASSI-AS (Node 45) A-14

Figure A-26 SCV Outrigger Response Spectra – X Direction Due to X Input – CLASSIinco, CLASSIinco-SRSS, SASSI-SRSS, SASSI Simulation Mean, SASSI-AS (Node 145) A-15

Figure A-27 SCV Outrigger Response Spectra – Y Direction Due to X Input – CLASSIinco, CLASSIinco-SRSS, SASSI-SRSS, SASSI Simulation Mean, SASSI-AS (Node 145) A-15

Figure A-28 SCV Outrigger Response Spectra – Z Direction Due to X Input – CLASSIinco, CLASSIinco-SRSS, SASSI-SRSS, SASSI Simulation Mean, SASSI-AS (Node 145) A-16

Figure A-29 Center of Foundation Response Spectra – X Direction Due to Y Input – CLASSIinco, CLASSIinco-SRSS, SASSI-SRSS, SASSI Simulation Mean, SASSI-AS (Node 1) A-16

Figure A-30 Center of Foundation Response Spectra – Y Direction Due to Y Input – CLASSIinco, CLASSIinco-SRSS, SASSI-SRSS, SASSI Simulation Mean, SASSI-AS (Node 1) A-17

Figure A-31 Center of Foundation Response Spectra – Z Direction Due to Y Input – CLASSIinco, CLASSIinco-SRSS, SASSI-SRSS, SASSI Simulation Mean, SASSI-AS (Node 1) A-17

Figure A-32 Edge of Foundation Response Spectra –XX Rotation Due to Y Input – CLASSIinco, CLASSIinco-SRSS, SASSI-SRSS, SASSI Simulation Mean, SASSI-AS (Node 1) A-18

Figure A-33 Edge of Foundation Response Spectra –YY Rotation Due to Y Input – CLASSIinco, CLASSIinco-SRSS, SASSI-SRSS, SASSI Simulation Mean, SASSI-AS (Node 1) A-18

Figure A-34 Edge of Foundation Response Spectra –ZZ Rotation Due to Y Input – CLASSIinco, CLASSIinco-SRSS, SASSI-SRSS, SASSI Simulation Mean, SASSI-AS (Node 1) A-19

Figure A-35 Top of ASB Response Spectra – X Direction Due to Y Input – CLASSIinco, CLASSIinco-SRSS, SASSI-SRSS, SASSI Simulation Mean, SASSI-AS (Node 18) A-19

Figure A-36 Top of ASB Response Spectra – Y Direction Due to Y Input – CLASSIinco, CLASSIinco-SRSS, SASSI-SRSS, SASSI Simulation Mean, SASSI-AS (Node 18) A-20

Figure A-37 Top of ASB Response Spectra – Z Direction Due to Y Input – CLASSIinco, CLASSIinco-SRSS, SASSI-SRSS, SASSI Simulation Mean, SASSI-AS (Node 18) A-20

Figure A-38 ASB Outrigger Response Spectra – X Direction Due to Y Input – CLASSIinco, CLASSIinco-SRSS, SASSI-SRSS, SASSI Simulation Mean, SASSI-AS (Node 118) A-21

Figure A-39 ASB Outrigger Response Spectra – Y Direction Due to Y Input – CLASSIinco, CLASSIinco-SRSS, SASSI-SRSS, SASSI Simulation Mean, SASSI-AS (Node 118) A-21

Figure A-40 ASB Outrigger Response Spectra – Z Direction Due to Y Input – CLASSIinco, CLASSIinco-SRSS, SASSI-SRSS, SASSI Simulation Mean, SASSI-AS (Node 118) A-22

Figure A-41 Top of CIS Shear Center Response Spectra – X Direction Due to Y Input – CLASSIinco, CLASSIinco-SRSS, SASSI-SRSS, SASSI Simulation Mean, SASSI-AS (Node 29) A-22

Figure A-42 Top of CIS Shear Center Response Spectra – Y Direction Due to Y Input – CLASSIinco, CLASSIinco-SRSS, SASSI-SRSS, SASSI Simulation Mean, SASSI-AS (Node 29) A-23

Figure A-43 Top of CIS Shear Center Response Spectra – Z Direction Due to Y Input – CLASSIinco, CLASSIinco-SRSS, SASSI-SRSS, SASSI Simulation Mean, SASSI-AS (Node 29) A-23

Figure A-44 Top of CIS Horizontal Mass Center Response Spectra – X Direction Due to Y Input – CLASSIinco, CLASSIinco-SRSS, SASSI-SRSS, SASSI Simulation Mean, SASSI-AS (Node 129) A-24

Figure A-45 Top of CIS Horizontal Mass Center Response Spectra – Y Direction Due to Y Input – CLASSIinco, CLASSIinco-SRSS, SASSI-SRSS, SASSI Simulation Mean, SASSI-AS (Node 129) A-24

Figure A-46 Top of CIS Horizontal Mass Center Response Spectra – Z Direction Due to Y Input – CLASSIinco, CLASSIinco-SRSS, SASSI-SRSS, SASSI Simulation Mean, SASSI-AS (Node 129) A-25

Figure A-47 CIS Outrigger Response Spectra – X Direction Due to Y Input – CLASSIinco, CLASSIinco-SRSS, SASSI-SRSS, SASSI Simulation Mean, SASSI-AS (Node 229) A-25

Figure A-48 CIS Outrigger Response Spectra – Y Direction Due to Y Input – CLASSIinco, CLASSIinco-SRSS, SASSI-SRSS, SASSI Simulation Mean, SASSI-AS (Node 229) A-26

Figure A-49 CIS Outrigger Response Spectra – Z Direction Due to Y Input – CLASSIinco, CLASSIinco-SRSS, SASSI-SRSS, SASSI Simulation Mean, SASSI-AS (Node 229) A-26

Figure A-50 Top of SCV Response Spectra – X Direction Due to Y Input – CLASSIinco, CLASSIinco-SRSS, SASSI-SRSS, SASSI Simulation Mean, SASSI-AS (Node 45) A-27

Figure A-51 Top of SCV Response Spectra – Y Direction Due to Y Input – CLASSIinco, CLASSIinco-SRSS, SASSI-SRSS, SASSI Simulation Mean, SASSI-AS (Node 45) A-27

Figure A-52 Top of SCV Response Spectra – Z Direction Due to Y Input – CLASSIinco, CLASSIinco-SRSS, SASSI-SRSS, SASSI Simulation Mean, SASSI-AS (Node 45) A-28

Figure A-53 SCV Outrigger Response Spectra – X Direction Due to Y Input – CLASSIinco, CLASSIinco-SRSS, SASSI-SRSS, SASSI Simulation Mean, SASSI-AS (Node 145) A-28

Figure A-54 SCV Outrigger Response Spectra – Y Direction Due to Y Input – CLASSIinco, CLASSIinco-SRSS, SASSI-SRSS, SASSI Simulation Mean, SASSI-AS (Node 145) A-29

Figure A-55 SCV Outrigger Response Spectra – Z Direction Due to Y Input – CLASSIinco, CLASSIinco-SRSS, SASSI-SRSS, SASSI Simulation Mean, SASSI-AS (Node 145) A-29

Figure A-56 Center of Foundation Response Spectra – X Direction Due to Z Input – CLASSIinco, CLASSIinco-SRSS, SASSI-SRSS, SASSI Simulation Mean, SASSI-AS (Node 1) A-30

Figure A-57 Center of Foundation Response Spectra – Y Direction Due to Z Input – CLASSIinco, CLASSIinco-SRSS, SASSI-SRSS, SASSI Simulation Mean, SASSI-AS (Node 1) A-30

Figure A-58 Center of Foundation Response Spectra – Z Direction Due to Z Input – CLASSIinco, CLASSIinco-SRSS, SASSI-SRSS, SASSI Simulation Mean, SASSI-AS (Node 1) A-31

Figure A-59 Edge of Foundation Response Spectra –XX Rotation Due to Z Input – CLASSIinco, CLASSIinco-SRSS, SASSI-SRSS, SASSI Simulation Mean, SASSI-AS (Node 1) A-31

Figure A-60 Edge of Foundation Response Spectra –YY Rotation Due to Z Input – CLASSIinco, CLASSIinco-SRSS, SASSI-SRSS, SASSI Simulation Mean, SASSI-AS (Node 1) A-32

Figure A-61 Edge of Foundation Response Spectra –ZZ Rotation Due to Z Input – CLASSIinco, CLASSIinco-SRSS, SASSI-SRSS, SASSI Simulation Mean, SASSI-AS (Node 1) A-32

Figure A-62 Top of ASB Response Spectra – X Direction Due to Z Input – CLASSIinco, CLASSIinco-SRSS, SASSI-SRSS, SASSI Simulation Mean, SASSI-AS (Node 18) A-33

Figure A-63 Top of ASB Response Spectra – Y Direction Due to Z Input – CLASSIinco, CLASSIinco-SRSS, SASSI-SRSS, SASSI Simulation Mean, SASSI-AS (Node 18) A-33

Figure A-64 Top of ASB Response Spectra – Z Direction Due to Z Input – CLASSIinco, CLASSIinco-SRSS, SASSI-SRSS, SASSI Simulation Mean, SASSI-AS (Node 18) A-34

Figure A-65 ASB Outrigger Response Spectra – X Direction Due to Z Input – CLASSIinco, CLASSIinco-SRSS, SASSI-SRSS, SASSI Simulation Mean, SASSI-AS (Node 118) A-34

Figure A-66 ASB Outrigger Response Spectra – Y Direction Due to Z Input – CLASSIinco, CLASSIinco-SRSS, SASSI-SRSS, SASSI Simulation Mean, SASSI-AS (Node 118) A-35

Figure A-67 ASB Outrigger Response Spectra – Z Direction Due to Z Input – CLASSIinco, CLASSIinco-SRSS, SASSI-SRSS, SASSI Simulation Mean, SASSI-AS (Node 118) A-35

Figure A-68 Top of CIS Shear Center Response Spectra – X Direction Due to Z Input – CLASSIinco, CLASSIinco-SRSS, SASSI-SRSS, SASSI Simulation Mean, SASSI-AS (Node 29) A-36

Figure A-69 Top of CIS Shear Center Response Spectra – Y Direction Due to Z Input – CLASSIinco, CLASSIinco-SRSS, SASSI-SRSS, SASSI Simulation Mean, SASSI-AS (Node 29) A-36

Figure A-70 Top of CIS Shear Center Response Spectra – Z Direction Due to Z Input – CLASSIinco, CLASSIinco-SRSS, SASSI-SRSS, SASSI Simulation Mean, SASSI-AS (Node 29) A-37

Figure A-71 Top of CIS Horizontal Mass Center Response Spectra – Z Direction Due to X Input – CLASSIinco, CLASSIinco-SRSS, SASSI-SRSS, SASSI Simulation Mean, SASSI-AS (Node 129) A-37

Figure A-72 Top of CIS Horizontal Mass Center Response Spectra – Y Direction Due to Z Input – CLASSIinco, CLASSIinco-SRSS, SASSI-SRSS, SASSI Simulation Mean, SASSI-AS (Node 129) A-38

Figure A-73 Top of CIS Horizontal Mass Center Response Spectra – Z Direction Due to Z Input – CLASSIinco, CLASSIinco-SRSS, SASSI-SRSS, SASSI Simulation Mean, SASSI-AS (Node 129) A-38

Figure A-74 CIS Outrigger Response Spectra – X Direction Due to Z Input – CLASSIinco, CLASSIinco-SRSS, SASSI-SRSS, SASSI Simulation Mean, SASSI-AS (Node 229) A-39

Figure A-75 CIS Outrigger Response Spectra – Y Direction Due to Z Input – CLASSIinco, CLASSIinco-SRSS, SASSI-SRSS, SASSI Simulation Mean, SASSI-AS (Node 229) A-39

Figure A-76 CIS Outrigger Response Spectra – Z Direction Due to Z Input – CLASSIinco, CLASSIinco-SRSS, SASSI-SRSS, SASSI Simulation Mean, SASSI-AS (Node 229) A-40

Figure A-77 Top of SCV Response Spectra – X Direction Due to Z Input – CLASSIinco, CLASSIinco-SRSS, SASSI-SRSS, SASSI Simulation Mean, SASSI-AS (Node 45) A-40

Figure A-78 Top of SCV Response Spectra – Y Direction Due to Z Input – CLASSIinco, CLASSIinco-SRSS, SASSI-SRSS, SASSI Simulation Mean, SASSI-AS (Node 45) A-41

Figure A-79 Top of SCV Response Spectra – Z Direction Due to Z Input – CLASSIinco, CLASSIinco-SRSS, SASSI-SRSS, SASSI Simulation Mean, SASSI-AS (Node 45) A-41

Figure A-80 SCV Outrigger Response Spectra – X Direction Due to Z Input – CLASSIinco, CLASSIinco-SRSS, SASSI-SRSS, SASSI Simulation Mean, SASSI-AS (Node 145) A-42

Figure A-81 SCV Outrigger Response Spectra – Y Direction Due to Z Input – CLASSIinco, CLASSIinco-SRSS, SASSI-SRSS, SASSI Simulation Mean, SASSI-AS (Node 145) A-42

Figure A-82 SCV Outrigger Response Spectra – Z Direction Due to Z Input – CLASSIinco, CLASSIinco-SRSS, SASSI-SRSS, SASSI Simulation Mean, SASSI-AS (Node 145) A-43

Figure B-1 Comparison of Hard Rock (Abrahamson, 2007) and Soil (Abrahamson, 2005, 2006) Coherency Functions B-2

Figure B-2 Locations on the AP1000-Based Stick Model where In-Structure Response Spectra are Computed B-3

Figure B-3 Foundation Response Spectra – X Direction –SSI Coherent, SSI Incoherent NAA2005-2006, SSI Incoherent NAA2007, (Node 1) and Free-Field B-8

Figure B-4 Foundation Response Spectra – Y Direction –SSI Coherent, SSI Incoherent NAA2005-2006, SSI Incoherent NAA2007, (Node 1) and Free-Field B-8

Figure B-5 Foundation Response Spectra – Z Direction –SSI Coherent, SSI Incoherent NAA2005-2006, SSI Incoherent NAA2007, (Node 1) and Free-Field B-9

Figure B-6 Top of Shield Building Response Spectra – X Direction –SSI Coherent, SSI Incoherent NAA2005-2006, SSI Incoherent NAA2007 (Node 310) B-9

Figure B-7 Top of Shield Building Response Spectra – Y Direction –SSI Coherent, SSI Incoherent NAA2005-2006, SSI Incoherent NAA2007 (Node 310) B-10

Figure B-8 Top of Shield Building Response Spectra – Z Direction –SSI Coherent, SSI Incoherent NAA2005-2006, SSI Incoherent NAA2007 (Node 310)..... B-10
Figure B-9 Top of Auxiliary Building Response Spectra – X Direction –SSI Coherent, SSI Incoherent NAA2005-2006, SSI Incoherent NAA2007 (Node 120mc)..... B-11
Figure B-10 Top of Auxiliary Building Response Spectra – Y Direction –SSI Coherent, SSI Incoherent NAA2005-2006, SSI Incoherent NAA2007 (Node 120mc)..... B-11
Figure B-11 Top of Auxiliary Building Response Spectra – Z Direction –SSI Coherent, SSI Incoherent NAA2005-2006, SSI Incoherent NAA2007 (Node 120)..... B-12
Figure B-12 Low on ASB Response Spectra – X Direction – SSI Coherent, SSI Incoherent NAA2005-2006, SSI Incoherent NAA2007 (Node 80mc)..... B-12
Figure B-13 Low on ASB Response Spectra – Y Direction – SSI Coherent, SSI Incoherent NAA2005-2006, SSI Incoherent NAA2007 (Node 80mc)..... B-13
Figure B-14 Low on ASB Response Spectra – Z Direction – SSI Coherent, SSI Incoherent NAA2005-2006, SSI Incoherent NAA2007 (Node 80)..... B-13
Figure B-15 Shield Building Outrigger Response Spectra – X Direction – SSI Coherent, SSI Incoherent NAA2005-2006, SSI Incoherent NAA2007 (Node 310out)..... B-14
Figure B-16 Shield Building Outrigger Response Spectra – Y Direction – SSI Coherent, SSI Incoherent NAA2005-2006, SSI Incoherent NAA2007 (Node 310out)..... B-14
Figure B-17 Shield Building Outrigger Response Spectra – Z Direction – SSI Coherent, SSI Incoherent NAA2005-2006, SSI Incoherent NAA2007 (Node 310out)..... B-15
Figure B-18 Auxiliary Building Outrigger Response Spectra – X Direction – SSI Coherent, SSI Incoherent NAA2005-2006, SSI Incoherent NAA2007 (Node 120out).... B-15
Figure B-19 Auxiliary Building Outrigger Response Spectra – Y Direction – SSI Coherent, SSI Incoherent NAA2005-2006, SSI Incoherent NAA2007 (Node 120out).... B-16
Figure B-20 Auxiliary Building Outrigger Response Spectra – Z Direction – SSI Coherent, SSI Incoherent NAA2005-2006, SSI Incoherent NAA2007 (Node 120out).... B-16
Figure B-21 Top of SCV Response Spectra – X Direction –SSI Coherent, SSI Incoherent NAA2005-2006, SSI Incoherent NAA2007 (Node 417) B-17
Figure B-22 Top of SCV Response Spectra – Y Direction –SSI Coherent, SSI Incoherent NAA2005-2006, SSI Incoherent NAA2007 (Node 417) B-17
Figure B-23 Top of SCV Response Spectra – Z Direction –SSI Coherent, SSI Incoherent NAA2005-2006, SSI Incoherent NAA2007 (Node 417) B-18
Figure B-24 Low on SCV Response Spectra – X Direction – SSI Coherent, SSI Incoherent NAA2005-2006, SSI Incoherent NAA2007 (Node 406)..... B-18
Figure B-25 Low on SCV Response Spectra – Y Direction – SSI Coherent, SSI Incoherent NAA2005-2006, SSI Incoherent NAA2007 (Node 406)..... B-19
Figure B-26 Low on SCV Response Spectra – Z Direction – SSI Coherent, SSI Incoherent NAA2005-2006, SSI Incoherent NAA2007 (Node 406)..... B-19
Figure B-27 SCV Outrigger Response Spectra – X Direction – SSI Coherent, SSI Incoherent NAA2005-2006, SSI Incoherent NAA2007 (Node 417out)..... B-20
Figure B-28 SCV Outrigger Response Spectra – Y Direction – SSI Coherent, SSI Incoherent NAA2005-2006, SSI Incoherent NAA2007 (Node 417out)..... B-20
Figure B-29 SCV Outrigger Response Spectra – Z Direction – SSI Coherent, SSI Incoherent NAA2005-2006, SSI Incoherent NAA2007 (Node 417out)..... B-21

Figure B-30 Top of CIS Response Spectra – X Direction –SSI Coherent, SSI Incoherent NAA2005-2006, SSI Incoherent NAA2007 (Node 538mc) B-21
Figure B-31 Top of CIS Response Spectra – Y Direction –SSI Coherent, SSI Incoherent NAA2005-2006, SSI Incoherent NAA2007 (Node 538mc) B-22
Figure B-32 Top of CIS Response Spectra – Z Direction –SSI Coherent, SSI Incoherent NAA2005-2006, SSI Incoherent NAA2007 (Node 538) B-22
Figure B-33 Low on CIS Response Spectra – X Direction –SSI Coherent, SSI Incoherent NAA2005-2006, SSI Incoherent NAA2007 (Node 535mc) B-23
Figure B-34 Low on CIS Response Spectra – Y Direction –SSI Coherent, SSI Incoherent NAA2005-2006, SSI Incoherent NAA2007 (Node 535mc) B-23
Figure B-35 Low on CIS Response Spectra – Z Direction –SSI Coherent, SSI Incoherent NAA2005-2006, SSI Incoherent NAA2007 (Node 535) B-24
Figure B-36 CIS Outrigger Response Spectra – X Direction – SSI Coherent, SSI Incoherent NAA2005-2006, SSI Incoherent NAA2007 (Node 538out) B-24
Figure B-37 CIS Outrigger Response Spectra – Y Direction – SSI Coherent, SSI Incoherent NAA2005-2006, SSI Incoherent NAA2007 (Node 538out) B-25
Figure B-38 CIS Outrigger Response Spectra – Z Direction – SSI Coherent, SSI Incoherent NAA2005-2006, SSI Incoherent NAA2007 (Node 538out) B-25
Figure C-1 Effects of Smoothing on the ITF Computed at Node 118, Y-Dof and Z-Shaking C-9
Figure C-2 Node 229 ITF Rosette at 20 Hz C-10
Figure C-3 Effect of ITF Phase Adjustment C-10
Figure C-4 Phase Adjustment Effect for Node 145Y for X-Shaking – Comparative ISRS Results C-11
Figure C-5 Phase Adjustment Effect for Node 145Y for Z-Shaking – Comparative ISRS Results C-12
Figure C-6 Base-Center ITF Under Horizontal Shaking Using SASSI-AS and Simulation Mean C-13
Figure C-7 Base-Center ITF Under Vertical Shaking Using SASSI-AS and Simulation Mean C-13
Figure C-8 Top-Edge ITF Under Vertical Shaking Using SASSI-AS and Simulation Mean.... C-14

LIST OF TABLES

Table 2-1 Coherency Function Coefficients 2-1
Table 2-2 Layers and Properties for the Rock Site (EQ Strain) 2-5
Table 2-3 Nodes and Mass Properties for Structural Model 2-10
Table 2-4 Element Properties for Structural Model 2-12
Table 3-1 Procedure to Evaluate Incoherency Transfer Function 3-6
Table 3-2 Procedure to Evaluate the Foundation and Structure Incoherent Response Spectra by CLASSIinco 3-8
Table 3-3 Procedure to Evaluate the Foundation and Structure Incoherent Response Spectra by CLASSIinco-SRSS 3-9
Table 6-1 Frequencies Used in CLASSI, CLASSIinco, and CLASSIinco-SRSS Analyses 6-5
Table 6-2 Frequencies Used in SASSI Simulation and SASSI-AS Analyses 6-11

1
INTRODUCTION AND BACKGROUND

Task S2.1 of the New Plant Seismic Issues Resolution Program is a multi-phase research project to assess the effects of seismic wave incoherence on the response of foundations and structures similar to those being considered for advanced reactor designs. The initial phases of this task focused on the objective of systematically studying seismic wave incoherence effects on structures/foundations. These phases were documented in *Program on Technology Innovation: Effect of Seismic Wave Incoherence on Foundation and Building Response* (Short et al., 2006). Results of these initial phases are summarized later in this chapter.

The final phase of Task S2.1 is presented in Chapters 3-7 of this report. This phase entails the validation of analytical methods and their implementation in the soil-structure interaction (SSI) computer programs CLASSI and SASSI. The objective of this final phase is to complete the validation which demonstrates that CLASSI and SASSI adequately calculate the seismic response of foundations and structures when subjected to seismic wave fields including incoherence effects. In addition, guidelines on the appropriate application of both CLASSI and SASSI to accurately reflect the seismic response incorporating incoherency effects are developed and presented.

Background on Seismic Wave Incoherence

Seismic wave incoherence consists of spatial variation of both horizontal and vertical ground motion. Two sources of incoherence or horizontal spatial variation of ground motion are:

- Local wave scattering: Spatial variation from scattering of waves due to the heterogeneous nature of the soil or rock along the propagation paths of the incident wave fields.
- Wave passage effects: Systematic spatial variation due to difference in arrival times of seismic waves across a foundation due to inclined waves.

The focus of all phases of Task S2.1 is on local wave scattering

The effect of seismic wave incoherence is that motions recorded on foundations of structures differ from those measured in the adjacent free-field. Generally, the motion measured on the foundation is less than the motion recorded in the free-field, especially at high-frequencies. Two aspects of soil-structure interaction contribute to the observations of foundation motion being less than the free-field: kinematic and inertial interaction. Kinematic interaction is due to the spatial variation of the free-field ground motion over the portion of the foundation/structure system abutting the soil or rock. For nuclear power plant structures, which have large and stiff foundation mats, the amplitudes of high-frequency seismic response of the foundation mat are expected to be significantly less than those in the free-field due to horizontal spatial variation of ground motion including incoherence.

The phenomenon of seismic wave incoherence has been recognized for many years, but the lack of an adequately large set of recorded data prevented quantification of the phenomenon and the development of approaches for the incorporation of the effect into the dynamic analysis of NPP structures. Dr. Norm Abrahamson has developed state-of-the-art representations of the coherency functions based on the most applicable data available (Abrahamson, 2005, 2006, 2007). These coherency functions are based on a large number of densely spaced ground motion recordings. Coherency functions define the relationships between ground motion at separate locations as a function of the separation distance between the locations and the frequency of the ground motion. Coherency of motion decreases significantly with increasing frequency and increasing distance between points of interest. The coherency functions (Abrahamson, 2005, 2006, 2007) account for this effect of incoherence at all frequencies of interest and all discretized points on the foundation. For the purposes of this research study on the effects to foundations and structures to coherent/incoherent response, the original coherency function developed by Dr. Abrahamson (Abrahamson 2006) for soil sites has been utilized. This soil coherency model contains less coherency (more reduction from the coherent response) than the currently being developed rock site coherency model and was judged to be appropriate for benchmarking methods of calculating structural response to incoherent ground motion.

Summary – Effect of Seismic Wave Incoherence on Foundation and Building Response (Short et al., 2006)

The initial phases of the Task S2.1 focused on evaluating seismic response for rigid, massless foundations and for example structural models on rigid foundation mats. CLASSI was the primary soil-structure interaction analysis program used for assessing seismic response including seismic wave incoherence. By the CLASSI methodology, the basic relationship between motion in the free-field and motion on the rigid massless foundation is developed based on random vibration theory. Basic inputs to incoherent SSI analyses are the coherency functions developed by Dr. Abrahamson (Abrahamson, 2005, 2006, 2007). As stated above, the coherency functions of Abrahamson (2005, 2006) were used in the initial phases and in this final phase of Task S2.1. Earlier vintage coherency functions by Luco and Wong (1986) are also employed in this final phase for comparisons of calculated response with that from published literature.

Seismic response of example structures considering seismic wave incoherence was calculated using the CLASSI family of SSI analysis programs. An important observation from these seismic analyses was that incoherence produced reduction in translational response but also induced rotational response. In general, each component of horizontal ground motion induces a horizontal translation and a companion torsional component. The vertical component of ground motion induces a vertical translation of the foundation and companion rocking components about the horizontal axes.

The CLASSI approach for seismic wave incoherence analysis was initially validated during the study by an independent comparison with different methodology and software. The random vibration approach used with CLASSI produced excellent agreement with an eigenfunction decomposition approach used with SASSI for a limited subset of analysis conditions, i.e., locations with in the structures where the effect of induced rotations on the foundation are minimal. Note that in SASSI analyses, the rigid basemat is simulated by very stiff material properties. Response is checked to verify that rigid foundation response is achieved. Expanding the validation of CLASSI and SASSI to more complex situations is the subject of the current phase of Task S2.1.

The conclusions of the initial phases of Task S2.1, which are directly relevant to this phase, are:

- Soil-structure interaction (SSI) analysis is important to calculating seismic response to structures mounted on rock sites and subjected to high-frequency ground motion. SSI produces significant reductions in high-frequency response for these conditions.
- Consideration of incoherence is important for the proper evaluation of the response of large base mat structures to high-frequency ground motions (primarily greater than 10 Hz). Realistically accounting for ground motion incoherence on the seismic response of nuclear power plant structures is significant and should be properly incorporated into seismic design analyses.
- The effects of incoherence are three-dimensional. Induced torsion couples horizontal response in the two horizontal directions. Induced rocking couples horizontal and vertical response, i.e., incoherent vertical ground motion induces horizontal response in the structure. Incoherency-induced rocking and torsion are shown to be important to in-structure response depending on the structure and its dynamic characteristics.

Scope of Current Research Effort

The scope of the final phase of Task S2.1 is to further validate the analytical methods and their implementation in the SSI computer programs CLASSI and SASSI. The objective is to demonstrate that both CLASSI and SASSI adequately calculate the seismic response of foundations and structures when subjected to seismic wave fields including incoherence effects. Theoretical aspects of the approaches are expanded beyond those presented by Short et al. (2006). Validation of the individual methodologies includes theoretical (e.g. randomness in modes and phasing) and practical (e.g. number of spatial modes selected within SASSI for computational efficiency) aspects. Guidelines on their application are developed and presented as a part of this report.

Validation of CLASSI and SASSI to treat seismic wave incoherence in SSI analyses is accomplished by:

- Comparison of results computed using CLASSI and SASSI to those available from published literature.
- Comparison of CLASSI computed incoherent seismic response with SASSI computed incoherent seismic response for an example rock/structure model.

As mentioned above, CLASSI and SASSI computed incoherent seismic response were compared and showed to be in good agreement by Short et al. (2006). However, the example soil/structure model considered in those benchmark analyses did not produce significant incoherency-induced torsion and rocking response. The example soil/structure model used for benchmark comparisons in this final phase has offsets of mass centers from the shear centers and significant “outriggers” (nodes extended from the mass center to simulate the response at the perimeter of the building) to overemphasize seismic response from incoherency-induced rotations. It is judged that the example soil/structure model utilized in this phase provide an extreme (conservative) level of torsion and rocking response induced by seismic wave incoherence that validates the use of either CLASSI or SASSI for seismic analysis.

Incoherency induced rotations are a random phenomena resulting from the horizontal spatial variation of ground motion over the foundation area. For response quantities where several components of foundation motion contribute significantly, the phasing of those components must be adequately represented in order to produce reasonable seismic response. As a result, enhancements to the CLASSI and SASSI approaches as described by Short et al. (2006) were required to capture the random nature of multi-component seismic response. These enhancements have led to the review and recognition of two CLASSI methods and three SASSI methods for evaluating seismic response including seismic wave incoherence. These approaches include:

- CLASSIinco – deterministic phasing of foundation component response
- CLASSIinco-SRSS – SRSS combination of structural response computed from random phasing of foundation component response
- SASSI-SRSS – SRSS combination of modal transfer functions to represent random phasing of spatial modes
- SASSI Simulation Mean – Monte Carlo simulations to represent random phasing of spatial modes
- SASSI-AS – Algebraic summation of spatial modes with assumed deterministic phasing

Comparisons of seismic response by all of these methods are presented in this report for the example structure with mass offsets and outriggers that exaggerates incoherency induced rotations. The results from these comparison studies form the basis for the validation of CLASSI and SASSI to treat seismic wave incoherence in SSI analyses of nuclear power plant structures.

Contents of the Report

Chapter 2 defines the input parameters for this study: ground motion coherency functions, rock site conditions and the corresponding free-field ground motions, and structure/foundation parameters for the seismic analyses performed. Chapter 3 presents the derivation of the CLASSI/random vibration approach, including enhancements from the approach reported by Short et al. (2006). Chapter 4 presents the SASSI technical approach. This entails the decomposition of the ground motion coherency matrix into its eigen-system termed spatial modes and calculation of foundation/structure response. Three approaches to treating the spatial modes are highlighted: randomization, square-root-of-the-sum-of the squares (SRSS), and algebraic combination. Chapter 5 presents comparisons of foundation and in-structure responses calculated by the various methodologies described within Chapters 3 and 4. Chapter 6 summarizes guidelines for the application of CLASSI and SASSI as a function of physical and calculational characteristics. Chapter 7 presents a summary of the results, conclusions and recommendations from this research study. Chapter 8 documents the references and Appendix A contains CLASSI/SASSI response data for individual earthquake input directions. Appendix B contains in-structure response spectra comparing the effect of the ground motion coherency function for soil with that for rock for the example advanced reactor model. Appendix C contains descriptions of the SASSI-Simulation and SASSI-AS approaches authored by Ghiocel. A description of the SASSI-SRSS approach and guidelines on its use authored by Ostadan and Deng (2007) is under a separate cover.

2
STUDY INPUT PARAMETERS

Coherency Function

For this phase of Task S2.1, the Abrahamson plane wave (i.e., no wave passage effects) coherency functions (2005, 2006) were used. Coherency functions describe the relationship between ground motion at separate locations as a function of the separation distance and the frequency of the ground motion. The coherency functions take the following form:

$$\gamma_{PW} = \left[1+\left(\frac{f\,Tanh(a_3\xi)}{a_1 f_c}\right)^{n1}\right]^{-1/2}\left[1+\left(\frac{f\,Tanh(a_3\xi)}{a_2 f_c}\right)^{n2}\right]^{-1/2}$$ **Equation 2-1**

Where γ_{PW} is the plane wave coherency representing random horizontal spatial variation of ground motion. The parameter f is ground motion frequency and ξ is the separation distance between locations in meters. Coefficients to be used in Equation 2-1 for horizontal and vertical ground motion are presented in Table 2-1.

Table 2-1
Coherency Function Coefficients

Coefficient	Horizontal Ground Motion	Vertical Ground Motion
a_1	1.647	3.15
a_2	1.01	1.0
a_3	0.4	0.4
n_1	7.02	4.95
n_2	5.1-0.51ln(ξ+10)	1.685
f_c	-1.886+2.221ln(4000/(ξ+1)+1.5)	Exp(2.43-0.025 ln(ξ+1)-0.048 (ln(ξ+1))^2)

The coherency function is plotted as a function of frequency for a number of separation distances in Figures 2-1 and 2-2 for horizontal and vertical ground motion, respectively. These figures show plane wave coherency (random spatial variation of ground motion) per Equation 2-1.

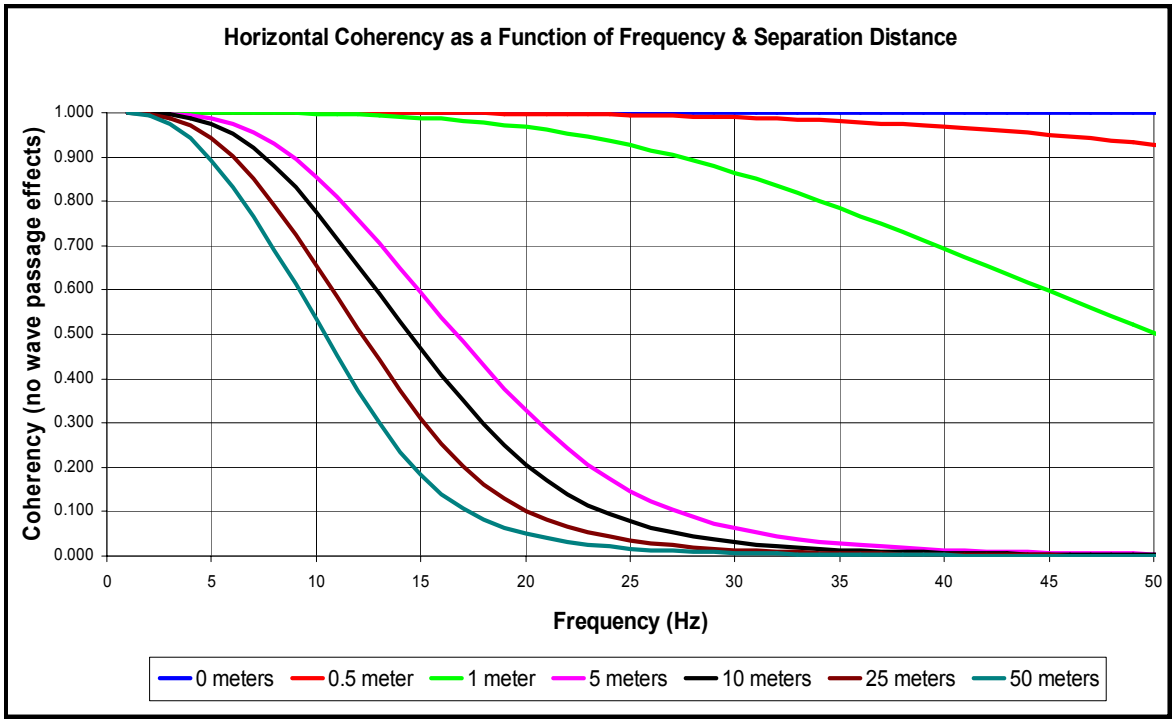

Figure 2-1
Coherency Function for Horizontal Ground Motion

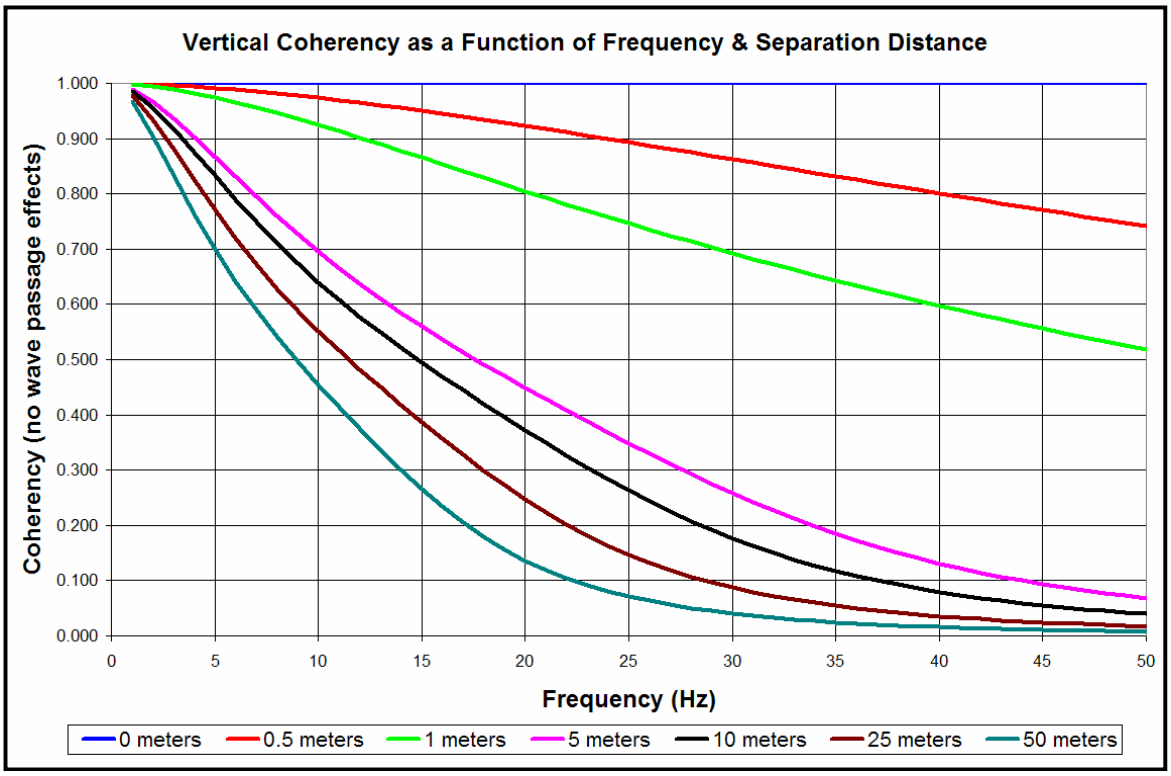

Figure 2-2
Coherency Function for Vertical Ground Motion

The coherency functions presented above have been developed from all available and applicable recorded ground motion from dense instrument arrays. Data are from a variety of site conditions and earthquake magnitudes. In the development of these functions, Dr. Abrahamson has reached the following conclusions (Abrahamson, 2005, 2006, 2007):

- Coherency functions are appropriate for all frequencies (including those above 20 Hz). Ground motion data analyzed to develop the coherency functions have frequency content of 20 Hz and less. It is logical that the trends observed should extrapolate to higher frequencies.
- Coherency is strongly affected by topography. Data with strong topographic effects were not included for development of the coherency function.
- Coherency does not vary as a function of earthquake magnitude. This is true for magnitudes of interest that are greater than magnitude 4.5 to 5.0.
- Each component of earthquake input can be treated as uncorrelated. The coherency of cross-components is near zero.
- Coherency varies as a function of site shear wave velocity, especially for "hard rock "sites, i.e., with shear wave velocities greater than about 1,000 m/sec (Abrahamson, 2007). For "hard rock" sites, ground motion coherency is greater than for soil sites for frequencies greater than 10 Hz. The ground motion coherency functions of Equation 2-1 and Table 2-1 are most appropriate for soil sites and surface-founded structures. In spite of this recent development, these ground motion coherency functions are used in the current study to maintain consistency with all previous sensitivity studies and results. In addition, these ground motion coherency functions are likely to produce a more severe test of the validation of the approaches and their implementation since the effect on foundation/structure response will be greater than the impact of the "hard rock" coherency functions on foundation/ structure response. The hard rock coherency function will produce reduced incoherency-induced rotations, which have been the more challenging aspect of the phenomena to achieve agreement between alternative approaches.

For the design of nuclear power plant structures, mean input ground motion is the goal. As a result, the goal is to use mean coherency. The functions of Equation 2-1 and Table 2-1 model median coherency. Median coherency is slightly larger (only a few percent difference) than mean coherency.

Site Parameters and Input Ground Motion

The initial phases of the Task S2.1 (Short et al., 2006) used two representative site profiles; one for soil and one for rock. These site profiles were selected to be representative of sites in the Central and Eastern United States. Site-specific response spectra compatible with each of the sites were developed and used in the initial study. The current phase only considers the rock site. For the rock site profile, shear wave velocities as a function of depth beneath the free-field ground surface are shown in Figure 2-3. The site profile shown in the figure extends down to the Central and Eastern United States (CEUS) generic rock that has shear wave velocity of about 9200 fps (McCann, 2004).

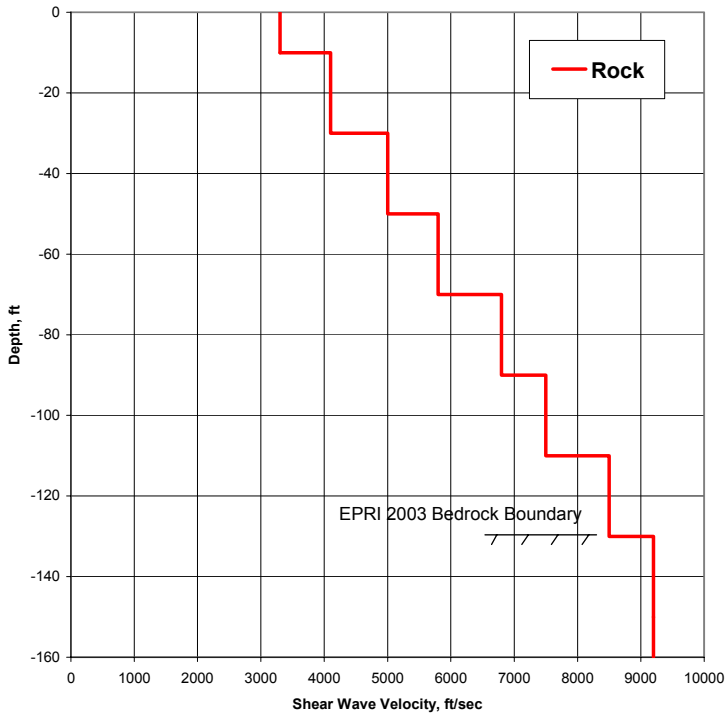

Figure 2-3
Rock Site Profile Shear Wave Velocities vs. Depth

For the foundation areas considered for this incoherence study, it is sufficient to define the site profile to a depth of about 300 feet beneath the foundation. The soil layers and properties shown in Table 2-2 have been used for the evaluation of coherency effects in this study. These properties were taken from information provided within the advanced reactor submittals (North Anna contained on the NRC web site).

For CLASSI modeling purposes, the rock site is represented by nine layers extending to 130-ft below the surface, and underlain by a half-space of bedrock at a shear wave velocity of 9200 fps as shown in Table 2-2. Note that CLASSI layers were originally developed for analyses up to 50 Hz. CLASSI analyses with the layer thicknesses used in SASSI that were developed for analyses up to 100 Hz show no significant differences at any frequency. Rock is assumed to have the low strain shear modulus (shear wave velocity) and no variation of damping at earthquake strain levels (i.e., linear elastic behavior). A damping ratio of 0.02 is assumed, which corresponds to about 0.001% shear strain.

For SASSI modeling purposes, the rock site is represented by thirteen layers extending to 130-ft below the surface, and underlain by a half-space of bedrock at a shear wave velocity of 9200 fps as shown in Table 2-2. In the SASSI model, layers 5, 6, 7, and 8 are all 10 feet thick as opposed to 20 feet thick in the CLASSI model as shown in Table 2-2. The same rock stiffness and damping properties are used for CLASSI and SASSI modeling.

Table 2-2
Layers and Properties for the Rock Site (EQ Strain)

CLASSI Layer	SASSI Layer	Shear Wave Velocity (fps)	Weight Density (pcf)	Poisson's Ratio	Damping (Fraction)	Thickness (ft)	Layer Top Depth (ft)
1	1	3300	160	0.33	0.02	5	0
2	2	3300	160	0.33	0.02	5	5
3	3	4100	160	0.33	0.02	10	10
4	4	4100	160	0.33	0.02	10	20
5	5	5000	160	0.33	0.02	10	30
	6	5000	160	0.33	0.02	10	30
6	7	5800	160	0.33	0.02	10	50
	8	5800	160	0.33	0.02	10	50
7	9	6800	160	0.33	0.02	10	70
	10	6800	160	0.33	0.02	10	70
8	11	7500	160	0.33	0.02	10	90
	12	7500	160	0.33	0.02	10	90
9	13	8500	160	0.33	0.02	20	110
10	14	9200	160	0.33	0.02	Half-space	130

Site-specific ground response spectra appropriate at the free ground surface at Elevation 0 for the rock site profile, as shown in Figure 2-3, were used for this coherency study. Five percent damped site-specific response spectra are illustrated in Figure 2-4 for the rock site. Also, plotted on the figure are the U.S. NRC Regulatory Guide 1.60 design ground response spectra anchored to 0.3 g peak ground acceleration (PGA) for comparison purposes. The rock site-specific ground response spectra have peak amplification in the 20 to 30 Hz range.

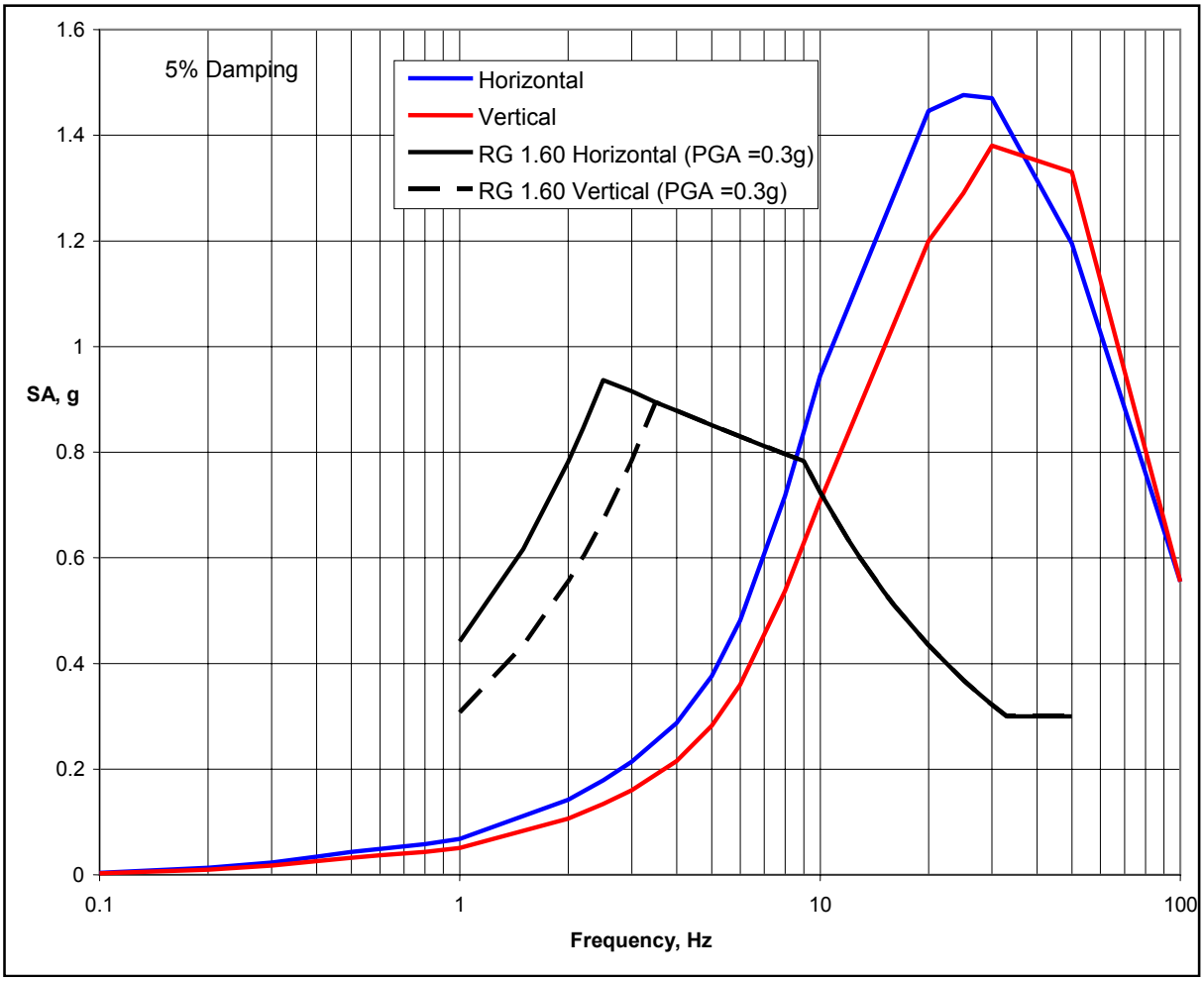

Figure 2-4
Site-Specific Response Spectra for Rock Site at Ground Surface (Depth 0-ft)

For soil-structure interaction analyses and the evaluation of structure response including the effects of seismic wave incoherence, spectrum compatible time histories for the rock site were required. These were developed by Dr. Abrahamson. The computed spectra and the target spectra (Figure 2-4) are shown in Figure 2-5. Three uncorrelated components were generated for two horizontal directions and the vertical direction.

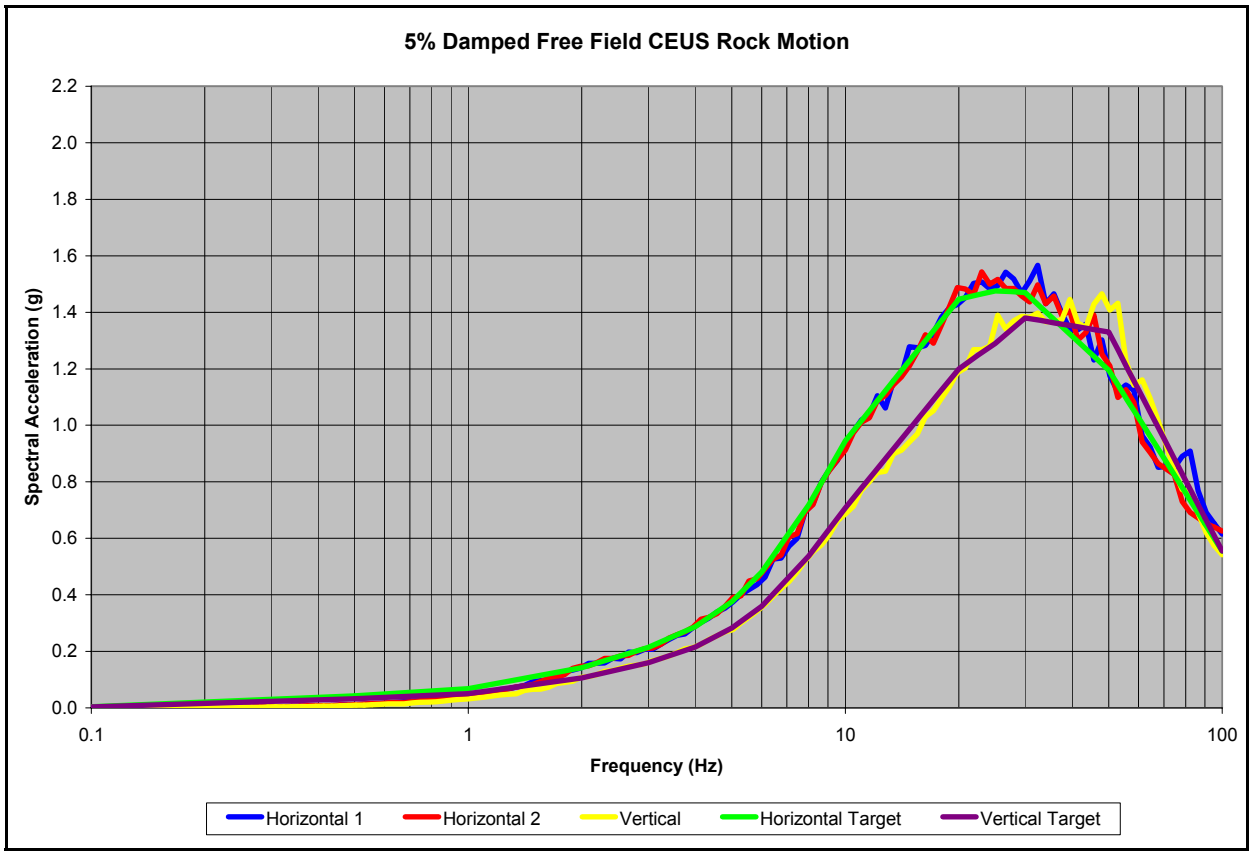

Figure 2-5
Computed and Target Response Spectra for Rock Site

Foundation Parameters

Initially, descriptions of two advanced reactor designs (AP1000 and ESBWR) were reviewed in order to understand the foundation and building configurations. Based on the foundation configurations presented for these two new plant designs, two foundations were studied - a rectangular foundation that is 225 x 100-ft in plan, and a square foundation that is 150 x 150-ft in plan. In addition, for validation purposes, a circular foundation footprint of the same area was considered. The foundation circle had a radius of 84.63 feet.

For the present phase of Task S2.1, the SSI seismic analyses, by CLASSI and SASSI, were performed for the 150-ft square foundation footprint. For these analyses, the foundation was assumed to be 15-ft thick. The resulting diagonal mass matrix terms are 1572 kip-sec2/ft in the horizontal and vertical directions, 2.98 x 106 kip-ft-sec2 about the horizontal axes, and 5.90 x 106 kip-ft-sec2 about the vertical axes.

Structure Properties

Soil-structure interaction seismic analyses for the purpose of evaluating structure and foundation response including the effects of seismic wave incoherence have been performed using a stick model with three concentric sticks representing the Coupled Auxiliary and Shield Building (ASB), the Steel Containment Vessel (SCV), and the Containment Internal Structure (CIS). The original model (Orr, 2003) was modified to enable the appropriate effects of incoherence induced rotations. This model is illustrated in Figure 2-6 with model properties presented in Tables 2-3 and 2-4. Modifications to the original model include:

- At the top of the shield building, auxiliary building, steel containment vessel, and containment internal structure massless outrigger nodes have been added connected to the centerline by rigid links. The ASB and CIS outriggers extend 75 feet from the centerline in the X-direction. The SCV outrigger extends 65 feet from the centerline in the X-direction.
- Mass centers have been offset from the shear center at locations in the auxiliary building and the CIS to introduce natural torsion into the models. The shear centers of the three sticks are coincident along the Z-axis.

For CLASSI SSI seismic analyses, the structure properties input are described by the fixed-base dynamic modal properties including frequencies, mode shapes and participation factors. These dynamic properties were developed using the finite element program, SAP2000 (CSI, 2004). One hundred and sixty (160) modes (maximum frequency of 141 Hz) were included with total mass participation in each direction of about 95 percent. The relative mass of the structures is approximately ASB – 86%, CIS – 11%, and SCV – about 3%.

The fixed-base modes of the three structure sticks provide some insight into their dynamic behavior. Fundamental fixed-base frequencies for each of the three structure concentric sticks are:

- Coupled Auxiliary and Shield Building (ASB)
  - X-Horizontal – 3.2 Hz
  - Y-Horizontal – 3.0 Hz
  - Z-Vertical – 9.9 Hz
- Steel Containment Vessel (SCV)
  - X-Horizontal – 5.5 Hz, 9.5 Hz, 9.9 Hz
  - Y-Horizontal – 6.10 Hz
  - Z-Vertical – 16.0 Hz
- Containment Internal Structure (CIS)
  - X-Horizontal – 13.3 Hz, 20.1 Hz, 28.9 Hz
  - Y-Horizontal – 12.0 Hz, 14.9 Hz, 17.5 Hz
  - Z-Vertical – 41.4 Hz

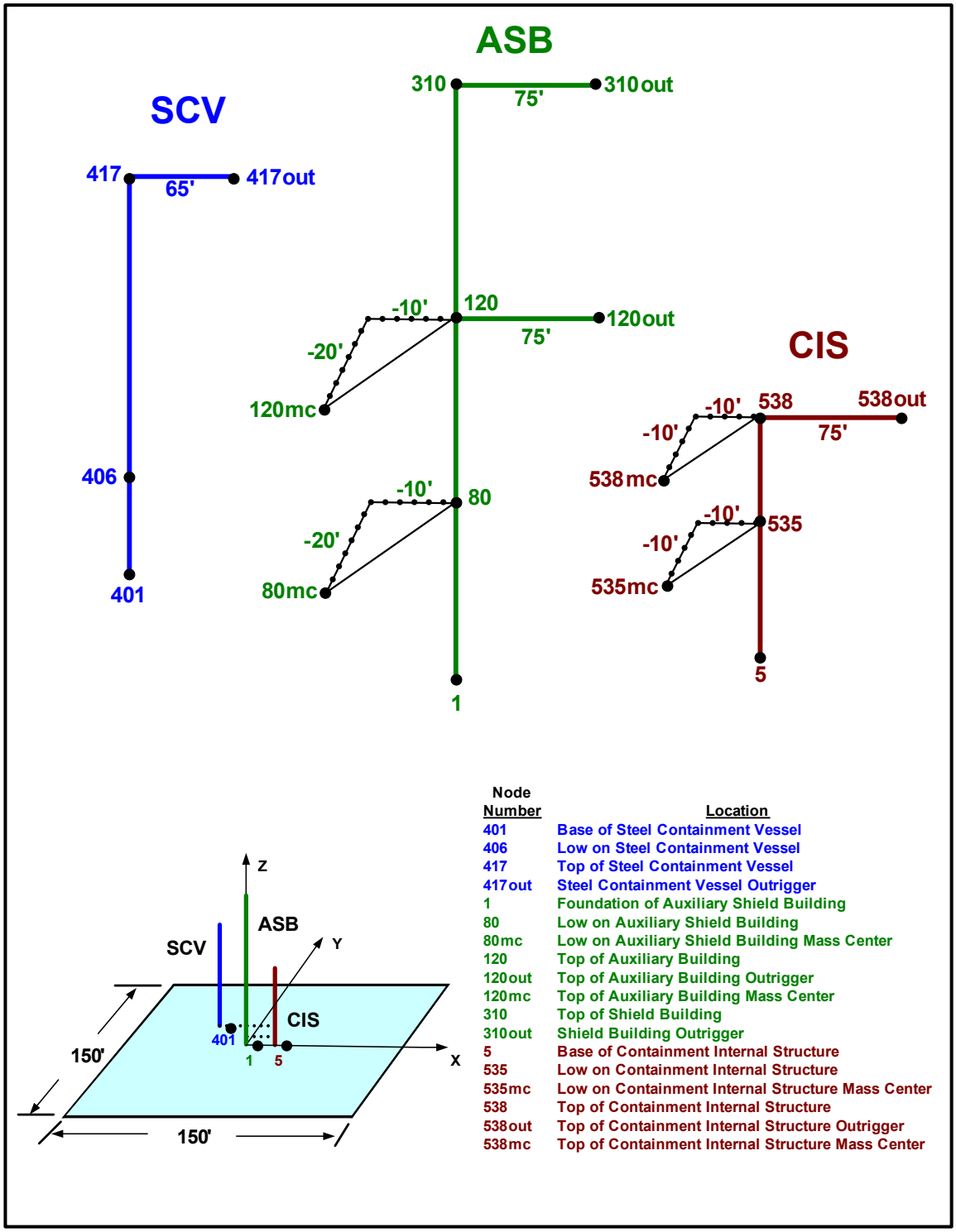

Node Number	Location
401	Base of Steel Containment Vessel
406	Low on Steel Containment Vessel
417	Top of Steel Containment Vessel
417out	Steel Containment Vessel Outrigger
1	Foundation of Auxiliary Shield Building
80	Low on Auxiliary Shield Building
80mc	Low on Auxiliary Shield Building Mass Center
120	Top of Auxiliary Building
120out	Top of Auxiliary Building Outrigger
120mc	Top of Auxiliary Building Mass Center
310	Top of Shield Building
310out	Shield Building Outrigger
5	Base of Containment Internal Structure
535	Low on Containment Internal Structure
535mc	Low on Containment Internal Structure Mass Center
538	Top of Containment Internal Structure
538out	Top of Containment Internal Structure Outrigger
538mc	Top of Containment Internal Structure Mass Center

Figure 2-6
Advanced Reactor Structure Stick Model With Outriggers and Offset Mass Centers

Table 2-3
Nodes and Mass Properties for Structural Model

				North-South Model			East-West Model		
NODE	**X**	**Y**	**Z**	**MX**	**MZ**	**Iy**	**MY**	**MZ**	**Ix**
ASB									
1	0	0	60.50						
11	0	0	66.50	236.400	236.400	1641500	236.400	236.400	466740
21	0	0	81.50	494.260	494.260	3612000	494.260	494.260	847820
31	0	0	91.50	307.080	439.280	1938300	307.080	439.280	456250
41	0	0	99.00	330.460	330.460	2619900	330.460	330.460	484190
51	0	0	106.17	210.100	210.100	1287500	210.100	210.100	390700
61	0	0	116.50	597.740	465.540	2526200	597.740	465.540	764330
80	0	0	134.87	0	441.849	3448492	0	441.849	710952
80mc	-10	-20	134.87	441.849	0	0	441.849	0	0
90	0	0	145.37	165.406	165.406	933560	165.406	165.406	293100
100	0	0	153.98	190.099	190.099	1022510	190.099	190.099	316650
110	0	0	164.51	164.371	164.371	422680	164.371	164.371	271344
120	0	0	179.56	0	200.431	323582	0	200.431	349825
120out	75	0	179.56	0	0	0	0	0	0
120mc	-10	-20	179.56	200.431	0.00	0.00	200.431	0.00	0.00
130	0	0	200.00	126.050	126.050	317710	126.050	126.050	317710
140	0	0	220.00	132.470	132.470	333900	132.470	132.470	333900
150	0	0	242.50	140.260	140.260	353540	140.260	140.260	353540
160	0	0	265.00	231.223	231.223	529020	231.223	231.223	529020
309	0	0	295.23	263.980	433.530	276470	263.980	433.530	276470
310	0	0	333.13	135.590	91.320	63050	135.590	91.320	63050
310out	75	0	333.13	0	0	0	0	0	0
320	0	0	296.77	0.000	0.000	0	0.000	0.000	0

Table 2-3
Nodes and Mass Properties for Structural Model (Continued)

				North-South Model			East-West Model		
NODE	**X**	**Y**	**Z**	**MX**	**MZ**	**Iy**	**MY**	**MZ**	**Ix**
CIS									
5	0	0	60.5						
500	0	0	66.5	595.3	593.4	568000	595.3	595.3	568000
531	0	0	82.5	927.6	927.6	1422000	927.6	927.6	137100
532	0	0	98	468.7	468.7	70800	468.7	468.7	680000
533	0	0	103	146.3	286.2	185000	146.3	286.2	177000
534	0	0	107.17	319.1	238.7	358900	319.1	238.7	319130
535	0	0	134.25	0	238.6	282150	0	238.6	255550
535mc	-10	-10	134.25	298.2	0	0	298.2	0	0
536	0	0	153	14.6	14.6	2019	14.6	14.6	2504
537	0	0	153	30.8	30.8	6065	30.8	30.8	4321
538	0	0	169	0	9.4	748	0	9.4	696
538out	75	0	169	0	0	0	0	0	0
538mc	-10	-10	169	9.4	0	0	9.4	0	0

				North-South Model			East-West Model		
NODE	**X**	**Y**	**Z**	**MX**	**MZ**	**Iy**	**MY**	**MZ**	**Ix**
SCV									
401	0	0	100.000	1.739	1.739	3636	1.739	1.739	3636
402	0	0	104.125	5.541	5.541	11732	5.541	5.541	11732
403	0	0	110.500						
404	0	0	112.500	15.388	15.388	33362	15.388	15.388	33362
406	0	0	131.677	17.907	17.907	37914	17.907	17.907	37914
407	0	0	138.583						
408	0	0	141.500	17.904	17.904	38689	17.904	17.904	38689
409	0	0	162.000	18.349	18.349	38850	18.349	18.349	38850
410	0	0	169.927	28.994	28.994	61388	28.994	28.994	61388
411	0	0	200.000	28.340	28.340	60003	28.340	28.340	60003
412	0	0	224.000	40.251	51.739	81602	51.522	51.739	81602
413	0	0	224.208	15.746	15.746	33338	15.746	15.746	33338
414	0	0	255.021	11.271	11.271	21897	11.271	11.271	21897
415	0	0	265.833	10.288	10.288	14610	10.288	10.288	14610
416	0	0	273.833	10.070	10.070	8149	10.070	10.070	8149
417	0	0	281.901	5.618	5.618	0	5.618	5.618	0
417out	65	0	281.901	0	0	0	0	0	0
425	0	0	224.000	28.439	16.951		17.168	16.951	

Note: All values are in kip, seconds, feet units.
Assume: **Iz = Ix + Iy.**

Table 2-4
Element Properties for Structural Model

		North-South Model				East-West Model				
ELEM	**NODES**		**A**	**IYY**	**AshearY**	**A**	**IZZ**	**AshearZ**	**Material**	**Modal Damping**
ASB										
1	1	11	15484.00	97176000	10322.67	15484.00	11236800	10322.67	Concrete	4 %
2	11	21	3462.50	6266240	1366.35	3462.50	4061440	1011.30	Concrete	4 %
3	21	31	3462.50	6266240	1366.35	3462.50	4061440	1011.30	Concrete	4 %
4	31	41	3462.50	6266240	1366.35	3462.50	4061440	1011.30	Concrete	4 %
5	41	51	3293.30	5744880	1214.35	3293.30	3562800	1008.14	Concrete	4 %
6	51	61	3293.30	5744880	1214.35	3293.30	3562800	1008.14	Concrete	4 %
7	61	80	3293.30	5744880	1214.35	3293.30	3562800	1008.14	Concrete	4 %
	80	80mc	Rigid Link							
31	80	90	3197.52	4196560	1185.61	3197.52	4412370	1360.04	Concrete	4 %
32	90	100	3197.52	4196560	1185.61	3197.52	4412370	1360.04	Concrete	4 %
33	100	110	2501.52	3676560	874.54	2501.52	3311570	1121.07	Concrete	4 %
34	110	120	1954.00	3083632	810.51	1954.00	3290960	746.70	Concrete	4 %
	120	120out	Rigid Link							
	120	120mc	Rigid Link							
35	120	130	1338.00	2700000	535.20	1338.00	2700000	535.20	Concrete	4 %
36	130	140	1338.00	2700000	535.20	1338.00	2700000	535.20	Concrete	4 %
37	140	150	1338.00	2700000	535.20	1338.00	2700000	535.20	Concrete	4 %
38	150	160	1338.00	2700000	535.20	1338.00	2700000	535.20	Concrete	4 %
301	160	309	50.45	1	0.000	50.45	1	0.000	Concrete	4 %
302	320	309	13.59	2680	10.872	13.59	2681.6	10.872	Concrete	4 %
303	309	310	704.50	431720	281.800	704.50	431720	281.800	Concrete	4 %
	310	310out	Rigid Link							
	160	320	Rigid	Rigid	Rigid	Rigid	Rigid	Rigid		

Table 2-4
Element Properties for Structural Model (Continued)

			North-South Model			East-West Model				
ELEM	**NODES**		**A**	**IYY**	**AshearY**	**A**	**IZZ**	**AshearZ**	**Material**	**Modal Damping**
CIS										
500	5	500	15175	1.24E+07	9228.29	15175	1.11E+07	8311.88	Concrete	4 %
501	500	531	15175	1.24E+07	9228.29	15175	1.11E+07	8311.88	Concrete	4 %
502	531	532	6732	4.50E+06	2976.99	6732	3.33E+-6	2965.86	Concrete	4 %
503	532	533	7944	6.74E+06	4411.70	7944	5.95E+06	3948.04	Concrete	4 %
504	533	534	5160	4.60E+06	3026.91	5160	2.93E+06	2702.19	Concrete	4 %
505	534	535	1705	7.83E+05	613.65	1705	5.75E+05	405.33	Concrete	4 %
	535	535mc	Rigid Link							
506	535	536	326	3.15E+03	13.10	326	1.77E+04	67.36	Concrete	4 %
507	535	537	484	3.89E+04	93.98	484	1.58E+04	64.30	Concrete	4 %
508	537	538	164	2.11E+03	29.24	164	2.47E+03	17.16	Concrete	4 %
	538	538out	Rigid Link							
	538	538mc	Rigid Link							
506	535	536	326	3.15E+03	13.10	326	1.77E+04	67.36	Concrete	4 %
507	535	537	484	3.89E+04	93.98	484	1.58E+04	64.30	Concrete	4 %
508	537	538	164	2.11E+03	29.24	164	2.47E+03	17.16	Concrete	4 %

Table 2-4
Element Properties for Structural Model (Continued)

			North-South Model			East-West Model				
ELEM	**NODES**		**A**	**IYY**	**AshearY**	**A**	**IZZ**	**AshearZ**	**Material**	**Modal Damping**
SCV										
401	401	402	14.49	29,107	27.6	14.49	29,107	27.6	Steel	4 %
402	402	403	59.63	126,243	29.81	59.63	126,243	29.81	Steel	4 %
403	403	404	59.63	126,243	29.81	59.63	126,243	29.81	Steel	4 %
405	404	406	59.63	126,243	29.81	59.63	126,243	29.81	Steel	4 %
406	406	407	59.63	126,243	29.81	59.63	126,243	29.81	Steel	4 %
407	407	408	59.63	126,243	29.81	59.63	126,243	29.81	Steel	4 %
408	408	409	59.63	126,243	29.81	59.63	126,243	29.81	Steel	4 %
409	409	410	59.63	126,243	29.81	59.63	126,243	29.81	Steel	4 %
410	410	411	59.63	126,243	29.81	59.63	126,243	29.81	Steel	4 %
411	411	412	59.63	126,243	29.81	59.63	126,243	29.81	Steel	4 %
412	412	413	59.63	126,243	29.81	59.63	126,243	29.81	Steel	4 %
413	413	414	13.15	110,115	27.1	13.15	110,115	27.1	Steel	4 %
414	414	415	4.58	83,714	24.6	4.58	83,714	24.6	Steel	4 %
415	415	416	1.74	46,047	19.89	1.74	46,047	19.89	Steel	4 %
416	416	417	0.55	13,850	8.56	0.55	13,850	8.56	Steel	4 %
	417	417out	Rigid Link							
	Spring		Kz	Kx		Kz	Ky			
	412	425	27630	80439		27630	9467			4 %

Notes:

All values are in kip, seconds, feet units

Material properties:

Concrete:

Elastic modulus = 519,120 ksf
Poisson's ratio = 0.17

Steel:
Elastic modulus = 4,248,000 ksf
Poisson's ratio = 0.30

3
CLASSI TECHNICAL APPROACH

General

In order to incorporate seismic wave incoherence into seismic analyses, a stochastic approach has been employed as described in this chapter. This approach is described in detail by Tseng and Lilhanand (1997) and briefly summarized in this chapter. By this approach, incoherency transfer functions have been developed for the rigid massless foundation and validated by comparison with published literature. As described in Chapter 2, coherency functions as a function of separation distance, frequency, apparent wave velocity, and direction of motion from Abrahamson (2005, 2006) are used as the basic input for all evaluations. The incoherency transfer functions have been generated for the rigid, massless foundation using the computer program, CLASSI. In addition, CLASSI has been used to evaluate seismic structural response of example rock/structure systems. The procedures used to evaluate incoherency transfer functions, to evaluate foundation response of rigid, massless foundations, and to evaluate structure and foundation response of example structural models accounting for soil-structure interaction and seismic wave incoherence are described in this Chapter. Following the description, validation of the approach in CLASSI is presented through benchmarking of the response of the rigid, massless foundation, i.e., the incoherency transfer functions (ITFs), for circular and square foundations by comparison with published literature.

Incorporation of the Coherency Function into CLASSI Procedures

To utilize CLASSI (Wong and Luco, 1980), one must first define the foundation footprint plan dimensions, underlying soil layers with properties of density, shear wave velocity, Poisson's ratio, material damping, and layer thickness, and frequencies for analysis. The foundation footprint is divided into n sub-regions for input to CLASSI. The coherency function is evaluated at the mid-point of each of these sub-regions with the separation distance being the distance between all of the combinations of sub-region mid-points.

Based on the assumption that ground motions can be represented by a stationary random process, the coherency function between ground motions $x_i(t)$ and $x_j(t)$, denoted by $\gamma(f)$, is a complex function of frequency, f, defined by:

$$\gamma(f) = \frac{S_{ij}(f)}{\sqrt{S_{ii}(f) S_{jj}(f)}} \qquad \textbf{Equation 3-1}$$

in which S_{ij} is the cross power spectral density function between motions $x_i(t)$ and $x_j(t)$ and S_{ii} and S_{jj} are the power spectral density functions for motions $x_i(t)$ and $x_j(t)$ in the same orthogonal direction, respectively.

The matrix [γ] is evaluated as a 3n by 3n matrix of the Abrahamson coherency function based on the separation distances between sub-regions for each selected frequency and for input apparent wave velocity or slowness. It should be noted that the motions in each orthogonal direction are not correlated with each other, thus the cross terms involving xy (yx), xz (zx), or yz (zy) motions of the coherency matrix [γ] are taken as zero.

Since the coherency function is defined in terms of power spectral density functions it is necessary to consider the CLASSI procedures reformulated into a random vibration analysis approach.

General CLASSI Approach: Rigid Massless Foundation

Let the modification of the free-field surface motion due to the presence of the rigid surface inclusion be represented by six component vector $\{U_0\}$. The average free-field surface motion of each of n sub-regions that represents the interface of the rigid foundation area with the half-space surface is represented by the 3n component vector $\{U_n\}$. The motion of a reference point of the rigid inclusion $\{U_0\}$ in terms of the set of sub-region motions $\{U_n\}$is related by the 6 x 3n scattering transfer function [F]:

$$\{U_0\} = [F]\{U_n\}$$ **Equation 3-2**

It may be noted that the 3n x6 rigid body transformation array $[\alpha_b]$ is defined by:

$$\{U_n\} = [\alpha_b]\{U_0\}$$ **Equation 3-3**

The matrix $[\alpha_b]$ is only a function of the foundation footprint geometry and the location of the n sub-regions and not of the properties of soil layers. As a result, comparison of Equations 3-2 and 3-3 shows that [F] must be independent of the soil conditions.

Using the CLASSI methodology, [F] is determined by:

$$[F] = [C]\,[T]^T$$ **Equation 3-4**

where [C] is the 6 by 6 compliance matrix (equal to the inverse of the impedance matrix $[K]^{-1}$); and [T] is a 3n by 6 traction matrix representing contact tractions on all n sub-regions subjected to unit rigid body motions.

$$[T]= [G]^{-1}\,[\alpha_b]$$ **Equation 3-5**

[G] is the 3n by 3n Green's function matrix containing displacement responses to unit harmonic loads on the surface of the soil/rock supporting the foundation and at each of the sub-regions and $[\alpha_b]$ is a 3n by 6 rigid body transformation matrix. One of the program modules to CLASSI uses soil profile properties to determine the Green's function.

The 6 x 6 impedance matrix [K] relates the driving forces applied to the rigid inclusion, $\{P_0\}$ to the displacements of the rigid inclusion, $\{U_0\}$ by:

$$\{P_0\} = [K]\{U_0\}$$ **Equation 3-6**

The impedance matrix may also be expressed in terms of the 3n x 3n array [G] of Green's functions integrated over each sub-region, and the 3n x6 rigid body transformation array $[\alpha_b]$ by:

$$[K] = [\alpha_b]^T[G]^{-1}[\alpha_b] \qquad \textbf{Equation 3-7}$$

Combining Equations 3-3, 3-6, and 3-7, it may be noted that $\{P_0\} = [\alpha_b]^T[G]^{-1}[\alpha_b]]\{U_0\} = [\alpha_b]^T[G]^{-1}\{U_n\}$. The array $[G]^{-1}[\alpha_b]$ may be identified as the 3n x 6 traction array [T] from Equation 3-5. Transposing Equation 3-5 gives $[T]^T = [\alpha_b]^T[G]^{-1}$. As a result:

$$\{P_0\} = [T]^T\{U_n\} \qquad \textbf{Equation 3-8}$$

Equating Equations 3-6 and 3-8 so that $\{P_0\} = [K]\{U_0\} = [T]^T\{U_n\}$, we may write express $\{U_0\}$ in terms of $\{U_n\}$ as:

$$\{U_0\} = [K]^{-1}[T]^T\{U_n\} = [C][T]^T\{U_n\} = [F]\ \{U_n\} \qquad \textbf{Equation 3-9}$$

where $[C] = [K]^{-1}$ is the 6 x 6 compliance array of the rigid, massless foundation reference point. The scattering transfer function, [F] may be identified as $[C][T]^T$ which was stated in Equation 3-4.

From Equation 3-3, $\{U_n\} = [\alpha_b]\{U_0\}$. Multiplying both sides to this equation gives $[\alpha_b]^T\{U_n\} = [\alpha_b]^T[\alpha_b]\{U_0\}$. $\{U_0\}$can then be related to $\{U_n\}$ by $\{U_0\} = ([\alpha_b]^T[\alpha_b])^{-1}[\alpha_b]^T\{U_n\}$ which may be identified as the least squares solution for the average motion of the rigid surface foundation given the over-determined free-field motion of the n sub-regions $\{U_n\}$. Hence, from Equation 3-2, it may be seen that the scattering transfer function [F] is given by:

$$[F] = ([\alpha_b]^T[\alpha_b])^{-1}[\alpha_b]^T \qquad \textbf{Equation 3-10}$$

Equation 3-10 shows that the scattering transfer function is independent of any soil properties, being determined only by the rigid body kinematics of the rigid foundation motion. The use of the identity $[F] = [C][T]^T$ is actually equivalent to the least squares solution, and is a convenient means of computation for the scattering transfer function given the CLASSI computation of [K] and [T] for solution of the SSI problem.

CLASSI Random Vibration Approach: Rigid Massless Foundation

The PSD of the rigid massless foundation considering incoherent input motion is determined using $[S_{UG}]$, a 3n by 3n covariance matrix of actual incoherent ground motions as determined by Equation 3-11.

$$[S_{UG}] = [S_o^{1/2}]\ [\gamma]\ [S_o^{1/2}] \qquad \textbf{Equation 3-11}$$

where $[S_o^{1/2}]$ is a 3n by 3n on-diagonal PSD matrix on the input ground motion and $S_o(f)$ is the power spectral density of the input free-field ground motion.

$[S_{Uo}]$, the 6 by 6 cross PSD of rigid massless foundation motion is determined from:

$$[S_{Uo}] = [F]\,[S_{UG}]\,[FC]^T \qquad \textbf{Equation 3-12}$$

where [F] is taken as the 6 by 3n scattering transfer function matrix relating sub-region displacements to rigid body displacements, along with its complex conjugate [FC], which is determined in the manner described above.

CLASSI is used to evaluate the impedance matrix [K] and the traction matrix [T] at each selected frequency. Normal outputs are impedance and scattering matrices. Also, [T], a Green's function matrix [G], and $[\alpha_b]$ are generated internally by the program. Input is the foundation footprint and the definition of sub-regions along with soil properties. For this study, the foundation footprint was divided into 10-ft square sub-regions. Around the periphery of the foundation, the outside 10-ft was further divided into 5-ft square sub-regions. A sensitivity study was performed on the number of sub-regions and concluded that this discretization was adequate.

CLASSI Random Vibration Approach: Foundation and Structure Response

The 6 by 6 cross PSD of foundation response motion, $[S_{UF}]$ may be determined by pre-multiplying $[S_{Uo}]$, the 6 by 6 cross PSD of rigid massless foundation motion by $[H_F]$ a 6 by 6 transfer function matrix between foundation response and the scattered foundation input motions and post-multiplying by $[H_FC]$, the complex conjugate of $[H_F]$:

$$[S_{UF}] = [H_F]\,[S_{Uo}]\,[H_FC]^T \qquad \textbf{Equation 3-13}$$

The foundation transfer function matrix is given by:

$$[H_F] = ([I]-\omega^2\,[C]\,([M_b] + [M_s(f)]))^{-1} \qquad \textbf{Equation 3-14}$$

In the above equation, [I] is an identity matrix, ω is the frequency of interest in radians per second, [C] is the compliance matrix previously defined, $[M_b]$ is the 6 by 6 diagonal mass matrix containing the foundation mass and mass moment of inertia, and $[M_s(f)]$ is the 6 by 6 equivalent mass matrix of the structure about its base computed by:

$$[M_s] = [\alpha_s]^T\,[M]\,[\alpha_s] + [\Gamma_s]^T\,[D(f)]\,[\Gamma_s] \qquad \textbf{Equation 3-15}$$

where [D(f)] is the k by k diagonal modal amplification matrix (k is the number of fixed-base structure modes) given by:

$$[D] = \left[\frac{(\omega/\omega_r)^2}{\left(1-\frac{\omega^2}{\omega_r^2}\right) + 2i\beta_r(\omega/\omega_r)}\right] \qquad \text{where r goes from 1 to k} \qquad \textbf{Equation 3-16}$$

$[\alpha_s]$ is a q by 6 rigid body transformation matrix of the structure about its base where q is the number of structure dynamic degrees of freedom above its base. $[\alpha_s]$ is given by:

$$[\alpha_s] = \begin{bmatrix} \cdots\cdots & & & & & \\ \cdots\cdots & & & & & \\ 1 & 0 & 0 & 0 & z^j & -y^j \\ 0 & 1 & 0 & -z^j & 0 & x^j \\ 0 & 0 & 1 & y^j & -x^j & 0 \\ 0 & 0 & 0 & 1 & 0 & 0 \\ 0 & 0 & 0 & 0 & 1 & 0 \\ 0 & 0 & 0 & 0 & 0 & 1 \end{bmatrix}$$ **Equation 3-17**

where j goes from 1 to q, the number of structure nodes with coordinates x, y, and z. [Γs] is a k by 6 matrix of modal participation factors given by:

$$[\Gamma_s] = [\phi_s]^T [M] [\alpha_s]$$ **Equation 3-18**

in which $[\phi_s]$ is the q by k fixed-base mode shape matrix of the structure and [M] is the q by q structure mass matrix.

The q by q cross PSD of structural response motion, $[S_{US}]$ is determined by pre-multiplying $[S_{Uo}]$, the 6 by 6 cross PSD of rigid massless foundation motion by $[H_T]$ (a q by 6 transfer function matrix between structural response and the scattered foundation input motions) and post-multiplying by $[H_TC]$, the complex conjugate of $[H_T]$:

$$[S_{Us}] = [H_T] [S_{Uo}] [H_TC]^T$$ **Equation 3-19**

The structure transfer function matrix is given by:

$$[H_T] = ([\alpha_s] + [\phi_s] [D] [\Gamma_s]) [H_F]$$ **Equation 3-20**

where all matrices and terms have been previously defined.

Procedure to Evaluate the Incoherency Transfer Function (ITF)

The diagonal terms of $[S_{Uo}]$, the 6 by 6 cross PSD of rigid massless foundation motion, given by Equation 3-12, provide the spectral density functions for the constrained rigid body motion of the reference point of the rigid massless foundation. If these terms are normalized by the respective free-field functions (two horizontal and torsion terms normalized by the horizontal free-field PSD; vertical and two rocking terms normalized by the vertical free-field PSD), then the square root of these normalized terms may be interpreted as transfer functions (Luco and Wong, 1986). Symbolically, the normalization can be accomplished by consideration of the evaluation of Equation 3-12 using a unit PSD input function.

The incoherency transfer function, ITF(f) is then defined as the amplitude of the square root of the diagonal terms of $[S_{UoI}]$ where $[S_{UoI}]$ is the 6 by 6 cross PSD matrix of rigid massless foundation motion subjected to unit PSD input.

$$[S_{UoI}] = [F]\,[S_{UGI}]\,[FC]^T \qquad \textbf{Equation 3-21}$$

where [F] is a 6 by 3n scattering transfer function matrix relating sub-region displacements to rigid body displacements and [FC] is the complex conjugate of [F] and $[S_{UGI}]$ is a 3n by 3n covariance matrix of incoherent ground motions for unit PSD input given by [I] [γ] [I] where [I] is an identity matrix.

The difference between $[S_{UGI}]$ and $[S_{UG}]$, used in Equation 3-12, is that the identity matrix, [I] is used instead of $[S_o^{1/2}]$. The procedure used is shown in Table 3-1.

Based on CLASSI determined [K], [T], [G], and $[\alpha_b]$ the 6 by 6 cross PSD, $[S_{UoI}]$ of the rigid massless foundation to unit PSD input due to incoherent input motion is generated. For this purpose, the coherency matrix, [γ], the covariance matrix for unit PSD input, $[S_{UGI}]$ and the scattering transfer function, [F] are evaluated. Also, incoherency transfer function, ITF, which is equal to the amplitude of the square root of the diagonal terms of $[S_{UoI}]$ is calculated.

Table 3-1
Procedure to Evaluate Incoherency Transfer Function

• Define soil profile and specify properties by soil layers Define foundation footprint and specify as n sub-regions
• Input coherency function, γ(f,s) as a function of frequency, f and separation distance, s
• Run CLASSI modules to evaluate the impedance matrix and Green's function matrix
• From Green's function matrix and rigid foundation assumption, evaluate the traction matrix, [T]. Invert the impedance matrix to evaluate the compliance matrix, [C]
• Evaluate $[S_{UoI}]$, the cross PSD matrix of rigid massless foundation motion subjected to unit PSD input $[S_{UoI}] = [F]\,[S_{UGI}]\,[FC]^T$ where $[F] = [C]\,[T]^T$ and $[S_{UGI}] = [I]\,[\gamma]\,[I]$
• Evaluate the incoherency transfer function, ITF(f) as the amplitude of the complex square root of the diagonal terms of $[S_{UoI}]$

Procedure to Evaluate the Foundation and Structure Incoherent Response Spectra by CLASSI

The complete random vibration approach could be employed to generate foundation and structure response including the conversion of ground motion response spectra into power spectral density functions (PSDFs) and reversing the process at the foundation and structure response locations. However, the formulation of CLASSI and its ease of use permitted implementation of a more direct approach to the SSI analysis of structure/foundation.

Elements of the substructure approach as implemented in CLASSI are shown schematically in Figure 3-1. The CLASSI program modules generate the complex impedance and scattering matrices at each frequency considered. The impedance matrix represents the stiffness and energy dissipation of the underlying soil medium. The foundation input motion is related to the free-field ground motion by means of a transformation defined by a scattering matrix. The term "foundation input motion" refers to the result of kinematic interaction of the foundation with the free-field ground motion. In general, the foundation input motion differs from the free-field ground motion in all cases, except for surface foundations subjected to vertically incident coherent waves. The soil-foundation interface scatters waves because points on the foundation are constrained to move according to its geometry and stiffness. Modeling of incoherent ground motions is one aspect of this phenomena and the focus of this study.

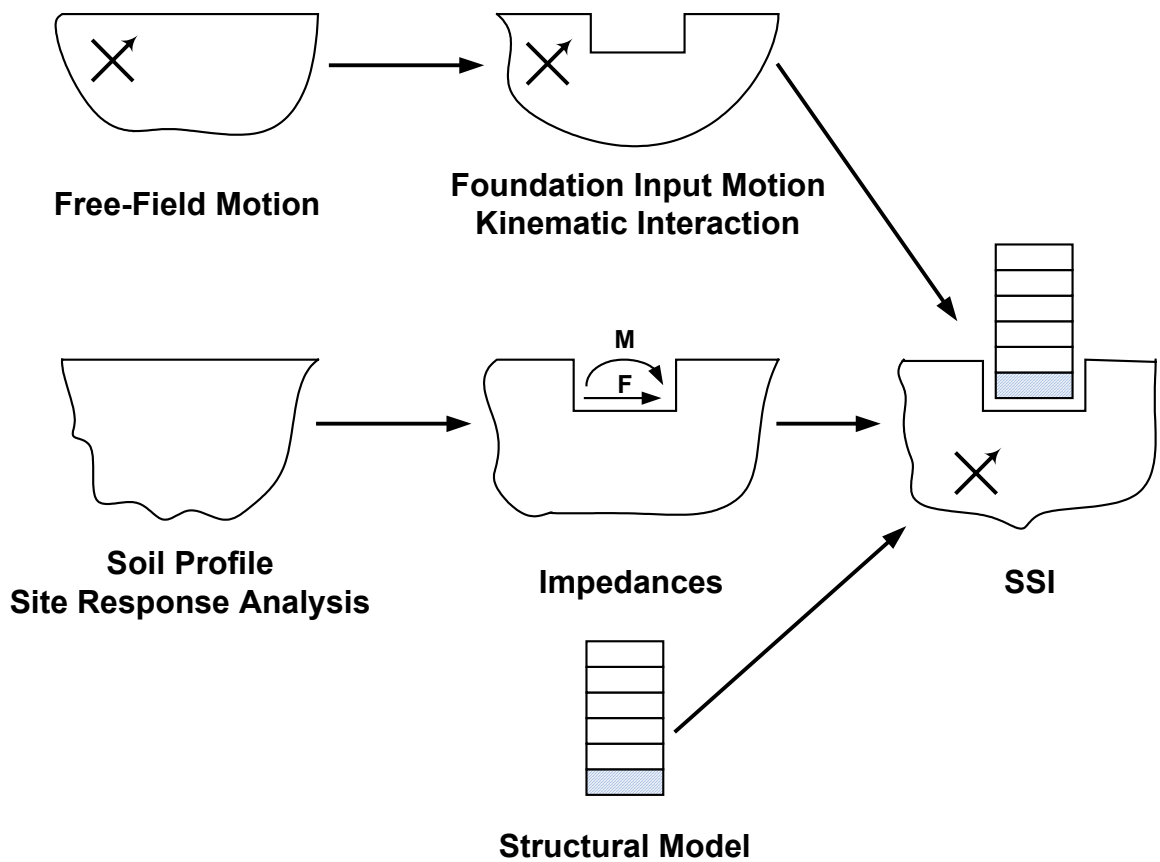

Figure 3-1
Elements of the Substructure Approach to SSI Analysis as Implemented in CLASSI

In essence, the incoherency transfer function may be interpreted as a scattering matrix accounting for the effects of seismic wave incoherency over the dimensions of the foundation. For this application, a 6 by 6 complex incoherency transfer function matrix [ITF] is evaluated by taking the square root of the diagonal terms of $[S_{UoI}]$, the 6 by 6 complex cross PSD matrix of rigid massless foundation motion to unit PSD input for each direction of translational input. Since the free-field motions are uncorrelated in each orthogonal direction, we may consider the evaluation of Equation 3-21 using each free-field input direction separately. Three sets of ITF vectors are obtained by taking the square root of each PSD evaluation. The CLASSI scattering

matrix (6 x 3) is comprised of 3 vectors each of which determines the foundation input motion for the three components of free-field ground motion. Each vector of the scattering matrix is replaced by the incoherency transfer function vectors that correspond to each component of free-field ground motion. Each frequency is treated independently. CLASSI SSI analyses are then performed in a conventional manner to evaluate the structure and foundation in-structure response spectra. CLASSI solves the SSI problem in the frequency domain. Ground motion time histories are transformed into the frequency domain, SSI parameters (impedances and scattering matrices) are complex-valued, frequency-dependent, and the structure is modeled using its fixed-base eigen-systems.

Two variations of the CLASSI approach have been implemented and applied to the example structure. The difference in the two approaches is the treatment of the phase of the foundation scattering terms or ITFs. The following describes the two approaches:

- CLASSIinco – Retain the deterministic phasing of the foundation scattering functions as determined from the complex square root of the diagonal terms of the matrix $[S_{UoI}]$. This is most appropriate for the case of phenomena, such as wave passage. However, the benchmarking reported by Short et al. (2006) and those presented herein demonstrate its potential validity in producing engineering acceptable solutions in many situations for seismic wave incoherence effects. Table 3-2 summarizes this approach.
- CLASSIinco-SRSS – SRSS combination of the structure response induced by the individual foundation scattering terms (ITFs) applied independently, i.e., assuming the relationship between the phases of the scattering terms behaves randomly. This results in performing six SSI analyses for each direction of ground motion and SRSSing the end quantity of interest. In this report, the end items of interest are in-structure response spectra. Table 3-3 summarizes this approach.

Table 3-2
Procedure to Evaluate the Foundation and Structure Incoherent Response Spectra by CLASSIinco

• Define free-field ground motion time histories compatible with response spectra, $[Rs_o]$
• Define soil profile and specify properties by soil layers Define foundation footprint and specify as n sub-regions Define foundation thickness and mass properties Define a fixed-base structural model
• Input coherency function, $\gamma(F,S)$ as a function of frequency, F and separation distance, S
• Run CLASSI modules to evaluate the impedance matrix
• Evaluate the scattering matrix as the incoherency transfer function. Each column of the scattering matrix corresponds to a direction of input excitation and is given by the diagonal terms from the incoherency transfer function at each frequency of interest.
• Evaluate fixed-base modal properties of the structure
• Run CLASSI modules that combine the structure properties, impedance matrix, scattering matrix, and input time histories, and evaluates output time histories
• Run standard response spectrum evaluation program to determine in-structure response spectra for the foundation and structure locations

Table 3-3
Procedure to Evaluate the Foundation and Structure Incoherent Response Spectra by CLASSIinco-SRSS

• Define free-field ground motion time histories compatible with response spectra, [Rs_o]
• Define soil profile and specify properties by soil layers Define foundation footprint and specify as n sub-regions Define foundation thickness and mass properties Define a fixed-base structural model
• Input coherency function, γ(F,S) as a function of frequency, F and separation distance, S
• Run CLASSI modules to evaluate the impedance matrix
• Evaluate the scattering matrix as the incoherency transfer function. Each column of the scattering matrix corresponds to a direction of input excitation and is given by the diagonal terms from the incoherency transfer function at each frequency of interest.
• Evaluate fixed-base modal properties of the structure
• Run CLASSI modules that combine the structure properties, impedance matrix, scattering matrix, and input time histories, and evaluates output time histories. Perform analyses with CLASSI for each component of the scattering matrix independently (for three components of free-field motion and a 3D structure, eighteen CLASSI analyses are performed.
• Run standard response spectrum evaluation program to determine in-structure response spectra for the foundation and structure locations for each of the eighteen analysis results. Perform SRSS of the ISRS.

In CLASSI, the dynamic characteristics of the structures to be analyzed are described by their fixed-based eigen-system and modal damping factors. Modal damping factors are the viscous damping factors for the fixed-base structure expressed as a fraction of critical damping. The structures' dynamic characteristics are then projected to a point on the foundation at which the total motion of the foundation, including SSI effects, is determined.

The final step in the CLASSI substructure approach is the actual SSI analysis. The results of the previous steps – foundation input motion (scattering matrix defined by the incoherency transfer function), foundation impedances, and structure model – are combined to solve the equations of motion for the coupled soil-structure system. For a single rigid foundation, the SSI response computation requires solution of, at most, six simultaneous equations – the response of the foundation. The derivation of the solution is obtained by first representing the response in the structure in terms of the foundation motions and then applying that representation to the equation defining the balance of forces at the soil/foundation interface. The formulation is in the frequency domain. Once the foundation motion is calculated (including all aspects of SSI), in-structure responses are determined for locations of interest in the structure, i.e., by solving the dynamic equations of motion in modal coordinates for the base excited system. The resulting in-structure response spectra at structure and foundation locations of interest include the effects of soil-structure interaction and seismic wave incoherence.

Validation of Rigid, Massless Foundation Response

Objective and Scope

The objective of this validation effort is to benchmark the procedure and results generated with CLASSI versus published literature. This version of CLASSI is denoted CLASSIinco for the purpose of identification. The theory and development of CLASSIinco is described in detail in the preceding sections.

The quantities of interest for benchmarking are the Incoherent Transfer Functions (ITFs), scattering functions in CLASSI nomenclature. Incoherent Transfer Functions relate the free-field ground motion to the response of a rigid massless foundation taking into account the spatial incoherence of the ground motion. One aspect of the benchmark problems is simplified, specifically the supporting media is a uniform visco-elastic half-space with the following properties:

Shear Wave Velocity, Vs = 6300 ft/sec = 1920.24 m/sec

Mass Density, ρ = .004969 k-sec2/ft^4

Poisson's Ratio, ν = 0.33

Damping, ξ = 0.01

Two foundation shapes are considered – a circular rigid disk of radius of 84.63 ft. and a square foundation 150 ft. on a side. These foundations have equal areas – 22,500 ft.*ft. The foundations are founded on the surface of the half-space. The ITFs of interest are the horizontal, vertical, rocking, and torsion components. Torsion is induced by the spatial incoherence of the horizontal ground motion. Rocking is induced by the spatial incoherence of the vertical ground motion. The bases of comparison are: Luco and Mita (1987) and Veletsos and Prasad (1989) for the circular disk; and Luco and Wong (1986) for the square foundation.

Ground Motion Coherence Function

The form of the ground motion coherency functions (horizontal and vertical directions) is exponential decay as a function of frequency and distance between observation points:

$$\Gamma(|r1 - r2|,\omega) = \exp[-(\gamma\omega|r1 - r2|/Vs)^2] \qquad \textbf{Equation 3-22}$$

where $|r1 - r2|$ is the distance between points on the foundation (subregion centroids)

γ is a dimensionless incoherence parameter,

ω is the angular frequency (radians/sec),

Vs is the representative shear wave velocity of the soil profile.

For benchmark purposes, calculations were made for values of $\gamma = 0.1$, 0.2, 0.3, 0.4 and 0.5.

Luco and Wong (1986) state that a reasonable value for γ might be

$$Vs * 2 \times 10^{-4} \text{ sec-m}^{-1} \leq \gamma \leq Vs * 3 \times 10^{-4} \text{ sec-m}^{-1}$$

For the uniform halfspace under consideration (Vs = 6300 ft/sec = 1920 m/sec), this yields a value of γ between about 0.4 and 0.6. Therefore, a value of $\gamma = 0.5$ is selected for comparison with the Abrahamson ground motion coherency function. However, comparison of ITFs are presented for the five values of γ.

The Abrahamson ground motion coherency functions, Equation 2-1 and Table 2-1, are compared with those of Equation 3-22 ($\gamma = 0.5$). The comparison of the Abrahamson ground motion coherency function for horizontal motion is plotted in Figure 3-2 for comparison with Equation 3-22 ($\gamma = 0.5$) for varying values of distance between observation points and frequency. One observes that for distances less than 50 m. and constant frequency, the Abrahamson coherency functions are significantly lower than Equation 3-1. For a distance of 50 m., the two functions are approximately the same. For distances greater than 50 m., the Abrahamson coherency functions are greater.

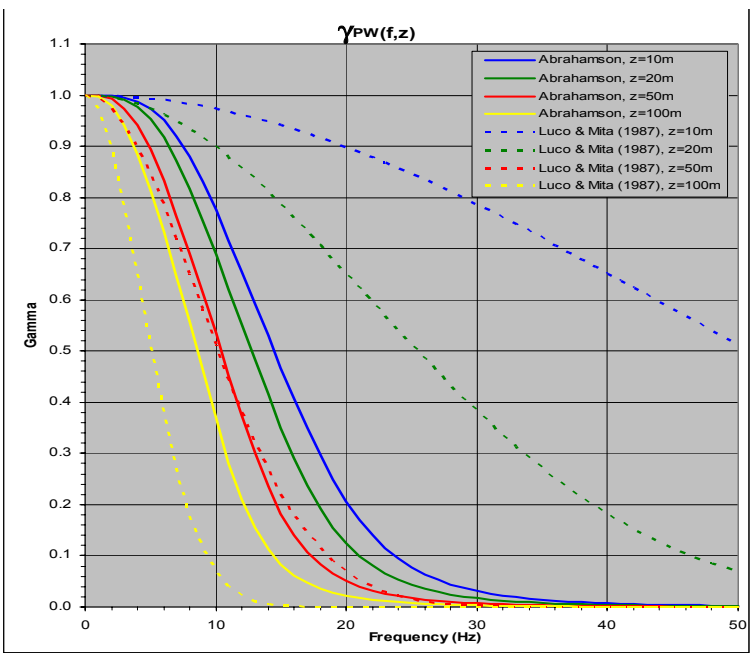

Figure 3-2
Comparison of Coherency Ground Motion Functions, Horizontal Direction – Abrahamson (2005, 2006) and Luco and Mita (1987) for $\gamma = 0.5$

Comparison of ITFs

CLASSIinco, modified to implement the ground motion coherency function of Equation.3-22, is used to calculate the ITFs or scattering functions. In the ensuing paragraphs, comparisons are made for rigid, massless foundation response: horizontal motion due to horizontal input (S11), induced torsion due to horizontal input motion (S61), vertical motion due to vertical input motion (S33), and induced rocking due to vertical input motion (S43).

The frequency axis in Figures 3-4 through 3-9 and 3-11 through 3-14 is in terms of dimensionless frequency:

$$a0 = \omega \text{ (rad/sec)} * Cl / Vs$$

where

Cl = characteristic length = 84.63 ft.

Vs = 6300 ft/sec.

The following table converts values of a0 to frequencies in Hz. for these cases.

Frequency (Hz)	a0
10	0.84404123
20	1.68808245
25	2.11010307
30	2.53212368
50	4.22020613

The legend in Figures 3-4 through 3-9 and 3-11 through 3-14 uses “g” to represent γ.

Circular Disk

The circular foundation model for the CLASSIinco analysis was discretized into 112 subregions as shown in Figure 3-2. This discretization was used in numerous previous studies, including as a foundation model of the Zion reactor building for the NRC Seismic Safety Margins Research Program.

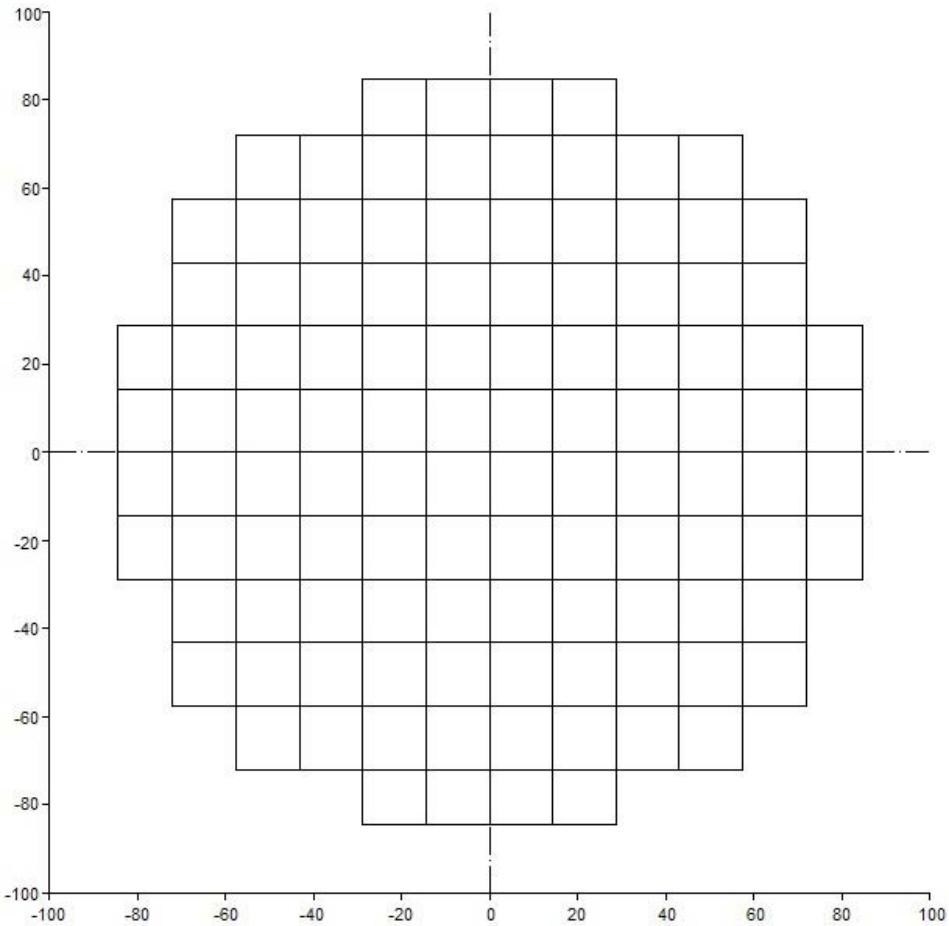

Figure 3-3
Foundation Model, Circular Disk, CLASSIinco

For the circular disk, Figures 3-4 through 3-7 show the comparisons of the scattering functions calculated with CLASSIinco and those tabulated in Luco and Mita (1987) Table 1. Further, a comparison was made with the approach of Veletsos and Prasad (1989) shown in Figures 3-8 and 3-9.

The comparisons with Luco and Mita demonstrate excellent agreement for all four scattering terms.

Figures 3-8 and 3-9 show comparisons of the CLASSIinco scattering functions for rigid, massless foundation response – horizontal and induced torsion – due to horizontal input motion with those of Veletsos and Prasad (1989), Equations 9a and 9b. These comparisons are plotted as functions of the dimensionless frequency $\tilde{a}0 = a0*\gamma$ for $\gamma = 0.5$. In this case, the CLASSIinco responses for horizontal foundation response are very close. For induced torsion, the CLASSIinco results are slightly lower than the results of the approach of Veletsos and Prasad (a maximum of about 15%).

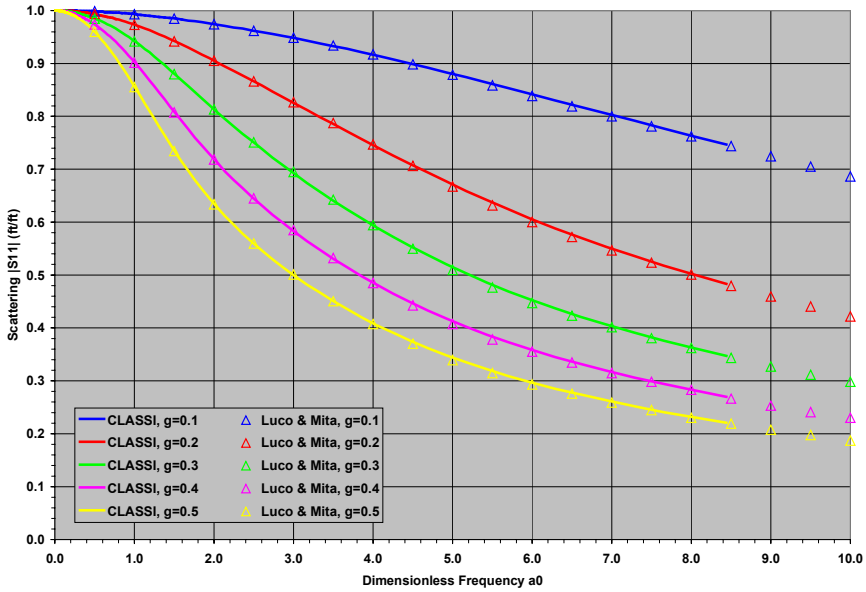

Figure 3-4
Circular Foundation, Comparison of CLASSlinco Results With Luco and Mita (1987), Horizontal Transfer Function S11

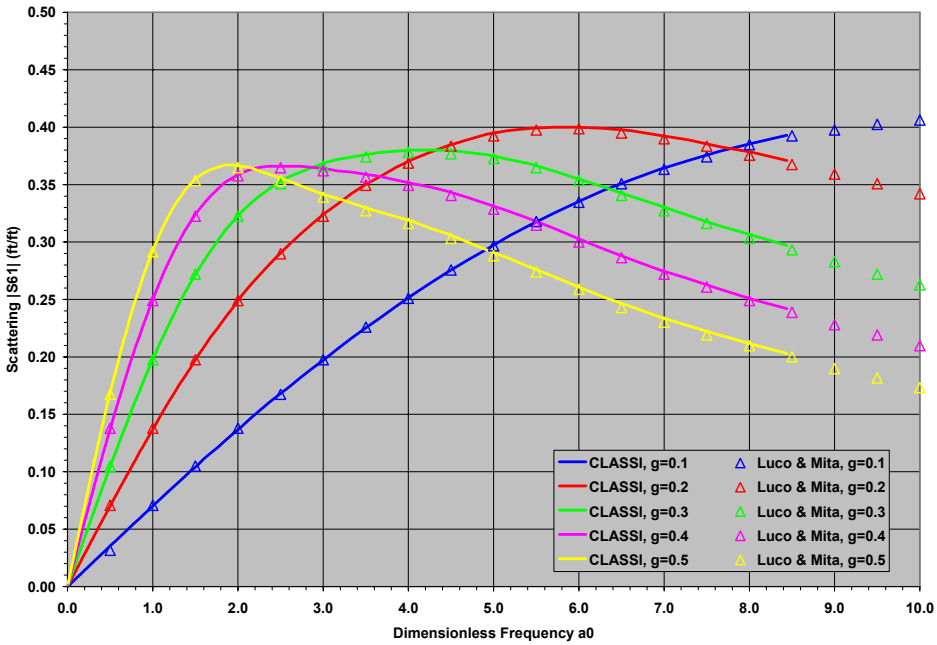

Figure 3-5
Circular Foundation, Comparison of CLASSlinco Results With Luco and Mita (1987), Torsional Transfer Function S61

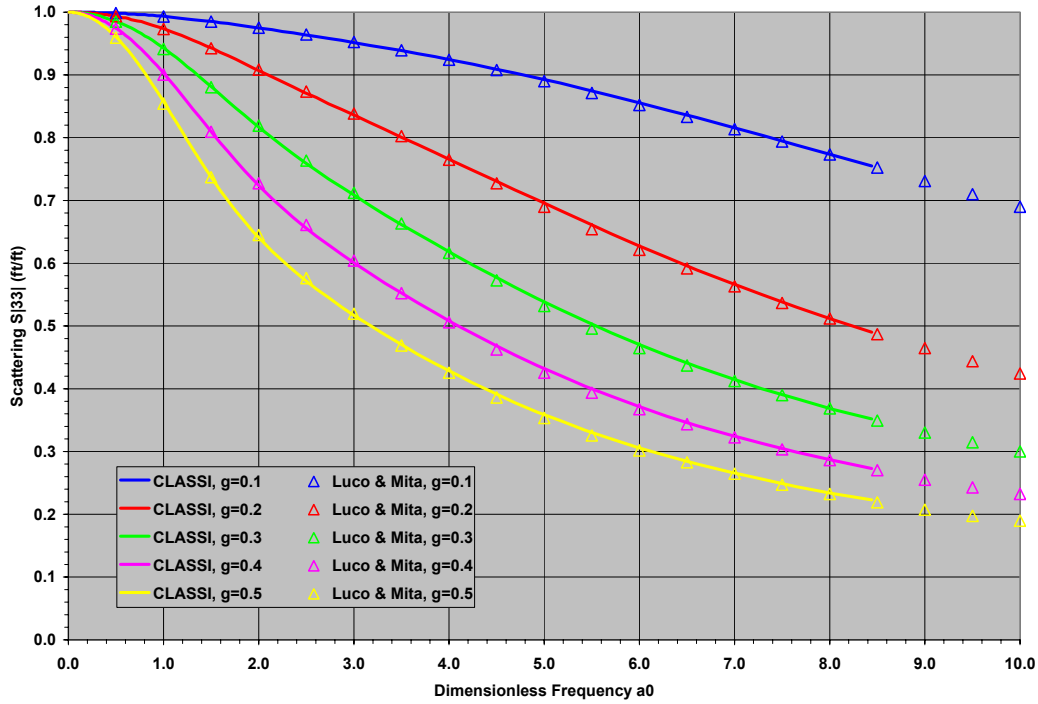

Figure 3-6
Circular Foundation, Comparison of CLASSlinco Results With Luco and Mita (1987), Vertical Transfer Function S33

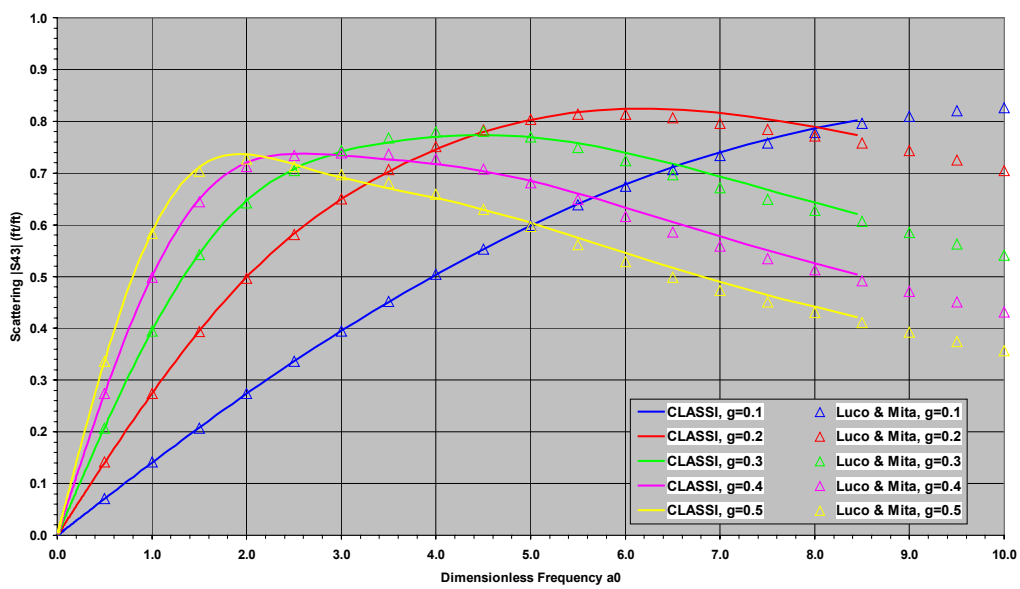

Figure 3-7
Circular Foundation, Comparison of CLASSlinco Results With Luco and Mita (1987), Rocking Transfer Function S43

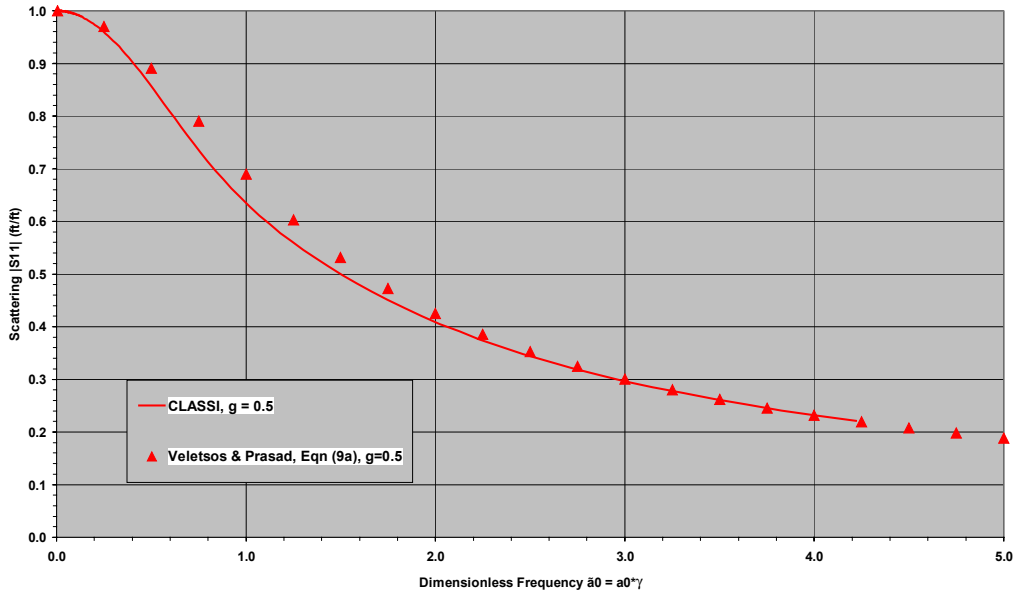

Figure 3-8
Circular Foundation, Comparison of CLASSlinco Results With Veletsos and Prasad (1989), Horizontal Transfer Function S11

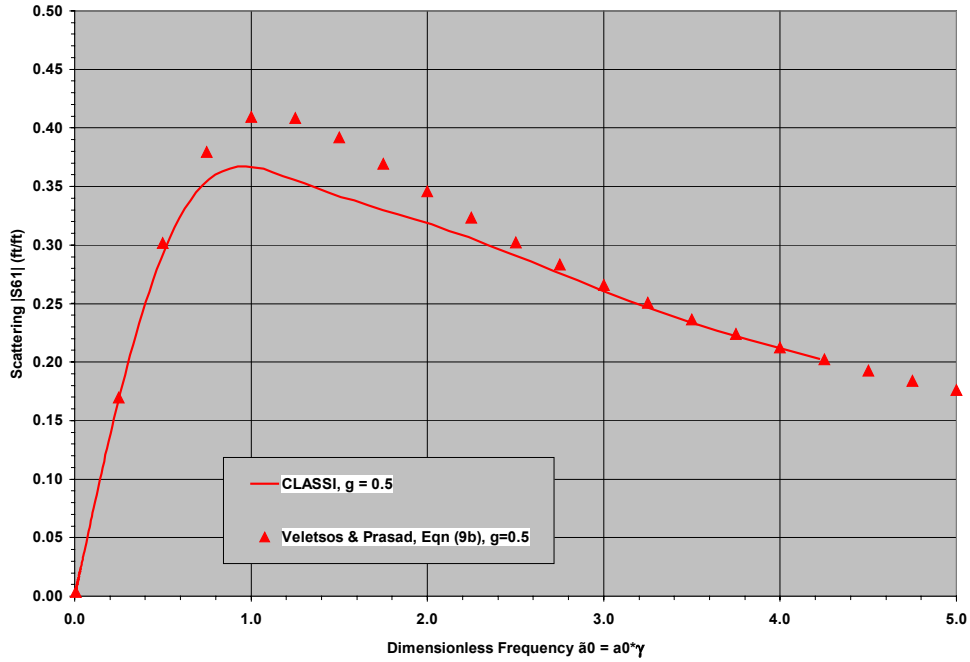

Figure 3-9
Circular Foundation, Comparison of CLASSlinco Results With Veletsos and Prasad (1989), Torsional Transfer Function S61

Square Foundation

The square foundation is the same as that used in the numerous sensitivity studies by Short et al. (2006) and in the current phase of the Program, i.e., 150 ft. on a side and discretized into 393 subregions as shown in Figure 3-9. The discretization consists of 169 (13 X 13) 10-ft square subregions surrounded by two rows of 5-ft square subregions. A sensitivity study confirmed the adequacy of this discretization during the execution of the effort reported by Short et al. (2006).

For the square foundation, the published data was taken from Luco and Wong (1986), Figures 2 and 3.

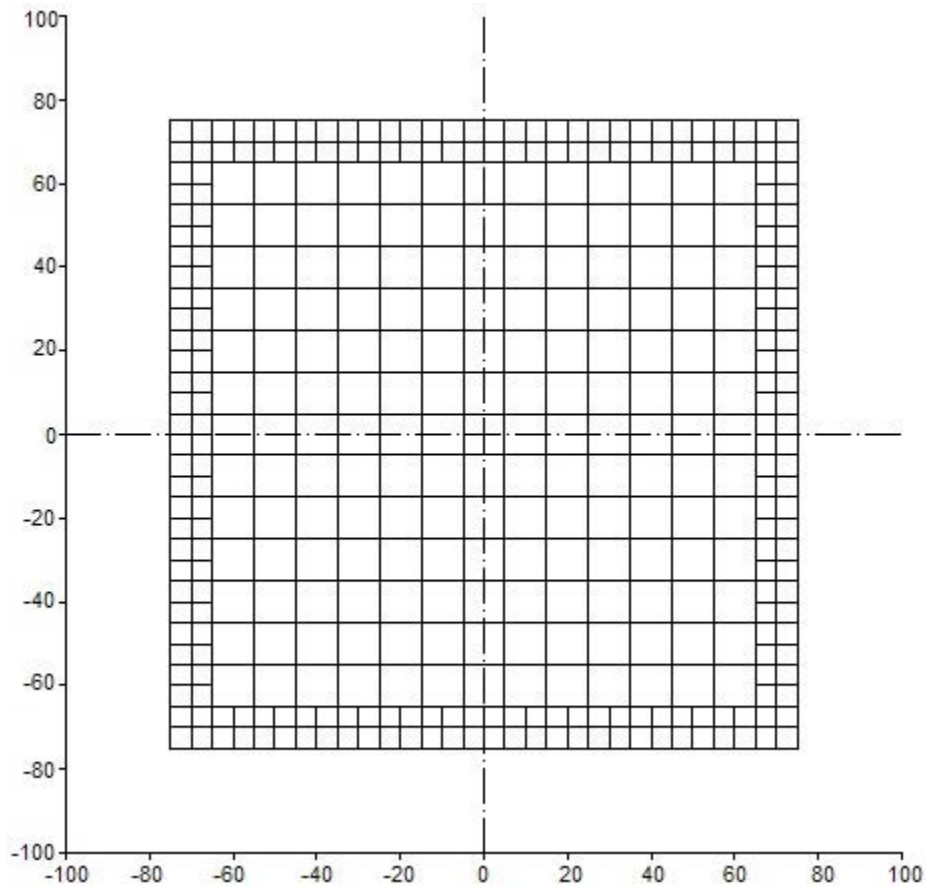

Figure 3-10
Square Foundation Model, CLASSIinco

For the square foundation, Figures 3-11 through 3-14 show the comparisons of the scattering functions calculated with CLASSIinco and those reported in Luco and Wong (1986), Figures 2 and 3. Note, the values reported in Luco and Wong were only in graphical form. Hence, the values plotted herein were read from the curves in Figures 2 and 3.

In general, the comparisons with Luco and Wong show the CLASSIinco results for translational scattering functions to be slightly less and the corresponding induced rotations are somewhat more than the values reported by Luco and Wong. The fact that the CLASSIinco approach and the approach of Luco and Wong apply differing simplifications and discretizations of the foundation lead to the conclusion that the benchmark comparison is very good.

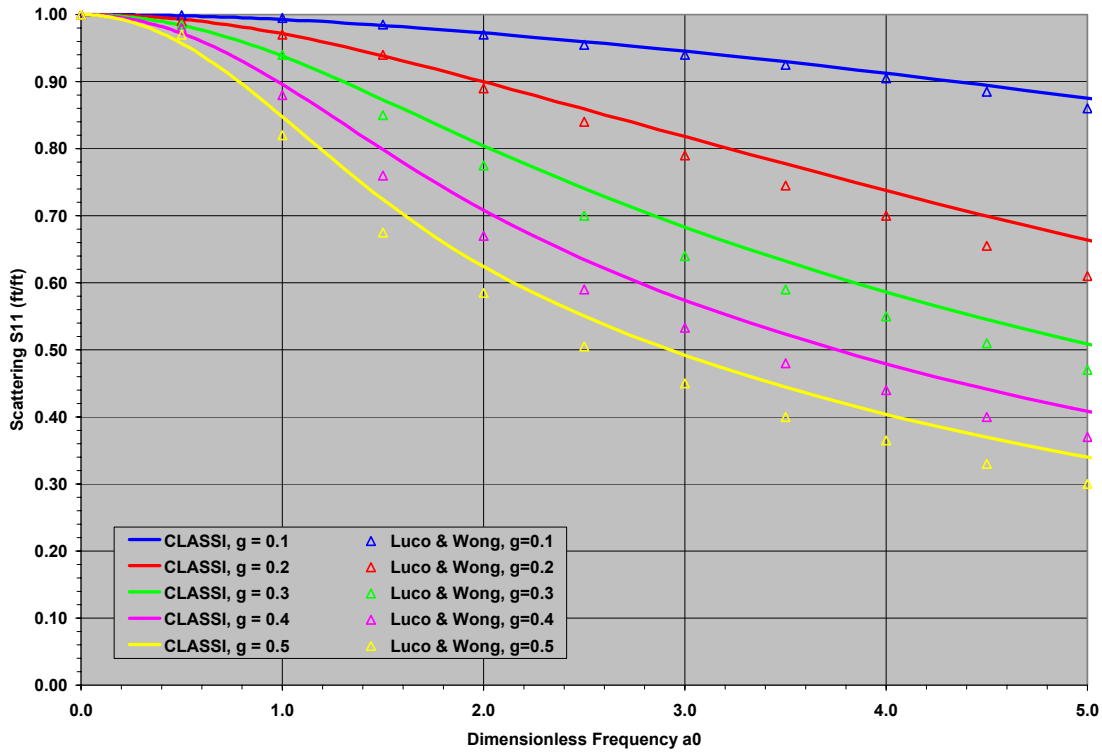

Figure 3-11
Square Foundation, Comparison of CLASSlinco Results With Luco and Wong (1986), Horizontal Transfer Function S11

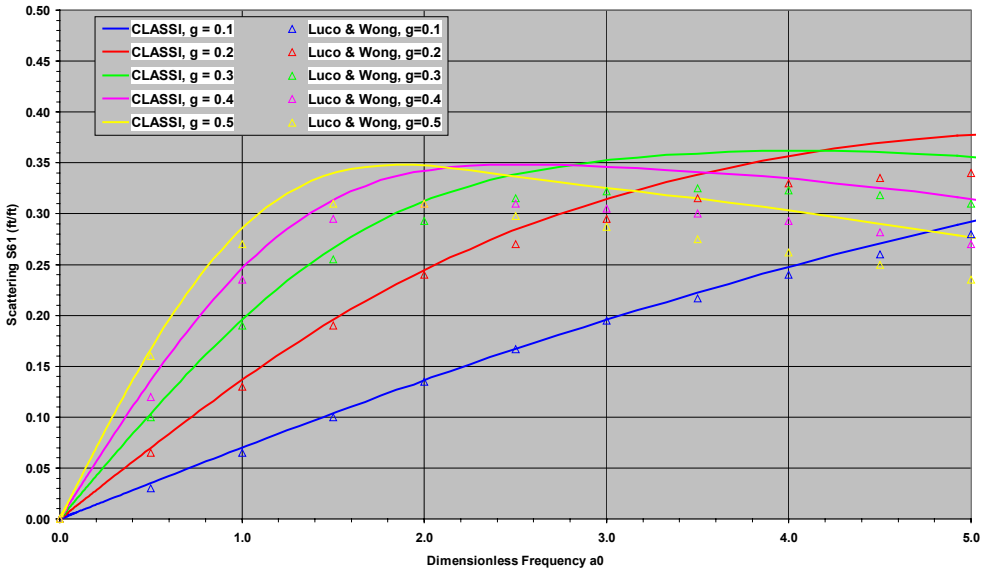

Figure 3-12
Square Foundation, Comparison of CLASSlinco Results With Luco and Wong (1986), Torsional Transfer Function S61

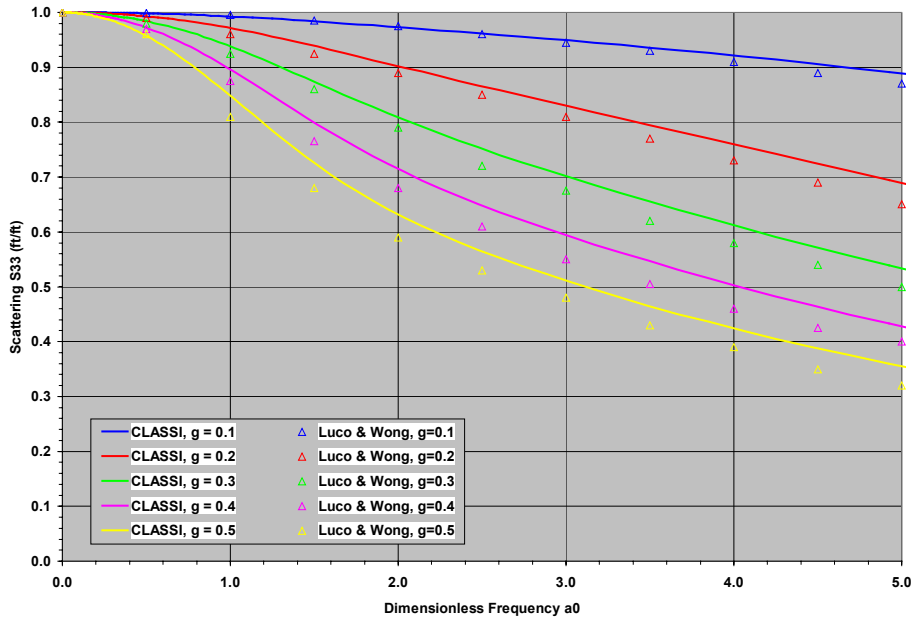

Figure 3-13
Square Foundation, Comparison of CLASSIinco Results With Luco and Wong (1986), Vertical Transfer Function S33

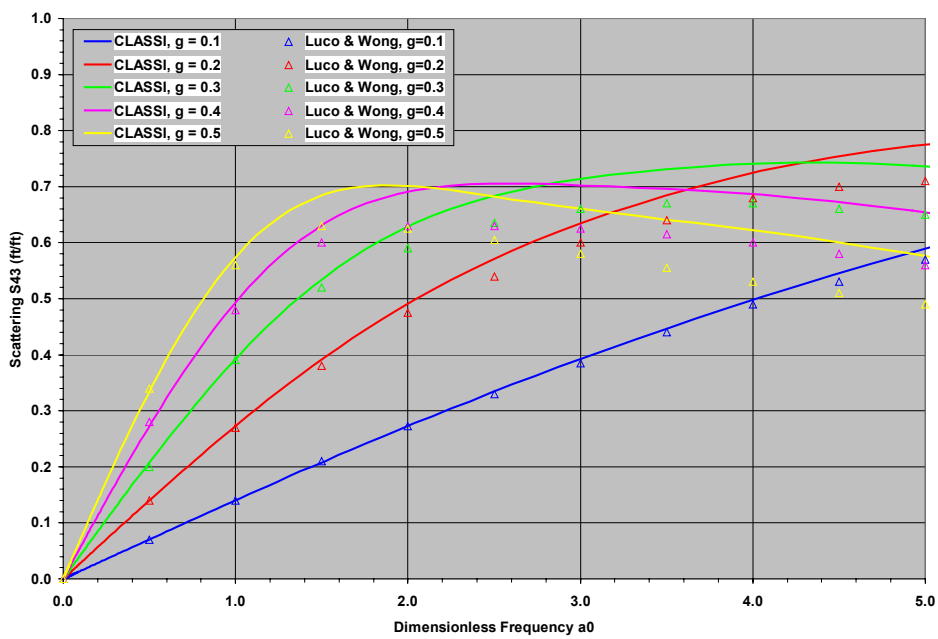

Figure 3-14
Square Foundation, Comparison of CLASSIinco Results With Luco and Wong (1986), Rocking Transfer Function S43

Conclusions

The benchmark performed of the amplitudes of the Incoherency Transfer Functions calculated with CLASSIinco when compared with published literature validates the procedure and implementation in CLASSIinco.

4
SASSI TECHNICAL APPROACH

General

A parallel effort to the stochastic approach described in Chapter 3 is denoted "Deterministic Method" by Tseng and Lilhanand (1997) from which the derivation implemented in several versions of SASSI is based. The key elements of the approach are summarized here and follow directly the Tseng and Lilhanand derivation. Ghiocel (2004) presents theoretical aspects of the approach itemized by Tseng and Lilhanand (1997) and provides the basis for the ACS SASSI treatment of the phenomena (Ghiocel, 2006). Short et al. (2006), Appendix C provides additional background on the SASSI analysis approaches. Tubino et al. (2003) present an approach to modeling multi-support systems accounting for spatial variation of input motion and lists several additional references on the subject.

The approaches described in Chapters 3 and 4 are general in the sense of treating local wave scattering and wave passage effects. However, as defined in Chapter 1, local wave scattering is the focus and ensuing discussion is limited to this case.

Coherency Matrix

The starting point is the matrix $[\gamma]$, a $3N$ by $3N$ matrix of the Abrahamson coherency function based on the separation distances between the "N" SASSI interaction node point DOFs. The factor 3 is for the three directions of free-field ground motion. As in the case of the stochastic approach, the effects of incoherence of ground motion are uncoupled for the three directions of free-field ground motion. This parallels the analysis procedure typically used in SASSI, i.e., treating each of the three directions independently and combining the response results appropriately. At each discrete frequency, the matrix $[\gamma]$ of Chapters 3 and 4 is identical when the centroids of the sub-regions of the CLASSI analysis coincide with the locations of the SASSI interaction node points.

The CLASSI approach applies the constraint of the rigid foundation behavior to determine the amplitude of the tractions on each of the sub-regions which produce the rigid body motion and the CPSD of the motion of the rigid massless foundation. The SASSI approach utilizes the characteristics of the matrix $[\gamma(\omega)]$, specifically the assurance that it can be decomposed into its eigensystem (termed spatial modes), to provide computational efficiency in the SSI analysis. Whereas the CLASSI approach requires determination of the scale factors for the sub-region tractions, the SASSI approach proceeds along a parallel path where a number of analysis decisions are required, as described next.

Before proceeding, some important observations concerning the coherency matrix, $[\gamma(\omega)]$ and its decomposition into its eigensystem are stated:

1. For a given frequency ω the coherency matrix is independent of all other frequencies.
2. The matrix $[\gamma(\omega)]$ is Hermitian and positive-definite and therefore, can be decomposed into its complex eigenvalues and associated eigenvectors (Equation 3-19, Tseng and Lilhanand, 1997):

$$([\gamma(\omega)] - \lambda_i^2[I])\ \{\phi(\omega)\}_i\ ) = \{0\},\ i = 1,2,\ldots N \qquad \textbf{Equation 4-1}$$

Where $[\gamma(\omega)]$ is the (N x N) coherency matrix for N SASSI interaction node points and considering a single component of input motion, $\lambda_i(\omega)$ is the ith eigenvalue, and $\{\phi(\omega)\}_i$ is the (N x 1) corresponding eigenvector to $\lambda_i(\omega)$.

If wave passage is not considered in the derivation of $[\gamma(\omega)]$, the eigensystem $[\phi(\omega)]$ and $[\lambda^2(\omega)]$ is real-valued.

3. Equation 3-22 of Tseng and Lilhanand (1997) yields the reconstruction of the matrix $[\gamma(\omega)]$:

$$[\gamma(\omega)] = [\phi(\omega)]\ [\lambda 2(\omega)][\phi c(\omega)]T \qquad \textbf{Equation 4-2}$$

Where $[\phi_c(\omega)]$ is the complex conjugate of $[\phi(\omega)]$ and "T" denotes transpose.

This equation defines a check that may be performed on the calculated eigensystem to determine the accuracy of the calculated eigensystem to represent the coherency matrix $[\gamma(\omega)]$.

SASSI Approach

Derivation of the approach to address the effects of incoherency of ground motion on SSI analysis of foundations and structures as implemented in SASSI (EPRI version SASSI-INCOH, Bechtel SASSI, and ACS SASSI) follows the approach of Tseng and Lilhanand (1997), Chap. 3 "Deterministic Method."

As noted above, the coherency matrix $[\gamma(\omega)]$ possesses special characteristics and thereby produces the following solution to the incoherent response at each SASSI interaction node, which follows the generalized solution denoted Karhunen-Loeve (KL) based on the spectral factorization of the coherency kernel (Ghiocel, 2004). Further, given the coherency kernel eigensystem decomposition, the resulting expression for the incoherent motion at SASSI interaction node points is:

$$\{Ugl\} = [\phi(\omega)]\ [\lambda(\omega)]\ \{\eta\theta(\omega)\}\ U0(\omega) \qquad \textbf{Equation 4-3}$$

Where $\{\eta_\theta(\omega)\}$ is a (N x 1) random phase vector of the form $e^{i\theta(\omega)}$ for each spatial mode and θ is uniformly distributed from $-\pi$ to π - therefore a median value of η is unity, and $U_0(\omega)$ is the single ground motion component of interest (i.e., X, Y, or Z). This expression includes all spatial modes, but a subset could be assumed. This is Equation 3-29 of Tseng and Lilhanand (1997).

In very general terms, this expression defines the transfer function of the input free-field ground motion to the interaction node points' degrees of freedom due to incoherence without effects of soil-structure interaction (SSI).

Approaches to Solve for SSI Response of Foundation and Structure

Recall that each frequency is treated independently and eigensystems or spatial modes are calculated independently for each frequency of solution. Therefore, in general, for N interaction degrees of freedom, there will be N spatial modes calculated at each solution frequency.

Three approaches have been identified as possible solution techniques.

Stochastic Approach or Randomization (SASSI – Simulation Mean)

Results presented in Chapter 5 and Appendix A calculated by this approach are denoted SASSI – Simulation Mean (implemented in ACS SASSI). The stochastic approach entails the following steps:

(i) For each SASSI frequency (rad/sec) to be solved explicitly - randomize the phase term in Equation 4-3 assuming a uniform distribution of the phase angle θ, sample the phase from this uniform distribution for each spatial mode of interest (N modes, if all are included), calculate the interaction node point transfer functions (input) from Equation 4-3 at this SASSI frequency (Equation 4-3 shows all spatial modes included, whereas, a subset may be considered, i.e., reduced to a limited number of spatial modes – it seems likely that a small number of spatial modes may be adequate at low frequencies and rigid foundations, whereas, a larger number of modes may be necessary at higher frequencies and flexible foundations). For this approach, the number of spatial modes included in the response calculation at each frequency does not dominate the computational effort – the number of statistical simulations is the dominant factor.

(ii) Repeat this process for all SASSI frequencies.

(iii) An intermediate output of this process is a single simulation of the transfer functions of interest, e.g., foundation quantities (translational or rotational displacements, velocities, accelerations) and in-structure quantities, e.g., displacements, velocities, accelerations. These transfer functions include all SSI effects.

(iv) Calculate SSI time history response of foundation and structure and derived quantities such as in-structure response spectra; this represents one realization or simulation of the process – one random sample.

(v) Repeat the process for an appropriate number of simulations to calculate the statistical mean of the end responses of interest, e.g., peak values of displacements, accelerations, forces, or in-structure response spectra. Calculate statistics of these end items for use in the seismic design or qualification process. For this effort, we seek mean response conditional on the free-field ground motion. The input coherency ground motion functions are assumed to be mean. Hence, mean values of the responses of interest for seismic design should be calculated.

This approach appears to be straight-forward to apply, but it is relatively computationally intensive. It should be noted that statistical simulations are not complete SSI analysis runs, but restart analyses that preserve the structural model and soil layering. These restart runs are about three to five times faster than an initiation SSI analysis run. It is estimated that for 10 statistical simulations, the overall run time is about three times that for an initiation SSI analysis run.

This stochastic simulation approach (SASSI Simulation Mean) is a repeated application of the Linear Algebraic Sum (SASSI-AS) approach assuming random phases instead of zero phases between coherency matrix spatial modes. The final mean results are obtained by statistical averaging of response from the individual random simulations.

The results of 20 simulations of random phasing for vertical input to the three stick model of a representative NPP structure are presented below. Response spectra at 5 percent of critical damping for the vertical response of the foundation and for the vertical response of node 229, the outrigger on the containment internal structure (CIS) are shown in Figures 4-1 and 4-2, respectively. From these figures, it may be seen that there is a wide variation of response as spectra peaks due to random phasing of the spatial modes. This is especially true up in the structure at the outrigger location as shown in Figure 4-2.

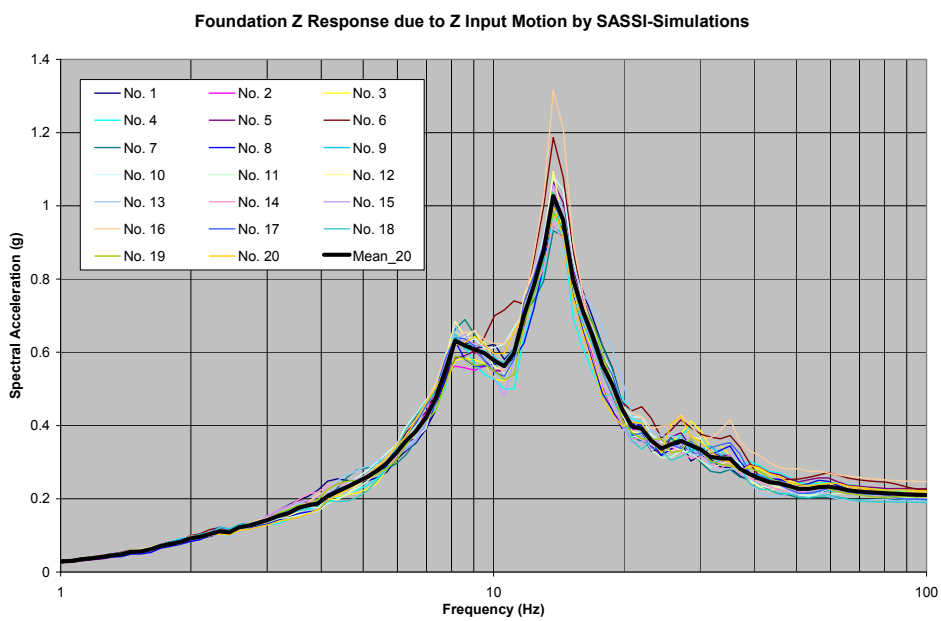

Figure 4-1
SASSI Simulation Calculated Foundation Vertical Response Spectra for Vertical Input Motion by 20 Simulations

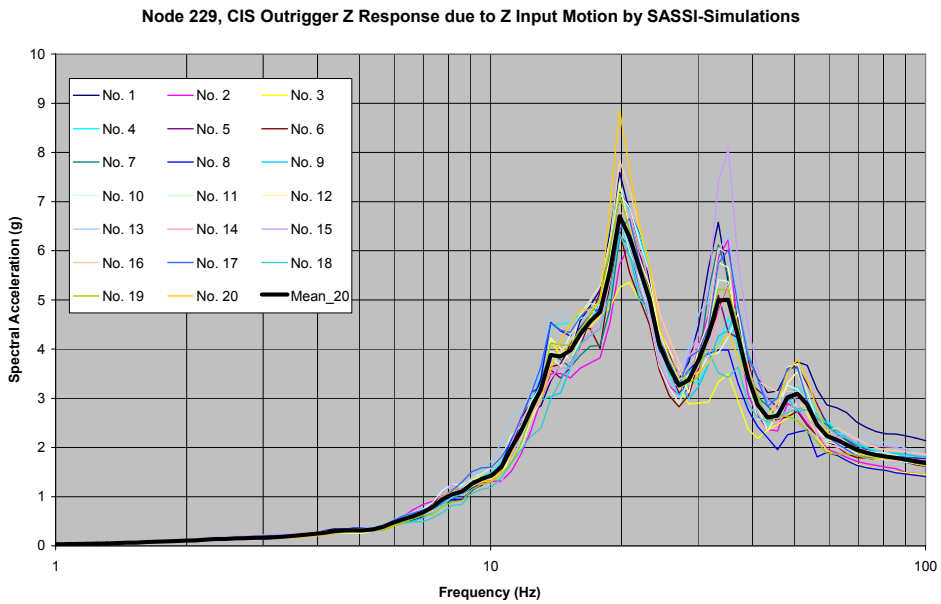

Figure 4-2
SASSI Simulation Calculated Node 229 CIS Outrigger Vertical Response Spectra for Vertical Input Motion by 20 Simulations

In Figures 4-3 and 4-4, the mean results for 5, 10, 15, and 20 simulations are shown for the vertical response of the foundation and the CIS outrigger, respectively. From these figures, it may be seen that the mean is accurately captured with few simulations. The mean from 5 simulations agrees with the mean from 20 simulations within engineering accuracy. The response spectra presented in Chapter 5 and Appendix A under the label, SASSI Simulation Mean, were generated from 15 simulations. In Figures 4-3 and 4-4, the mean from 15 and 20 simulations is essentially identical.

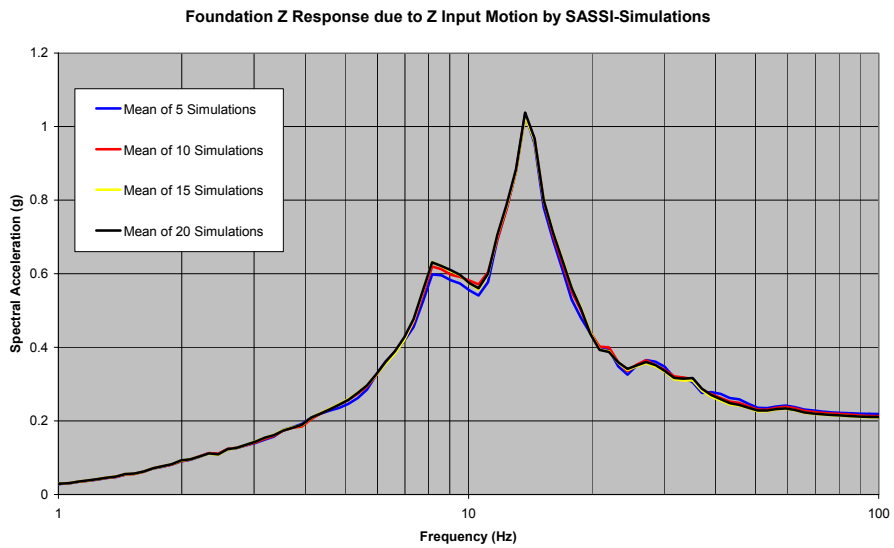

Figure 4-3
SASSI Simulation Calculated Foundation Vertical Response Spectra for Vertical Input Motion – Mean Spectra by 5, 10, 15, and 20 Simulations

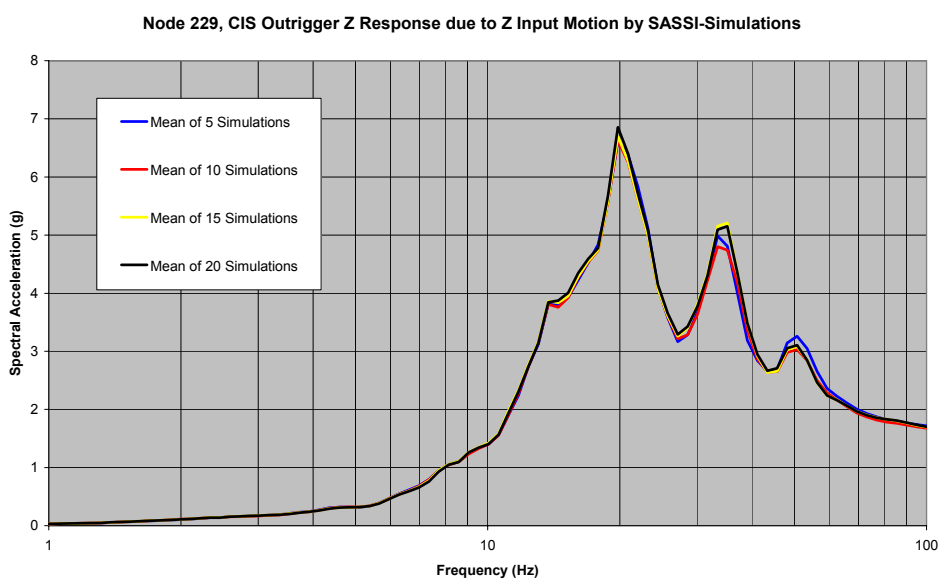

Figure 4-4
SASSI Simulation Calculated Node 229 CIS Outrigger Vertical Response Spectra for Vertical Input Motion – Mean Spectra by 5, 10, 15 and 20 Simulations

Square Root of the Sum of the Squares (SASSI-SRSS)

Conceptually, the SRSS approach can be implemented at the transfer function or at the SSI dynamic response stage. Equation 4-4 (Equation 3-33, Tseng and Lilhanand, 1997) is of interest:

$$\{Us(\omega)\}i = [Hs(\omega)]\ [\phi(\omega)]i\ [Hc(\omega)]\ \lambda i(\omega)\ U0(\omega);\ i = 1, 2, \ldots, m \qquad \textbf{Equation 4-4}$$

Where $\{Us(\omega)\}_i$ is the Fourier transform of the response at a given foundation/structure degree of freedom due to spatial mode i, $[Hs(\omega)]$ is the transfer function relating structure response to the input motion at the SASSI interaction nodes, $[H^c(\omega)]$ is the transfer function that relates the coherent ground motion vector at the SASSI interaction nodes to the control motion at the reference station $U_0(\omega)$ accounting for wave passage effects (for no wave passage effects, this is unity), $[\phi(\omega)]_i$ and $\lambda_i(\omega)$ represent the spatial mode(s) i, and $\eta_\theta(\omega) = 1$, for all values of i.

SRSS Transfer Functions

This approach is described in detail in Ostadan & Deng, 2007 and is implemented in the Bechtel version of SASSI2000. For each SASSI frequency (rad/sec) to be solved explicitly:

(i) The transfer functions for foundation and structure response are calculated for each of the spatial modes independently assuming phase angle $\theta = 0$ and consequently $\eta_\theta(\omega) = 1$. The transfer function (complex-valued) calculated for each of the spatial modes assuming zero phase are combined by SRSS.

$$TFj(\omega) = \sqrt{\sum} \left(\sum \langle Hsj(\omega)\rangle\ [\{\phi_1(\omega)\ \lambda_1(\omega)\} \ldots \{\phi_i(\omega)\ \lambda_i(\omega)\} \ldots \{\phi_q(\omega)\ \lambda_q(\omega)\}]\right)^2$$

Where j denotes the foundation/structure degree of freedom of interest; Hsj is the transfer function between SASSI interaction nodes and response degree of freedom j (total of N SASSI interaction nodes) – Hsj is (1 x N); the inside summation is over the interaction node points 1 to N; the result is the transfer function for degree of freedom j due to each spatial mode i for a given ω; the outside summation represents the summation of these q values squared, q being the number of modes considered; and the square root of the result is taken.

(ii) Repeat this process for all SASSI frequencies.

(iii) The end result of steps (i) and (ii) are SRSS transfer functions for response quantities of interest of the foundation and structure.

(iv) Using these transfer functions, calculate SSI time history response of foundation and structure and derived quantities such as in-structure response spectra; this represents the SRSS response.

All results presented in Chapter 5 and Appendix A denoted SASSI – SRSS are for this approach.

SRSS – SSI Response

The SRSS – SSI response approach (implemented in the EPRI version of SASSI-INCOH) is the application of Equation 4-4, including the applying the condition of no wave passage, i.e., $U_0(\omega) = 1$, and $\eta_\theta(\omega) = 1$, for all values of i, to the stage of determining the Fourier transform of the response quantity of interest, performing the Inverse Fourier transform to calculate the time history of response, and then from this time history determining the specific item of interest, such as peak value, in-structure response spectrum, etc. If all spatial modes were included at all SASSI frequencies, this would lead to q values of the response. These q values could then be SRSSed as the end product.

Tseng and Lilhanand (1997) applied this approach. This approach has not been validated by the research study documented in this report.

Linear Algebraic Summation (SASSI – AS)

For each SASSI frequency to be solved explicitly, the Linear Algebraic Summation (algebraic sum) approach takes the phase angle associated with each spatial mode as zero ($\theta = 0$ and $\eta_\theta(\omega) = 1$). This approach is implemented in ACS SASSI. Consequently, the motion at each interaction node point degree of freedom is calculated by Equation 4-3 assuming a linear algebraic sum of the spatial modes scaled by the square root of their eigenvalues. It should be noted that the square roots of the mode eigenvalues are equal to the standard deviations of the random mode contribution factors to the total stochastic spatial variability of the input motion.

Since this approach is applied directly in the context of the complex Fourier transform representation of the input motion in SASSI, it assumes that the Fourier amplitudes of two neighbor frequencies are statistically uncorrelated. Thus, the power content of the input motion is described with a high frequency resolution without including any spectral averaging or smoothing of the Fourier amplitudes. As a result of the high frequency resolution of the incoherent transfer function amplitudes (obtained by convolution in frequency domain of complex structural transfer functions with complex Fourier spatial free-field input variation at interaction nodes), the original SASSI interpolation scheme (Tajirian et al., 1981) could produce spurious spectral peaks and valleys. To avoid these spurious peaks and valleys in the interpolated transfer functions, an improved interpolation scheme that bases on the original SASSI interpolation scheme but includes a parametric spectral smoothing capability of the interpolation error was implemented. More specifically, first, the differences between the original computed complex transfer functions at the selected frequencies and the interpolated transfer function at all Fourier frequencies are computed at all Fourier frequencies (separate for the Fourier amplitudes and phases) and then, these amplitude differences are smoothed using the Parzen windowing technique with a user specified smoothing parameter (Parzen, 1962). For small smoothing parameter values, the final complex transfer functions are closer to the interpolated transfer functions using original SASSI interpolation scheme, while for large smoothing parameter, they are closer to the original computed transfer functions. The smoothing parameter value represents the number of Fourier frequency steps that is used to define the bandwidth of the Parzen spectral window (equal to the standard deviation of the Gaussian function used).

To include the effects of motion incoherency stochasticity of complex response phasing, the SASSI-AS approach assumes that complex response phase angles are limited to a variation range from –pi/2 to pi/2 that ensures that the phase angle cosines for all frequency components are positive. This phase angle variation limitation avoids the random occurrence of out-of-phase components due to motion incoherency and by this generates higher energy response time histories for given Fourier amplitude spectra. The Linear Algebraic Summation approach incorporates smoothing and the above phase adjustment to linear mode combination to form an approximate approach for computing the mean incoherent response that produces similar results with the SASSI-SRSS and SASSI Simulation approaches as shown in this report.

5
CLASSI AND SASSI IN-STRUCTURE RESPONSE SPECTRA COMPARISONS

General

CLASSI and SASSI computed incoherent seismic response were compared and shown to be in good agreement by Short et al. (2006). However, the example rock/structure model considered in those benchmark analyses did not produce significant incoherency-induced torsion and rocking response. The example rock/structure model used for benchmark comparisons in this study has offsets of mass centers from the shear centers and significant outriggers to overemphasize seismic response from incoherency-induced rotations as described in Chapter 2. It is judged that this example rock/structure model provides an extreme (conservative) level of torsion and rocking response induced by seismic wave incoherence for validation of either CLASSI or SASSI for seismic analysis.

Incoherency induced rotations are a random phenomena resulting from the horizontal spatial variation of ground motion over the foundation area. In addition, there are response quantities where several components of foundation motion contribute significantly such that the phasing of those components must be adequately represented in order to produce reasonable seismic response. Based on these considerations, two CLASSI methods as described in Chapter 3 and three SASSI methods as described in Chapter 4 are used herein for evaluating seismic response including seismic wave incoherence. These approaches include:

- CLASSIinco – deterministic phasing of foundation component response
- CLASSIinco-SRSS – SRSS combination of structural response computed from random phasing of foundation component response
- SASSI-SRSS – SRSS combination of modal transfer functions to represent random phasing of spatial modes
- SASSI Simulation Mean – Monte Carlo simulations to represent random phasing of spatial modes
- SASSI-AS – Algebraic summation of spatial modes with assumed deterministic phasing

Comparisons of seismic response by all of these methods are presented in Chapter 5 for the example nuclear power plant structure model as illustrated in Figure 5-1. Note that node numbers as used in CLASSI and SASSI analyses have been superimposed on this figure as compared to the similar figure in Chapter 2. These node numbers are referred to in the response spectra comparison figures of this chapter.

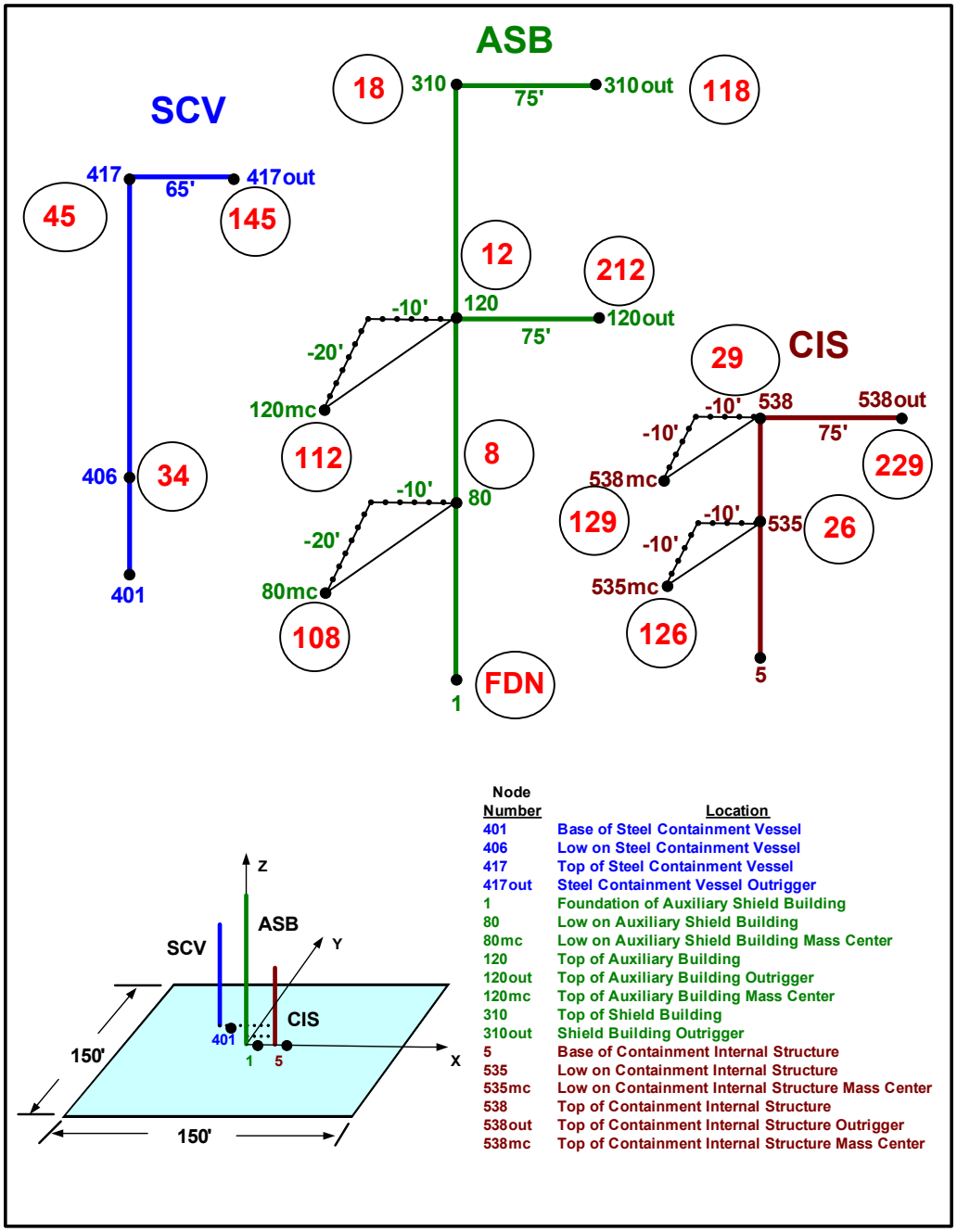

Figure 5-1
Locations on the AP1000-Based Stick Model With Offsets and Outriggers where In-Structure Response Spectra are Computed

Chapter 5 provides a summary of the results of the investigation into the effects of incoherence of ground motion on the response of a nuclear power plant structure. The structure being analyzed is a simplified model based on some of the AP1000 properties (described in Chapter 2). Note the structure model is comprised of three sticks with limited inter-connectivity at upper elevations. This model includes mass offsets and outriggers that exaggerate incoherency induced rotations. The structure is anchored to a 15-ft thick, 150-ft square foundation. This structure is

founded on the surface of the rock site profile described in Chapter 2. The high frequency content free-field ground motion compatible with the rock site profile also described in Chapter 2 was used. For all analyses, spectrum compatible time histories defined the free-field ground motion. All analyses reported in this chapter considered three directions of simultaneous earthquake input motion. Analyses were performed for three individual input motions (X, Y, and Z) and the resulting response spectra were combined by the square root of the sum of the squares (SRSS) to obtain response to the combined simultaneous input motion. This approach treats the effect of three components of ground motion for seismic analysis/design of nuclear power plant structures (ASCE, 2000). It does not treat other provisions, e.g., explicitly considering a range of site conditions (best estimate, lower bound, and upper bound), peak broadening and reductions of in-structure response spectra, etc. All other seismic analysis/design provisions will need to be addressed in the application of these methods to the seismic analysis/design process.

Note that the same coherency functions from Dr. Norm Abrahamson as were used by Short et al. (2006) are also used in this study (i.e., the soil site coherency functions). Recently, updated coherency functions have been developed by Dr. Abrahamson. However, the previous soil site coherency functions correspond to less coherent ground motion that will likely induce greater rotations that must be captured by the CLASSI and SASSI methods considered. Hence, the original coherency is judged to be a more stringent test for CLASSI-SASSI validation.

Six sets of analyses have been performed for the example structural model:

1. SSI analysis with coherent input motion determined by CLASSI (light blue curves in all Chapter 5 response spectra figures)
2. CLASSIinco with incoherent input motion (dark blue curves in all Chapter 5 response spectra figures)
3. CLASSIinco-SRSS with incoherent input motion (green curves in all Chapter 5 response spectra figures)
4. SASSI-SRSS with incoherent input motion (yellow curves in all Chapter 5 response spectra figures)
5. SASSI Simulations with incoherent input motion (black curves in all Chapter 5 response spectra figures). The mean of 15 simulations of randomly phased spatial modes is used for the analyses of this chapter
6. SASSI-AS with incoherent input motion (red curves in all Chapter 5 response spectra figures)

To evaluate the effects of incoherency on in-structure response, response spectra were calculated and compared for the various analyses at the foundation, at the tops of the structure sticks, and on outriggers extending 65 or 75-ft. from the top of each stick in the X direction. To evaluate the effects of induced rocking, the representative responses on the edge of the foundation, at the structure mass center and on the outrigger were examined. To evaluate the effects of induced torsion, the representative responses on the edge of the foundation and on the outriggers were examined.

CLASSI-SASSI Comparisons of In-Structure Response Spectra

Results presented are in-structure response spectra (5% damping) at the foundation and at representative points on each of the three models (ASB, SCV, CIS) as shown in Figure 5-1. Responses at the top of each model and on the foundation are calculated and compared for the six analysis methods listed above. Foundation response considered included X, Y, and Z foundation translation and XX, YY, and ZZ foundation rotation. The foundation rotation response is scaled by 75 feet to correspond to translation at the edge of the 150 foot square foundation. Two ASB, three CIS, and two SCV responses are considered. These correspond to the top of the structure shear center and an outrigger extending from the top of the structure. At the top of the ASB and SCV the shear and mass centers are assumed to be coincident. At the top of the CIS, the mass center is assumed to be offset from the shear center. In-structure response spectra at these eight locations for response in two horizontal directions, X and Y, and the vertical direction, Z, are presented in Figures 5-2 through 5-28. Again, all analyses considered three directions of simultaneous earthquake input motion. Results from the three individual input motion cases are presented in Appendix A.

Foundation Response

Foundation response is presented in Figures 5-2 through 5-7. Comparing the foundation translation response spectra including incoherency effects with results for coherent ground motion in Figures 5-2, 5-3, and 5-4, generally shows significant reductions over those due to coherent SSI effects at frequencies greater than 10 Hz. Comparing the foundation rotation response spectra including incoherency effects with results for coherent ground motion in Figures 5-5, 5-6, and 5-7, shows little or no reduction due to incoherency and, in some cases, increased response due to incoherency. Note that the response spectra for rotations are the rotation response times a lever arm of 75 feet such that they correspond to translation at an edge of the foundation. The horizontal spatial variation of ground motion comprising incoherency produces reduced translation response but also induces additional rotational response.

There is very close agreement in the incoherent results by all five methods considered for translational foundation response. Agreement is also quite good for the foundation rotational response. There is somewhat more deviation in rotational response between the various CLASSI and SASSI methods but it is judged to be acceptable for engineering purposes.

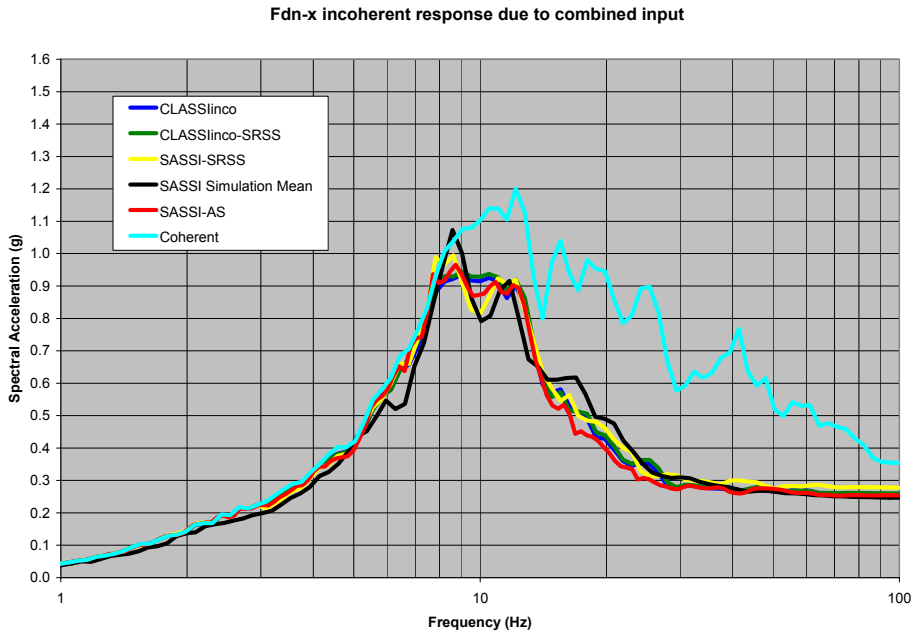

Figure 5-2
Center of Foundation Response Spectra – X Direction – CLASSlinco, CLASSlinco-SRSS, SASSI-SRSS, SASSI Simulation Mean, SASSI-AS (Node 1)

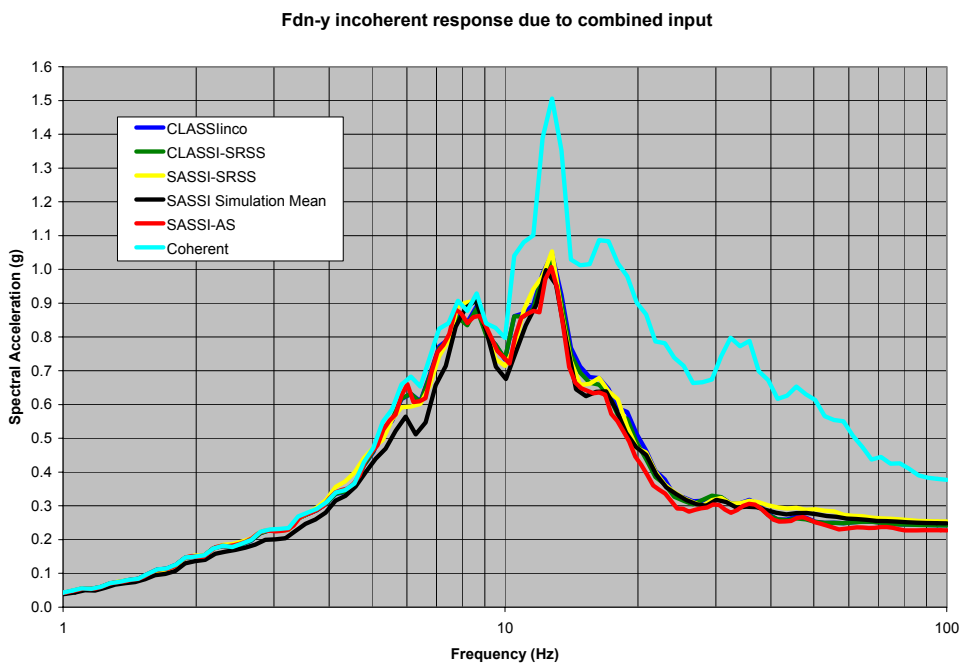

Figure 5-3
Center of Foundation Response Spectra – Y Direction – CLASSlinco, CLASSlinco-SRSS, SASSI-SRSS, SASSI Simulation Mean, SASSI-AS (Node 1)

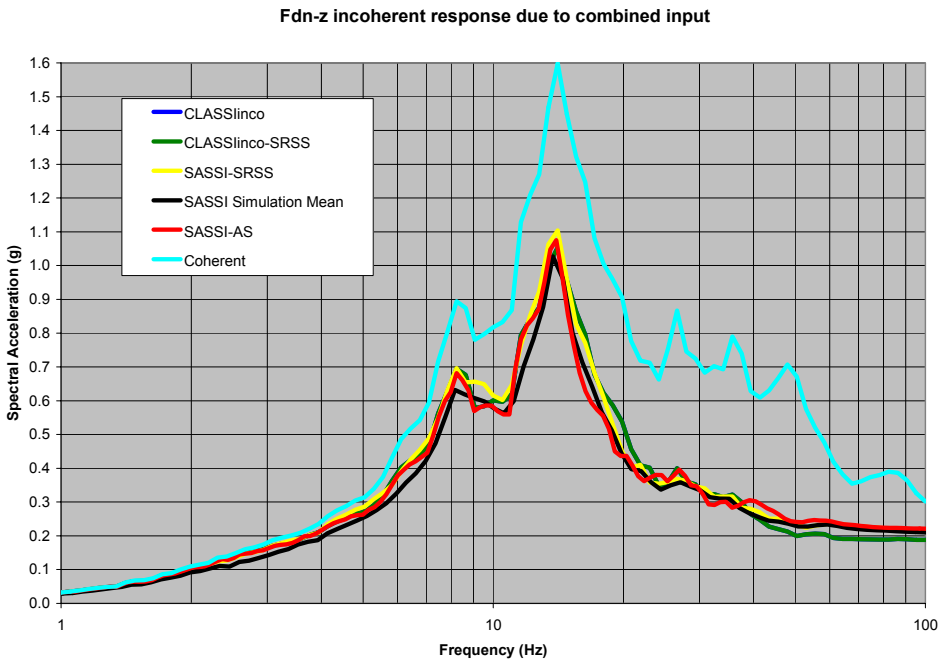

Figure 5-4
Center of Foundation Response Spectra – Z Direction – CLASSlinco, CLASSlinco-SRSS, SASSI-SRSS, SASSI Simulation Mean, SASSI-AS (Node 1)

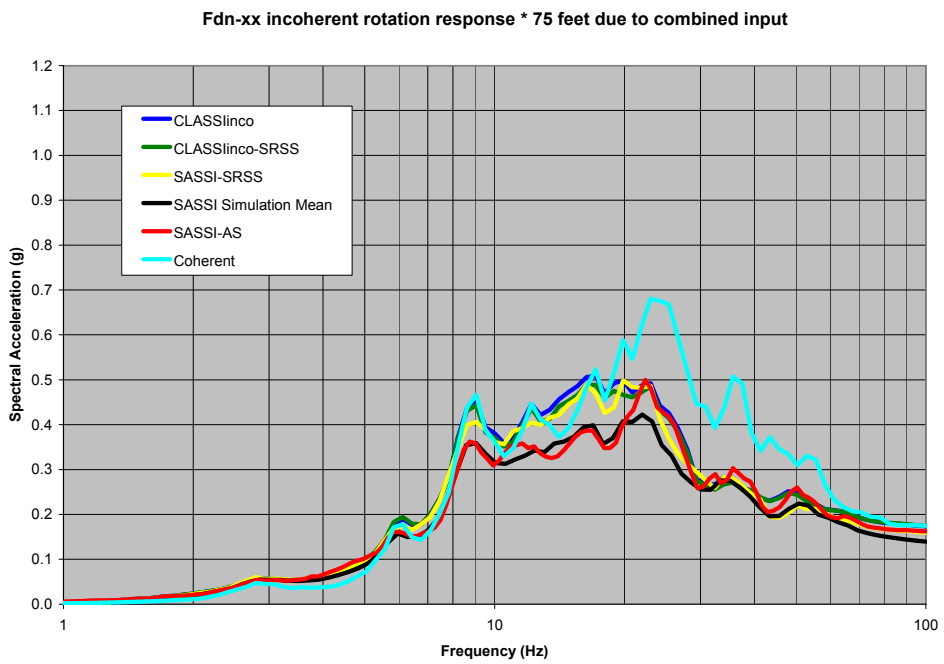

Figure 5-5
Edge of Foundation Response Spectra –XX Rotation – CLASSlinco, CLASSlinco-SRSS, SASSI-SRSS, SASSI Simulation Mean, SASSI-AS (Node 1)

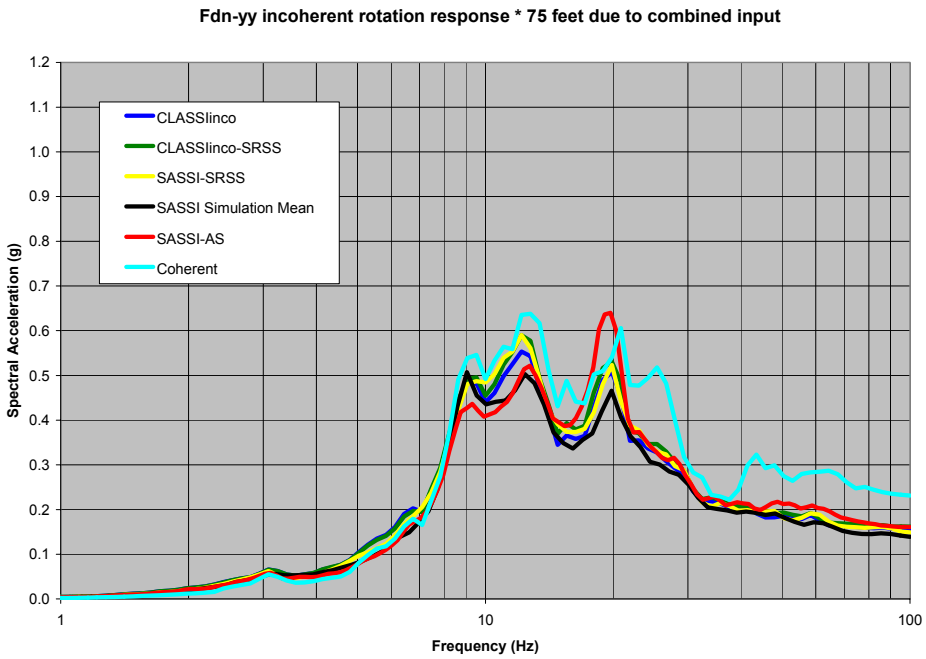

Figure 5-6
Edge of Foundation Response Spectra –YY Rotation – CLASSlinco, CLASSlinco-SRSS, SASSI-SRSS, SASSI Simulation Mean, SASSI-AS (Node 1)

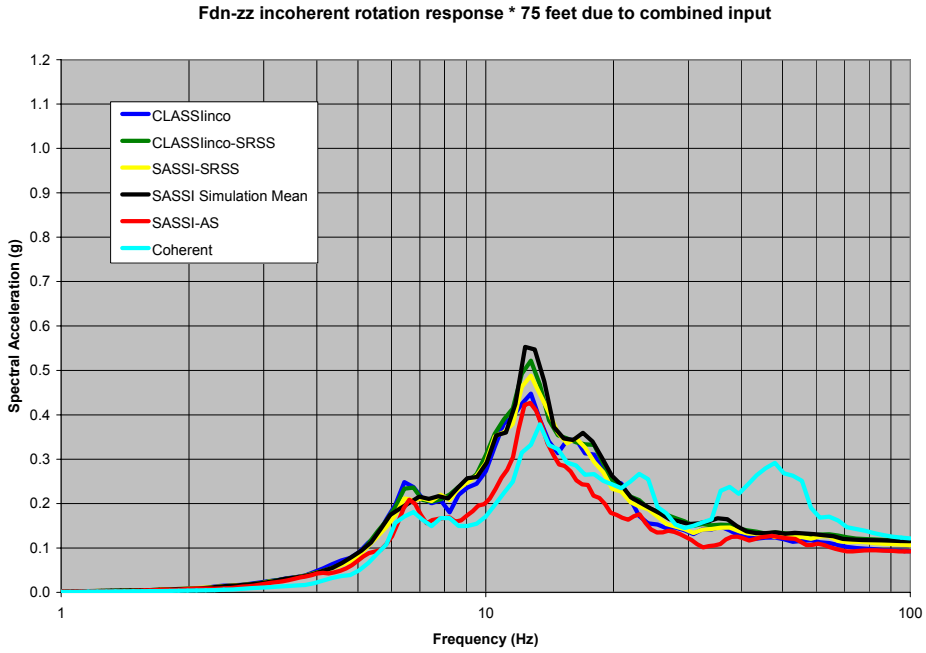

Figure 5-7
Edge of Foundation Response Spectra –ZZ Rotation – CLASSlinco, CLASSlinco-SRSS, SASSI-SRSS, SASSI Simulation Mean, SASSI-AS (Node 1)

Auxiliary and Shield Building (ASB)

- **Top of Shield Building.** Responses at the top of the coupled auxiliary and shield building (ASB) are presented in Figures 5-8, 5-9, and 5-10. Comparing the response spectra due to incoherency effects with the coherent results, generally, shows significant reductions due to incoherency for frequencies greater than 12 Hz for the horizontal directions and at frequencies greater than 10 Hz for the vertical direction. For horizontal directions, the reductions are, generally, greater than 30% up to 30 Hz and less as one approaches the ZPA frequency. For the vertical direction, substantial reductions are observed in the frequency range above 10 Hz, including at the ZPA frequency. At frequencies of peak amplification less than 10 Hz (X-direction 3.2 and 6.5 Hz; Y-direction 3 Hz and 6 Hz), slight increases in spectral accelerations of the incoherent case above the coherent case are observed. As was the case in earlier phases of this study, it was concluded that this effect is due to incoherency-induced rotations

  There is very close agreement among all five approaches for considering incoherency effects for the horizontal response. For vertical response, the agreement is good (acceptable for engineering purposes) but with somewhat greater deviations than for horizontal response.

  The responses of the outrigger, extending 75-ft. in the X-direction, are presented in Figures 5-11, 5-12, and 5-13. The reductions in response spectral accelerations generally follow the trend of the values on the centerline, but the reductions are observed to be less.

  There is very close agreement among all five approaches for considering incoherency effects for both horizontal and vertical response. The various CLASSI and SASSI methods agree within 10 percent at all frequencies, generally with differences much less than 10 percent.

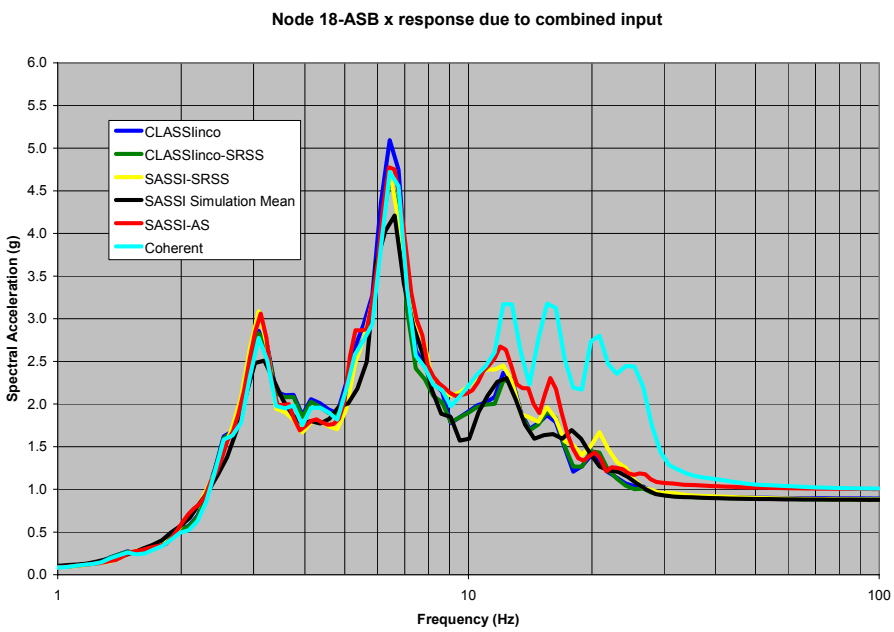

Figure 5-8
Top of ASB Response Spectra – X Direction – CLASSlinco, CLASSlinco-SRSS, SASSI-SRSS, SASSI Simulation Mean, SASSI-AS (Node 18)

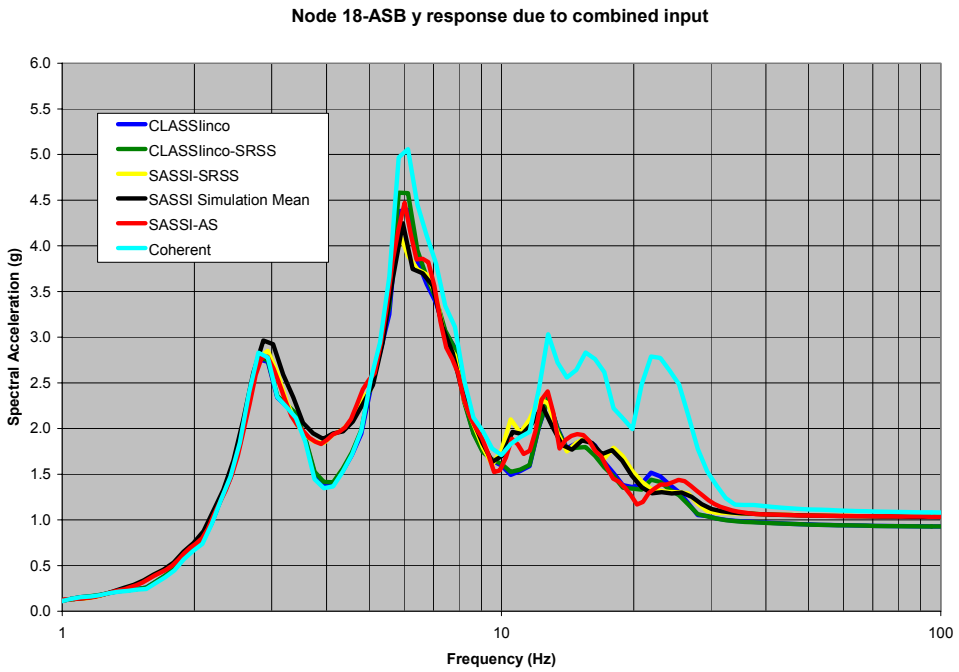

Figure 5-9
Top of ASB Response Spectra – Y Direction - CLASSIinco, CLASSIinco-SRSS, SASSI-SRSS, SASSI Simulation Mean, SASSI-AS (Node 18)

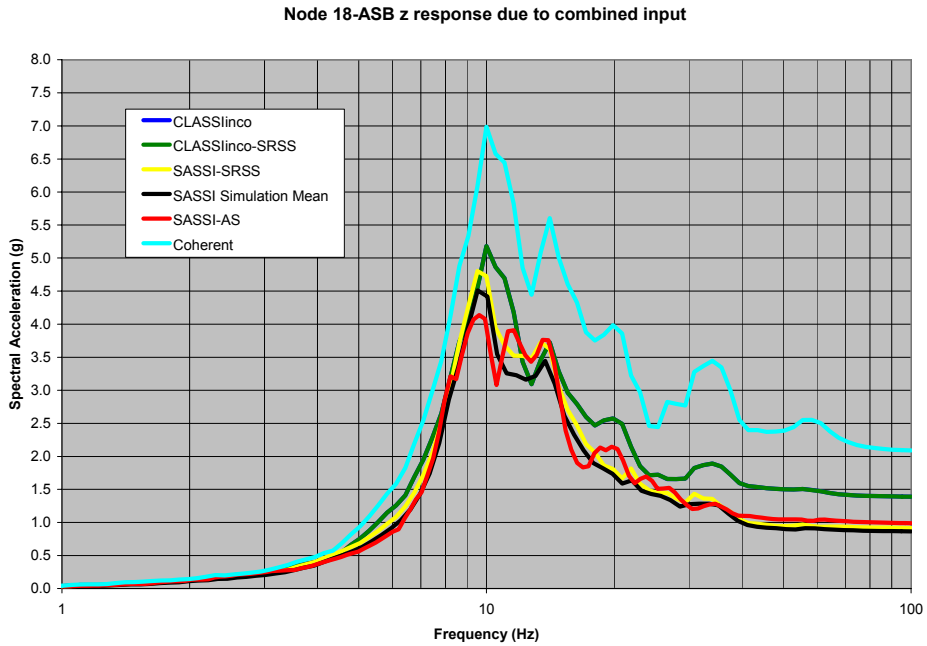

Figure 5-10
Top of ASB Response Spectra – Z Direction – CLASSIinco, CLASSIinco-SRSS, SASSI-SRSS, SASSI Simulation Mean, SASSI-AS (Node 18)

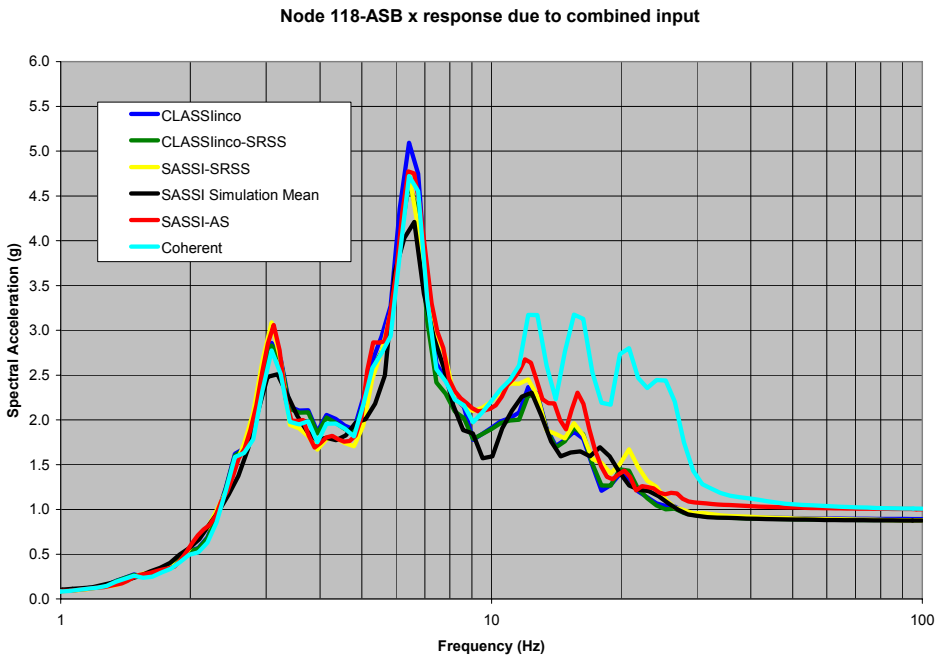

Figure 5-11
ASB Outrigger Response Spectra – X Direction – CLASSlinco, CLASSlinco-SRSS, SASSI-SRSS, SASSI Simulation Mean, SASSI-AS (Node 118)

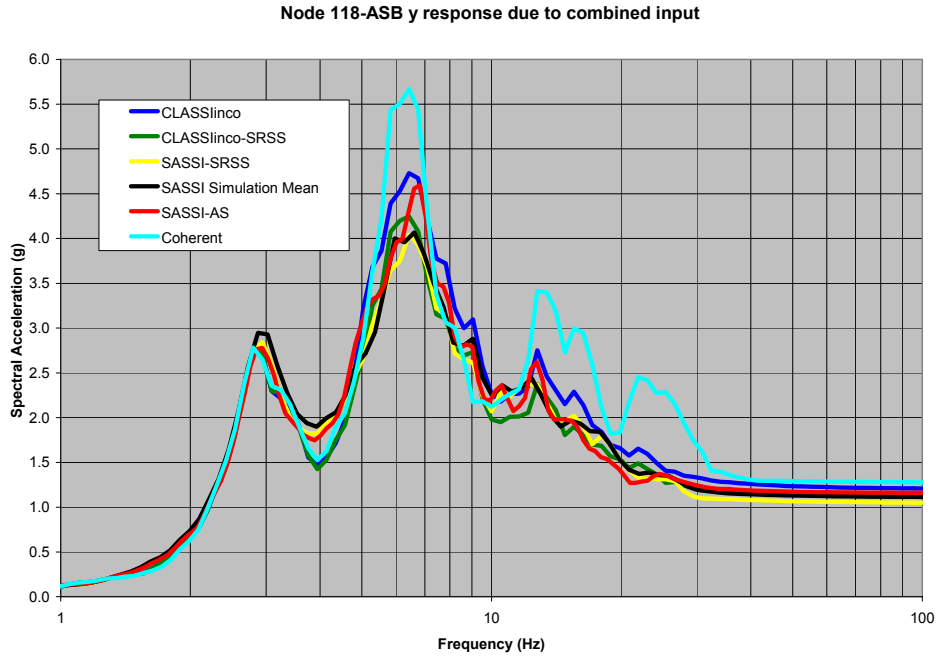

Figure 5-12
ASB Outrigger Response Spectra – Y Direction Due – CLASSlinco, CLASSlinco-SRSS, SASSI-SRSS, SASSI Simulation Mean, SASSI-AS (Node 118)

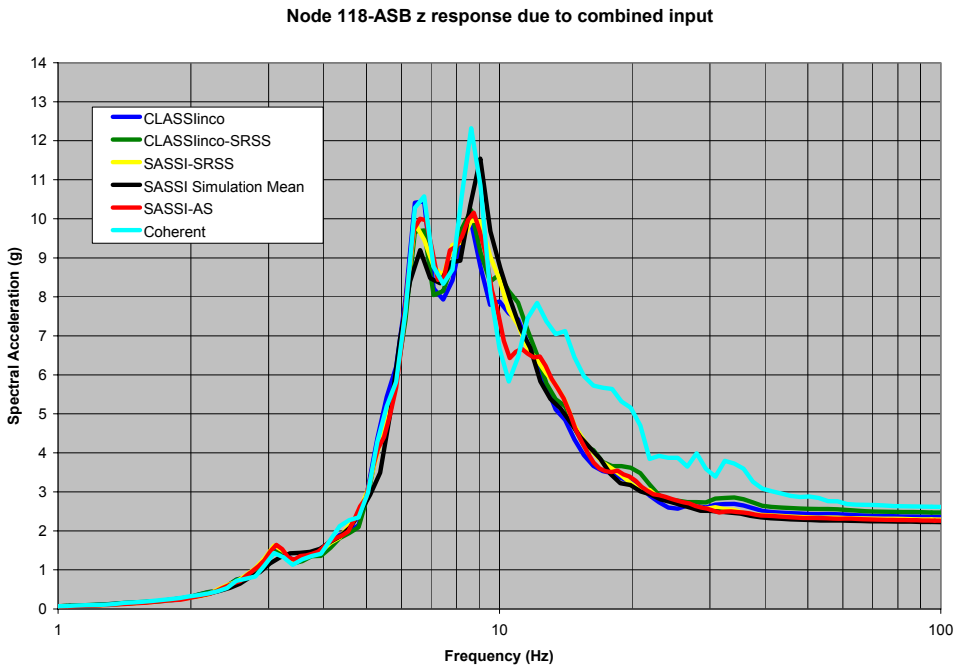

Figure 5-13
ASB Outrigger Response Spectra – Z Direction – CLASSlinco, CLASSlinco-SRSS, SASSI-SRSS, SASSI Simulation Mean, SASSI-AS (Node 118)

Containment Internal Structure (CIS)

- **Top of CIS.** Responses at the top of the containment internal structure (CIS) are presented in Figures 5-14 through 5-19. Responses of the outrigger extending 75-ft in the X direction from the top of the containment internal structure (CIS) are presented in Figures 5-20, 5-21, and 5-22. Comparing the response spectra due to incoherency effects with coherent seismic response, generally, shows significant reductions over those due to coherent SSI effects at frequencies greater than about 12 Hz. As expected for a high frequency structure like the CIS, these reductions are 50% or greater compared to the SSI coherent ground motion case.

  For this high frequency structure, there is very close agreement in incoherent seismic response at all frequencies for the CIS. The two CLASSI approaches and the three SASSI approaches agree well within engineering expectations.

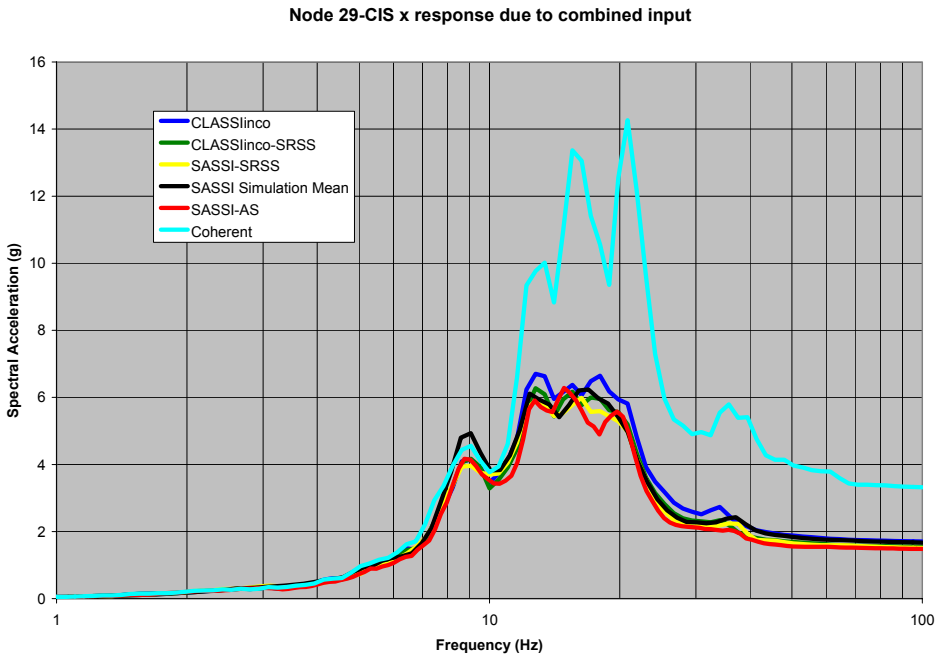

Figure 5-14
Top of CIS Shear Center Response Spectra – X Direction – CLASSlinco, CLASSlinco-SRSS, SASSI-SRSS, SASSI Simulation Mean, SASSI-AS (Node 29)

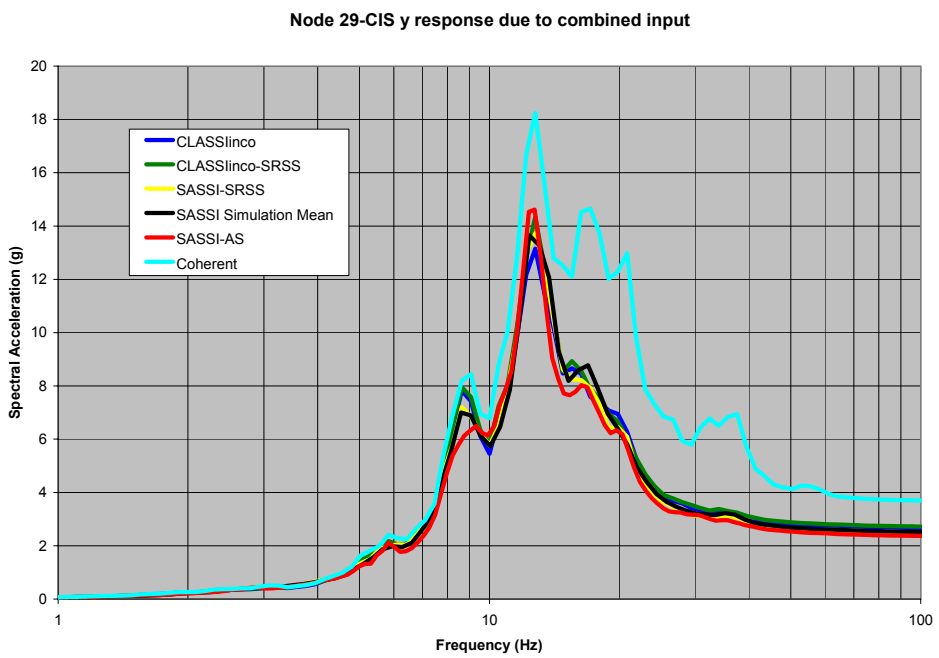

Figure 5-15
Top of CIS Shear Center Response Spectra – Y Direction – CLASSlinco, CLASSlinco-SRSS, SASSI-SRSS, SASSI Simulation Mean, SASSI-AS (Node 29)

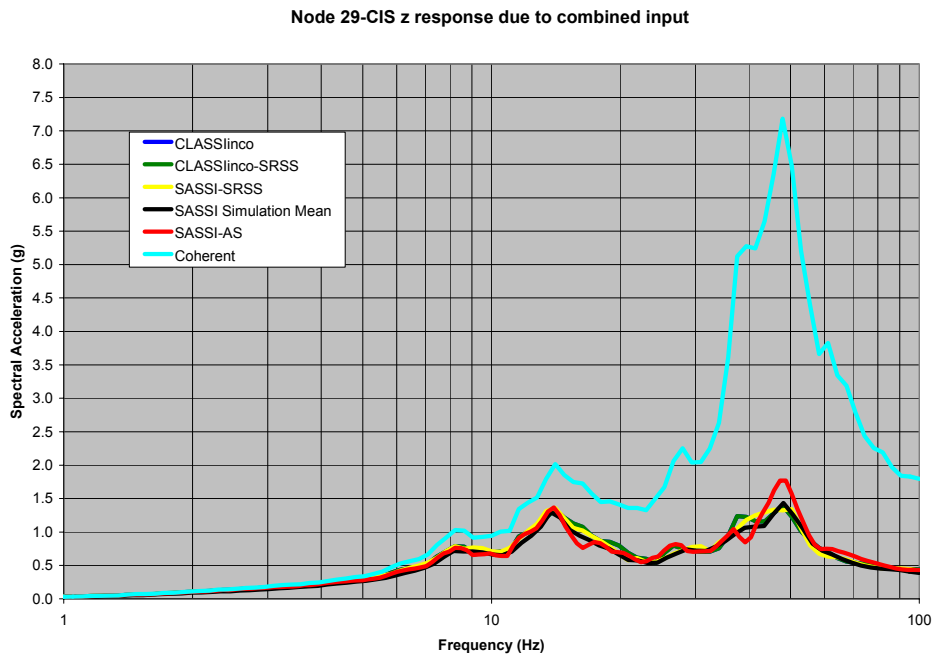

Figure 5-16
Top of CIS Shear Center Response Spectra – Z Direction – CLASSlinco, CLASSlinco-SRSS, SASSI-SRSS, SASSI Simulation Mean, SASSI-AS (Node 29)

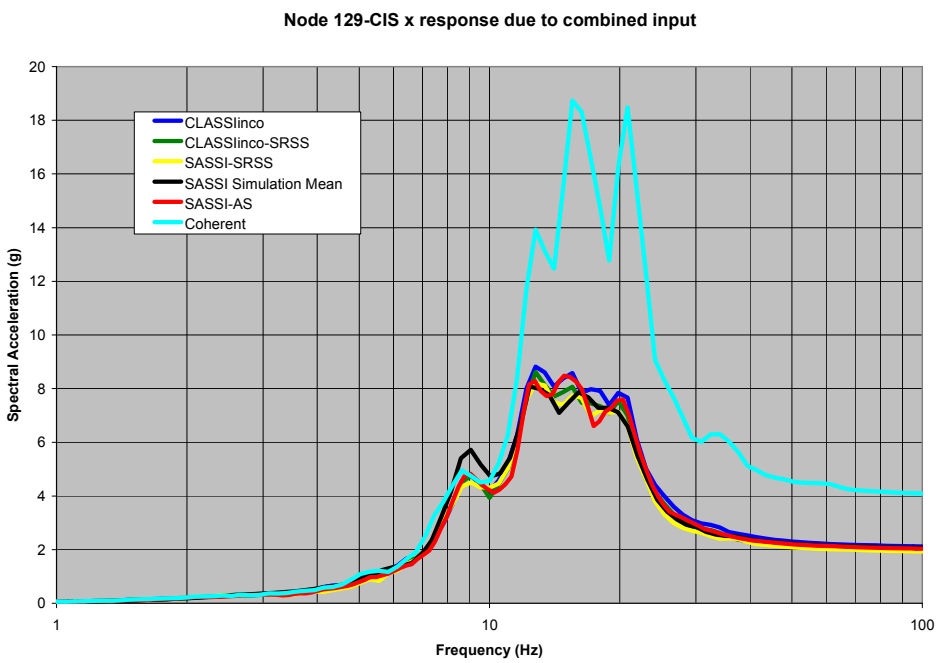

Figure 5-17
Top of CIS Horizontal Mass Center Response Spectra – X Direction – CLASSlinco, CLASSlinco-SRSS, SASSI-SRSS, SASSI Simulation Mean, SASSI-AS (Node 129)

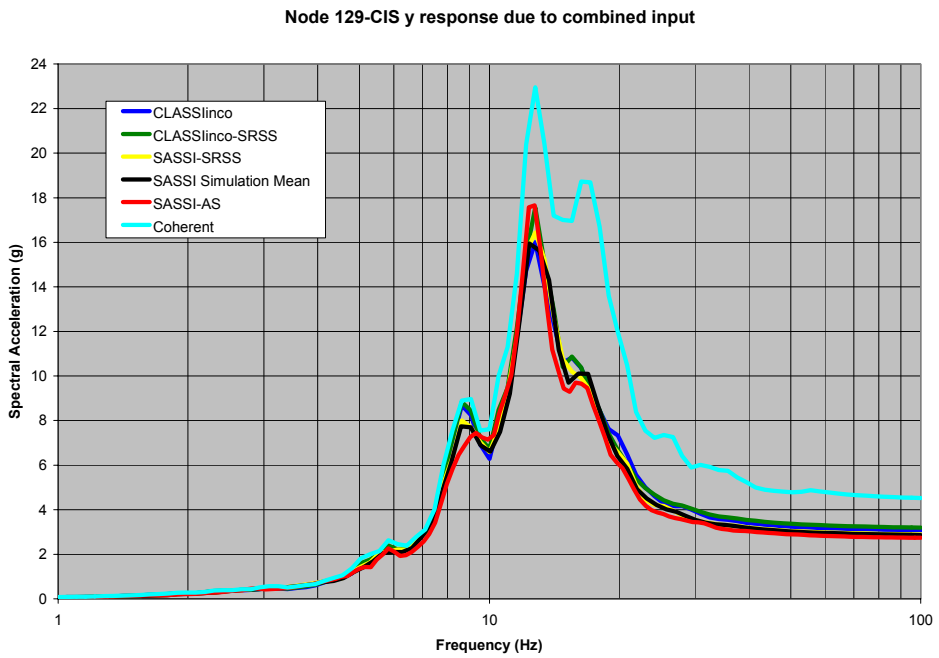

Figure 5-18
Top of CIS Horizontal Mass Center Response Spectra – Y Direction – CLASSlinco, CLASSlinco-SRSS, SASSI-SRSS, SASSI Simulation Mean, SASSI-AS (Node 129)

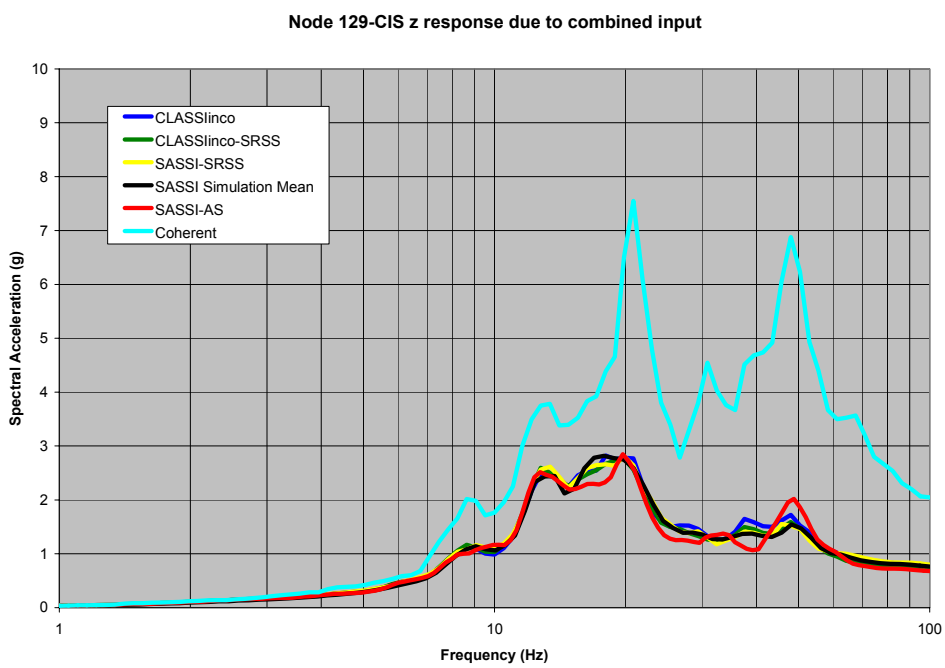

Figure 5-19
Top of CIS Horizontal Mass Center Response Spectra – Z Direction – CLASSlinco, CLASSlinco-SRSS, SASSI-SRSS, SASSI Simulation Mean, SASSI-AS (Node 129)

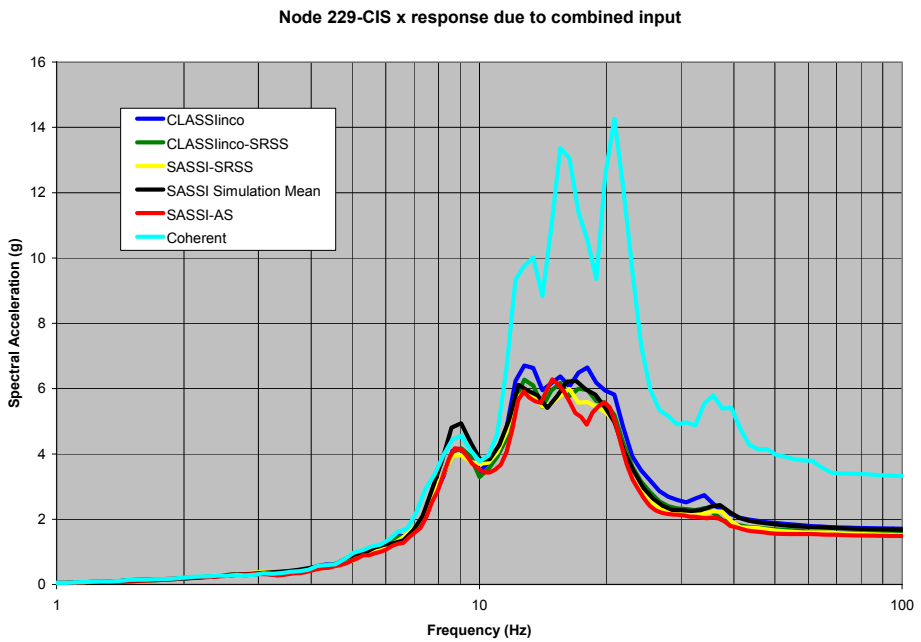

Figure 5-20
CIS Outrigger Response Spectra – X Direction – CLASSlinco, CLASSlinco-SRSS, SASSI-SRSS, SASSI Simulation Mean, SASSI-AS (Node 229)

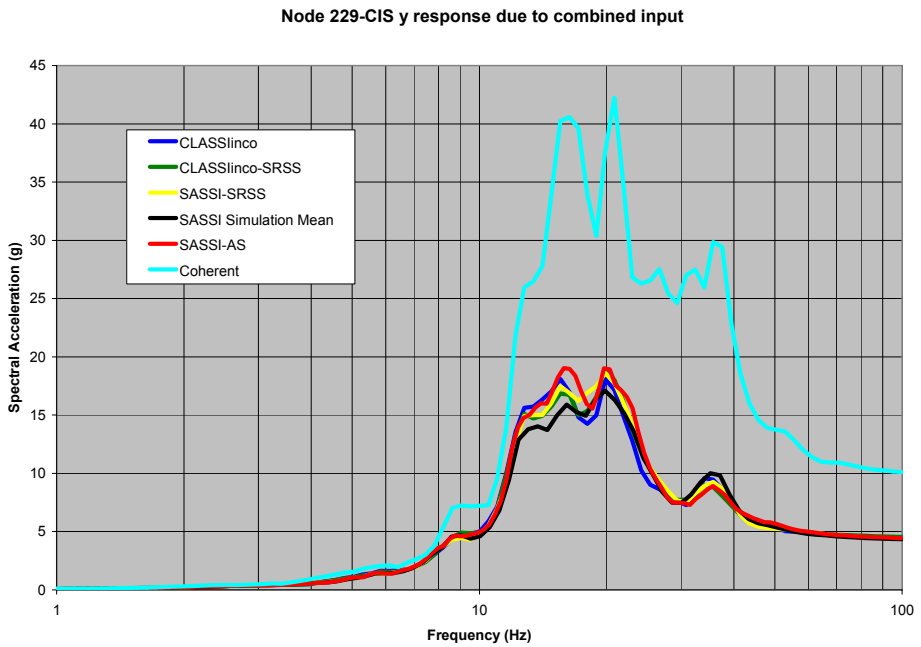

Figure 5-21
CIS Outrigger Response Spectra – Y Direction – CLASSlinco, CLASSlinco-SRSS, SASSI-SRSS, SASSI Simulation Mean, SASSI-AS (Node 229)

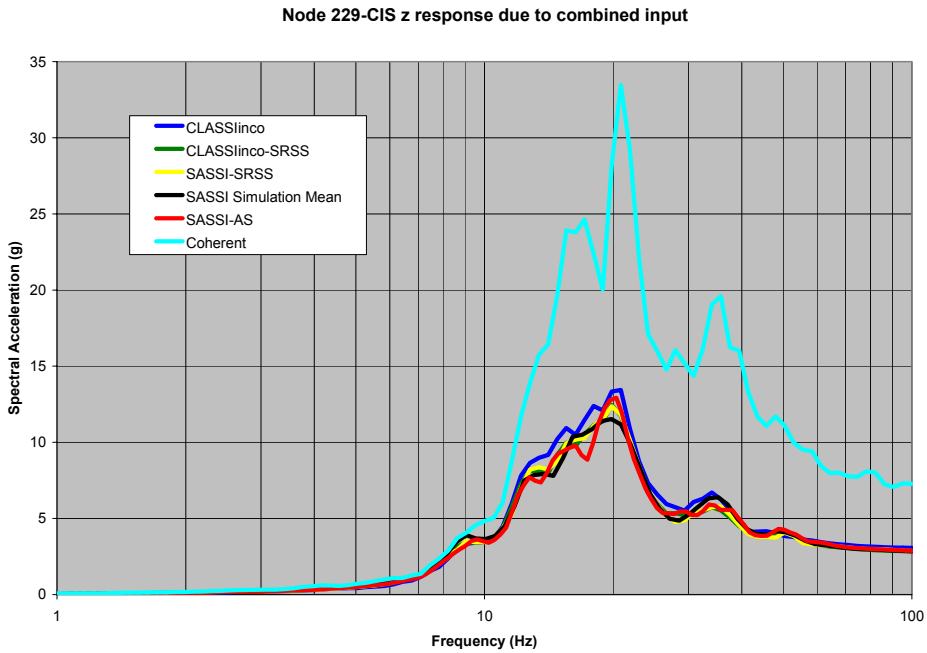

Figure 5-22
CIS Outrigger Response Spectra – Z Direction – CLASSIinco, CLASSIinco-SRSS, SASSI-SRSS, SASSI Simulation Mean, SASSI-AS (Node 229)

Steel Containment Vessel (SCV)

- **Top of SCV.** Response at the top of the steel containment vessel (SCV) at the centerline is presented in Figures 5-23, 5-24, and 5-25. The responses of the outrigger extending 75-ft in the X direction from the top of the steel containment vessel (SCV) are presented in Figures 5-26, 5-27, and 5-28. Comparing the response spectra due to incoherency effects with those for coherent ground motion, generally, show significant reductions in response for frequencies greater than about 12 Hz with less reductions at the ZPA. In the vertical direction, significant reductions are observed for all frequencies greater than 10 Hz.

  For the SCV, there is again very close agreement in incoherent seismic response at all frequencies. The two CLASSI approaches and the three SASSI approaches again agree well within engineering expectations.

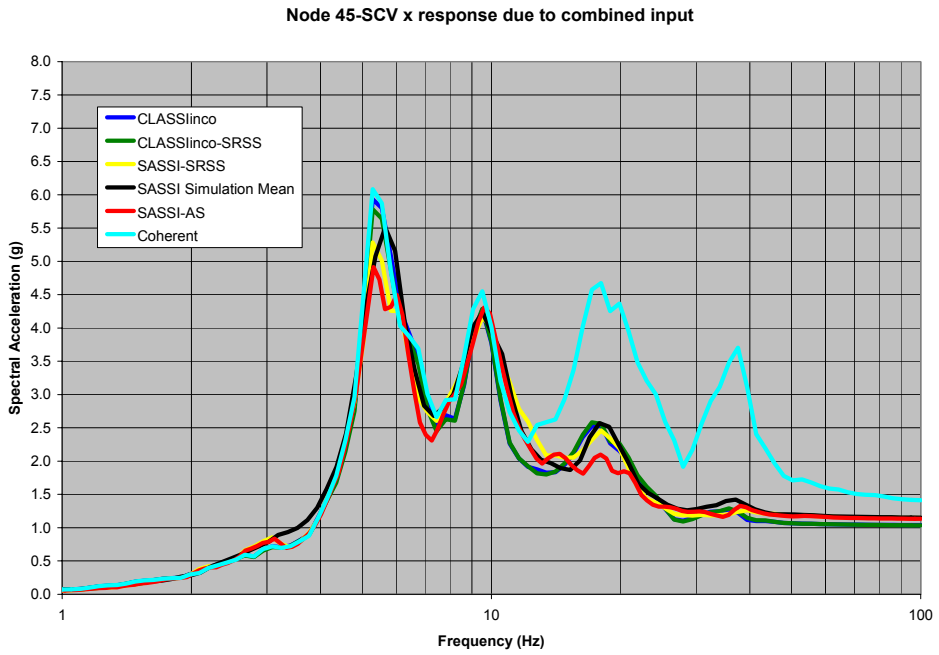

Figure 5-23
Top of SCV Response Spectra – X Direction – CLASSlinco, CLASSlinco-SRSS, SASSI-SRSS, SASSI Simulation Mean, SASSI-AS (Node 45)

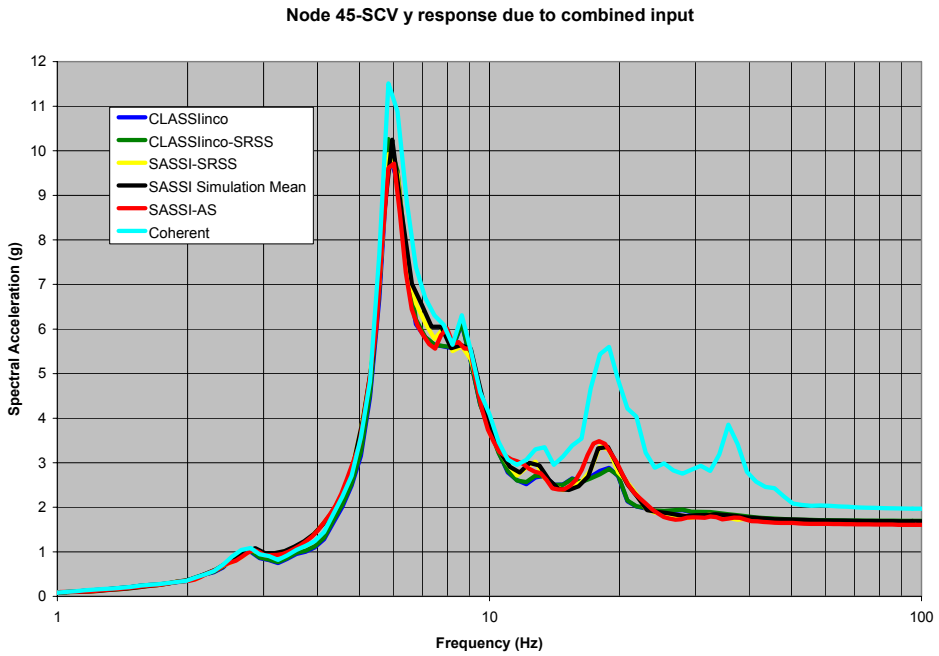

Figure 5-24
Top of SCV Response Spectra – Y Direction – CLASSlinco, CLASSlinco-SRSS, SASSI-SRSS, SASSI Simulation Mean, SASSI-AS (Node 45)

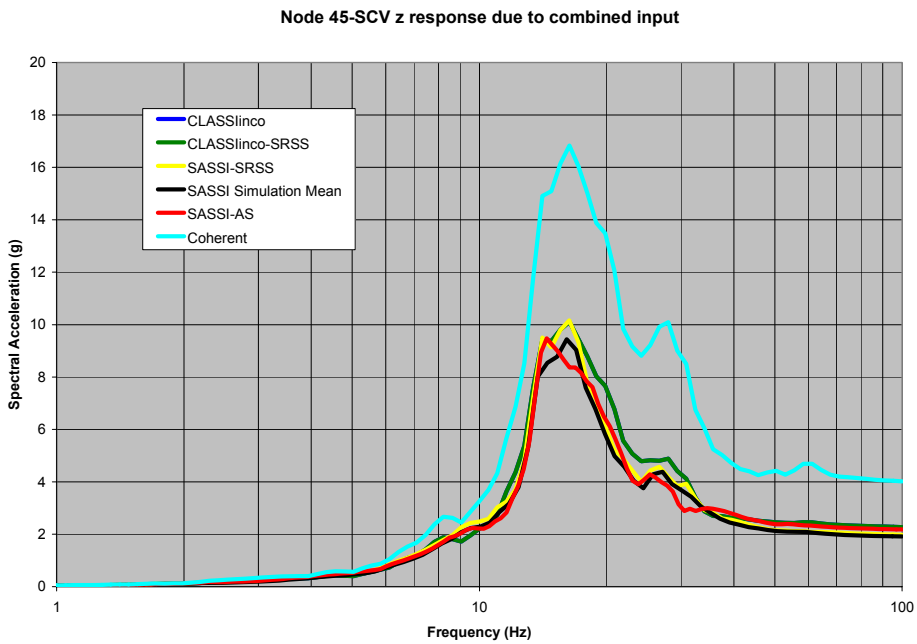

Figure 5-25
Top of SCV Response Spectra – Z Direction – CLASSlinco, CLASSlinco-SRSS, SASSI-SRSS, SASSI Simulation Mean, SASSI-AS (Node 45)

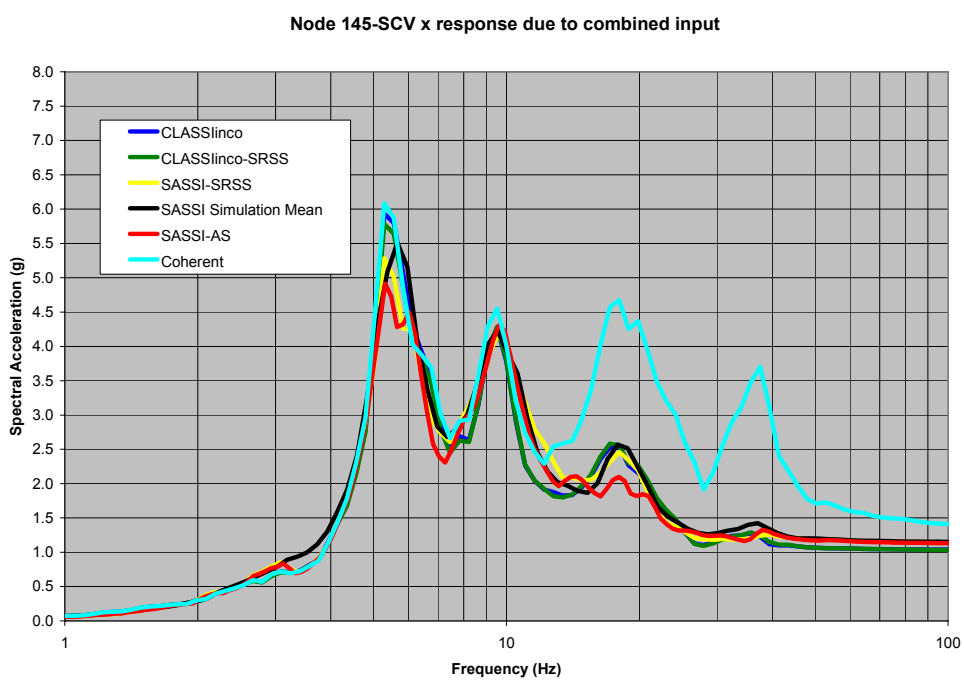

Figure 5-26
SCV Outrigger Response Spectra – X Direction – CLASSlinco, CLASSlinco-SRSS, SASSI-SRSS, SASSI Simulation Mean, SASSI-AS (Node 145)

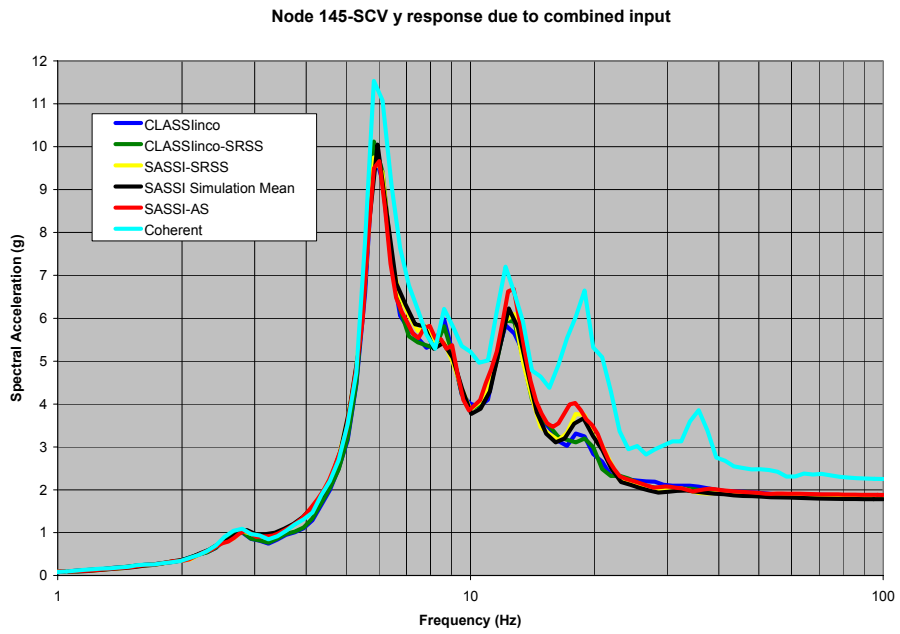

Figure 5-27
SCV Outrigger Response Spectra – Y Direction – CLASSlinco, CLASSlinco-SRSS, SASSI-SRSS, SASSI Simulation Mean, SASSI-AS (Node 145)

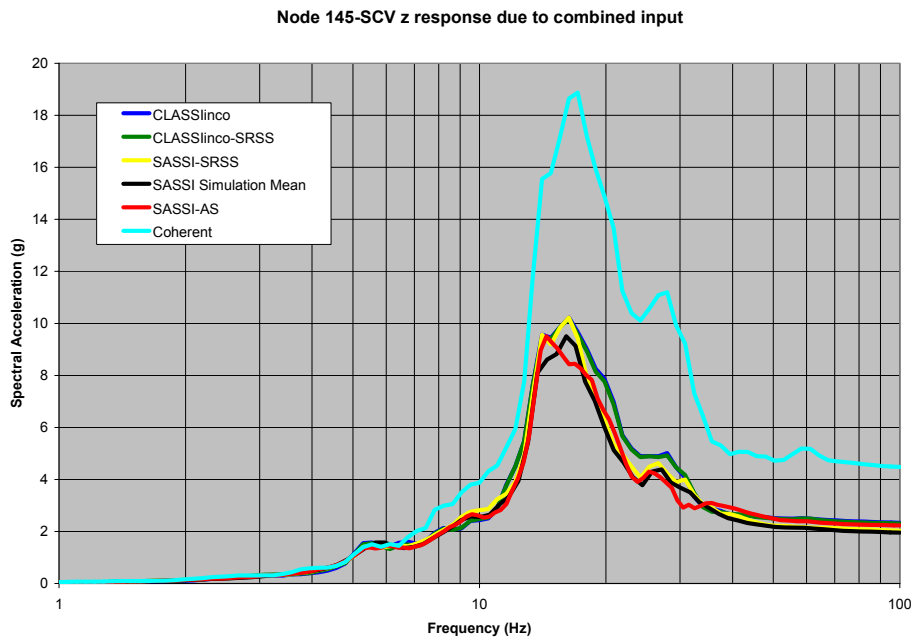

Figure 5-28
SCV Outrigger Response Spectra – Z Direction – CLASSlinco, CLASSlinco-SRSS, SASSI-SRSS, SASSI Simulation Mean, SASSI-AS (Node 145)

Summary of CLASSI-SASSI Comparisons

Figures 5-2 through 5-28 demonstrate significant reductions in high-frequency response as a result of seismic wave incoherence. In the horizontal response directions, these translational reductions in response spectra are tempered somewhat due to incoherency induced rocking and torsion. Even with this phenomena of incoherency induced rocking and torsion, the fundamental conclusion remains that there are significant reductions in high-frequency response due to seismic wave incoherence.

Figures 5-2 through 5-28 also demonstrate close agreement between the five methods of computing incoherent seismic response (i.e., CLASSIinco, CLASSIinco-SRSS, SASSI-SRSS, SASSI Simulations, and SASSI-AS). It is demonstrated by this study that any of these five methods is suitable for accurately determining seismic response to incoherent input ground motion. In Appendix A, response spectra for individual directions of input motion are presented. In the appendix, all methods agree well but there are some deviations by the CLASSIinco method and by the SASSI-AS method. The other methods (CLASSIinco-SRSS, SASSI-SRSS, SASSI Simulations) explicitly consider the random nature of incoherence and are preferable from a theoretical standpoint and produce slightly more accurate results. However, SASSI-SRSS and SASSI Simulations require significantly greater computation time than the CLASSIinco, CLASSIinco-SRSS, and SASSI-AS methods.

Based on the results presented in this chapter, CLASSI and SASSI are judged to be validated to treat seismic wave incoherence in SSI analyses of nuclear power plant structures. CLASSIinco, CLASSIinco-SRSS, SASSI-SRSS, SASSI Simulations, and SASSI-AS are all recommended for this use.

6
GUIDELINES FOR APPLICATION OF CLASSI AND SASSI

General

Both CLASSI (Wong and Luco, 1980) and SASSI (Lysmer, et.al.,1981) are computer programs for seismic analyses of structures founded on soil or rock that treat soil-structure interaction (SSI). Both of these programs treat both the inertial interaction and kinematic interaction aspects of SSI. In addition, both programs are actually a family of modules or sub-programs. Each module is an independent program that is executed in order to arrive at intermediate results for use in subsequent modules or the final desired result.

Typical usage of CLASSI and SASSI to perform seismic analyses of structures including the effects of SSI for coherent input ground motion. This application of the various program modules for both codes is briefly described in this chapter. CLASSI and SASSI have been modified to handle incoherent input ground motion for seismic analyses with SSI. The modifications that incorporate seismic wave incoherence into SSI analyses and guidance on their implementation are the primary subject of this chapter.

SASSI guidance presented in this chapter specifically applies to ACS SASSI (Ghiocel, 2006). ASC SASSI implements the SASSI-Simulation and SASSI-AS approaches for treatment of incoherent ground motion. There are detailed descriptions of these approaches in Appendix C. Guidance for other versions of SASSI that implement the SASSI-SRSS approach for treatment of seismic wave incoherence is available as a separate report (Ostadan and Deng, 2007).

CLASSI

The modules comprising the CLASSI family of SSI programs includes GLAY, CLAN, SAP, INSSIN, and SSIN. Each of these modules is briefly described below.

GLAY – Program GLAY was developed to calculate Green's functions that describe the steady-state dynamic force/displacement relationships between the source and observer points located on the surface of a layered visco-elastic halfspace. The calculations are performed at specified frequencies and at uniform intervals out to a specified maximum distance from the source. The results of these calculations are used by the Program CLAN to calculate impedance and wave scattering functions for surface functions of arbitrary shape.

Input to GLAY are soil properties defining the layered visco-elastic halfspace. These properties include shear wave velocity, mass density, Poisson's ratio, material damping ratio, and thickness of each soil layer. The equivalent-linear earthquake strain-compatible free field soil properties are used. Input for GLAY is given in GLAYIN. Output is given in two files, GLAYO and GRNFN.

CLAN – Program CLAN was developed to calculate dynamic soil impedance matrices and incident wave-scattering vectors for multiple rigid surface foundations of arbitrary shape, including through soil-coupling. CLAN uses the Green's functions calculated by GLAY, along with a user-defined discretized model of the soil-foundation interface. At the same frequencies specified for GLAY, the force-displacement relationships between each pair of foundation sub-regions are calculated by Gaussian integration of the Green's function over the sub-region areas. The impedance matrix and wave scattering vectors are then calculated by applying the constraints of rigid body motion. The standard version of CLASSI includes the option to consider the effects of wave passage; the modifications introduced as part of this program permit treatment of local wave scattering. These effects are modeled in the scattering functions.

Input to CLAN is GRNFN generated by GLAY and file, CLANIN. CLANIN contains control information as well as the definition and discretization of the geometry of the rigid foundation-soil interface. Output is given in two files, CLANO and IMPFN.

SAP – The structure is represented by its fixed base dynamic properties in CLASSI. These dynamic properties can be generated by any structural dynamics computer program such as SAP. The dynamic property output from the structural dynamics program must be properly formatted for the CLASSI SSI response calculation module, SSIN. This formatting is performed by the Program INSSIN. Hence, INSSIN must be compatible with the version of SAP used or other structural dynamics code, e.g., ANSYS, such that the structure fixed base dynamic characteristics can be properly read.

A finite element model of the structure is developed and input in the SAP input file, SAPI. This model is to be used for dynamic analyses and thus, must represent the mass and stiffness distribution of the structure. Eigenvalues and eigenvectors are extracted following guidance on the number of modes to consider per ASCE 4. An output file, SAPO with model and dynamic characteristic information is produced along with various other files for processing by INSSIN. Information, in the appropriate formats, required in other files include: node coordinates and mass properties, and the fixed-base modes and frequencies. In addition, if stress recovery is sought, an additional file of element stress/displacement is necessary.

INSSIN – Program INSSIN was developed to process the dynamic structural properties computed by SAP to generate structural data files for use by the program SSIN in the solution of soil-structure interaction problems.

Input for INSSIN is INSSINI, the input data file containing the control data defining the foundation reference point where the structure is attached to the rigid foundation. INSSINI also includes the control data defining in-structure responses to be calculated in the SSIN analyses. Other required input files for INSSIN are the SAP input file, SAPI, and files, as described above. Output for INSSIN is a file, INSSINO, containing a log of the execution of INSSIN and an output data file SSINST. SSINST contains modal frequencies, damping ratios, and participation factors for each mode, the rigid-body mass matrix of the model about the reference point, and the modal coordinates and rigid-body transformation vector for each user-specified response.

SSIN – Program SSIN was developed to perform soil-structure interaction response calculations of structures for multiple analyses that include random variation of soil and structure properties. To perform multiple SSI analyses, SSIN is computationally efficient. SSIN uses foundation impedance and incident wave scattering functions calculated by CLAN or, in some cases, by other programs where more general SSI solutions are sought (e.g., embedded structures). SSIN also uses the dynamic properties of the structure taken from INSSIN in combination with earthquake free-field acceleration time histories.

SSIN is capable of calculating the response of multiple structures supported on multiple rigid surfaces or embedded foundations depending on the program used to generate the impedance and wave scattering functions. Again, the dynamic representation of the structure is obtained by a fixed-base eigenvalue extraction analysis using a finite element analysis program such as SAP, with post-processors, such as INSSIN, to organize the data into the format that is expected by SSIN.

Input to SSIN includes four input files for its execution, SSININ, IMPFN, SSINST, and SSINTH. The file SSININ contains information such as the number of foundations, the number of structures on each foundation, the number of in-structure responses to calculate, and the number of earthquake cases. SSININ also contains the foundation mass matrices and control information for the input motion and wave scattering. IMPFN contains the impedance and scattering matrices for the foundations, as typically generated by CLAN. In general, the number of frequencies for which impedance and wave scattering data is calculated is much less than the number of frequencies used in the SSI analyses because these functions are much smoother than the Fourier spectra of the input and response time histories. Values for the Fourier analyses are obtained by linear interpolation of the input values. SSINST is the file with dynamic properties of the structure as generated by INSSIN. SSINTH is a file containing the input acceleration time histories (in the case of time history analysis) or the input Fourier spectra (in the case of pure Fourier analysis) to the problem. The format of the SSINTH file is specified in the SSININ file.

Output files for SSIN include SSINO and SSINP. SSINO contains a summary of the program execution including identification of the impedance and wave scattering data, structural data, and the input functions as well as a summary of the maximum values of foundation and structural response. SSINP contains selected in-structure response time histories or Fourier spectra determined from the analysis. Complete response of all foundation components is always included.

CLASSIinco

In order to consider incoherent ground motion, CLASSI was modified. The modifications consisted of revising the Program CLAN to CLANINCO in order to extract important information and of generating a new module, CLAN6 to compute incoherency transfer functions to describe wave scattering due to seismic wave incoherence. The output of CLAN6 is a revised IMPFN file with the impedance matrices and incoherent wave scattering vectors to be used with the remaining CLASSI modules in order to obtain seismic SSI response to incoherent ground motion. As a result, the sequence of modules to perform an SSI analysis for incoherent ground motion with the program, CLASSIinco is:

1. GLAY (same as for coherent analysis)
2. CLANINCO (creates input file for CLAN6; otherwise same as for coherent analysis)
3. CLAN6 (new module for incoherence)
4. Replace IMPFN with an incoherent IMPFN created by CLAN6 as input to SSIN
5. SAP (same as for coherent analysis)
6. INSSIN (same as for coherent analysis)
7. SSIN (same as for coherent analysis)

Note that modeling of the soil-structure system including the soil layers, the foundation discretization, and the finite element model of the structure are identical for either coherent or incoherent ground motion.

As described above, Program CLAN was developed to calculate dynamic soil impedance matrices and incident wave-scattering vectors for rigid surface foundations of arbitrary shape, including through soil-coupling. CLANINCO performs exactly the same function as CLAN and the input to CLANINCO is identical to that for CLAN, namely CLANIN and GRNFN.

The difference is that CLANINCO produces two output files, CLAN6dt and CLAN6db. CLAN6dt is a text file that includes control information as well as: (1) the frequencies of analysis; (2) information on foundation sub-regions including the differences in horizontal coordinates between every sub-region; (3) the impedance matrix at each frequency considered; and (4) the traction matrix at each frequency considered. CLAN6db is a binary file that includes the impedance matrix at each frequency considered and the traction matrix at each frequency considered. CLAN6 actually reads the impedance and traction data from the binary file.

The frequencies of the analysis, as stated above, are less than the total number in the Fourier analysis of input and response motions. These frequencies are input to GLAY and CLANinco (and CLAN) with an error created when they do not agree. These frequencies are output to the file CLAN6dt for use in CLAN6. The frequencies used in all CLASSI analyses including coherent runs and incoherent by CLASSIinco and CLASSIinco-SRSS are shown in Table 6-1. One hundred and forty two frequencies were used over the range from 0.1 Hz to 100 Hz. Note that for Fourier analysis, the intermediate frequencies are obtained by linear interpolation. Impedance functions and wave scattering vectors vary relatively smoothly with frequency such that linear interpolation accurately captures the response.

Table 6-1
Frequencies Used in CLASSI, CLASSlinco, and CLASSlinco-SRSS Analyses

No.	Frequency (Hz)	No.	Frequency (Hz)	No.	Frequency (Hz)	No.	Frequency (Hz)
1	0.1000	37	0.5834	73	3.4034	109	19.8550
2	0.1050	38	0.6127	74	3.5743	110	20.8520
3	0.1103	39	0.6434	75	3.7538	111	21.8990
4	0.1158	40	0.6758	76	3.9423	112	22.9990
5	0.1217	41	0.7097	77	4.1402	113	24.1530
6	0.1278	42	0.7453	78	4.3481	114	25.3660
7	0.1342	43	0.7827	79	4.5664	115	26.6400
8	0.1409	44	0.8220	80	4.7957	116	27.9770
9	0.1480	45	0.8633	81	5.0365	117	29.3820
10	0.1554	46	0.9067	82	5.2894	118	30.8580
11	0.1632	47	0.9522	83	5.5550	119	32.4070
12	0.1714	48	1.0000	84	5.8339	120	34.0340
13	0.1800	49	1.0502	85	6.1268	121	35.7430
14	0.1891	50	1.1029	86	6.4344	122	37.5380
15	0.1986	51	1.1583	87	6.7575	123	39.4230
16	0.2085	52	1.2165	88	7.0968	124	41.4020
17	0.2190	53	1.2776	89	7.4532	125	43.4810
18	0.2300	54	1.3417	90	7.8274	126	45.6640
19	0.2415	55	1.4091	91	8.2204	127	47.9570
20	0.2537	56	1.4798	92	8.6332	128	50.3650
21	0.2664	57	1.5541	93	9.0666	129	52.8940
22	0.2798	58	1.6322	94	9.5219	130	55.5500
23	0.2938	59	1.7141	95	10.0000	131	58.3390
24	0.3086	60	1.8002	96	10.5020	132	61.2680
25	0.3241	61	1.8906	97	11.0290	133	64.3440
26	0.3403	62	1.9855	98	11.5830	134	67.5750
27	0.3574	63	2.0852	99	12.1650	135	70.9680
28	0.3754	64	2.1899	100	12.7760	136	74.5320
29	0.3942	65	2.2999	101	13.4170	137	78.2740
30	0.4140	66	2.4153	102	14.0910	138	82.2040
31	0.4348	67	2.5366	103	14.7980	139	86.3320
32	0.4566	68	2.6640	104	15.5410	140	90.6660
33	0.4796	69	2.7978	105	16.3220	141	95.2190
34	0.5037	70	2.9382	106	17.1410	142	100.0000
35	0.5289	71	3.0858	107	18.0020		
36	0.5555	72	3.2407	108	18.9060		

In CLASSI (CLAN and CLANINCO) the foundation is discretized into rectangular sub-regions. The foundation sub-regions are defined by the X and Y (horizontal plane) coordinates of the center of each sub-region rectangle along with the sub-region shape number. For each sub-region shape defined, the X and Y dimensions of the rectangle are input. This information is input in the file CLANIN and output in the file CLAN6dt for use in CLAN6. The distances between sub-regions are important parameters needed for the development of the coherency matrix [γ] as discussed in Chapter 3 and defined by Equation 3-1.

The impedance matrix at each frequency is normal output of CLAN or CLANinco in file, IMPFN. However, the impedance matrices and the tractions matrices are needed in CLAN6 to perform the operations described in Chapter 3 and given in Equation 3-4. As a result, these matrices are written to files CLAN6dt and CLAN6db for use in CLAN6 for the evaluation of the scattering transfer function [F] by Equation 3-4.

CLAN6 is a new CLASSI module for analysis of incoherent ground motion. After reading in the frequencies of analysis, foundation sub-region information, and impedance and tractions matrices, the program produces a new file in IMPFN format with the name CIMPSCT. CIMPSCT is then renamed to IMPFN for incoherent runs completing the CLASSI SSI analysis (i.e., Steps 5, 6, and 7 above). The IMPFN file for coherent motion generated by CLANinco (and CLAN) is overwritten for the incoherent analysis.

Currently, there are three versions of CLAN6, each with a different coherency function programmed into the module. These are:

- CLAN6-Luco & Wong – Equation 3-22
- CLAN6-Abrahamson Soil – Equation 2-1
- CLAN6 Abrahamson Hard Rock (Abrahamson, 2007)

Results from CLAN6-Luco & Mita are presented in Chapter 3. Results from CLAN6-Abrahamson Soil are presented in Chapter 5 and Appendix A. For this validation study, the soil coherency function has been maintained for consistency with past results and consistency among the various approaches employed. Results for the hard rock coherency function are presented in Appendix B with comparisons to the results generated with the soil coherency functions. In the future, there will be a single version of CLAN6 in which the desired coherency function may be requested.

Input to CLAN6 is a brief input file, CLAN6IN and files CLAN6dt and CLAN6db, generated by CLANINCO. CLAN6IN contains control information. In addition, for rigid, massless foundation problems as described in Chapter 3, this file could also include the PSD matrix of the input motion, $[S_o^{1/2}]$ as used in Equation 3-11.

CLAN6 generates the coherency matrix $[\gamma]$, the scattering transfer function [F], and the incoherency transfer function, ITF as determined from Equation 3-21 and the associated discussion. As described in Chapter 3, the wave scattering vectors for X, Y, and Z input motion are determined from the ITF matrix and input into the file CIMPSCT along with the impedance matrix for each frequency considered. For CLASSIinco, the wave scattering vector for each direction includes the ITF terms for all 6 foundation degrees of freedom. Upon completion of the CLAN6 run, the CIMPSCT file is renamed IMPFN, overwriting the corresponding coherent motion file and the remainder of the CLASSI SSI analysis is performed.

CLASSIinco-SRSS

CLASSIinco-SRSS is identical to CLASSIinco with the exception that CLAN6-SRSS is used instead of CLAN6. The difference in CLAN6-SRSS and CLAN6 is that in addition to the output file CIMPSCT as described above, six additional output files with impedance function and wave scattering vectors are produced, CIMPSCTX, CIMPSCTY, CIMPSCTZ, CIMPSCTXX, CIMPSCTYY, and CIMPSCTZZ. For each direction of motion, each of these files only has the wave scattering term for one of the foundation degrees of freedom, translations X, Y, Z, and rotations XX, YY, ZZ, with the other five terms set to zero. For each direction, there are then six IMPFN files created from which 18 SSI analyses are performed. From the 18 SSIN analyses

there are 18 SSINP files with response time histories. For structural locations of interest, response spectra are computed. For example, for X-direction input motion, there will be 6 individual response spectra, RSi-x-x, RSi-x-y, RSi-x-z, RSi-x-xx, RSi-x-yy, and RSi-x-zz. The resulting response spectra at location i, due to x direction input, RSi-x is then determined by:

$$RS_{i-x} = \sqrt{(RS_{i-x} - x)^2 + (RS_{i-x} - y)^2 + (RS_{i-x} - z)^2 + (RS_{i-x} - xx)^2 + (RS_{i-x} - yy)^2 + (RS_{i-x} - zz)^2}$$

Results for individual directions of input motion as determined above are presented in Appendix A.

When the response of location i is desired for simultaneous occurrence of three directions of earthquake motion, RS_i may be determined by:

$$RS_i = \sqrt{(RS_{i-x})^2 + (RS_{i-y})^2 + (RS_{i-z})^2}$$

Results for combined directions of input motion as determined above are presented in Chapter 5.

The sequence of modules and actions to perform an SSI analysis for incoherent ground motion with the program, CLASSIinco-SRSS is:

1. GLAY (same as for coherent analysis; frequencies in Table 6-1)
2. CLANINCO (creates input file for CLAN6; otherwise same as for coherent analysis)
3. CLAN6-SRSS (new module for incoherence)
4. Replace IMPFN with incoherent IMPFNs created by CLAN6 as input to SSIN. Six IMPFN files are created for each foundation degree of freedom, 3 translations and 3 rotations.
5. SAP (same as for coherent analysis)
6. INSSIN (same as for coherent analysis)
7. SSIN (same as for coherent analysis, except that six SSIN runs are performed; one for each of the six IMPFN files)
8. Generate six response spectra corresponding to the excitation of each of the foundation degrees of freedom and combine by SRSS to obtain the in-structure response spectra for incoherent motion

SASSI

The modules comprising the SASSI family of SSI programs include SITE, POINT, HOUSE, ANALYS, COMBIN, MOTION, and STRESS. These modules are common to all available versions of SASSI. These modules are organized in such a way that each handles the calculation of a few analysis steps so that the site response analysis, the impedance analysis, the formation of the complex dynamic stiffness and mass matrices of the complete soil/structure system, the calculation of transfer functions, and the convolution of transfer functions with the input motion to obtain structural responses can all be performed separately with the results being stored on intermediate files. Each of these modules is briefly described below.

SITE – The SITE module solves the site response problem. Based on input site soil properties and the wave field specified for the control motion, free-field mode shapes are computed and written to TAPE1, and the information required to compute transmitting boundaries used in solving the impedance problem is computed and saved on TAPE2.

Important inputs to SITE are the frequencies at which calculations are to be made in frequency sets. Calculations at these frequencies may be combined at a later stage as described below. To be computationally efficient, it is necessary to perform calculations at much fewer frequencies than are used for Fourier analysis and calculated values at intermediate frequencies are determined by interpolation. Comparisons of calculated and interpolated values are compared to assure adequacy of the computation. In addition to the frequencies, the time step of the input control motion and the number of frequency values to be used in the Fourier transform of the control motion are input. From these data the frequency step is computed.

Other input to SITE includes information about soil layers. Individual soil layers and a halfspace beneath must be defined. Input for the layers and halfspace includes unit weight, shear wave velocity, compression wave velocity, shear wave associated damping ratio, and compression wave associated damping ratio. For the soil layers, the layer number and its thickness must be defined. For the halfspace, the number of layers to simulate the halfspace is input.

The last input to SITE is information on the control motion about the wave fields that comprise the motion and the soil layer number at which the control motion is to be applied. The convention used on this project is the horizontal motion in the X and Y directions consist of vertically propagating SH waves (acting independently), and vertical motion in the Z direction consists completely of vertically propagating P waves,

POINT – The POINT module solves for the Green's functions needed for computing the compliance matrix for all interaction nodes (i.e., nodes that are coincident between the soil and the structure) with pertinent information saved on TAPE3. For each frequency specified in the SITE program and for a given radius of the central zone as input to POINT, the program solves for point loads applied at the surface of the layered soil system and on the layer interfaces below the ground surface for embedded structures.

Input to POINT includes the maximum number of layers in the ground to which the structure is embedded and the radius of the central zone for the point load solution. The radius of the central zone depends on the geometry of foundation discretization by the finite element method.

HOUSE – The HOUSE module input has all the information describing the structure and its foundation including node locations, element connectivity, material properties, and structure/foundation mass. This module forms the frequency-independent mass and stiffness matrices for the structure and the soil in the embedded region and stores it to TAPE4.

HOUSE input is similar to any structural analysis finite element program such as SAP. It is our practice to develop the structural model in the computer program SAP2000 taking advantage of its graphical user interface and convert the resulting files to HOUSE format. An important parameter is the Z or vertical coordinate of the ground surface. This ties the structural finite element model defined in HOUSE to the soil layers defined in SITE in the vertical direction.

ANALYS – As stated in the SASSI manual, the ANALYS program is the heart of SASSI. This module consists of three sub-modules, namely MATRIX, LOADS, and SOLVE. The MATRIX sub-module uses Tapes 3 and 4 created by POINT and HOUSE, respectively, as input to form the impedance matrix for each frequency and store it on TAPE5. MATRIX also forms the modified complex stiffness matrices in triangularized form and saves them on TAPE6. The LOADS module used the input data from TAPE1 created by SITE to compute the load vector for each frequency and store it on TAPE7. The SOLVE module uses the input data on TAPE6 and TAPE7 created by MATRIX and LOADS to compute the transfer functions for the structural response motions relative to the control motions and save them to TAPE8.

There are limited input items for the ANALYS module. One important input item is the horizontal X and Y coordinates of the control point. Other input quantities are related to output of transfer functions.

COMBIN – The generation of structural response transfer functions by ANALYS is the most computationally intensive part of SASSI. As a result, it is common to run several sets of frequencies in order to limit individual run times and to assure that the proper frequencies are being used such that stable transfer functions at all frequencies are developed. The COMBIN module combines the structural response transfer functions from 2 frequency sets saved on TAPE8 created by ANALYS to a new TAPE8.

MOTION – The MOTION module reads the structural response transfer functions from TAPE8 created by ANALYS, performs the interpolation to all Fourier frequencies. At this point, calculated and interpolated transfer functions are compared to ensure that stable transfer functions are developed that capture the frequency content of soil-structure response. With stable transfer functions, it performs the convolution of the interpolated transfer functions with the control motions in the frequency domain and computes the inverse Fast Fourier Transforms of the structural response back to the time domain. For seismic analysis, in-structure acceleration time histories and response spectra are computed.

Input to MOTION includes the locations for computation of in-structure responses and the input motion acceleration time history. Also, the control information for generation of in-structure response spectra such as damping ratios and frequencies for spectra computation are specified.

STRESS – The STRESS module reads input from TAPE 4 and TAPE8 created by HOUSE and ANALYS, respectively and computes stress, strain, and force time histories and their corresponding peak values for structural elements as requested.

The input to STRESS consists primarily of the locations in the structural model where stress, strain, or force output is requested. The input acceleration time history is also specified for STRESS.

SASSI Simulations

The SASSI Simulation approach was executed for this study in ACS SASSI.

SITE - The initial step in SASSI analyses is to define the soil layers, the control point layer, the wave field characteristics of the control motion including the direction of the control motion, the frequencies of analysis, and the number of Fourier components. These are all input to the SITE module. All input items are identical between coherent analyses and incoherent analyses except for the number of frequencies.

A larger number of frequencies are required to perform incoherent analysis than is typically needed for coherent analysis. For coherent analysis, there must be sufficient frequencies to capture the dynamic amplification at the natural frequencies of the soil-structure system. For incoherent analysis, there are many additional frequencies of interest due to the stochastic nature of the incoherent foundation motion. This point will be illustrated later in this chapter when transfer functions are discussed. For the SASSI Simulation analyses performed in this study, 224 frequencies were specified in SITE. The specific frequencies used in these analyses are listed in Table 6-2.

POINT - The execution of POINT is identical between coherent and incoherent analyses. The radius of the central zone is specified based on the discretization of the foundation.

HOUSE - The input of the data describing the structure and the foundation to the HOUSE module is identical between coherent and incoherent analyses. In ACS SASSI, input parameters for selection of the coherency function are in the HOUSE module. At this point, one of five coherency functions may be selected:

1. Luco & Wong – Equation 3-22
2. Abrahamson, 1993
3. Abrahamson Soil Surface – Equation 2-1
4. Abrahamson Soil Embedded, December 2006
5. Abrahamson Hard Rock, April 2007

There is the option to consider wave passage effects for the Abrahamson coherency functions and the apparent wave velocity is another input quantity for HOUSE. All analyses for this study considered plane wave coherency only with no wave passage effects.

The number of spatial modes to use for incoherent SSI analyses is another input quantity in HOUSE. The 150 foot square foundation was discretized into 144 squares that are 12.5 feet on a side with 169 node points. These 169 nodes that are in contact with both the foundation and the soil are specified to be interaction nodes. As a result, there are a total of 169 spatial modes. In ACS SASSI, the first n spatial modes may be utilized in an incoherent analysis. For all SASSI Simulation analyses in this study, all 169 modes were selected.

Table 6-2
Frequencies Used in SASSI Simulation and SASSI-AS Analyses

No.	Frequency (Hz)	No.	Frequency (Hz)	No.	Frequency (Hz)	No.	Frequency (Hz)
1	0.049	57	10.600	113	21.780	169	44.970
2	0.342	58	10.790	114	21.970	170	46.000
3	0.684	59	10.990	115	22.170	171	46.970
4	0.977	60	11.230	116	22.360	172	48.000
5	1.172	61	11.430	117	22.560	173	48.970
6	1.367	62	11.620	118	22.750	174	50.000
7	1.562	63	11.820	119	22.950	175	50.980
8	1.660	64	12.010	120	23.140	176	52.000
9	1.758	65	12.210	121	23.340	177	52.980
10	1.855	66	12.400	122	23.540	178	54.000
11	2.002	67	12.600	123	23.730	179	54.980
12	2.100	68	12.790	124	23.930	180	56.010
13	2.197	69	12.990	125	24.120	181	56.980
14	2.295	70	13.180	126	24.320	182	58.010
15	2.490	71	13.380	127	24.510	183	58.980
16	2.588	72	13.570	128	24.710	184	60.010
17	2.686	73	13.770	129	24.900	185	60.990
18	2.832	74	14.010	130	25.100	186	62.010
19	2.930	75	14.210	131	25.290	187	62.990
20	3.125	76	14.400	132	25.490	188	64.010
21	3.320	77	14.600	133	25.680	189	64.990
22	3.516	78	14.790	134	25.880	190	66.020
23	3.711	79	14.990	135	26.070	191	66.990
24	3.906	80	15.190	136	26.270	192	68.020
25	4.150	81	15.380	137	26.460	193	68.990
26	4.395	82	15.580	138	26.660	194	70.020
27	4.590	83	15.770	139	26.860	195	71.000
28	4.785	84	16.020	140	27.050	196	72.020
29	4.980	85	16.210	141	27.250	197	73.000
30	5.176	86	16.410	142	27.440	198	74.020
31	5.371	87	16.600	143	27.640	199	75.000
32	5.566	88	16.800	144	27.830	200	76.030
33	5.762	89	16.990	145	28.030	201	77.000
34	6.006	90	17.240	146	28.320	202	78.030
35	6.201	91	17.430	147	28.610	203	79.000
36	6.396	92	17.630	148	28.910	204	80.030
37	6.592	93	17.820	149	29.100	205	81.010
38	6.787	94	18.020	150	29.350	206	82.030
39	6.982	95	18.210	151	29.690	207	83.010
40	7.227	96	18.410	152	30.030	208	84.030
41	7.422	97	18.600	153	30.520	209	85.010
42	7.617	98	18.800	154	31.010	210	86.040
43	7.812	99	18.990	155	31.540	211	87.010
44	8.008	100	19.240	156	32.030	212	88.040
45	8.203	101	19.430	157	33.010	213	89.010
46	8.398	102	19.630	158	34.030	214	90.040
47	8.594	103	19.820	159	35.010	215	91.020
48	8.789	104	20.020	160	36.040	216	92.040
49	8.984	105	20.210	161	37.010	217	93.020
50	9.180	106	20.410	162	38.040	218	94.040
51	9.375	107	20.610	163	39.010	219	95.020
52	9.570	108	20.800	164	39.990	220	96.040
53	9.766	109	21.000	165	40.970	221	97.020
54	10.010	110	21.190	166	41.990	222	98.000
55	10.210	111	21.390	167	42.970	223	99.020
56	10.400	112	21.580	168	43.990	224	100.000

The next decision that has to be made for execution of HOUSE is to decide on the means of incoherency motion simulation. The input choices are:

1. Deterministic Incoherency Input
2. Stochastically Simulated Incoherency Input

By the SASSI-Simulation approach described herein, option 2 is selected. In addition, horizontal and vertical random seed numbers must be selected as well as the range over which the random spatial mode phasing is uniformly distributed. The range for all analyses performed in this study is taken to be from minus 180 degrees to plus 180 degrees.

ANALYS – One important input quantity in ANALYS is the Z-coordinate of the control point. This parameter links the soil layer information in SITE with the structure and foundation information in HOUSE. In addition, ANALYS may be specified as an initial run or as a restart run. This is significant as ANALYS requires the longest computer run time of the SASSI modules. The transfer functions for all degrees of freedom at the input frequencies are calculated in ANALYS. There is no specific input that is unique to incoherent analysis for this module.

MOTION – Input to MOTION includes the specification of desired output locations and identification of the input control motion time history. This input is applicable for either coherent or incoherent analyses. For incoherent analysis, a smoothing parameter is specified that aids in interpolation of transfer functions.

A challenge in running SASSI SSI analyses is to develop stable transfer functions at all frequencies required in Fourier analysis. In MOTION, the calculated transfer functions from ANALYS combined with an interpolation scheme are used to evaluate the transfer functions at the Fourier frequencies and at specified response locations. The calculated and interpolated transfer functions are compared to decide if stable transfer functions are determined. A stable transfer function is achieved when the interpolated transfer function used in response analysis reflects only the behavior represented by the calculated transfer function values.

In coherent SSI analysis, where there is deviation between the calculated and interpolated transfer functions, additional calculated transfer functions are computed by repeating SITE, POINT, HOUSE, and ANALYS for another frequency set. All of the calculated transfer functions are combined in the module COMBIN when more than one frequency set is used.

In incoherent SSI analysis, it may be more challenging to achieve stable transfer functions with the SASSI interpolation scheme. Some transfer functions have a large number of peaks and valleys for which the interpolation scheme introduces unrealistic spurious peaks and valleys. The stochastic nature of the incoherent transfer functions does not necessarily enable achievement of stable transfer functions by the addition of more frequencies at which calculated transfer functions are obtained.

As a result, the approach for incoherent SSI analysis is to use a larger number of frequencies than would be used for coherent analysis to assure that the actual soil-structure dynamic behavior is being captured and then to aid the SASSI interpolation scheme by employing the smoothing technique described in Chapter 4. For all SASSI Simulation runs, 224 frequencies were used and smoothing parameter of 10 was specified in MOTION. It is believed that more frequencies than will be typically needed were used for these analyses and that the number of frequencies for incoherent analysis will be in the range of 100 to 200 based on the judgment of the analyst.

The smoothing parameter value represents the number of Fourier frequency steps that is used to define the bandwidth of the Parzen spectral window (the standard deviation of the Gaussian function). For small smoothing parameter values, say 1-5, the final smoothed complex transfer functions are closer to the interpolated transfer functions using original SASSI interpolation scheme and large deviations from the calculated transfer function values are reduced or eliminated when larger smoothing parameters are used. Depending on the selection of the frequency set for transfer function calculations, a smoothing parameter value from 10 to 100 is recommended. Before deciding the final smoothing parameter value to be used, the user should compare the original computed amplitude transfer functions with the interpolated amplitude transfer functions. If spurious spectral peaks or valleys are present in the interpolated transfer functions, then the smoothing parameter should be increased.

It should be noted that the spectral windowing is a smoothing or interpolation method that reconstructs the transfer functions. If the selected set of frequencies for SSI analysis is insufficient for capturing some key features of the response spectral content, then spectral windowing will not help to improve results. The selection of an appropriate set of frequencies for response calculations remains as an aspect of essence for the SSI analysis accuracy.

Examples of the effect of smoothing are seen in Figures 6-1 and 6-2. These figures show both calculated and interpolated transfer functions. The curve labeled TFI is the interpolated transfer function at all of the Fourier frequencies. The points labeled TFU are the calculated (or un-interpolated) transfer function values.

Figure 6-1 shows the transfer function for Z direction foundation response (node 1) due to Z input motion where Figure 6-1a is for no smoothing (smoothing parameter equals zero) and Figure 6-1b is for some smoothing with the smoothing parameter specified to be 10. For the relatively smooth transfer function of foundation z response due to z input, smoothing has very little effect; with 224 frequencies, the calculated and interpolated transfer functions are nearly equal. There is a very minor peak near 5 Hz that is removed by the smoothing process.

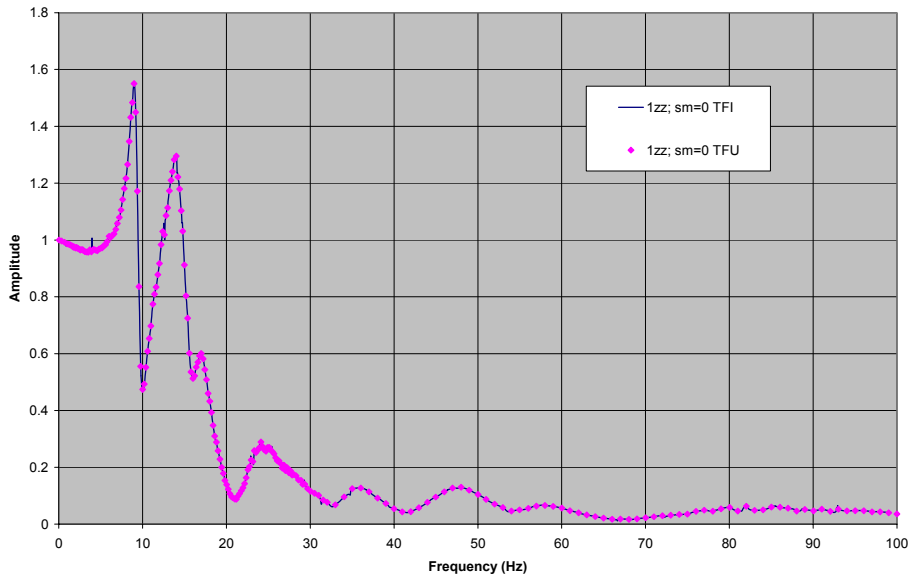

a. Smoothing parameter = 0

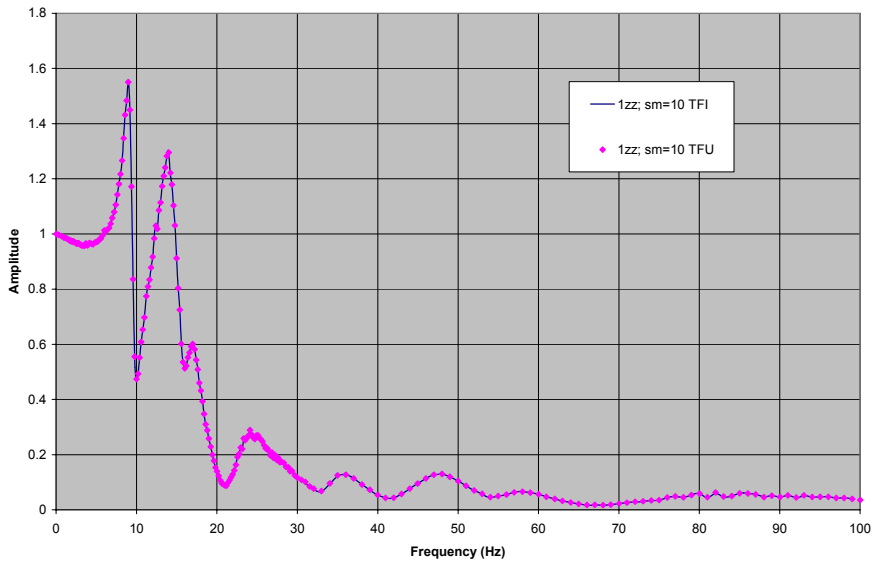

b. Smoothing parameter = 10

Figure 6-1
Foundation Transfer Function – Z Direction Due to Z Input– (Node 1)

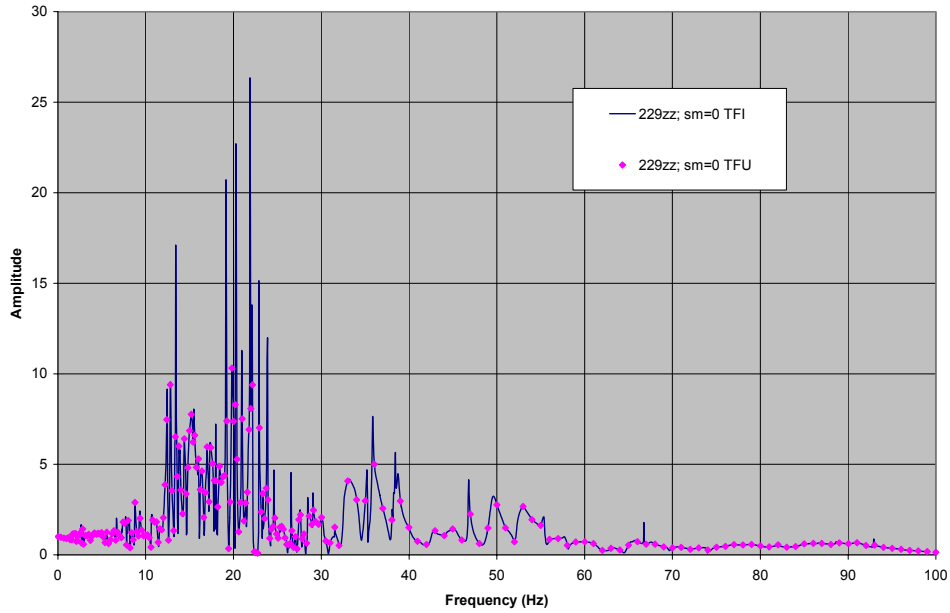

a. Smoothing parameter = 0

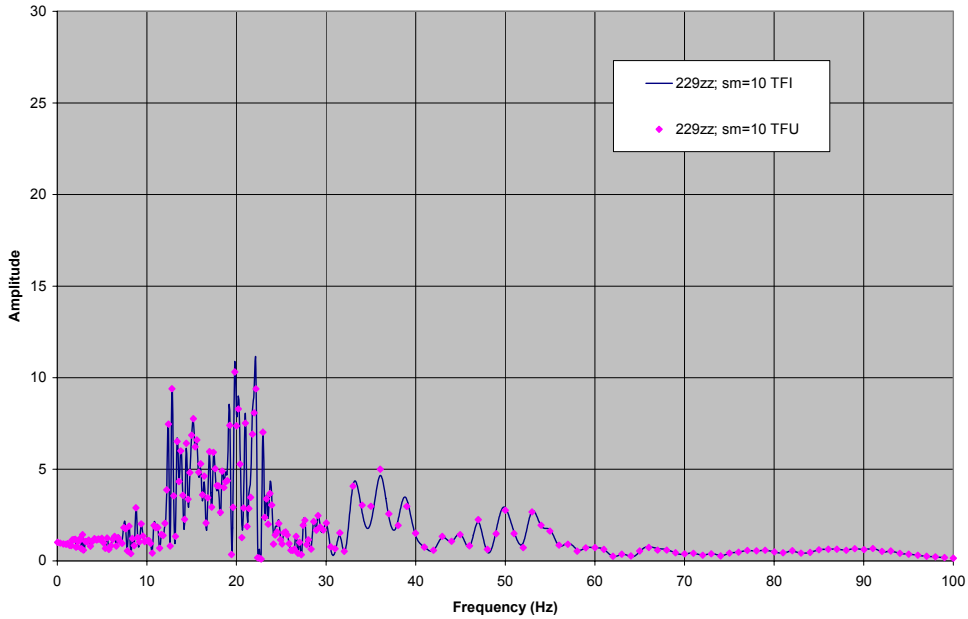

b. Smoothing parameter = 10

Figure 6-2
Top of CIS Outrigger Transfer Function – Z Direction Due to Z Input– (Node 229)

Figure 6-2 shows the transfer function for Z direction top of CIS outrigger response (node 229) due to Z input motion where Figure 6-2a is for no smoothing (smoothing parameter equals zero) and Figure 6-2b is for some smoothing with the smoothing parameter specified to be 10. For the very erratic transfer function of node 229 z response due to z input, smoothing has a large impact even for the 224 frequencies at which the transfer function is calculated. Without smoothing, there are very large peaks as a result of the SASSI interpolation scheme that are not reflected in the calculated transfer function values. These large spurious peaks are eliminated by the smoothing addition to the interpolation scheme. As a result, the interpolated transfer function resulting from smoothing reflects the calculated transfer function values closely. It has been found that this type of convergence between interpolated and calculated transfer functions cannot be achieved by just adding more calculated frequencies for transfer functions with many peaks and valleys such as Figure 6-2 and smoothing is required to achieve acceptable transfer functions for response analysis. Without smoothing, nearly all of the Fourier frequencies would have to be included in the ANALYS transfer function calculation. This would generally be prohibitively time consuming and expensive.

For the SASSI Simulation approach, there is an adjustment of response phasing as is used for the SASSI-AS approach and as described in Chapter 4. The phase adjustment limits complex response phase angles to a variation range from –pi/2 to pi/2. This adjustment ensures that the phase angle cosines for all frequency components are positive to avoid random occurrence of out-of-phase components due to motion incoherency and hence generates higher energy response time histories for given Fourier amplitude spectra.

SIMULATIONS – Once stable transfer functions are developed in the manner described above, the MOTION output will include response time histories and/or response spectra at requested locations. Each set of random seeds input in module HOUSE begins a simulation from which stable transfer functions and, in turn, in-structure response spectra are determined. The results presented in Chapter 5 and Appendix A are the mean in-structure response spectra evaluated frequency by frequency from 15 simulations. The analyst must decide on the appropriate number of simulations. As shown in Chapter 4, for this problem, a stable mean is achieved with as low as 5 simulations. It is recommended that at least 10 simulation runs be performed.

The sequence of modules and actions to perform an SSI analysis for incoherent ground motion with the program, ACS SASSI by the SASSI Simulation approach is:

1. SITE (same as for coherent analysis except an expanded number of frequencies are used)
2. POINT (same as for coherent analysis)
3. HOUSE (same as for coherent analysis for foundation and structure input data; input coherency function selection, specify simulation approach and input random seeds, and input number of spatial modes for incoherent analysis)
4. ANALYS (same as for coherent analysis)
5. MOTION (same as for coherent analysis for ground motion time history; input smoothing parameter for incoherent analysis). Assure that interpolated transfer functions reflect the calculated transfer functions without spurious peaks and valleys but still capture the actual structure-soil dynamic behavior (this is the same task for either coherent or incoherent analysis but it may be more demanding for incoherent analysis due to the stochastic nature of the incoherent response such that more frequencies and smoothing are employed). ISRS are output from the MOTION run

6. STRESS (same as for coherent analysis; not used in this study as the response quantities of interest are ISRS)
7. Repeat Steps 3 through 5 as a restart run with new random seeds for each simulation
8. Compute the mean ISRS from spectra generated from each simulation. Perform enough simulations that the mean ISRS are stable.

SASSI-AS

The input for performing SASSI-AS incoherent analyses is very similar to that for SASSI Simulations since a SASSI-AS analysis is essentially a single simulation. As a result, there is some repetition in the discussion of the SASSI-AS input. The SASSI-AS approach was also executed for this study in ACS SASSI.

SITE – The initial step in SASSI analyses is to define the soil layers, the control point layer, the wave field characteristics of the control motion including the direction of the control motion, the frequencies of analysis, and the number of Fourier components. These are all input to the SITE module. All input items are identical between coherent analyses and incoherent analyses except for the number of frequencies.

A larger number of frequencies are required to perform incoherent analysis than is typically needed for coherent analysis. For coherent analysis, there must be sufficient frequencies to capture the dynamic amplification at the natural frequencies of the soil-structure system. For incoherent analysis, there are many additional frequencies of interest due to the stochastic nature of the incoherent foundation motion. This point will be illustrated later in this chapter when transfer functions are discussed. For the SASSI-AS analyses performed in this study, the 224 frequencies listed in Table 6-2 were specified in SITE.

POINT – The execution of POINT is identical between coherent and incoherent analyses. The radius of the central zone is specified based on the discretization of the foundation.

HOUSE – The input of the data describing the structure and the foundation to the HOUSE module is identical between coherent and incoherent analyses. In ACS SASSI, input parameters for selection of the coherency function are in the HOUSE module. At this point, one of five coherency functions may be selected:

1. Luco & Wong – Equation 3-22
2. Abrahamson, 1993
3. Abrahamson Soil Surface – Equation 2-1
4. Abrahamson Soil Embedded. December 2006
5. Abrahamson Hard Rock, April 2007

There is the option to consider wave passage effects for the Abrahamson coherency functions and the apparent wave velocity is another input quantity for HOUSE. All analyses for this study considered plane wave coherency only with no wave passage effects.

The number of spatial modes to use for incoherent SSI analyses is another input quantity in HOUSE. The 150 foot square foundation was discretized into 144 squares that are 12.5 feet on a side with 169 node points. These 169 nodes that are in contact with both the foundation and the soil are specified to be interaction nodes. As a result, there are a total of 169 spatial modes. In ACS SASSI, the first n spatial modes may be utilized in an incoherent analysis. For all SASSI-AS analyses in this study, all 169 modes were selected.

The next decision that has to be made for execution of HOUSE is to decide on the means of incoherency motion simulation. The input choices are:

1. Deterministic Incoherency Input
2. Stochastically Simulated Incoherency Input

By the SASSI-AS approach described herein, option 1 is selected. There are no other input parameters in HOUSE for incoherent analysis for the SASSI-AS approach.

ANALYS – One important input quantity in ANALYS is the Z-coordinate of the control point. This parameter links the soil layer information in SITE with the structure and foundation information in HOUSE. In addition, ANALYS may be specified as an initial run or as a restart run. This is significant as ANALYS requires the longest computer run time of the SASSI modules. The transfer functions for all degrees of freedom at the input frequencies are calculated in ANALYS. There is no specific input that is unique to incoherent analysis for this module.

MOTION – Input to MOTION includes the specification of desired output locations and identification of the input control motion time history. This input is applicable for either coherent or incoherent analyses. For incoherent analysis, a smoothing parameter is specified that aids in interpolation of transfer functions.

A challenge in running SASSI SSI analyses is to develop stable transfer functions at all frequencies required in Fourier analysis. In MOTION, the calculated transfer functions from ANALYS combined with an interpolation scheme are used to evaluate the transfer functions at the Fourier frequencies and at specified response locations. The calculated and interpolated transfer functions are compared to decide if stable transfer functions are determined. A stable transfer function is achieved when the interpolated transfer function used in response analysis reflects only the behavior represented by the calculated transfer function values.

In coherent SSI analysis, where there is deviation between the calculated and interpolated transfer functions, additional calculated transfer functions are computed by repeating SITE, POINT, HOUSE, and ANALYS for another frequency set. All of the calculated transfer functions are combined in the module COMBIN when more than one frequency set is used.

In incoherent SSI analysis, it may be more challenging to achieve stable transfer functions with the SASSI interpolation scheme. Some transfer functions have a large number of peaks and valleys for which the interpolation scheme introduces unrealistic spurious peaks and valleys. The stochastic nature of the incoherent transfer functions does not necessarily enable achievement of stable transfer functions by the addition of more frequencies at which calculated transfer functions are obtained.

As a result, the approach for incoherent SSI analysis is to use a larger number of frequencies than would be used for coherent analysis to assure that the actual soil-structure dynamic behavior is being captured and then to aid the SASSI interpolation scheme by employing the smoothing technique described in Chapter 4. For all SASSI-AS runs, 224 frequencies were used and smoothing parameter of 10 was specified in MOTION. It is believed that more frequencies than will be typically needed were used for these analyses and that the number of frequencies for incoherent analysis will be in the range of 100 to 200 based on the judgment of the analyst.

The smoothing parameter value represents the number of Fourier frequency steps that is used to define the bandwidth of the Parzen spectral window (the standard deviation of the Gaussian function). For small smoothing parameter values, say 1-5, the final smoothed complex transfer functions are closer to the interpolated transfer functions using original SASSI interpolation scheme and large deviations from the calculated transfer function values are reduced or eliminated when larger smoothing parameters are used. Depending on the selection of the frequency set for transfer function calculations, a smoothing parameter value from 10 to 100 is recommended. Before deciding the final smoothing parameter value to be used, the user should compare the original computed amplitude transfer functions with the interpolated amplitude transfer functions. If spurious spectral peaks or valleys are present in the interpolated transfer functions, then the smoothing parameter should be increased.

It should be noted that the spectral windowing is a smoothing or interpolation method that reconstructs the transfer functions. If the selected set of frequencies for SSI analysis is insufficient for capturing some key features of the response spectral content, then spectral windowing will not help to improve results. The selection of an appropriate set of frequencies for response calculations remains as an aspect of essence for the SSI analysis accuracy.

For the SASSI-AS approach, there is an adjustment of response phasing as described in Chapter 4. The phase adjustment limits complex response phase angles to a variation range from –pi/2 to pi/2. This adjustment ensures that the phase angle cosines for all frequency components are positive to avoid random occurrence of out-of-phase components due to motion incoherency and hence generates higher energy response time histories for given Fourier amplitude spectra.

The sequence of modules and actions to perform an SSI analysis for incoherent ground motion with the program, ACS SASSI by the SASSI AS approach is:

1. SITE (same as for coherent analysis except an expanded number of frequencies are used)
2. POINT (same as for coherent analysis)
3. HOUSE (same as for coherent analysis for foundation and structure input data; input coherency function selection, specify deterministic approach, and input number of spatial modes for incoherent analysis; note that leaving the number of modes blank or setting it to zero defaults to using all of the spatial modes)
4. ANALYS (same as for coherent analysis)

5. MOTION (same as for coherent analysis for ground motion time history; input smoothing parameter for incoherent analysis). Assure that interpolated transfer functions reflect the calculated transfer functions without spurious peaks and valleys but still capture the actual structure-soil dynamic behavior (this is the same task for either coherent or incoherent analysis but it may be more demanding for incoherent analysis due to the stochastic nature of the incoherent response such that more frequencies and smoothing are employed). ISRS are output from the MOTION run
6. STRESS (same as for coherent analysis; not used in this study as the response quantities of interest are ISRS)

SASSI-SRSS

Guidelines and description of SASSI-SRSS are presented under separate cover (Ostadan and Deng, 2007).

7
CONCLUSIONS AND RECOMMENDATIONS

1. Soil-structure interaction (SSI) analysis is important to calculating seismic response to structures mounted on rock sites and subjected to high-frequency ground motion. SSI produces significant reductions in high-frequency response for these conditions.
2. CLASSIinco and CLASSIinco-SRSS are computationally efficient methods for conducting SSI analyses including incoherency, but are limited to rigid surface foundations. For structures with foundations for which the combined behavior of foundation/structure is deemed flexible and for embedded foundations/partial structure, a version of SASSI is required to accurately capture seismic response.
3. Utilization of SASSI-AS to compute the response for incoherent input requires computational effort comparable to standard SASSI analysis for coherent input. SASSI-SRSS and SASSI Simulation require significantly greater computational effort to analyze the incoherent response for complex structural models.
4. The SSI analysis programs CLASSIinco-SRSS, SASSI-SRSS, and SASSI-Simulation have been fully validated to treat the phenomena of incoherency for nuclear power plant structures when applied in the seismic design/qualification process. The bases of the validation are:
   - Agreement of results computed using CLASSI and SASSI to those available from published literature (Chapter 3 and Appendix C).
   - Comparison of CLASSI computed incoherent seismic response with SASSI computed incoherent seismic response for an example rock/structure model with agreement within engineering accuracy (Chapter 5 and Appendix A).
5. CLASSIinco-SRSS, SASSI-SRSS, and SASSI-Simulation are the most theoretically correct techniques since they recognize and treat the random nature of the phase of the incoherent SSI response. The results of the analyses where the three input directions are treated independently (Appendix A) demonstrates that the agreement between these three is excellent.
6. The more simplified approach of SASSI-AS has been shown to agree with other methods for response to combined excitations (i.e., Chapter 5 and Appendix C of Short, et.al., 2006). SASSI-AS results deviate from other methods for some instances where single excitation directions are considered (i.e., Appendix A). As a result, SASSI-AS may be used to treat the phenomena of incoherency for nuclear power plant structures with the following restrictions:
   - SASSI-AS is acceptable for foundation/structural systems demonstrated to have minimal incoherency-induced rotation effects. SASSI-AS may be used for structure configurations where it can be demonstrated that induced rotation effects are adequately treated with this methodology, (e.g., for large plan dimension/low height structures).
   - SASSI-AS may be used if its applicability is demonstrated by sensitivity studies.

7. Even though CLASSIinco results were in close agreement with the other approaches that computed incoherent seismic response for the example rock/structure model (Chapter 5), it is recommended that the CLASSIinco-SRSS approach be used for incoherent analysis by CLASSI. CLASSIinco would require the same sensitivity studies as SASSI-AS in order to be used. However, CLASSIinco-SRSS is very computationally efficient, which precludes the need for the simpler version, CLASSIinco.

8
REFERENCES

Abrahamson, N. (2007). *Hard Rock Coherency Functions Based on the Pinyon Flat Data*, April 2.

Abrahamson, N. (2006). *Program on Technology Innovation: Spatial Coherency for Soil-Structure Interaction.* Electric Power Research Institute, Palo Alto, CA, and U.S. Department of Energy, Germantown, MD: December. Report 1014101.

Abrahamson, N. (2005). *Spatial Coherency for Soil-Structure Interaction*. Electric Power Research Institute, Palo Alto, CA: December. Technical Update Report 1012968.

ASCE (2000). *Seismic Analysis of Safety-Related Nuclear Structures and Commentary,* American Society Civil Engineers, Report. ASCE 4-98.

Chang, C.-Y., M.S. Power, I.M. Idriss, P. Sommerville, W. Silva, and P.C. Chen. (1986). *Engineering Characterization of Ground Motion, Task I1: Observational Data on Spatial Variations of Earthquake Ground Motion, NUREG/CR-3805,* Vol. 3.

CSI (2004). *Computers and Structures Incorporated, SAP2000, Integrated Software for Structural Analysis and Design, Version 9.*

Der Kiureghian, A. *(1980). Structural Response to Stationary Excitation,* Journal of the Engineering Mechanics Division, American Society Civil Engineers, December.

EPRI (1993). *Guidelines for Determining Design Basis Ground Motions, Volume 1: Method and Guidelines for Estimating Earthquake Ground Motion in Eastern North America.* Electric Power Research Institute, Palo Alto, CA: November. Report TR-102293.

EPRI (1991). *A Methodology for Assessment of Nuclear Power Plant Seismic Margin (Rev 1).* Electric Power Research Institute, Palo Alto, CA: August. Report NP-6041-SL.

Ghiocel, D (2004). *Stochastic Simulation Methods for Engineering Predictions, CRC* Engineering Design Reliability Handbook, Chapter 20, CRC Press, New York, NY.

Ghiocel Predictive Technologies, Inc. (2006). *ACS-SASSI, An Advanced Computational Software for 3D Dynamic Analysis Including Soil-Structure Interaction,* Version 2.2, Pittsford, New York.

Johnson, J.J. (2003). *Soil-Structure Interaction, Earthquake Engineering Handbook,* Chapter 10, W-F Chen, C. Scawthorn, eds., CRC Press, New York, NY.

Kim, S. and J.P. Stewart (2003). *Kinematic Soil-Structure Interaction from Strong Motion Recordings*, Journal of Geotechnical and Geoenvironmental Engineering, ASCE, April.

Luco, J.E. and A. Mita (1987). *Response of Circular Foundation to Spatially Random Ground Motion,* Journal of Engineering Mechanics, American Society of Civil Engineers, Vol. 113, No. 1, January. 1987, pp. 1-15.

Luco, J.E. and H.L. Wong (1986). *Response of a Rigid Foundation Subjected to a Spatially Random Ground Motion,* Earthquake Engineering and Structural Dynamics, Vol. 14, pp. 891-908.

Lysmer, J., M. Tabatabaie-Raissi, F. Tajirian, S. Vahdani, and F. Ostadan (1981), "SASSI-A System for Analysis of Soil-Structure Interaction," Report no. UCB/GT/81-02, Department of Civil Engineering, University of California, Berkeley, April.

McCann, M., J. Marrone, and R. Youngs (2004). CEUS *Ground Motion Project Final Report*. Electric Power Research Institute, Palo Alto, CA, December. TR-1009684.

Orr, R. (2003). *AP1000 Inputs for 2D SASSI Analyses*, Calculation No. APP-1000-S2C-052, Rev. 0, Westinghouse.

Orr, R., Westinghouse Corporation (2006). Personal email communication on AP1000 Model Properties to Greg Hardy, ARES Corporation, August.

Ostadan, F., Bechtel Corporation (2006). Personal email communication on SASSI SSI Analysis Results to Steve Short, ARES Corporation, August.

Ostadan, F. and N. Deng (2007), "SASSI-SRSS Approach for SSI Analysis with Incoherent Ground Motions," Bechtel National, San Francisco, CA.

Parzen E. (1962). "On Estimation of a Probability Density Function and Mode", Ann. Math. Stat. 33, pp. 1065-1076.

Short, S.A., G.S. Hardy, K.L. Merz, and J.J. Johnson (2006). *Program on Technology Innovation: Effect of Seismic Wave Incoherence on Foundation and Building Response*, *Electric Power Research Institute, Palo Alto, CA and U.S. Department of Energy, Germantown, MD. Report No. TR-1013504. November.*

Tseng, W.S. and K.I. Lilhanand (1997)**.** *Soil-Structure Interaction Analysis Incorporating Spatial Incoherence of Ground Motions*. Electric Power Research Institute, Palo Alto, CA: November. Report TR-102631 2225.

Tubino, F., L. Carassale, and G. Solari (2003). Seismic Response of Multi-Supported Structures by Proper Orthogonal Decomposition, Earthquake Engineering and Structural Dynamics, Vol. 32, pp. 1639-1654.

U.S. Department of Energy (2002). *Natural Phenomena Hazards Design and Evaluation Criteria for Department of Energy Facilities*, DOE-STD-1020-2002, January.

Veletsos, A.S. and A.M. Prasad (1989). *Seismic Interaction of Structures and Soils: Stochastic Approach,* ASCE Journal of Structural Engineering, Vol. 115, pp. 935-956, April.

Veletsos, A.S. and Y. Tang (1990). *Deterministic Assessment of Effects of Ground-Motion Incoherence,* ASCE Journal of Engineering Mechanics, Vol. 116, pp. 1109-1124, May.

Wong, H.L. and J.E. Luco (1980). *Soil-Structure Interaction: A Linear Continuum Mechanics Approach (CLASSI),* Report CE, Department of Civil Engineering, University of Southern California, Los Angeles, California.

A
CLASSI-SASSI IN-STRUCTURE RESPONSE SPECTRA COMPARISONS FOR INDIVIDUAL INPUT DIRECTION COMPONENTS

In Chapter 5, in-structure response spectra computed by two CLASSI methods and three SASSI methods for evaluating seismic response including seismic wave incoherence were presented. Again, these approaches include:

- CLASSIinco – deterministic phasing of foundation component response
- CLASSIinco-SRSS – SRSS combination of structural response computed from random phasing of foundation component response
- SASSI-SRSS – SRSS combination of modal transfer functions to represent random phasing of spatial modes
- SASSI Simulation Mean – Monte Carlo simulations to represent random phasing of spatial modes
- SASSI-AS – Algebraic summation of spatial modes with assumed deterministic phasing

The comparisons of response spectra in Chapter 5 were for response in the x, y, and z directions for simultaneous application of input motion in the x, y, and z directions. These spectra were determined from the square root of the sum of the squares combination of spectra due to individual x, y, and z input motion. The response spectra for the individual x, y, and z input motion are presented in this appendix for the 5 computational methods listed above. Response locations are identified by the node numbers of the CLASSI and SASSI models as shown in Figure A-1. Response spectra for x input motion are presented in Figures A-2 through A-28. Response spectra for y input motion are presented in Figures A-29 through A-55. Response spectra for z input motion are presented in Figures A-56 through A-82.

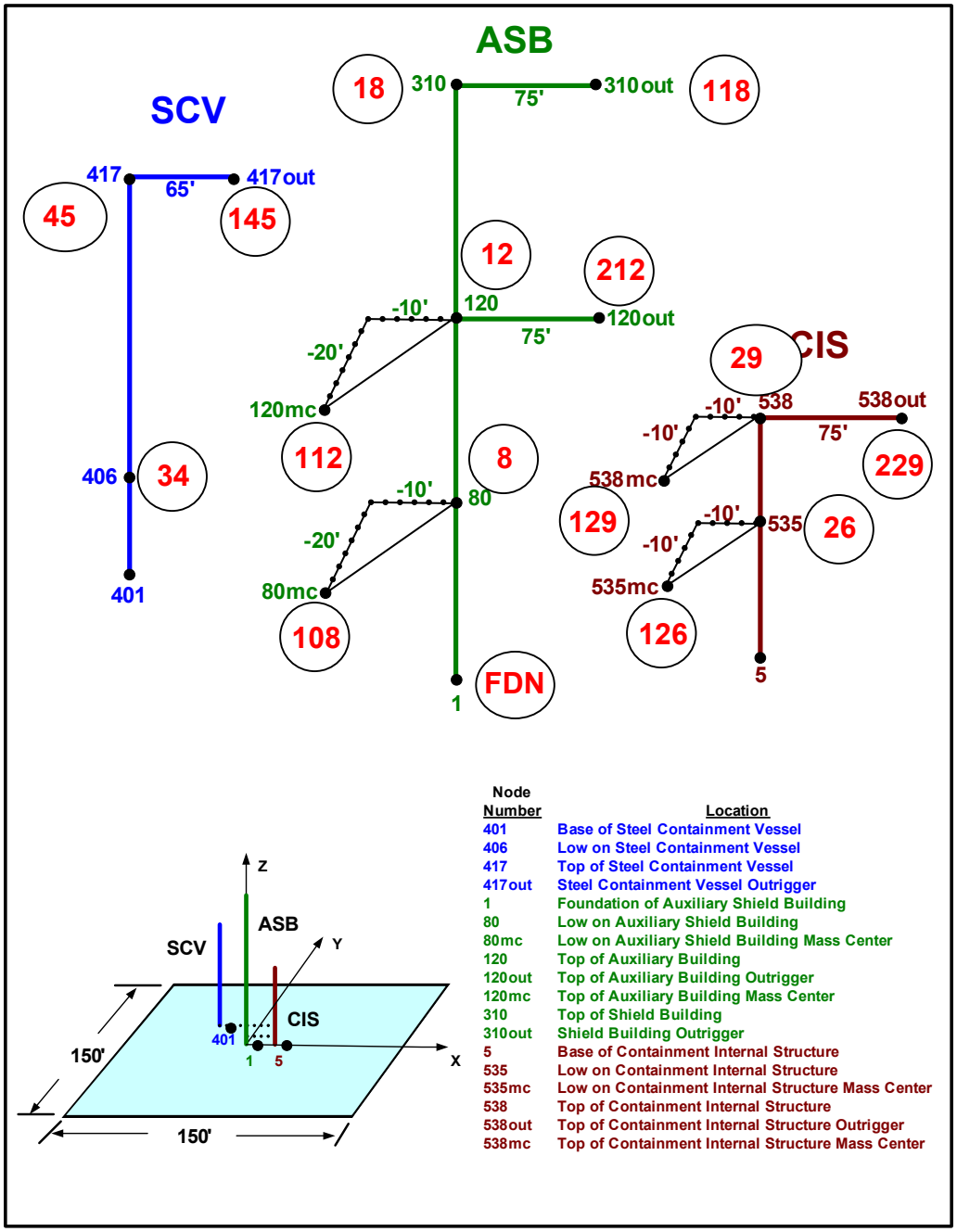

Figure A-1
Locations on the AP1000-Based Stick Model where In-Structure Response Spectra are Computed

X-Direction Input Ground Motion

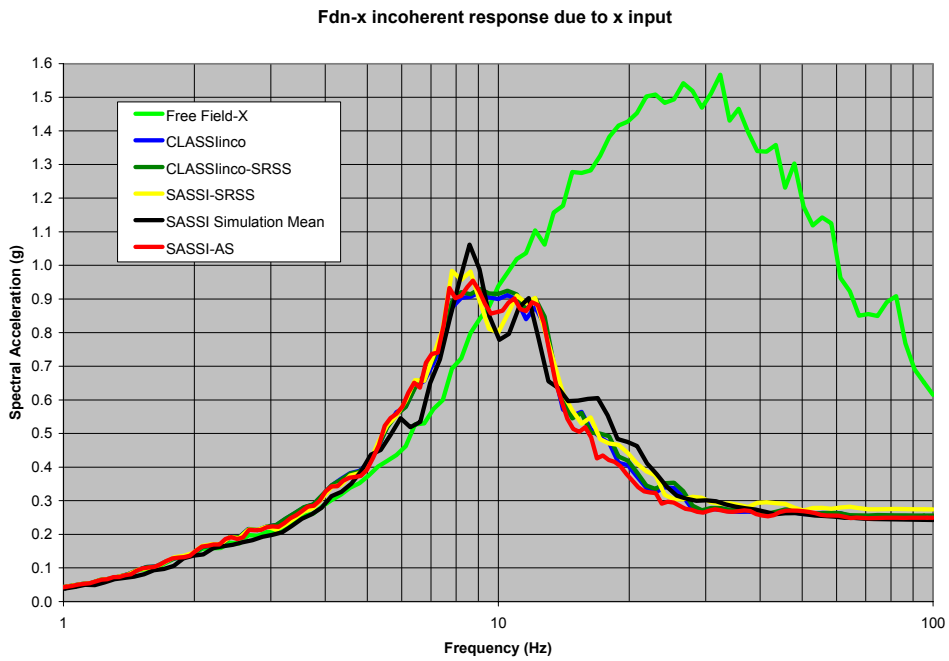

Figure A-2
Center of Foundation Response Spectra – X Direction Due to X Input – CLASSlinco, CLASSlinco-SRSS, SASSI-SRSS, SASSI Simulation Mean, SASSI-AS (Node 1)

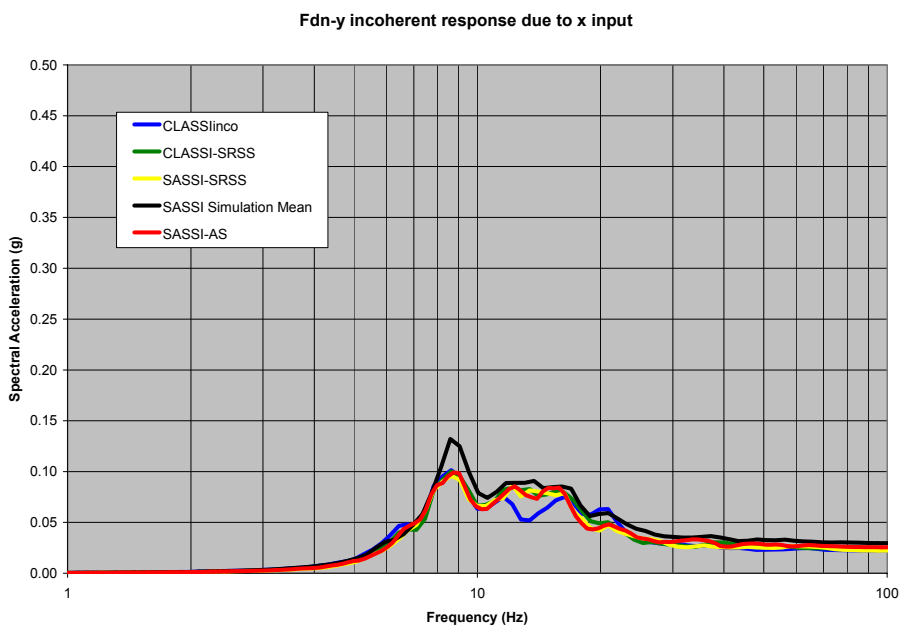

Figure A-3
Center of Foundation Response Spectra – Y Direction Due to X Input – CLASSlinco, CLASSlinco-SRSS, SASSI-SRSS, SASSI Simulation Mean, SASSI-AS (Node 1)

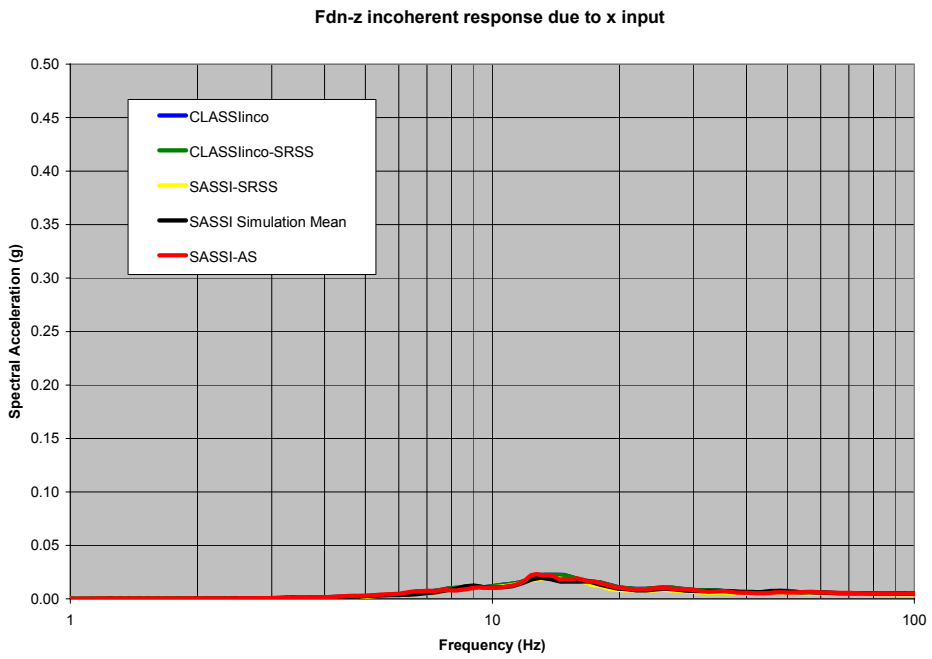

Figure A-4
Center of Foundation Response Spectra – Z Direction Due to X Input – CLASSlinco, CLASSlinco-SRSS, SASSI-SRSS, SASSI Simulation Mean, SASSI-AS (Node 1)

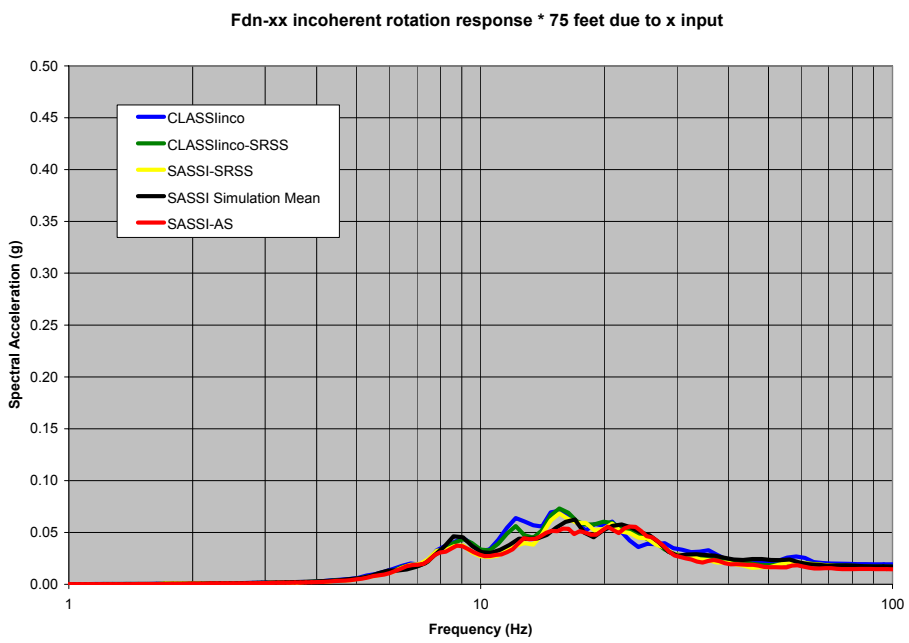

Figure A-5
Edge of Foundation Response Spectra –XX Rotation Due to X Input – CLASSlinco, CLASSlinco-SRSS, SASSI-SRSS, SASSI Simulation Mean, SASSI-AS (Node 1)

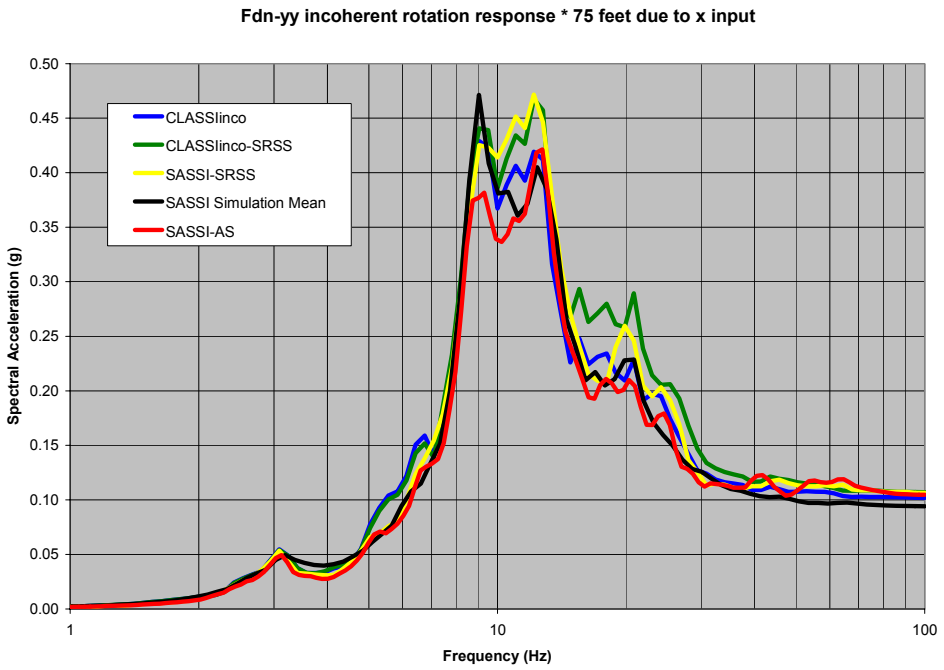

Figure A-6
Edge of Foundation Response Spectra –YY Rotation Due to X Input – CLASSlinco, CLASSlinco-SRSS, SASSI-SRSS, SASSI Simulation Mean, SASSI-AS (Node 1)

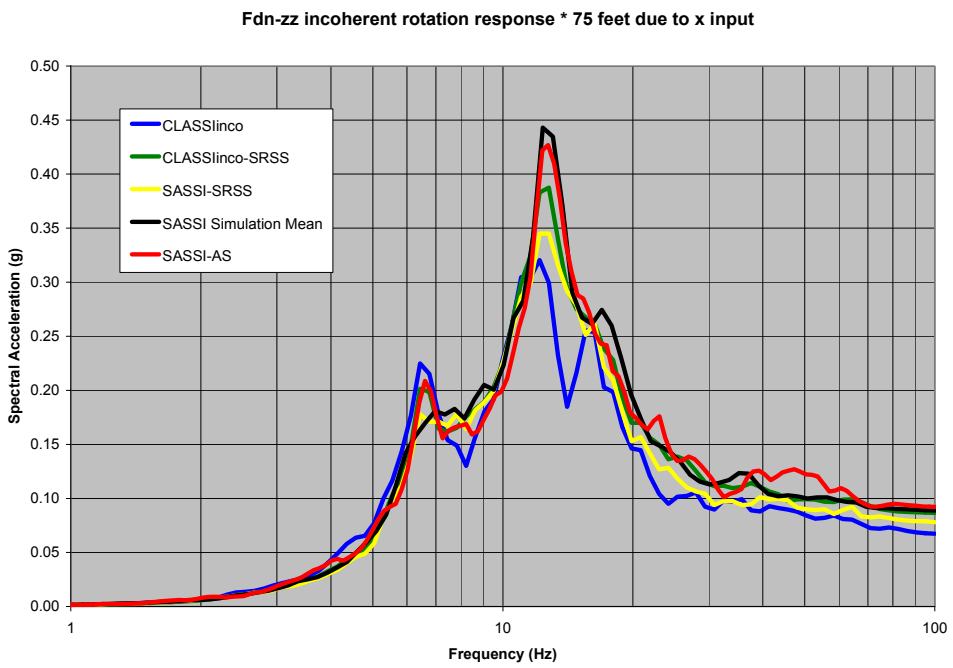

Figure A-7
Edge of Foundation Response Spectra –ZZ Rotation Due to X Input – CLASSlinco, CLASSlinco-SRSS, SASSI-SRSS, SASSI Simulation Mean, SASSI-AS (Node 1)

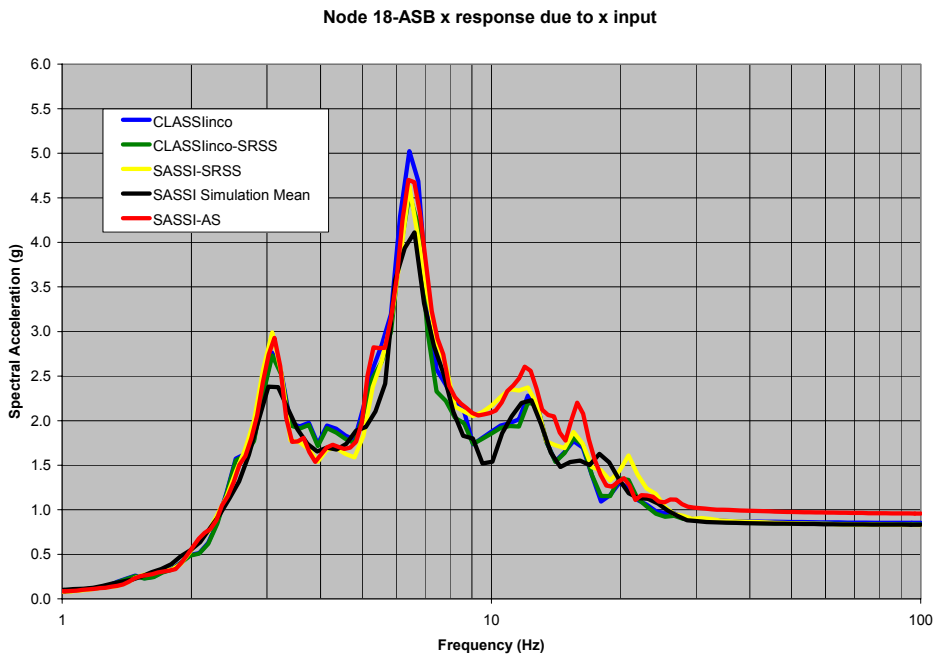

Figure A-8
Top of ASB Response Spectra – X Direction Due to X Input – CLASSlinco, CLASSlinco-SRSS, SASSI-SRSS, SASSI Simulation Mean, SASSI-AS (Node 18)

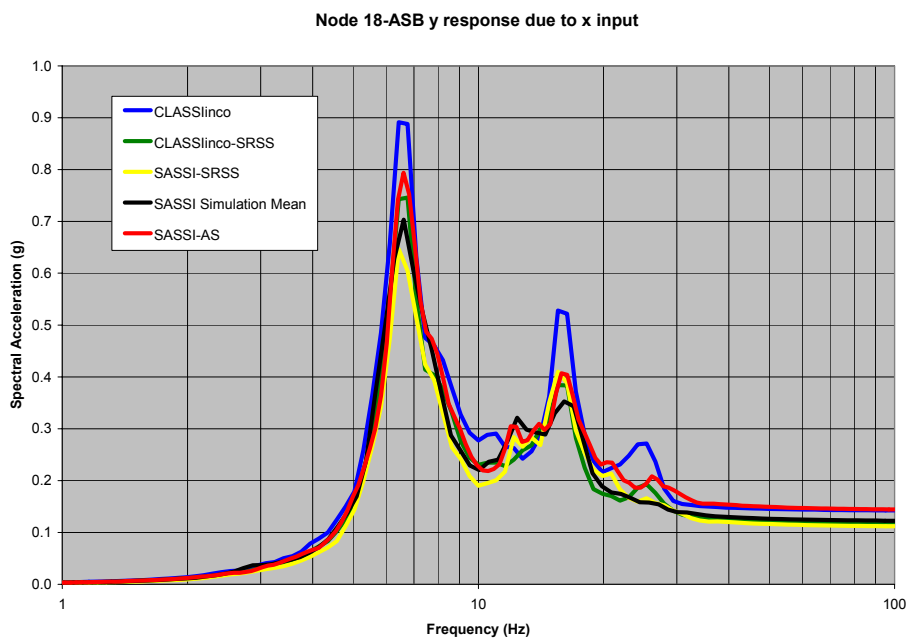

Figure A-9
Top of ASB Response Spectra – Y Direction Due to X Input – CLASSlinco, CLASSlinco-SRSS, SASSI-SRSS, SASSI Simulation Mean, SASSI-AS (Node 18)

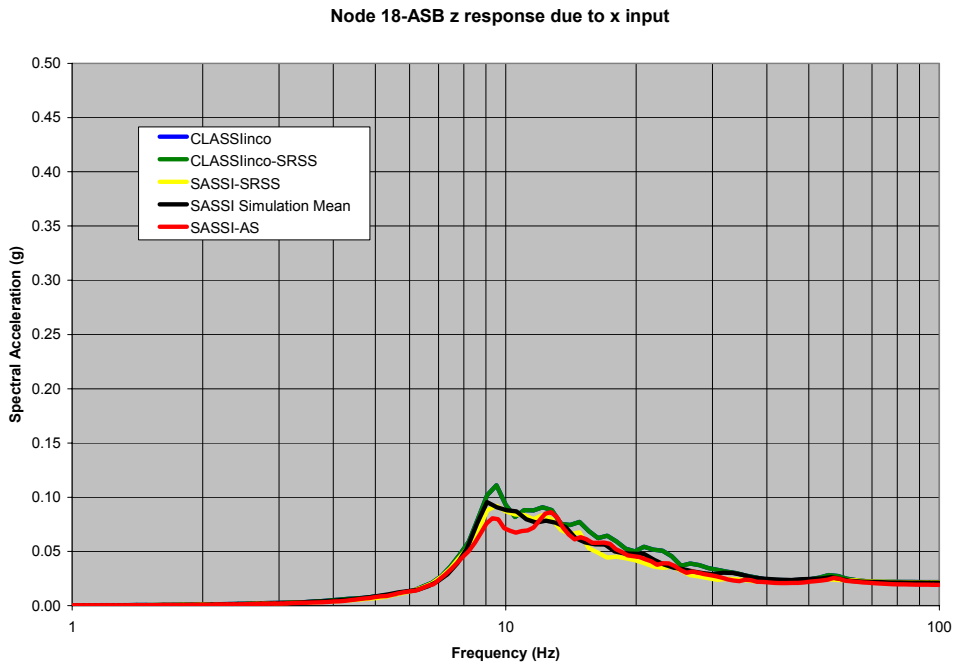

Figure A-10
Top of ASB Response Spectra – Z Direction Due to X Input – CLASSlinco, CLASSlinco-SRSS, SASSI-SRSS, SASSI Simulation Mean, SASSI-AS (Node 18)

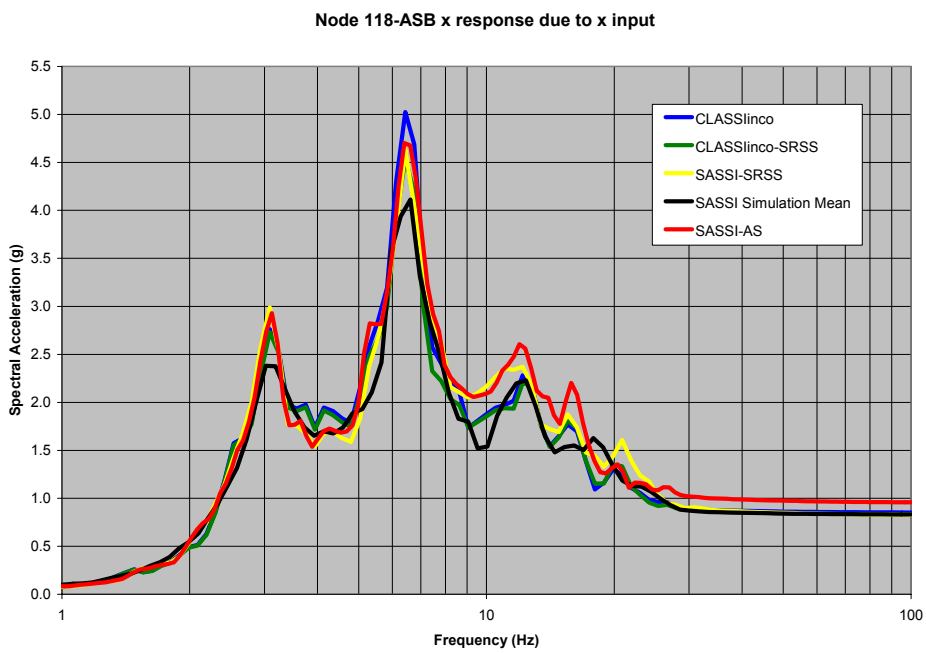

Figure A-11
ASB Outrigger Response Spectra – X Direction Due to X Input – CLASSlinco, CLASSlinco-SRSS, SASSI-SRSS, SASSI Simulation Mean, SASSI-AS (Node 118)

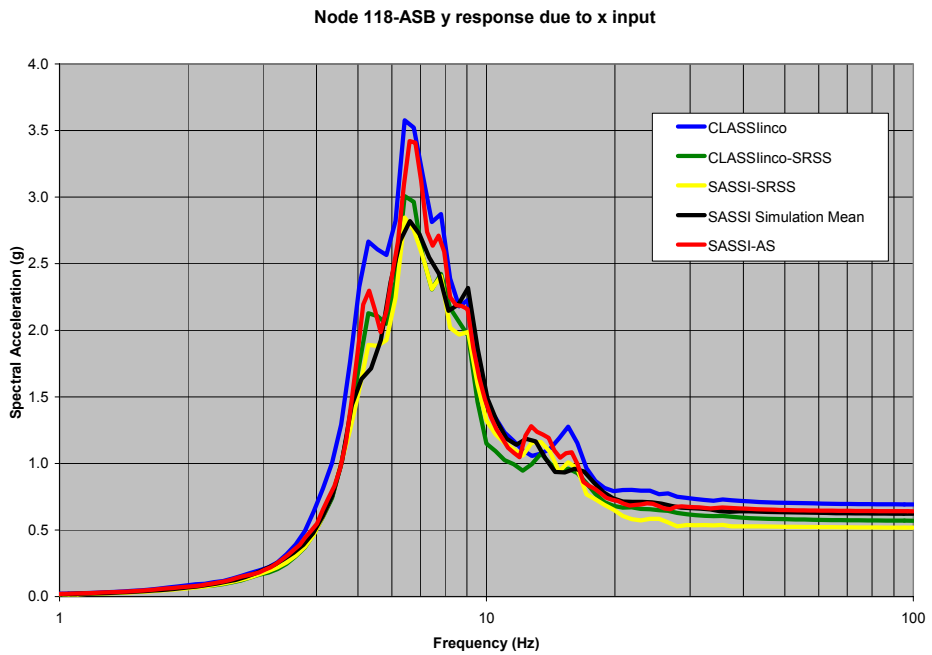

Figure A-12
ASB Outrigger Response Spectra – Y Direction Due to X Input – CLASSlinco, CLASSlinco-SRSS, SASSI-SRSS, SASSI Simulation Mean, SASSI-AS (Node 118)

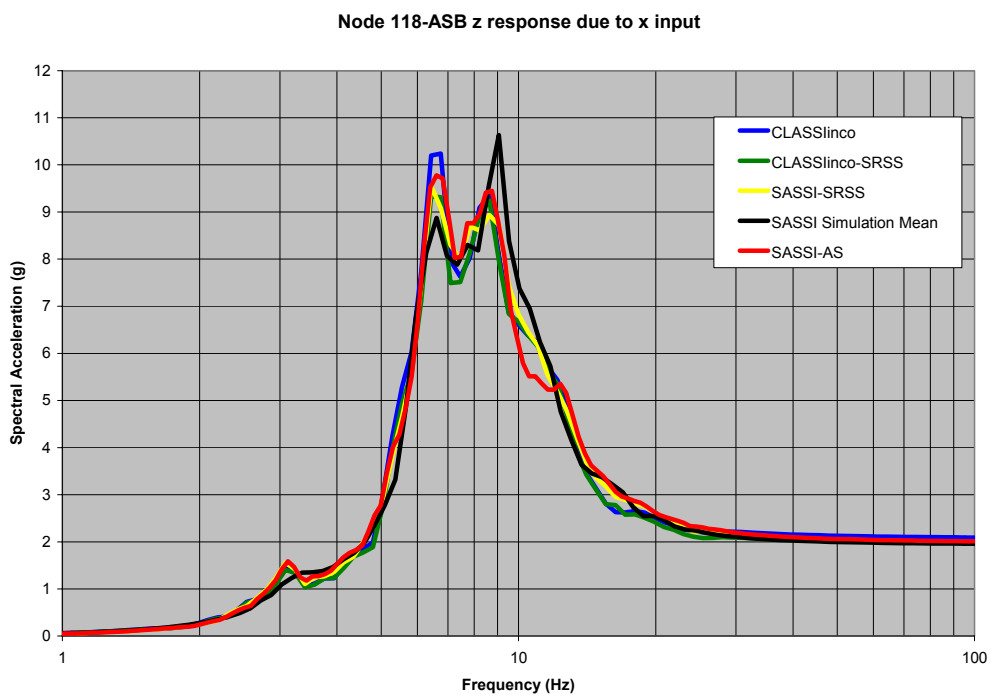

Figure A-13
ASB Outrigger Response Spectra – Z Direction Due to X Input – CLASSlinco, CLASSlinco-SRSS, SASSI-SRSS, SASSI Simulation Mean, SASSI-AS (Node 118)

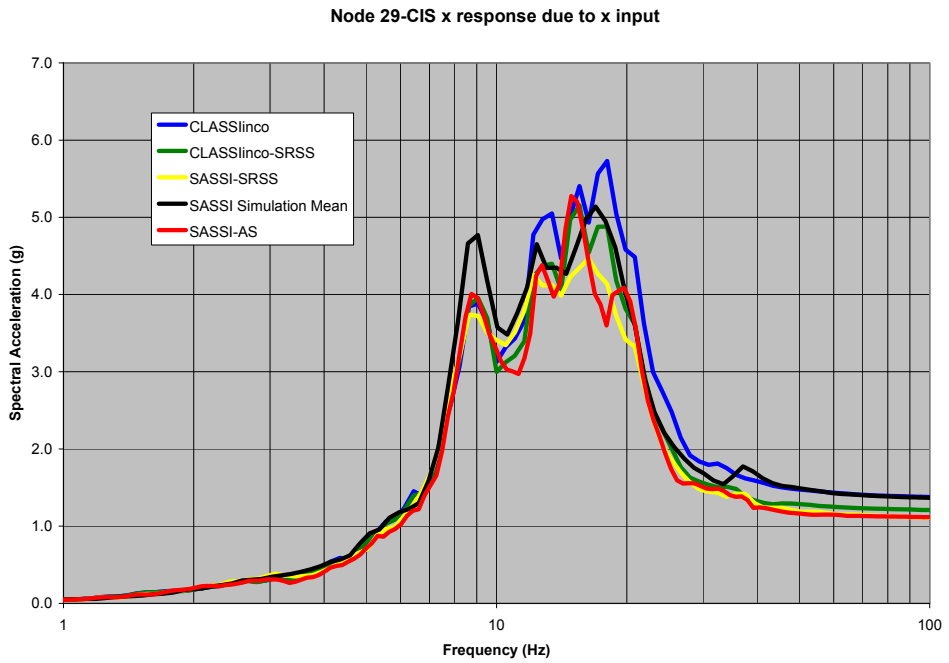

Figure A-14
Top of CIS Shear Center Response Spectra – X Direction Due to X Input – CLASSlinco, CLASSlinco-SRSS, SASSI-SRSS, SASSI Simulation Mean, SASSI-AS (Node 29)

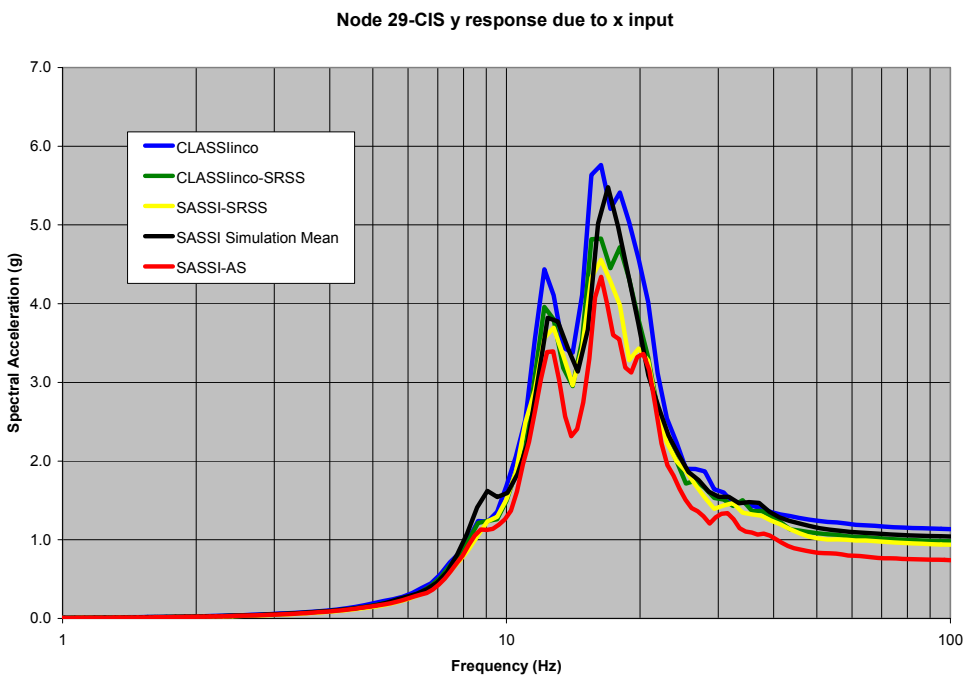

Figure A-15
Top of CIS Shear Center Response Spectra – Y Direction Due to X Input – CLASSlinco, CLASSlinco-SRSS, SASSI-SRSS, SASSI Simulation Mean, SASSI-AS (Node 29)

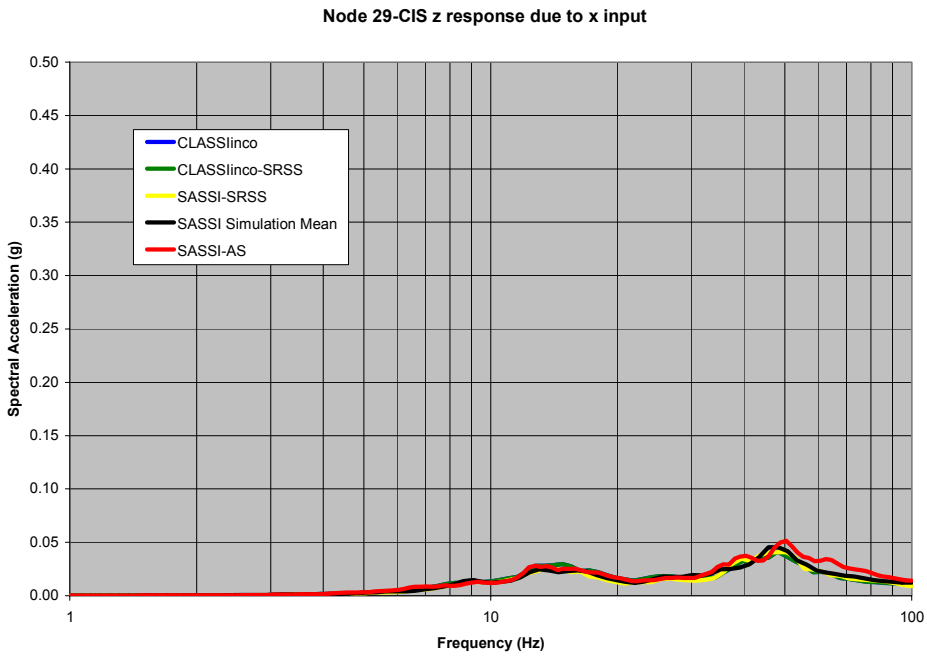

Figure A-16
Top of CIS Shear Center Response Spectra – Z Direction Due to X Input – CLASSlinco, CLASSlinco-SRSS, SASSI-SRSS, SASSI Simulation Mean, SASSI-AS (Node 29)

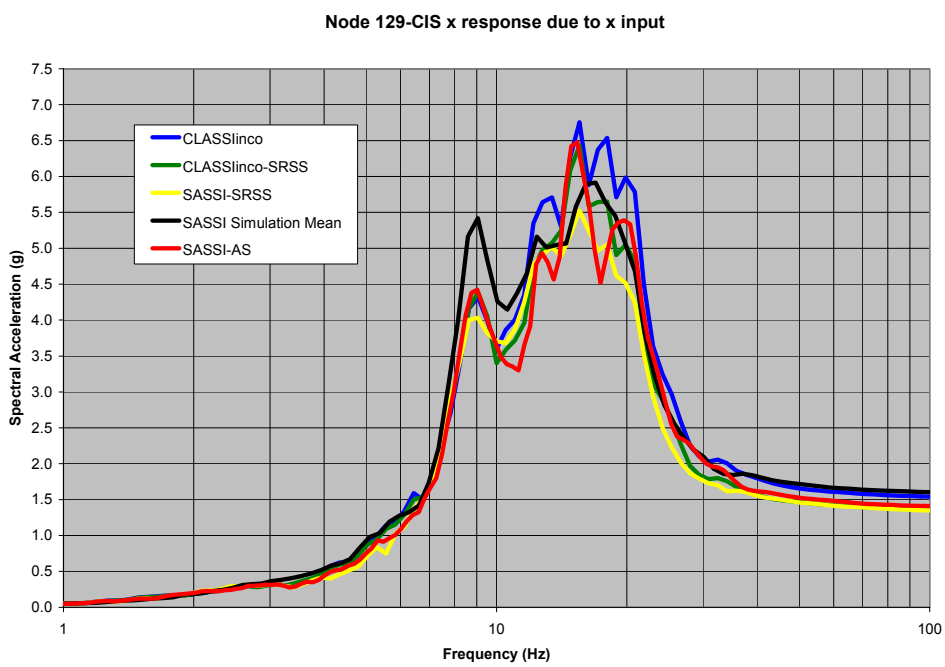

Figure A-17
Top of CIS Horizontal Mass Center Response Spectra – X Direction Due to X Input – CLASSlinco, CLASSlinco-SRSS, SASSI-SRSS, SASSI Simulation Mean, SASSI-AS (Node 129)

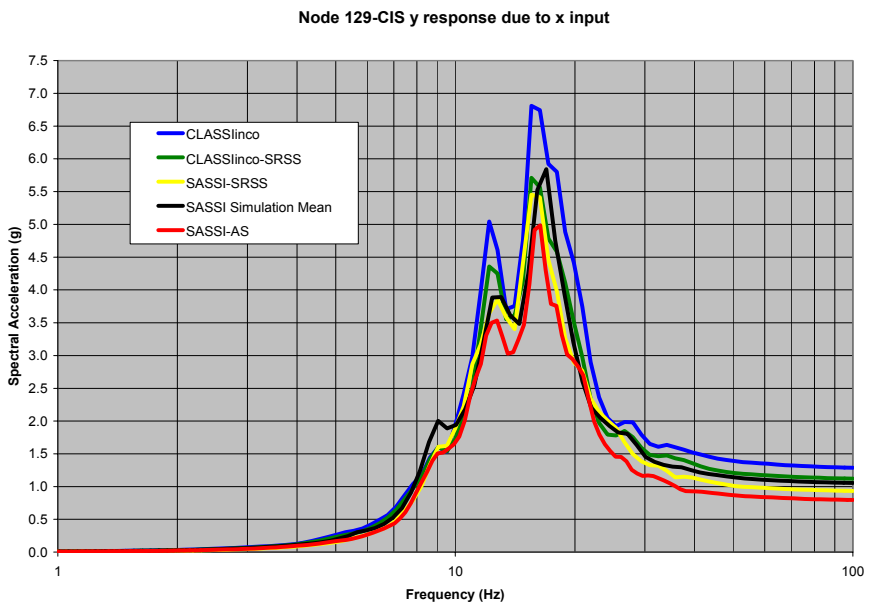

Figure A-18
Top of CIS Horizontal Mass Center Response Spectra – Y Direction Due to X Input – CLASSlinco, CLASSlinco-SRSS, SASSI-SRSS, SASSI Simulation Mean, SASSI-AS (Node 129)

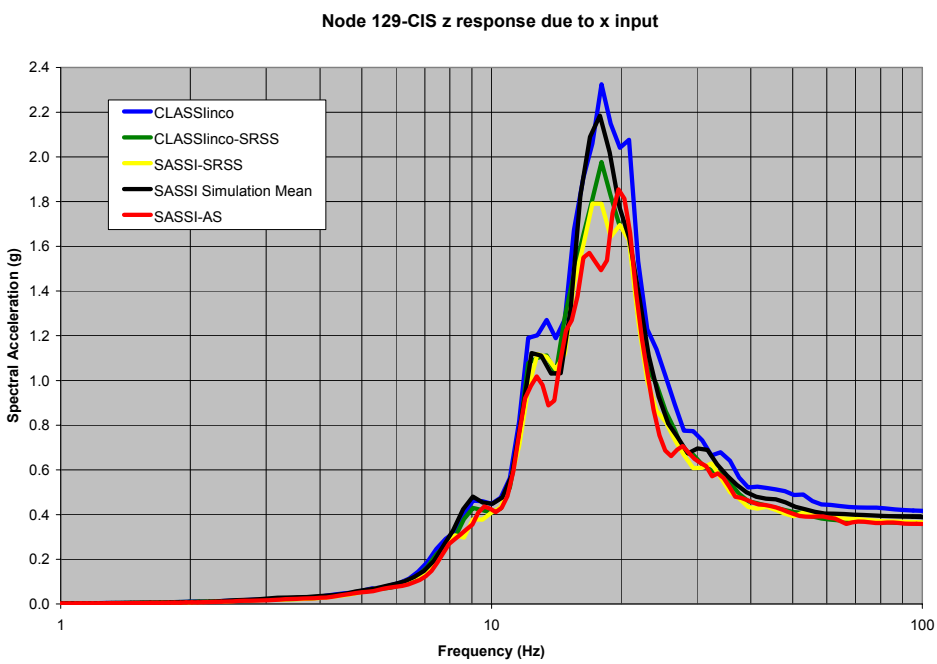

Figure A-19
Top of CIS Horizontal Mass Center Response Spectra – Z Direction Due to X Input – CLASSlinco, CLASSlinco-SRSS, SASSI-SRSS, SASSI Simulation Mean, SASSI-AS (Node 129)

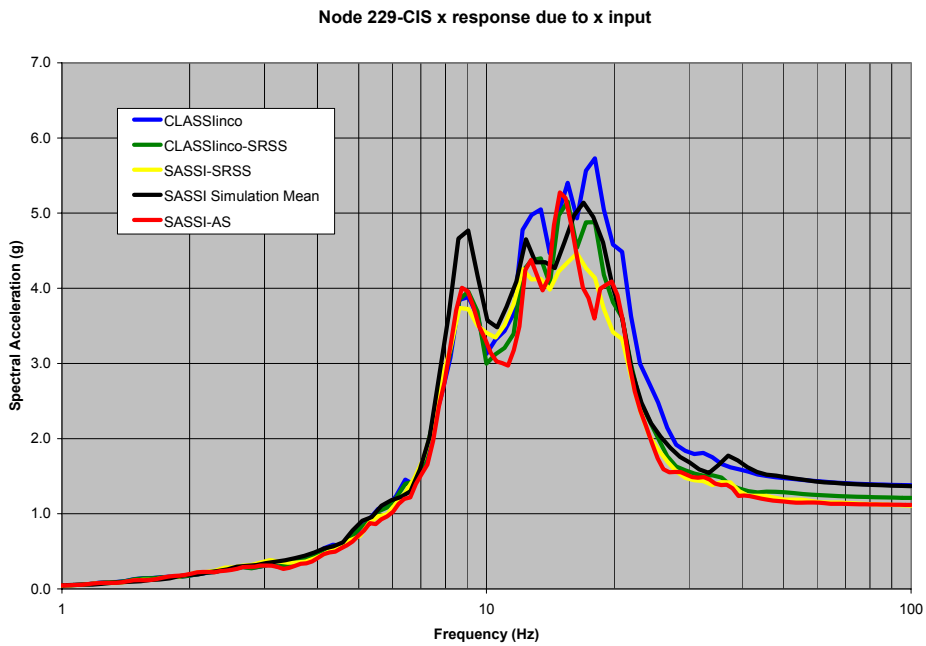

Figure A-20
CIS Outrigger Response Spectra – X Direction Due to X Input – CLASSlinco, CLASSlinco-SRSS, SASSI-SRSS, SASSI Simulation Mean, SASSI-AS (Node 229)

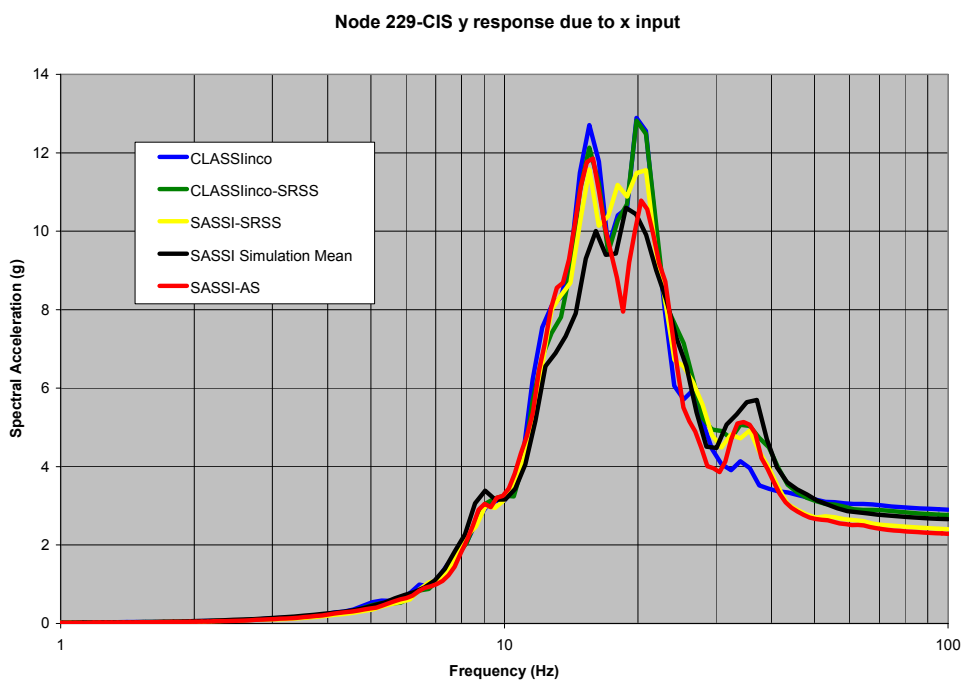

Figure A-21
CIS Outrigger Response Spectra – Y Direction Due to X Input – CLASSlinco, CLASSlinco-SRSS, SASSI-SRSS, SASSI Simulation Mean, SASSI-AS (Node 229)

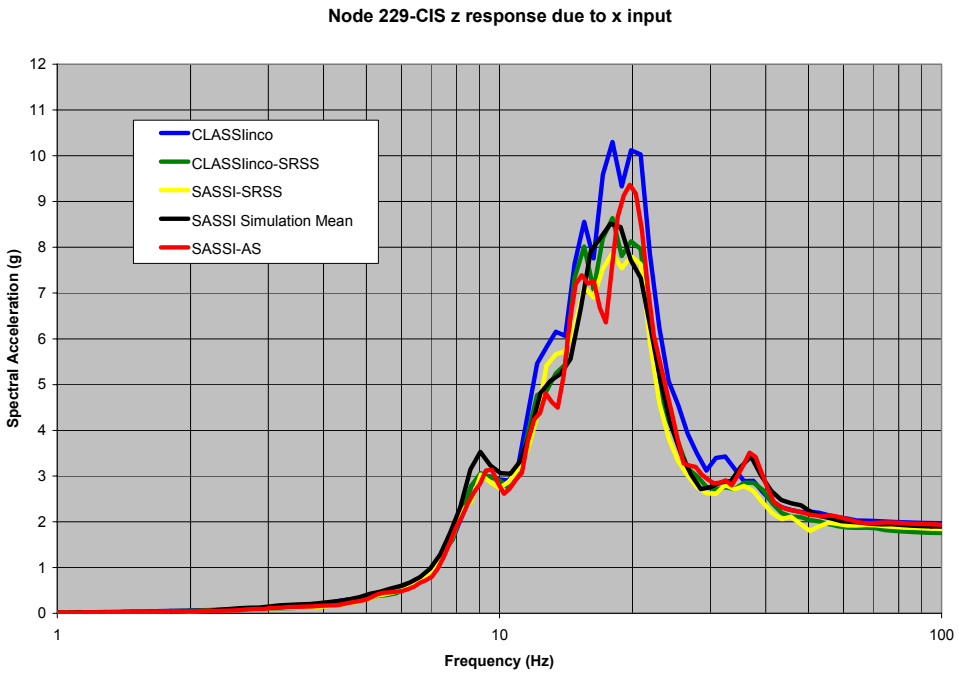

Figure A-22
CIS Outrigger Response Spectra – Z Direction Due to X Input – CLASSlinco, CLASSlinco-SRSS, SASSI-SRSS, SASSI Simulation Mean, SASSI-AS (Node 229)

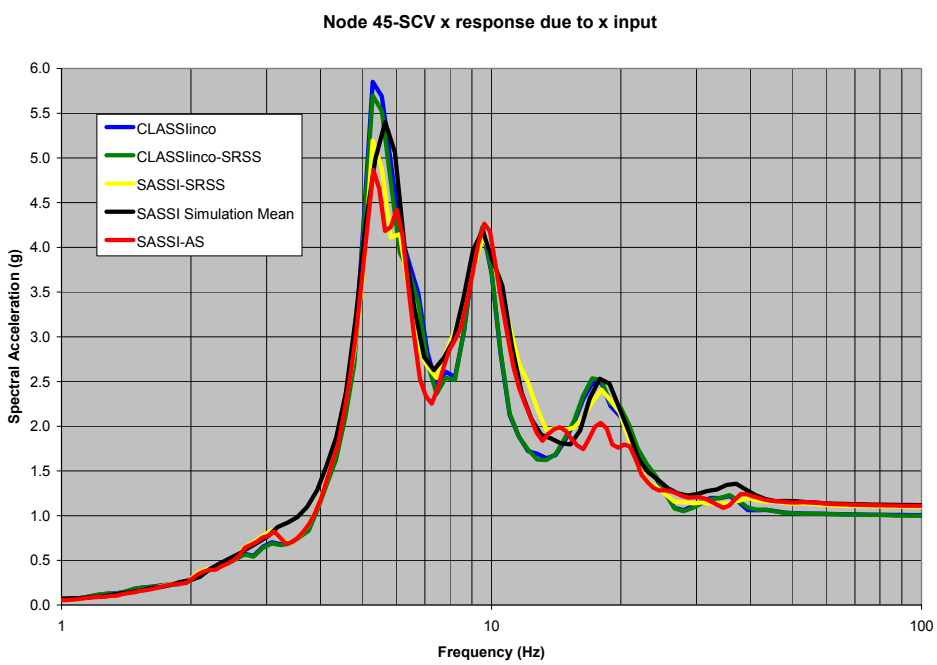

Figure A-23
Top of SCV Response Spectra – X Direction Due to X Input – CLASSlinco, CLASSlinco-SRSS, SASSI-SRSS, SASSI Simulation Mean, SASSI-AS (Node 45)

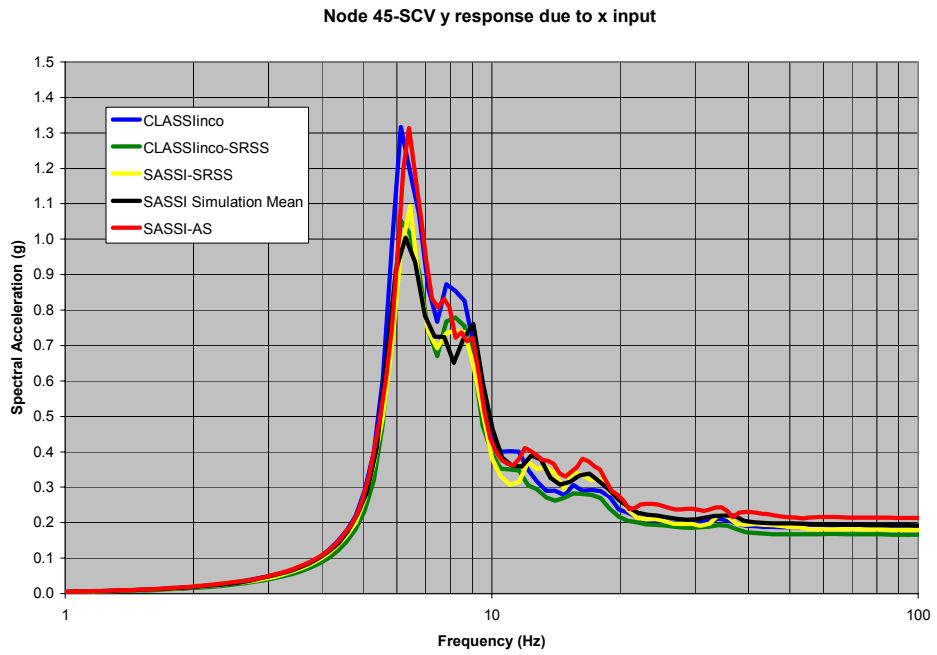

Figure A-24
Top of SCV Response Spectra – Y Direction Due to X Input – CLASSlinco, CLASSlinco-SRSS, SASSI-SRSS, SASSI Simulation Mean, SASSI-AS (Node 45)

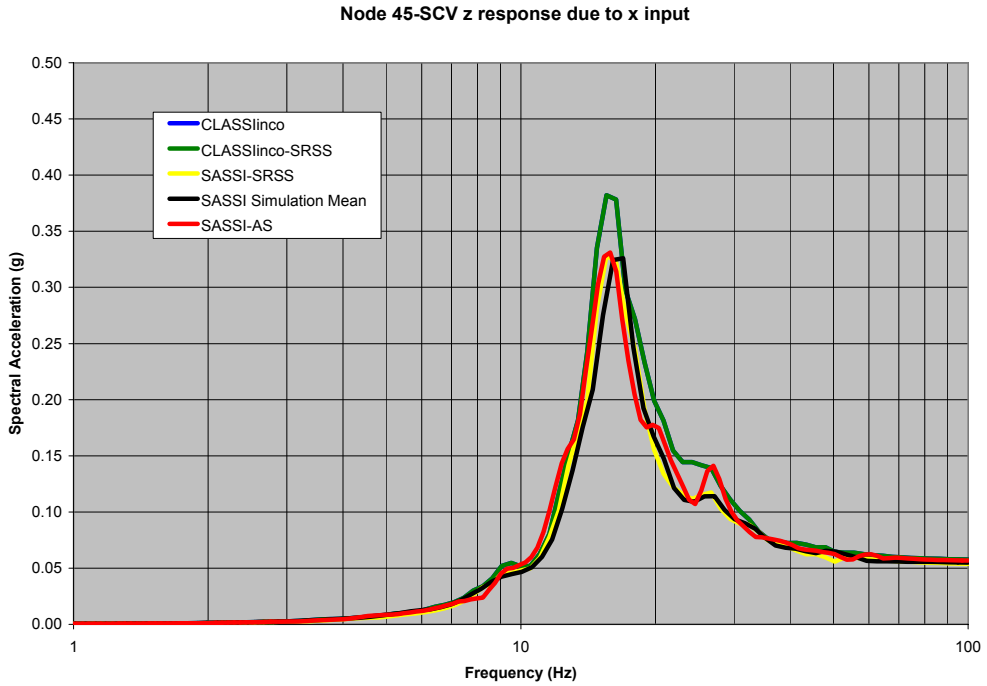

Figure A-25
Top of SCV Response Spectra – Z Direction Due to X Input – CLASSlinco, CLASSlinco-SRSS, SASSI-SRSS, SASSI Simulation Mean, SASSI-AS (Node 45)

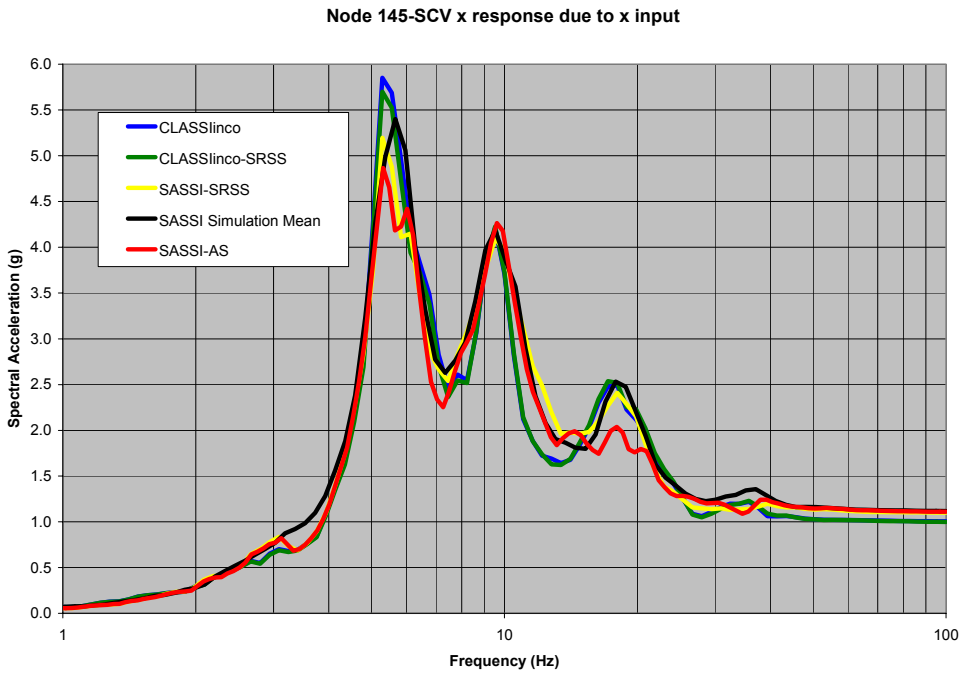

Figure A-26
SCV Outrigger Response Spectra – X Direction Due to X Input – CLASSlinco, CLASSlinco-SRSS, SASSI-SRSS, SASSI Simulation Mean, SASSI-AS (Node 145)

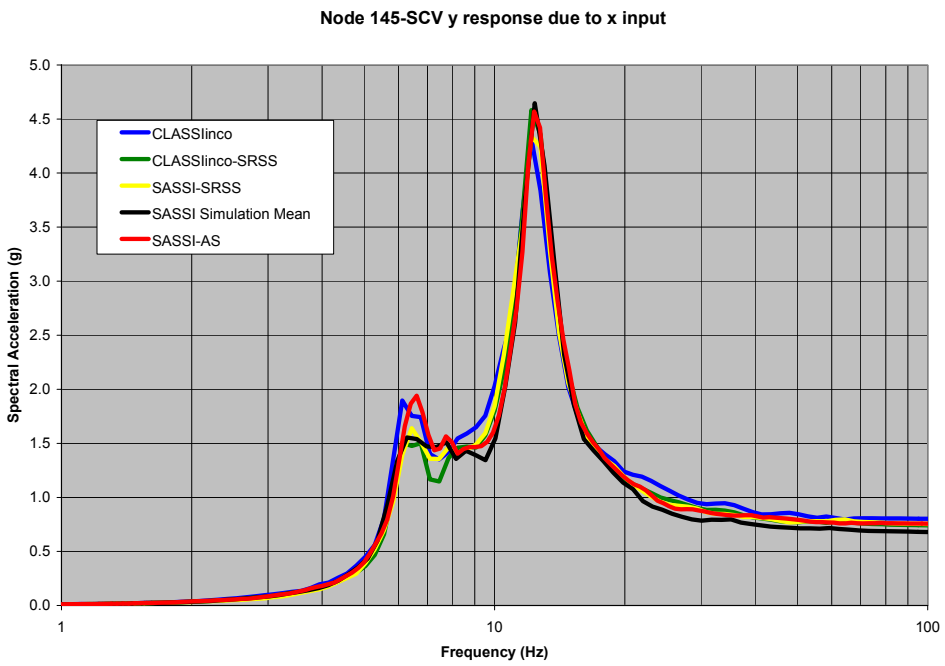

Figure A-27
SCV Outrigger Response Spectra – Y Direction Due to X Input – CLASSlinco, CLASSlinco-SRSS, SASSI-SRSS, SASSI Simulation Mean, SASSI-AS (Node 145)

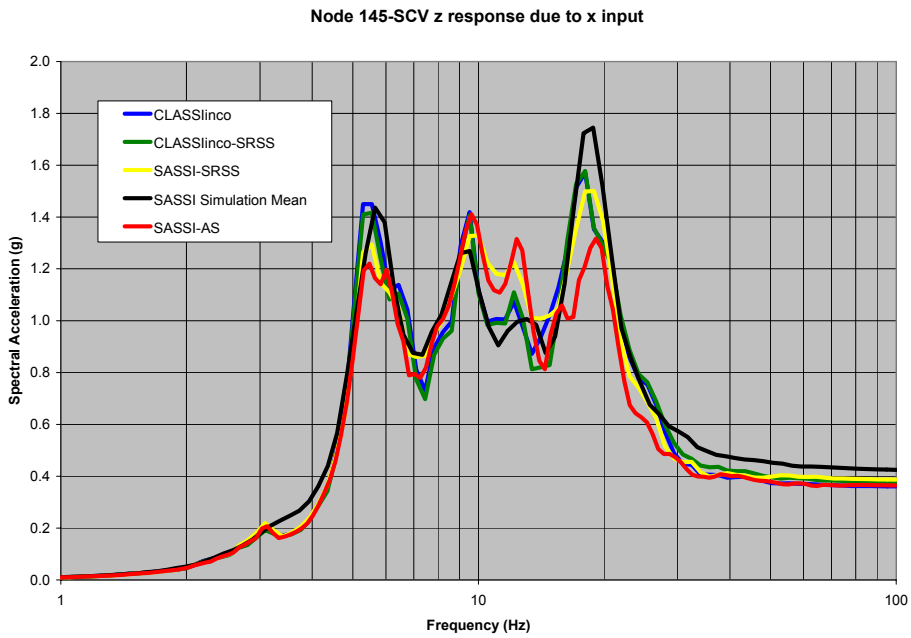

Figure A-28
SCV Outrigger Response Spectra – Z Direction Due to X Input – CLASSlinco, CLASSlinco-SRSS, SASSI-SRSS, SASSI Simulation Mean, SASSI-AS (Node 145)

Y-Direction Input Ground Motion

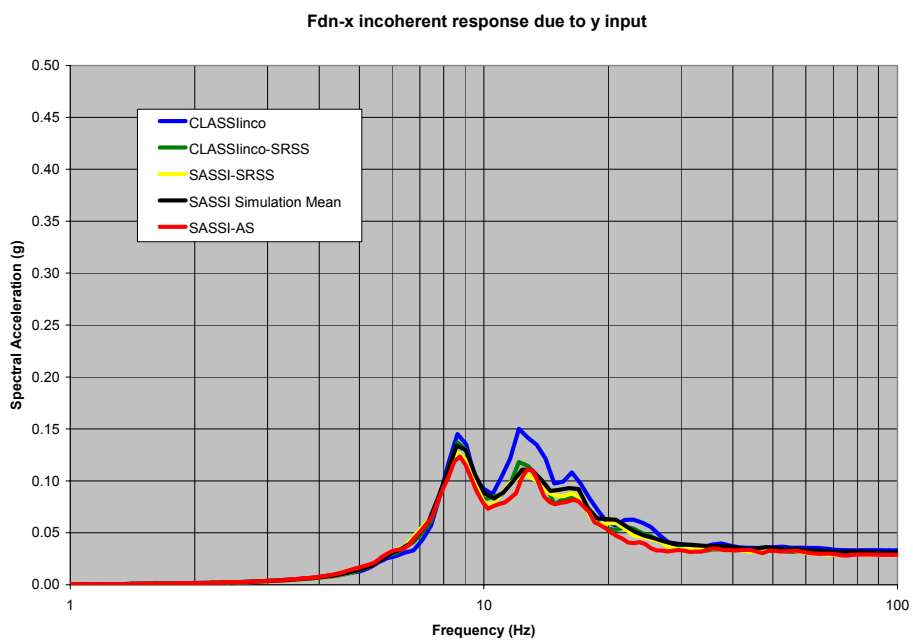

Figure A-29
Center of Foundation Response Spectra – X Direction Due to Y Input – CLASSlinco, CLASSlinco-SRSS, SASSI-SRSS, SASSI Simulation Mean, SASSI-AS (Node 1)

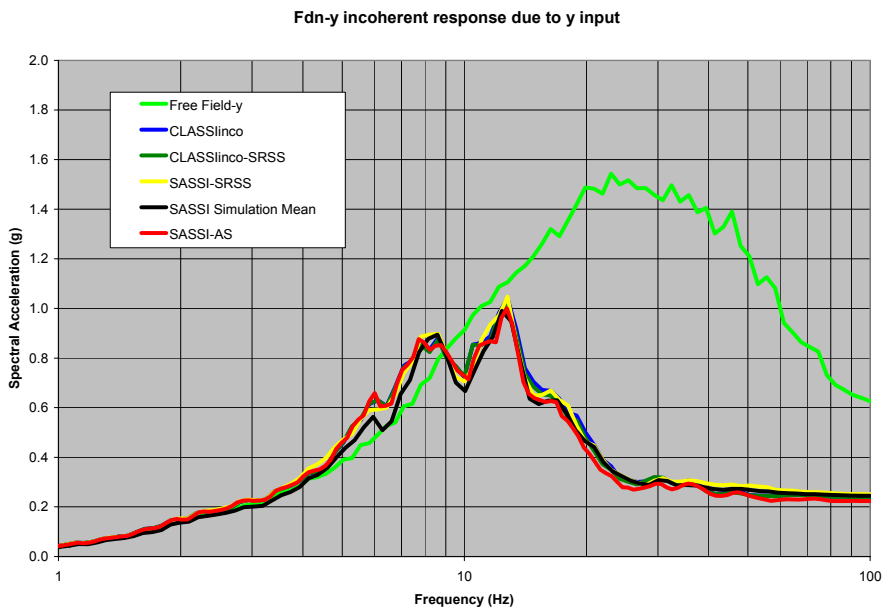

Figure A-30
Center of Foundation Response Spectra – Y Direction Due to Y Input – CLASSlinco, CLASSlinco-SRSS, SASSI-SRSS, SASSI Simulation Mean, SASSI-AS (Node 1)

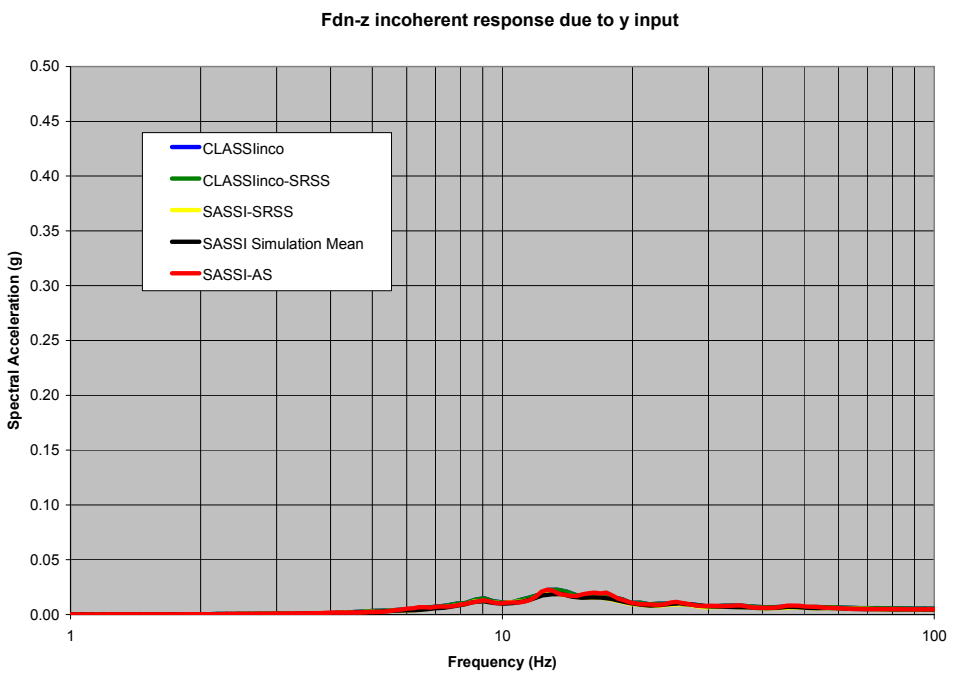

Figure A-31
Center of Foundation Response Spectra – Z Direction Due to Y Input – CLASSlinco, CLASSlinco-SRSS, SASSI-SRSS, SASSI Simulation Mean, SASSI-AS (Node 1)

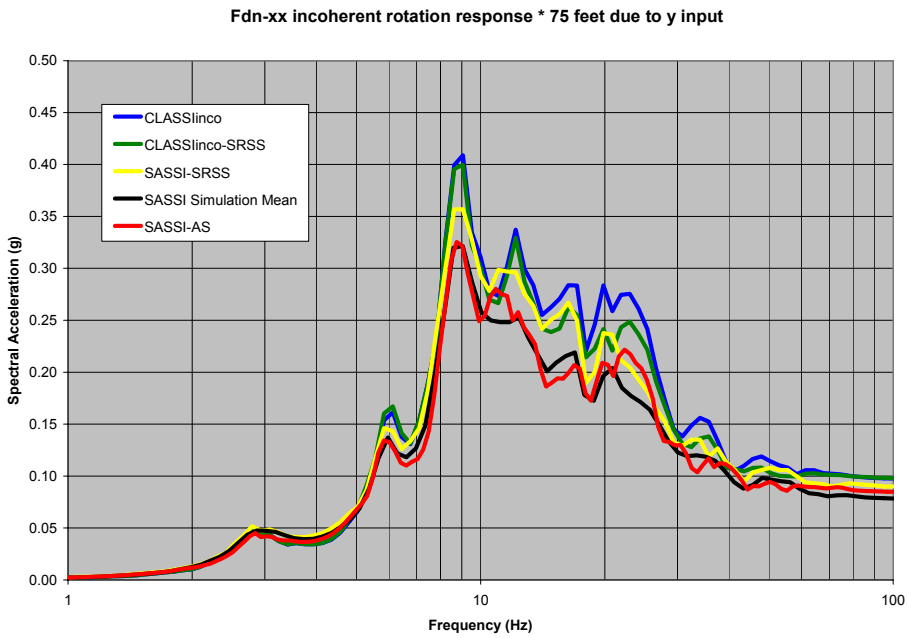

Figure A-32
Edge of Foundation Response Spectra –XX Rotation Due to Y Input – CLASSlinco, CLASSlinco-SRSS, SASSI-SRSS, SASSI Simulation Mean, SASSI-AS (Node 1)

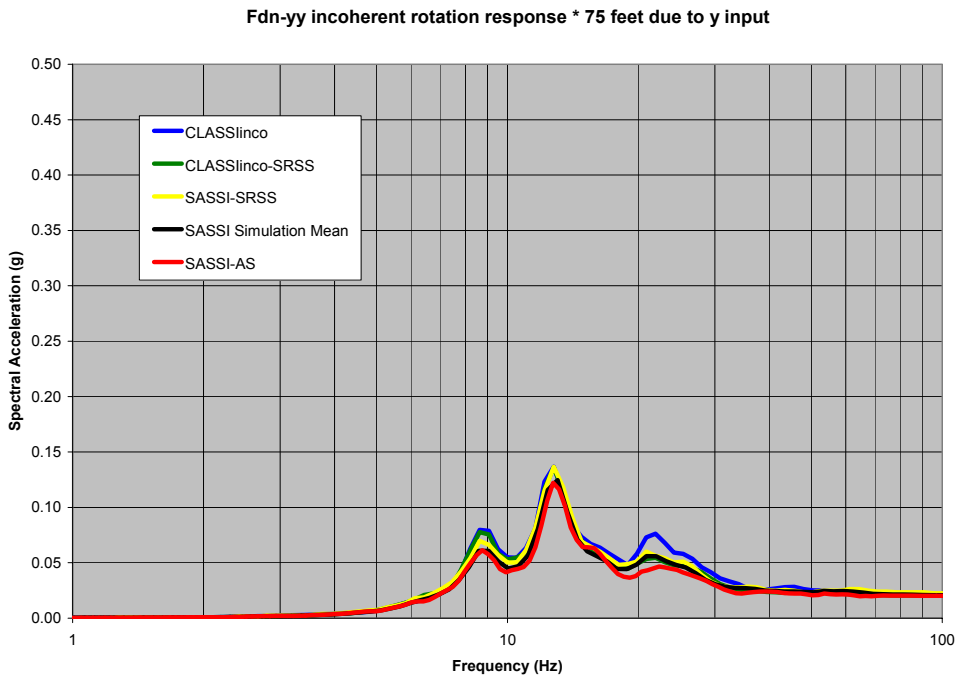

Figure A-33
Edge of Foundation Response Spectra –YY Rotation Due to Y Input – CLASSlinco, CLASSlinco-SRSS, SASSI-SRSS, SASSI Simulation Mean, SASSI-AS (Node 1)

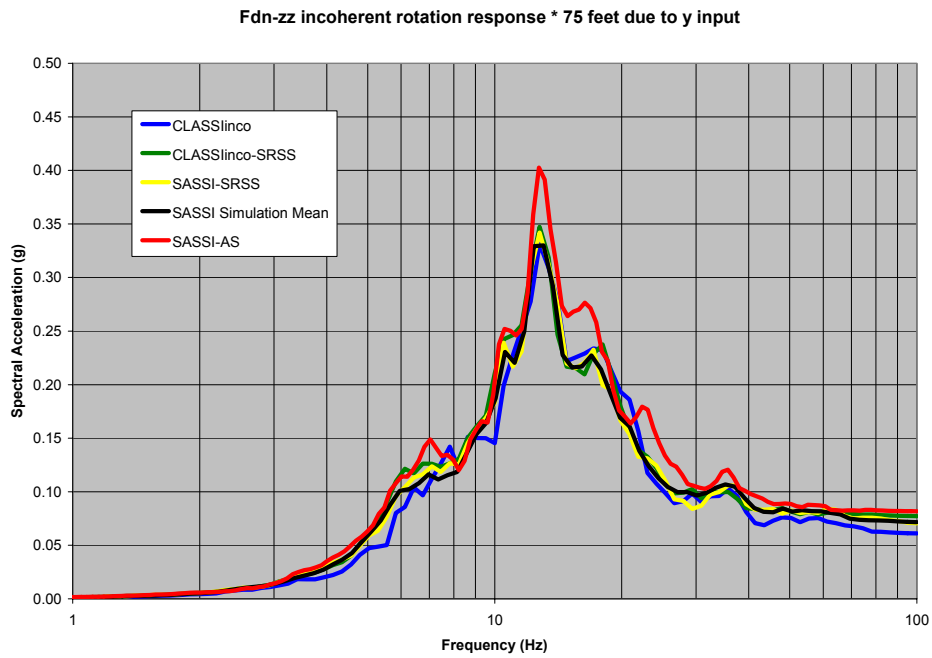

Figure A-34
Edge of Foundation Response Spectra –ZZ Rotation Due to Y Input – CLASSlinco, CLASSlinco-SRSS, SASSI-SRSS, SASSI Simulation Mean, SASSI-AS (Node 1)

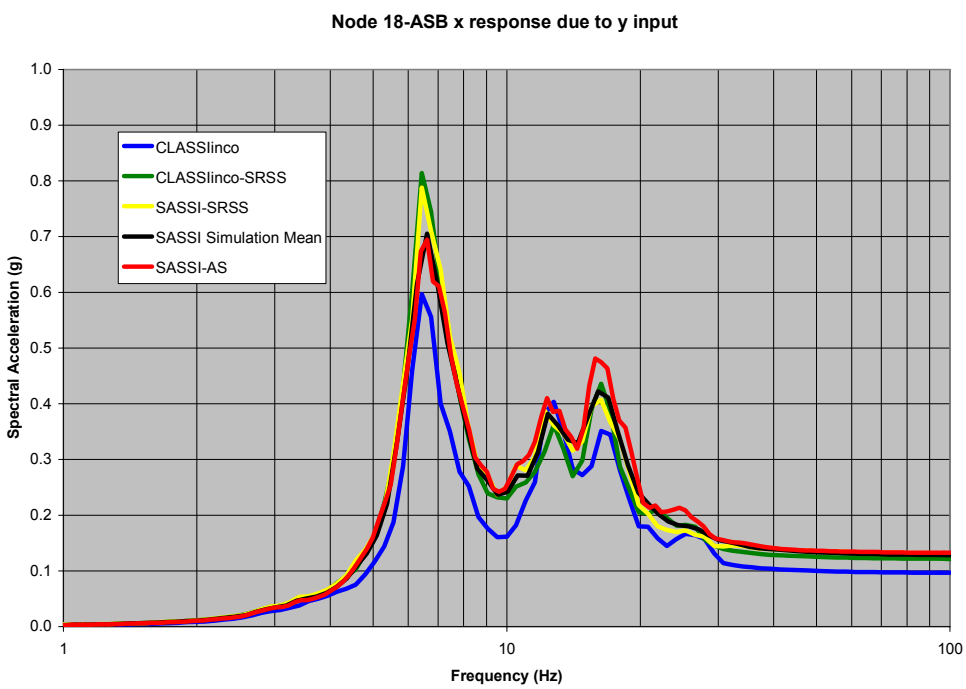

Figure A-35
Top of ASB Response Spectra – X Direction Due to Y Input – CLASSlinco, CLASSlinco-SRSS, SASSI-SRSS, SASSI Simulation Mean, SASSI-AS (Node 18)

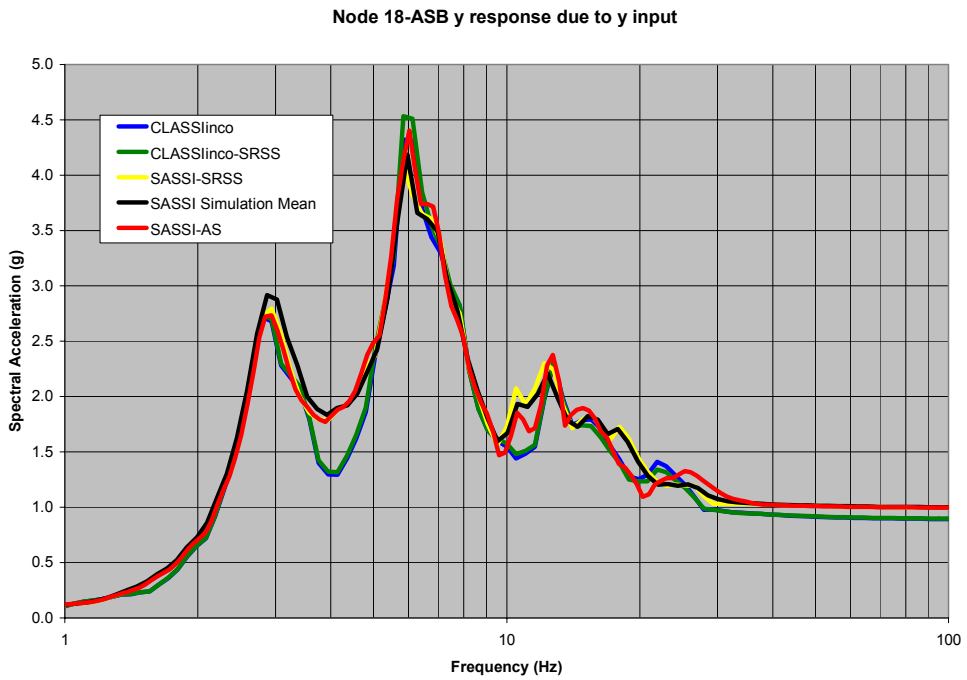

Figure A-36
Top of ASB Response Spectra – Y Direction Due to Y Input – CLASSIinco, CLASSIinco-SRSS, SASSI-SRSS, SASSI Simulation Mean, SASSI-AS (Node 18)

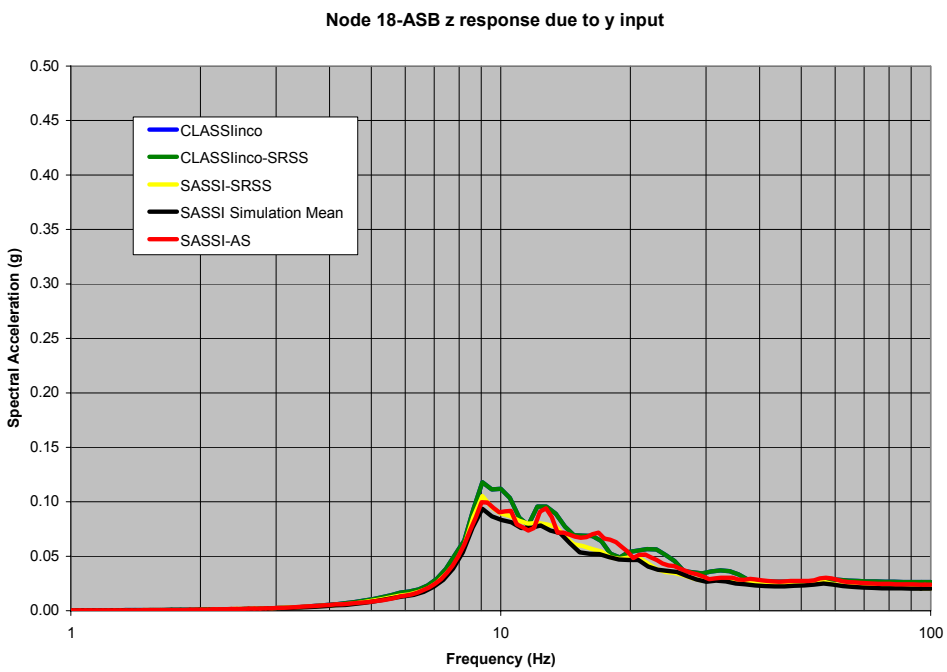

Figure A-37
Top of ASB Response Spectra – Z Direction Due to Y Input – CLASSIinco, CLASSIinco-SRSS, SASSI-SRSS, SASSI Simulation Mean, SASSI-AS (Node 18)

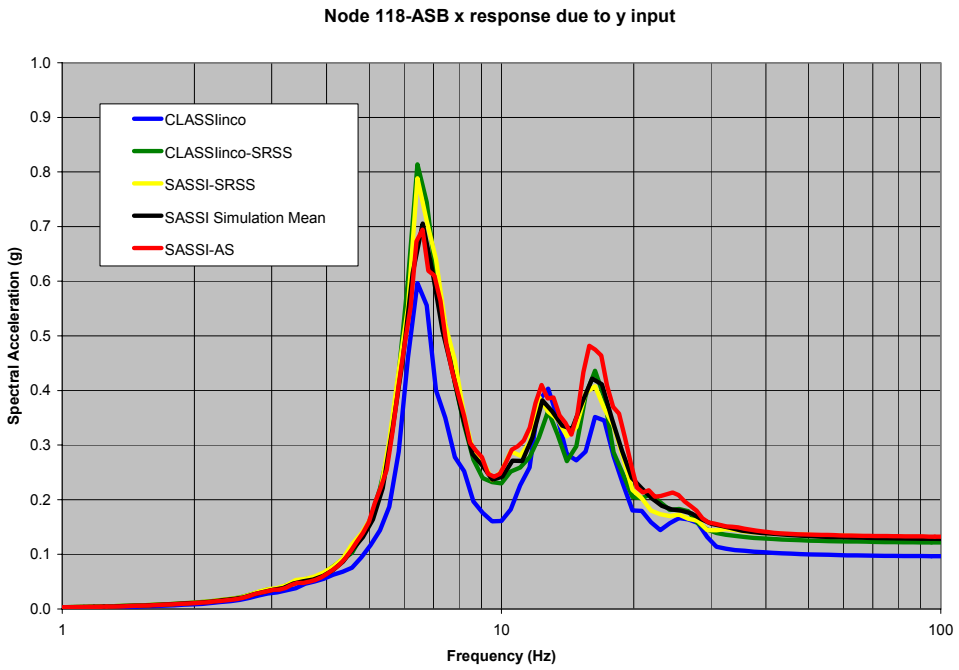

Figure A-38
ASB Outrigger Response Spectra – X Direction Due to Y Input – CLASSlinco, CLASSlinco-SRSS, SASSI-SRSS, SASSI Simulation Mean, SASSI-AS (Node 118)

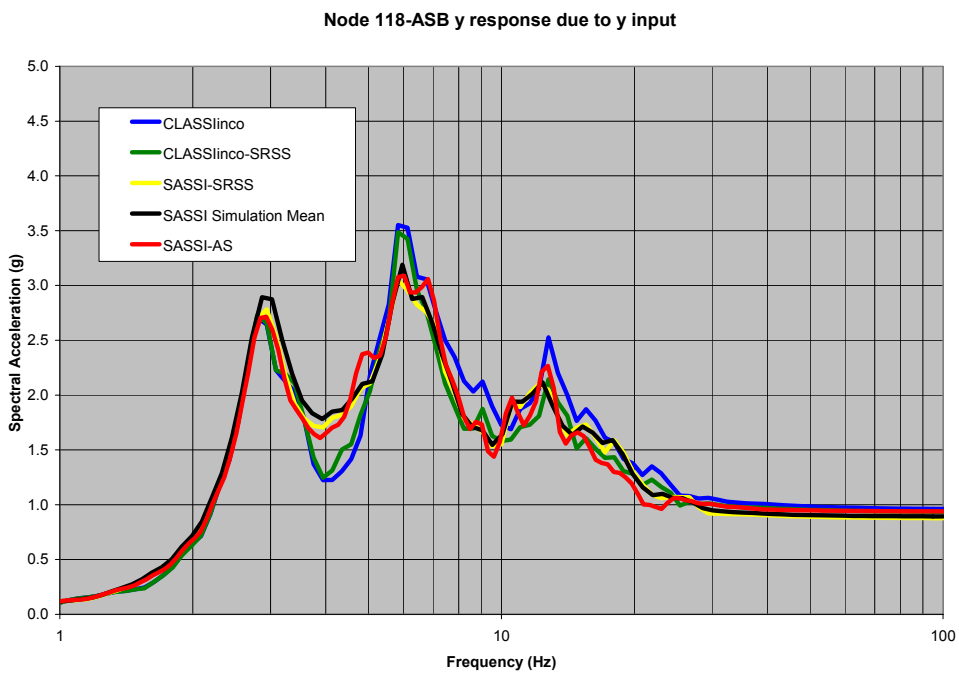

Figure A-39
ASB Outrigger Response Spectra – Y Direction Due to Y Input – CLASSlinco, CLASSlinco-SRSS, SASSI-SRSS, SASSI Simulation Mean, SASSI-AS (Node 118)

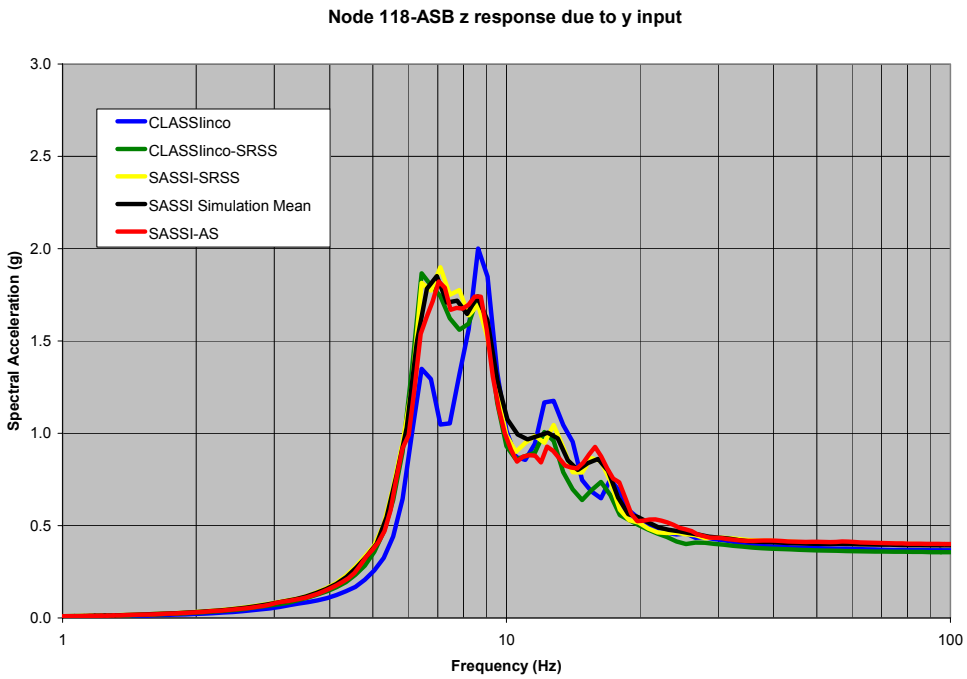

Figure A-40
ASB Outrigger Response Spectra – Z Direction Due to Y Input – CLASSlinco, CLASSlinco-SRSS, SASSI-SRSS, SASSI Simulation Mean, SASSI-AS (Node 118)

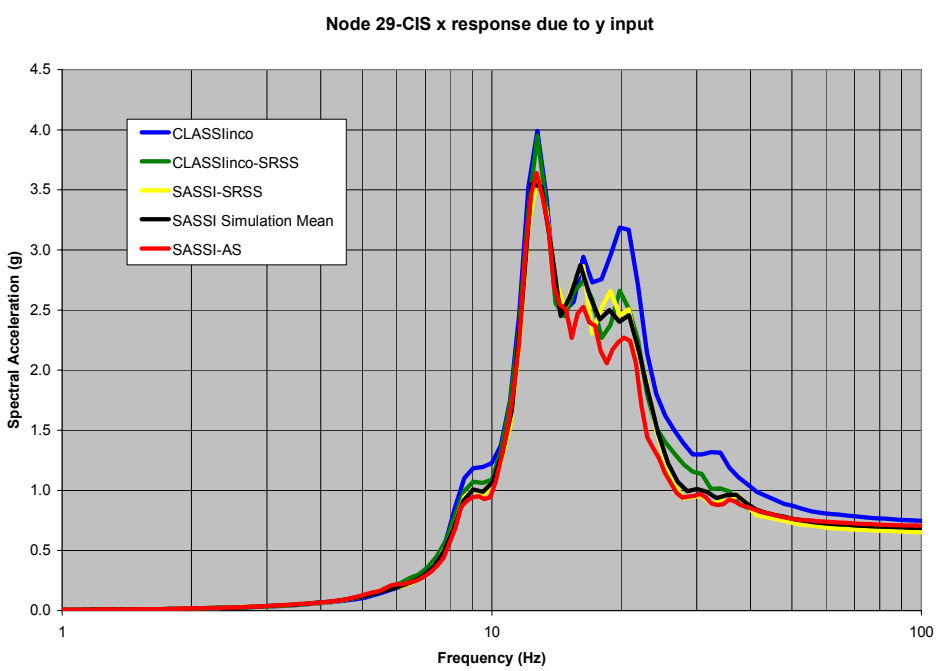

Figure A-41
Top of CIS Shear Center Response Spectra – X Direction Due to Y Input – CLASSlinco, CLASSlinco-SRSS, SASSI-SRSS, SASSI Simulation Mean, SASSI-AS (Node 29)

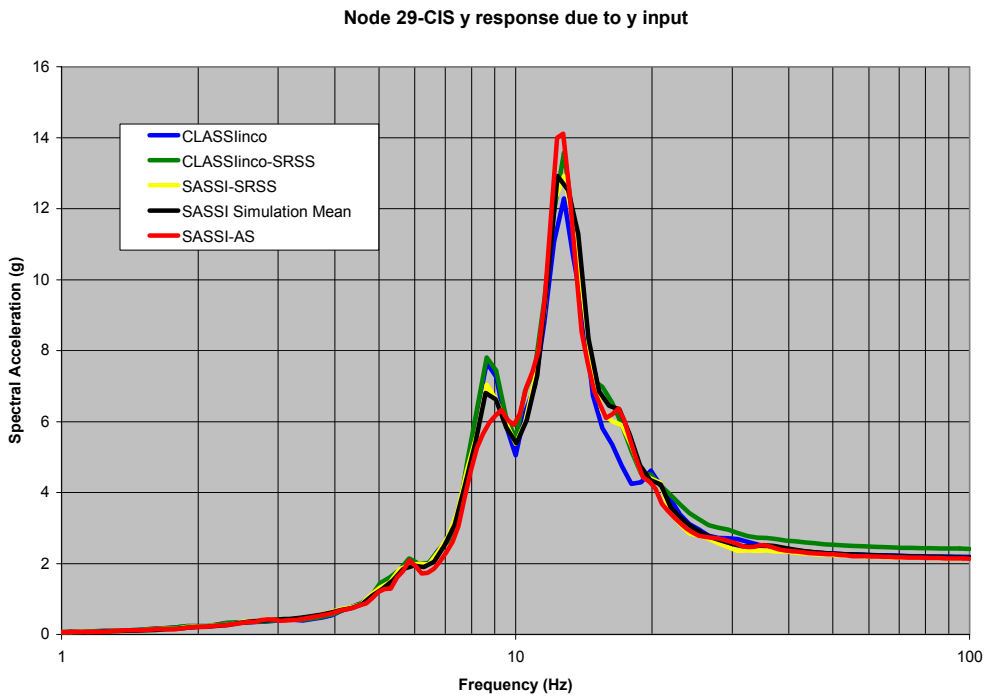

Figure A-42
Top of CIS Shear Center Response Spectra – Y Direction Due to Y Input – CLASSlinco, CLASSlinco-SRSS, SASSI-SRSS, SASSI Simulation Mean, SASSI-AS (Node 29)

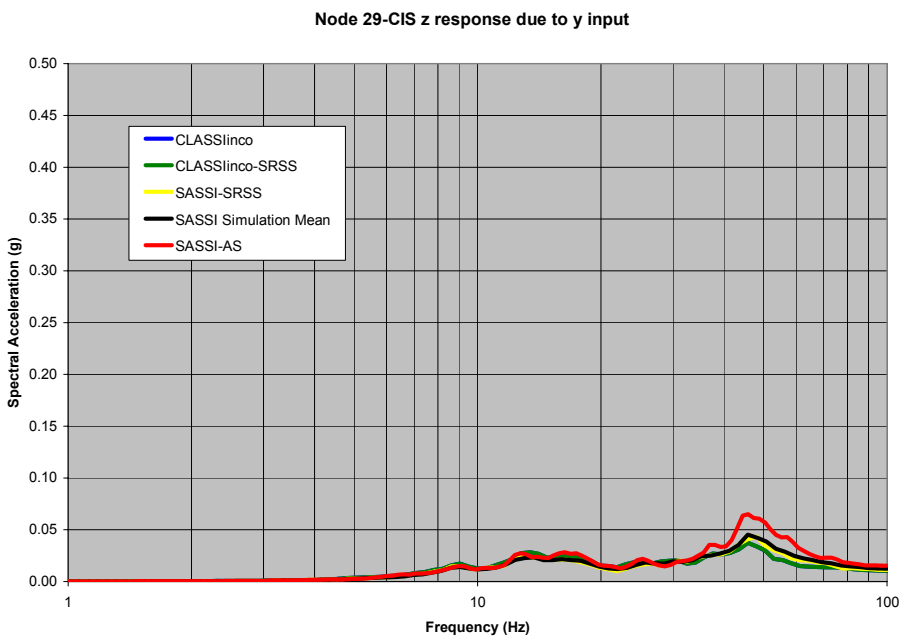

Figure A-43
Top of CIS Shear Center Response Spectra – Z Direction Due to Y Input – CLASSlinco, CLASSlinco-SRSS, SASSI-SRSS, SASSI Simulation Mean, SASSI-AS (Node 29)

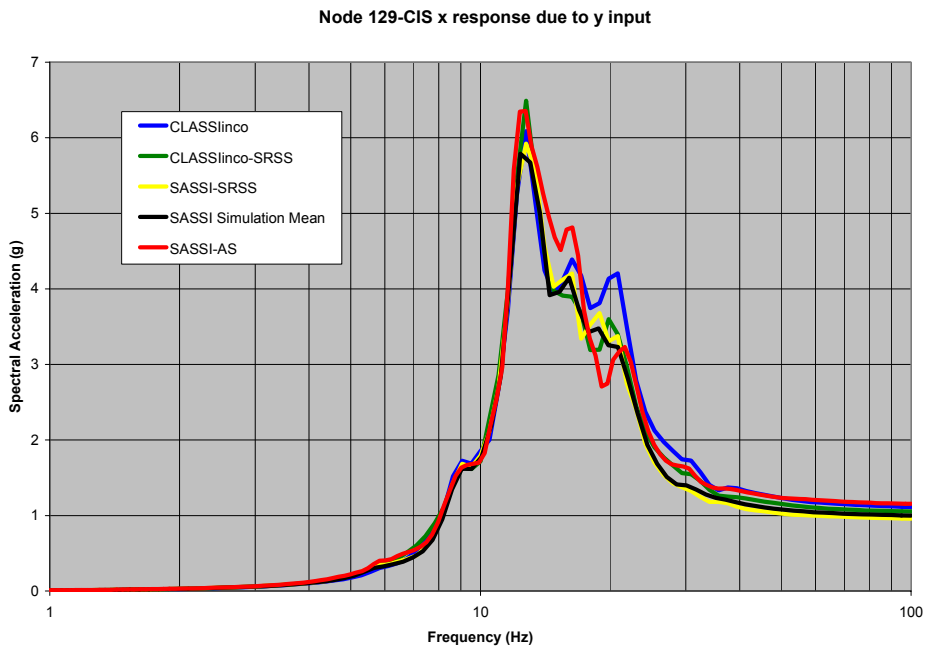

Figure A-44
Top of CIS Horizontal Mass Center Response Spectra – X Direction Due to Y Input – CLASSlinco, CLASSlinco-SRSS, SASSI-SRSS, SASSI Simulation Mean, SASSI-AS (Node 129)

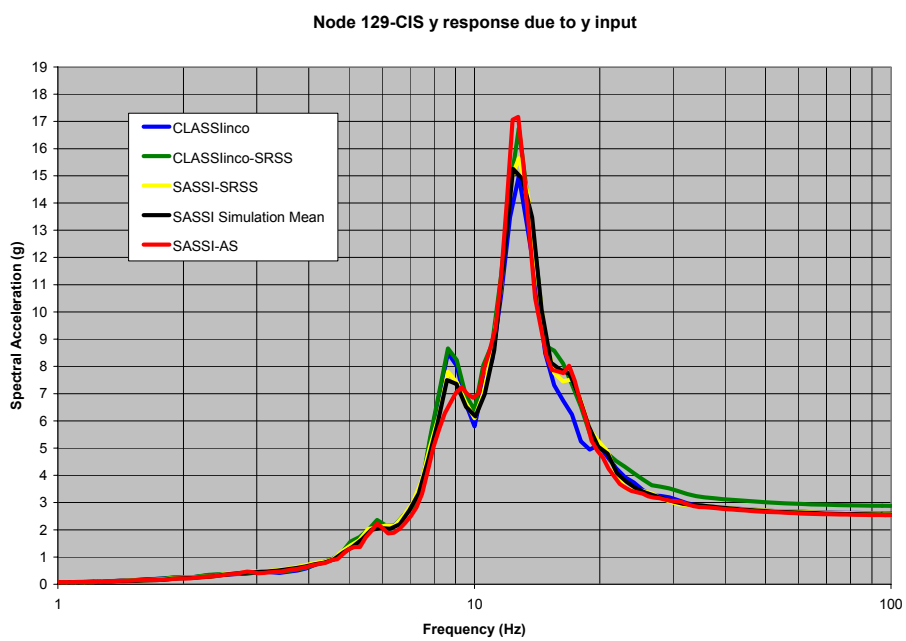

Figure A-45
Top of CIS Horizontal Mass Center Response Spectra – Y Direction Due to Y Input – CLASSlinco, CLASSlinco-SRSS, SASSI-SRSS, SASSI Simulation Mean, SASSI-AS (Node 129)

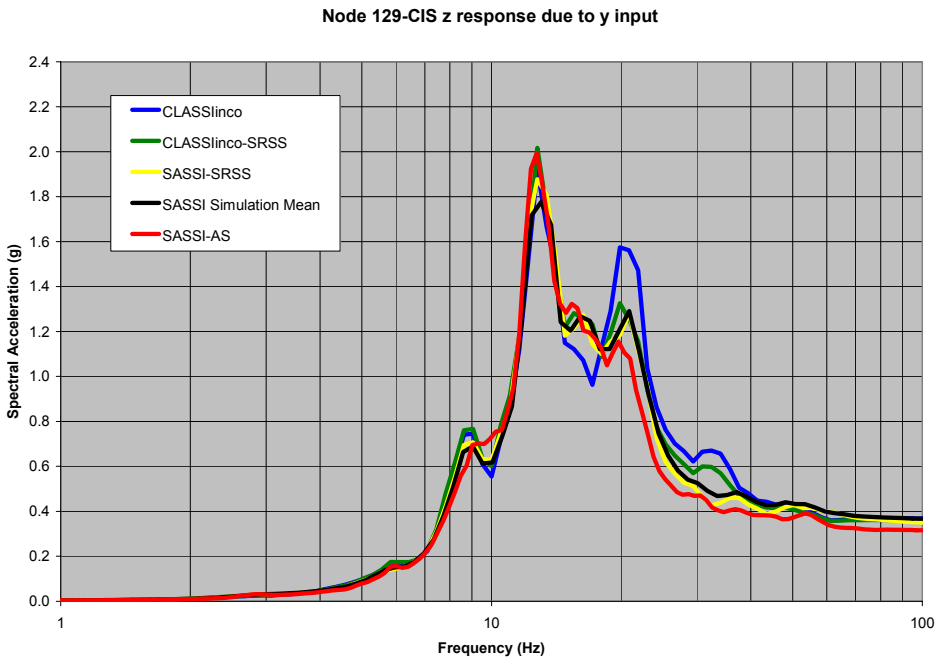

Figure A-46
Top of CIS Horizontal Mass Center Response Spectra – Z Direction Due to Y Input – CLASSlinco, CLASSlinco-SRSS, SASSI-SRSS, SASSI Simulation Mean, SASSI-AS (Node 129)

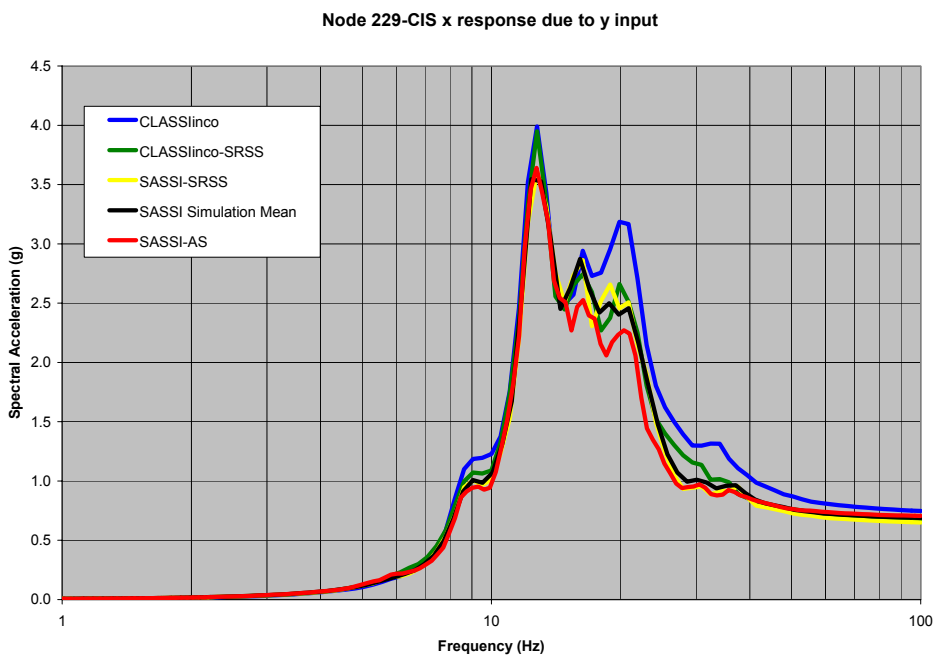

Figure A-47
CIS Outrigger Response Spectra – X Direction Due to Y Input – CLASSlinco, CLASSlinco-SRSS, SASSI-SRSS, SASSI Simulation Mean, SASSI-AS (Node 229)

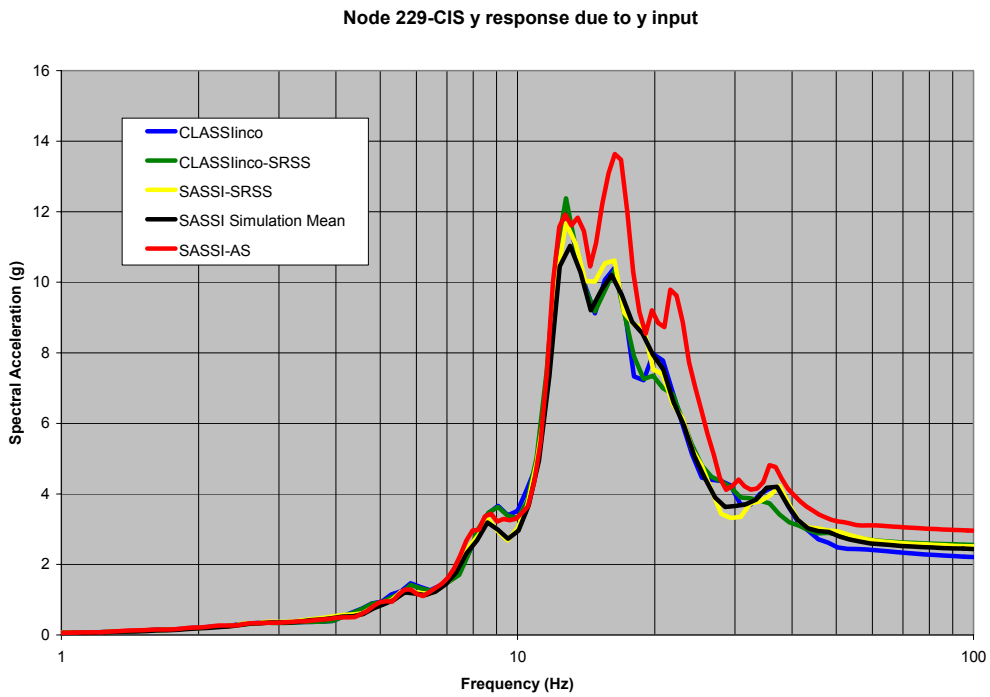

Figure A-48
CIS Outrigger Response Spectra – Y Direction Due to Y Input – CLASSlinco, CLASSlinco-SRSS, SASSI-SRSS, SASSI Simulation Mean, SASSI-AS (Node 229)

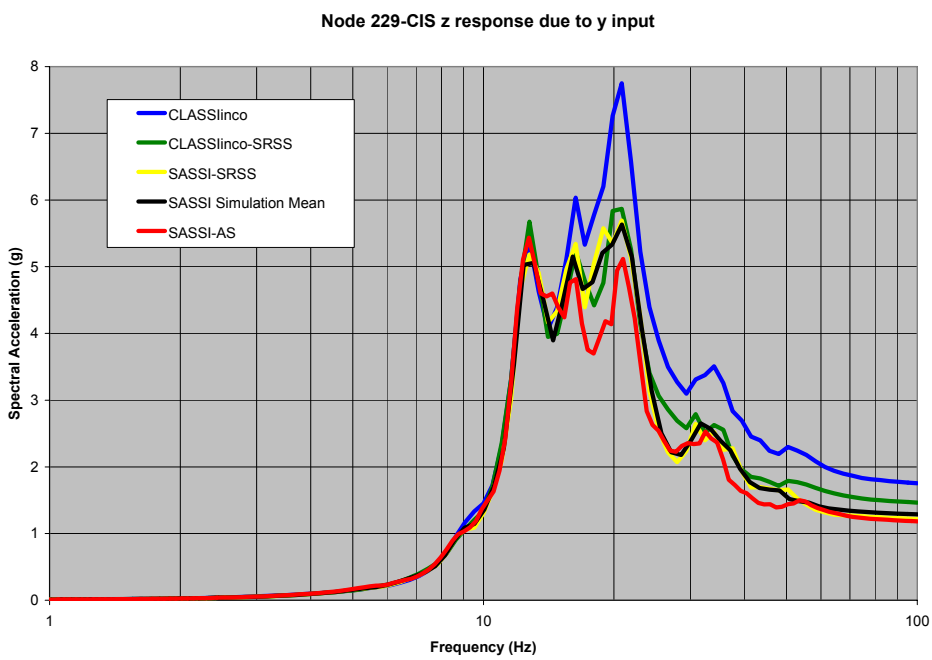

Figure A-49
CIS Outrigger Response Spectra – Z Direction Due to Y Input – CLASSlinco, CLASSlinco-SRSS, SASSI-SRSS, SASSI Simulation Mean, SASSI-AS (Node 229)

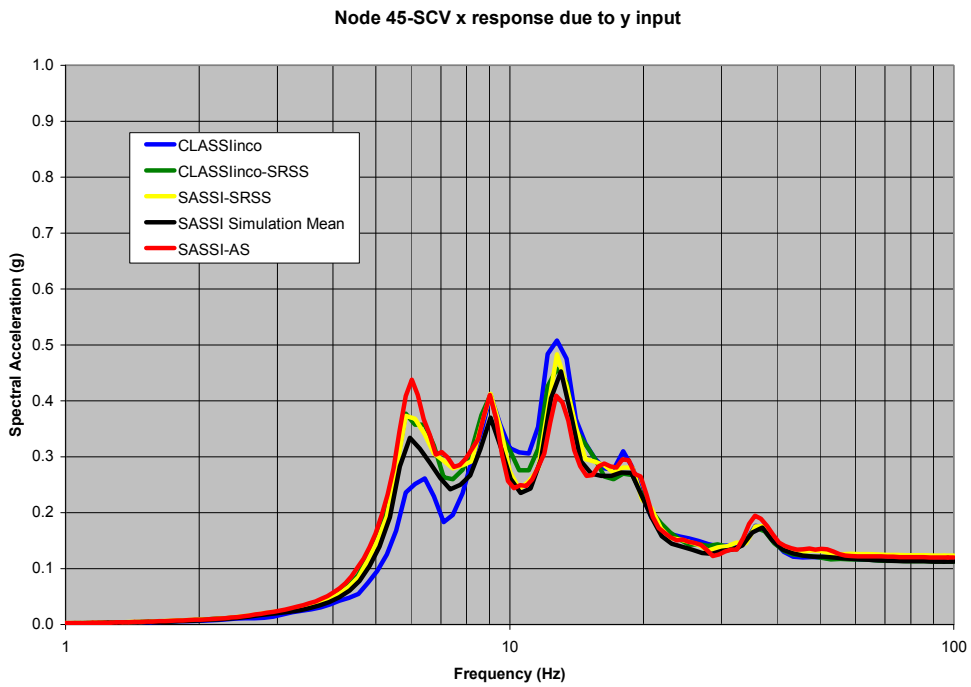

Figure A-50
Top of SCV Response Spectra – X Direction Due to Y Input – CLASSIinco, CLASSIinco-SRSS, SASSI-SRSS, SASSI Simulation Mean, SASSI-AS (Node 45)

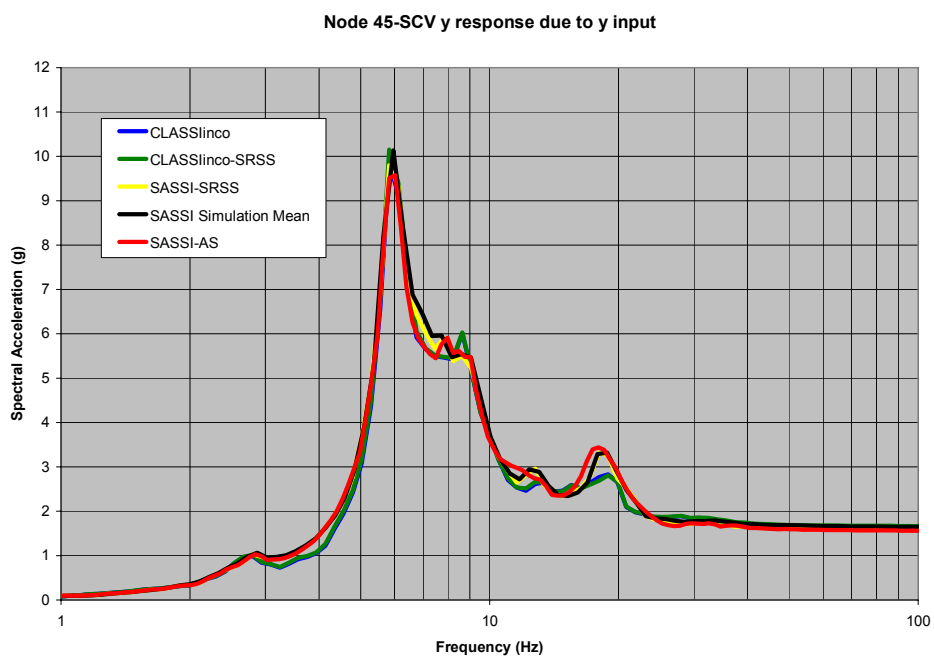

Figure A-51
Top of SCV Response Spectra – Y Direction Due to Y Input – CLASSIinco, CLASSIinco-SRSS, SASSI-SRSS, SASSI Simulation Mean, SASSI-AS (Node 45)

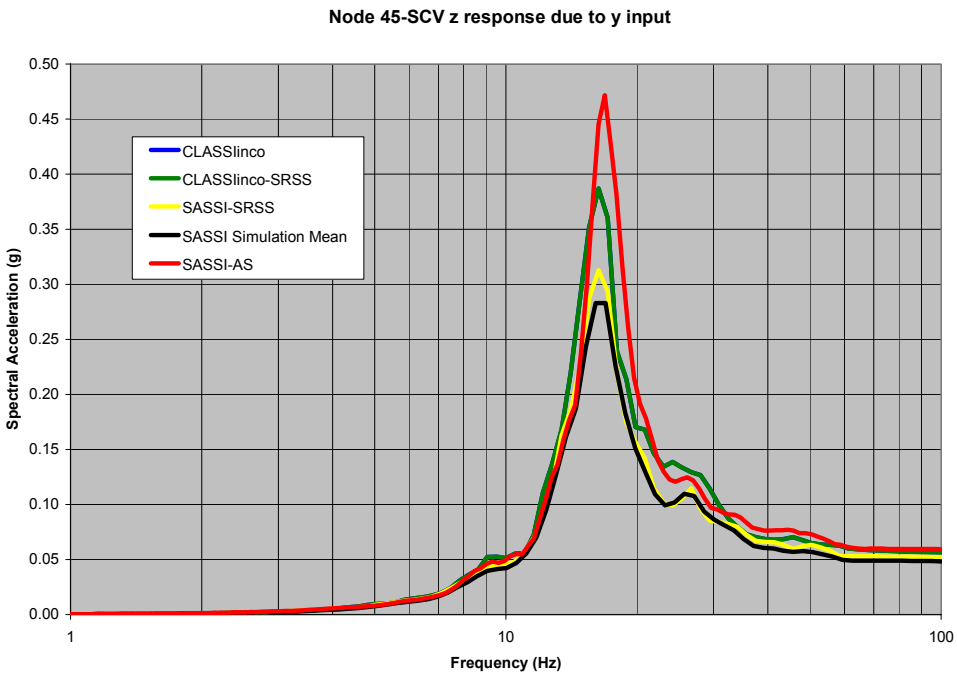

Figure A-52
Top of SCV Response Spectra – Z Direction Due to Y Input – CLASSlinco, CLASSlinco-SRSS, SASSI-SRSS, SASSI Simulation Mean, SASSI-AS (Node 45)

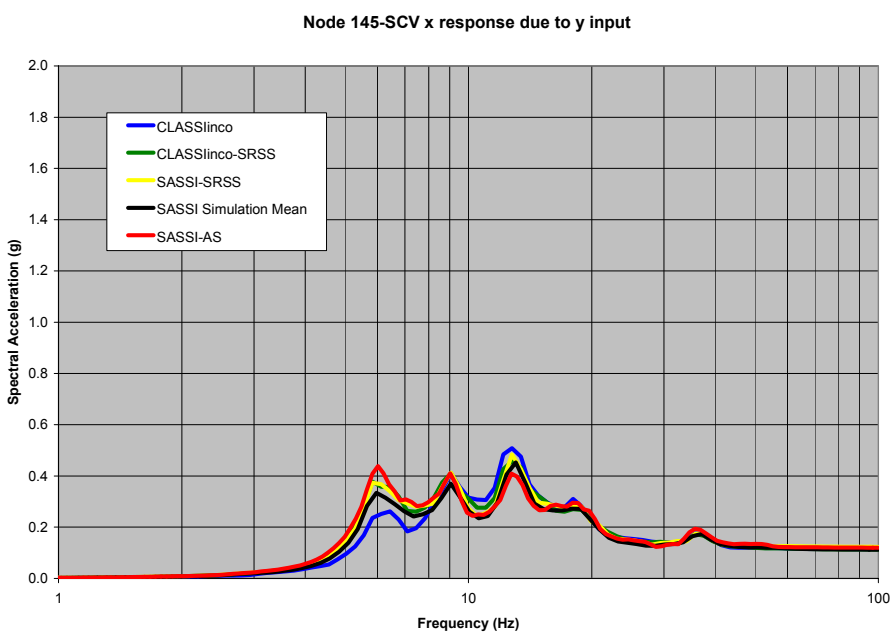

Figure A-53
SCV Outrigger Response Spectra – X Direction Due to Y Input – CLASSlinco, CLASSlinco-SRSS, SASSI-SRSS, SASSI Simulation Mean, SASSI-AS (Node 145)

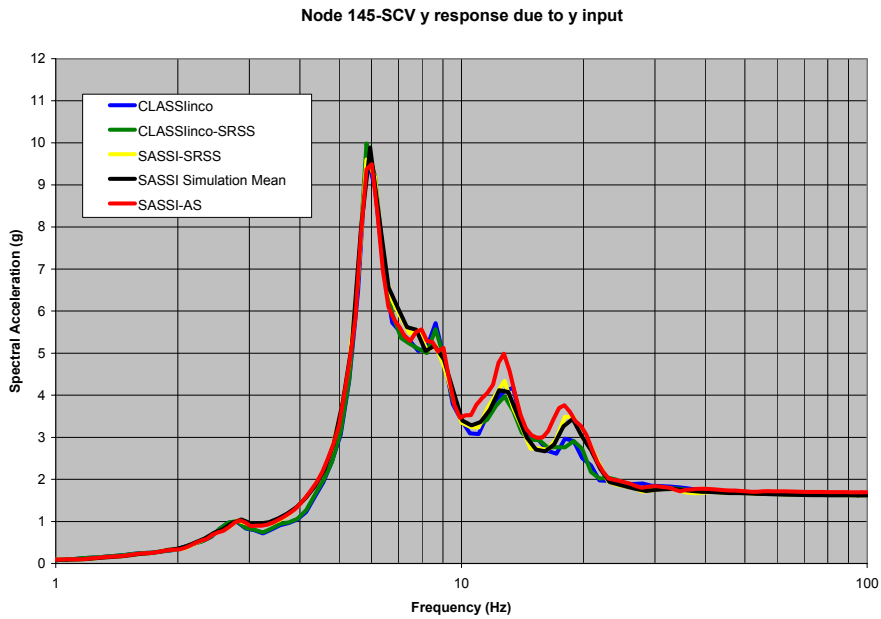

Figure A-54
SCV Outrigger Response Spectra – Y Direction Due to Y Input – CLASSIinco, CLASSIinco-SRSS, SASSI-SRSS, SASSI Simulation Mean, SASSI-AS (Node 145)

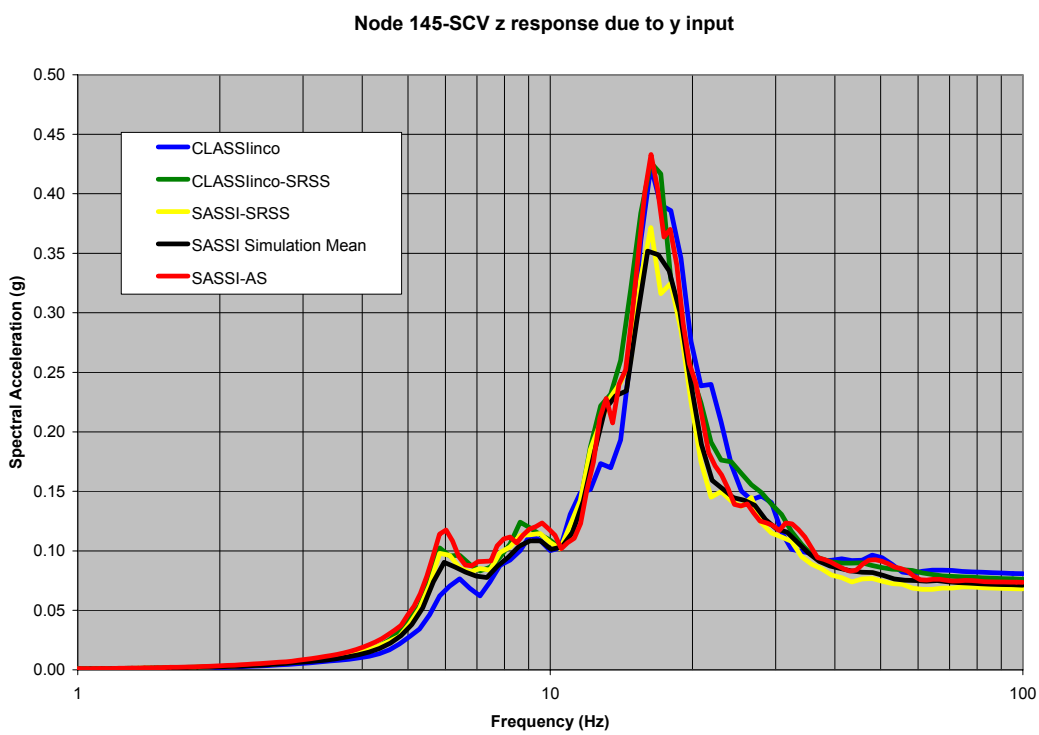

Figure A-55
SCV Outrigger Response Spectra – Z Direction Due to Y Input – CLASSIinco, CLASSIinco-SRSS, SASSI-SRSS, SASSI Simulation Mean, SASSI-AS (Node 145)

Z-Direction Input Ground Motion

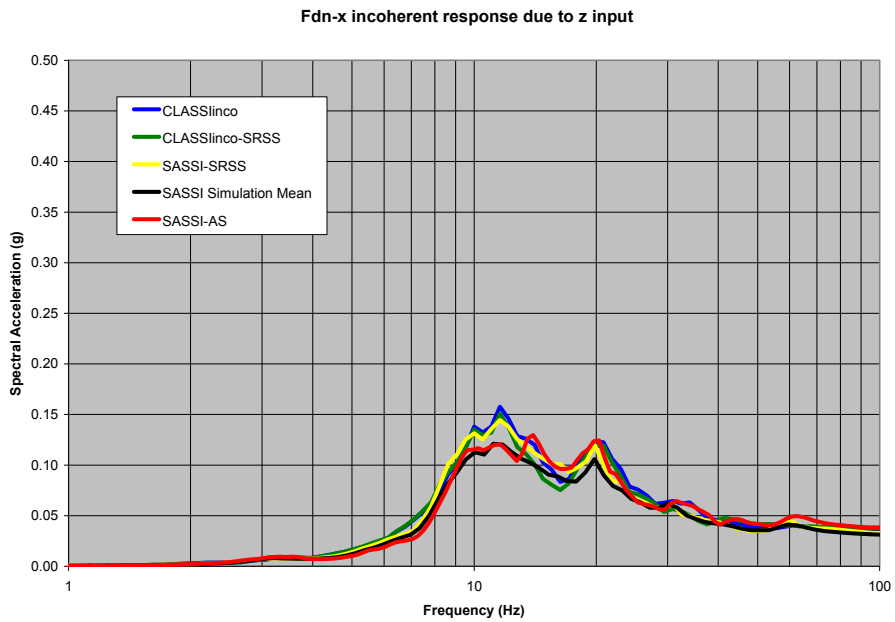

Figure A-56
Center of Foundation Response Spectra – X Direction Due to Z Input – CLASSlinco, CLASSlinco-SRSS, SASSI-SRSS, SASSI Simulation Mean, SASSI-AS (Node 1)

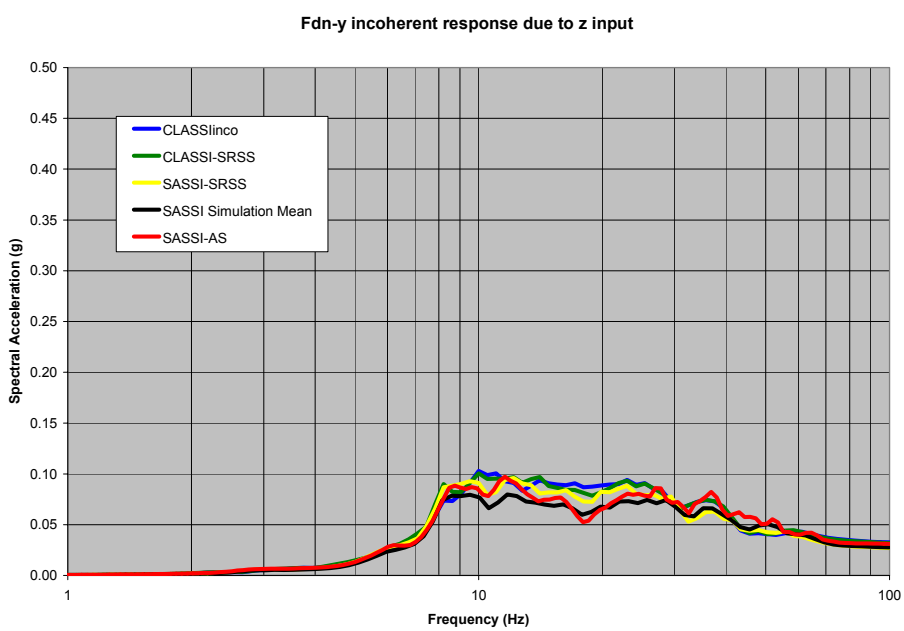

Figure A-57
Center of Foundation Response Spectra – Y Direction Due to Z Input – CLASSlinco, CLASSlinco-SRSS, SASSI-SRSS, SASSI Simulation Mean, SASSI-AS (Node 1)

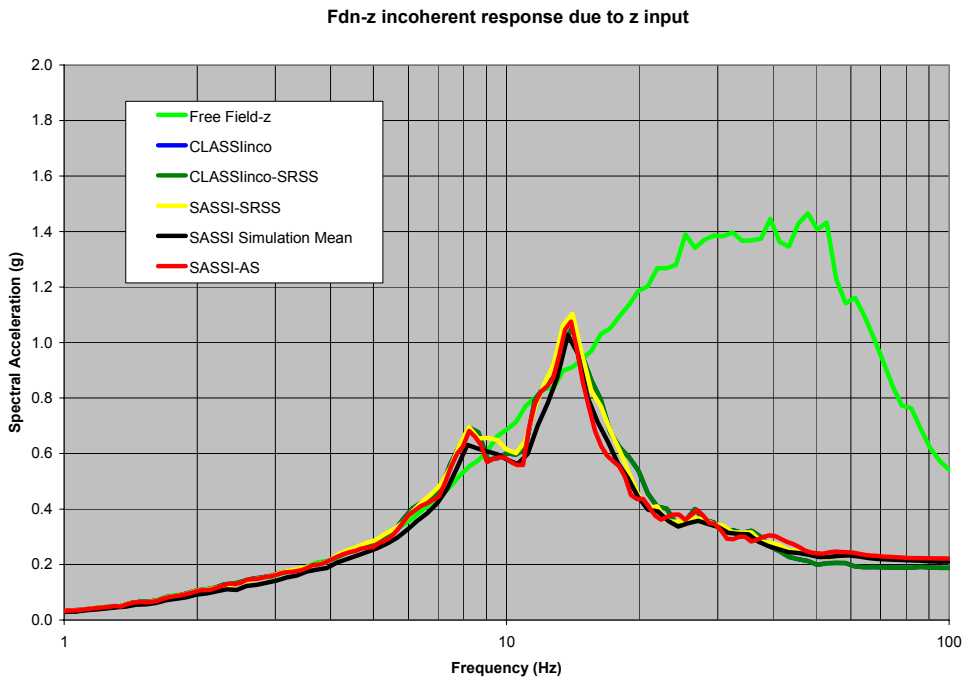

Figure A-58
Center of Foundation Response Spectra – Z Direction Due to Z Input – CLASSlinco, CLASSlinco-SRSS, SASSI-SRSS, SASSI Simulation Mean, SASSI-AS (Node 1)

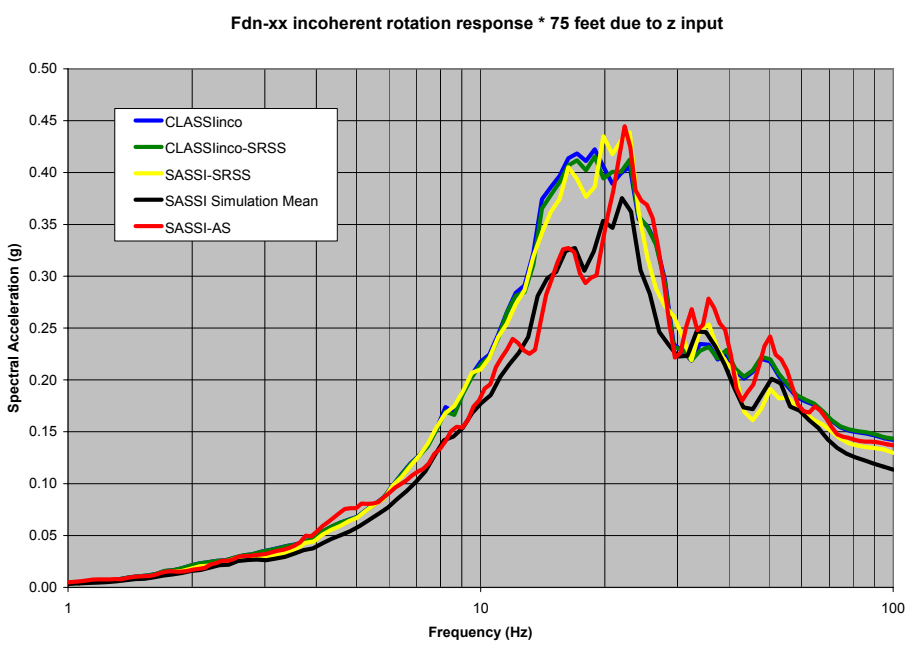

Figure A-59
Edge of Foundation Response Spectra –XX Rotation Due to Z Input – CLASSlinco, CLASSlinco-SRSS, SASSI-SRSS, SASSI Simulation Mean, SASSI-AS (Node 1)

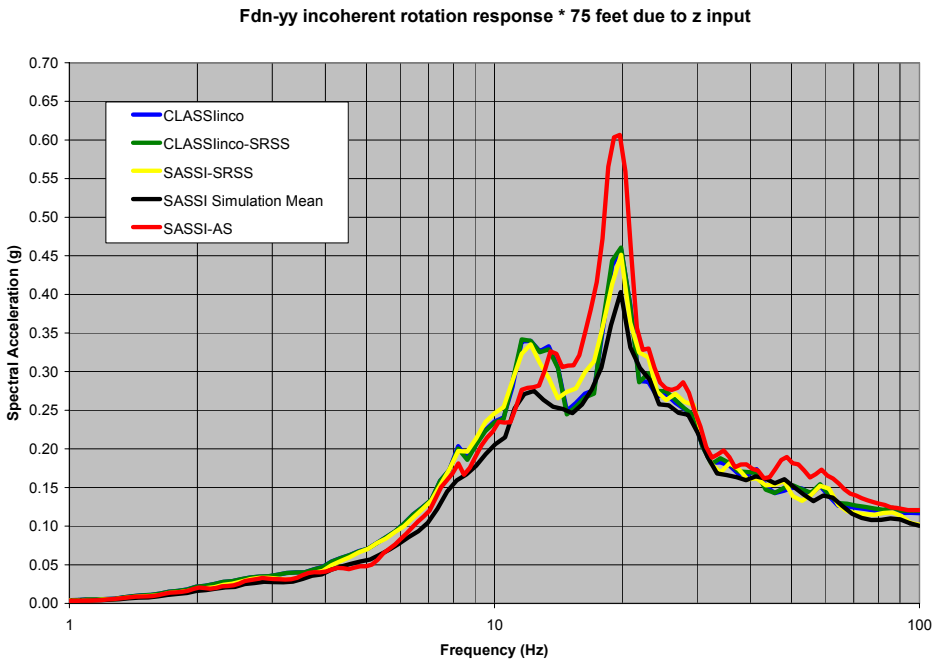

Figure A-60
Edge of Foundation Response Spectra –YY Rotation Due to Z Input – CLASSlinco, CLASSlinco-SRSS, SASSI-SRSS, SASSI Simulation Mean, SASSI-AS (Node 1)

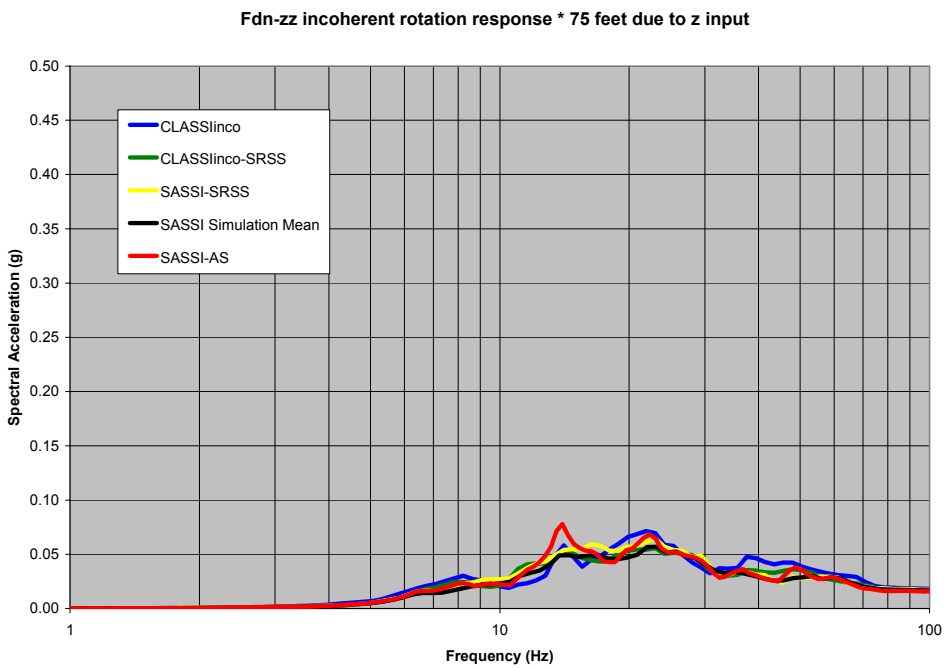

Figure A-61
Edge of Foundation Response Spectra –ZZ Rotation Due to Z Input – CLASSlinco, CLASSlinco-SRSS, SASSI-SRSS, SASSI Simulation Mean, SASSI-AS (Node 1)

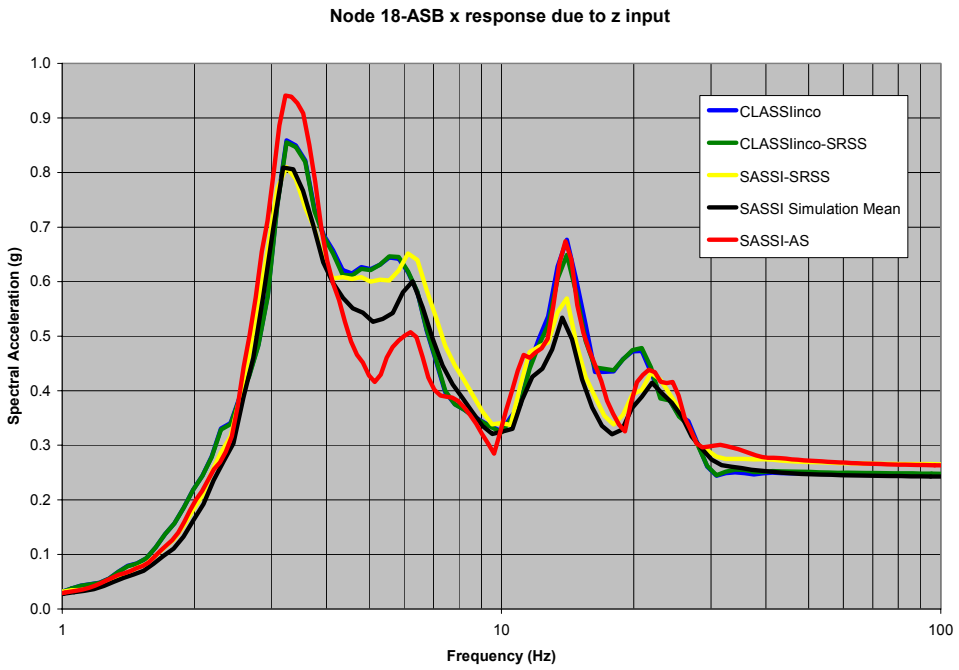

Figure A-62
Top of ASB Response Spectra – X Direction Due to Z Input – CLASSlinco, CLASSlinco-SRSS, SASSI-SRSS, SASSI Simulation Mean, SASSI-AS (Node 18)

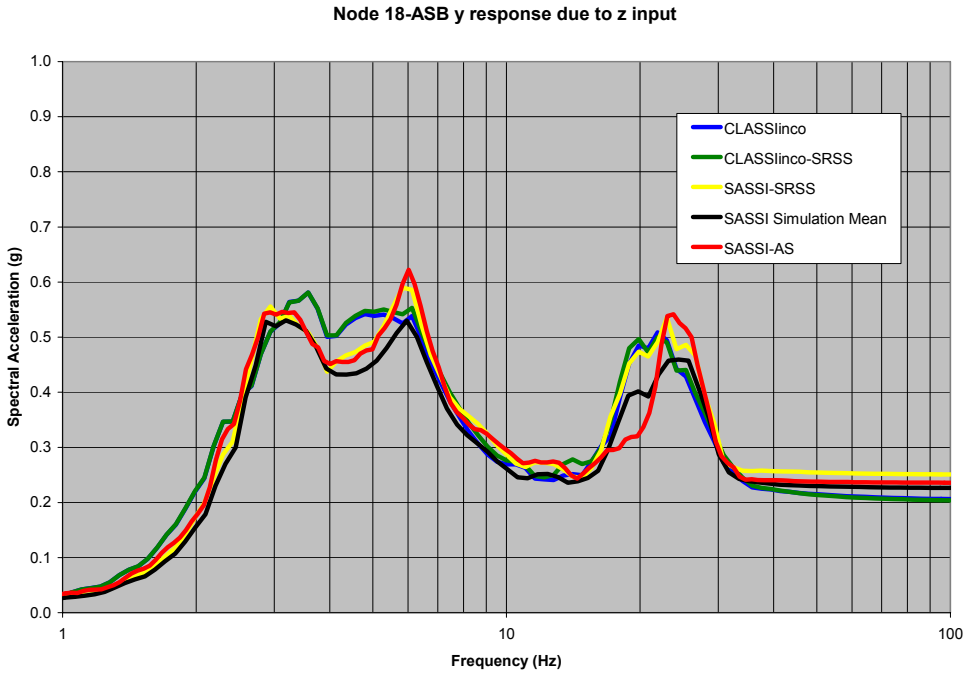

Figure A-63
Top of ASB Response Spectra – Y Direction Due to Z Input – CLASSlinco, CLASSlinco-SRSS, SASSI-SRSS, SASSI Simulation Mean, SASSI-AS (Node 18)

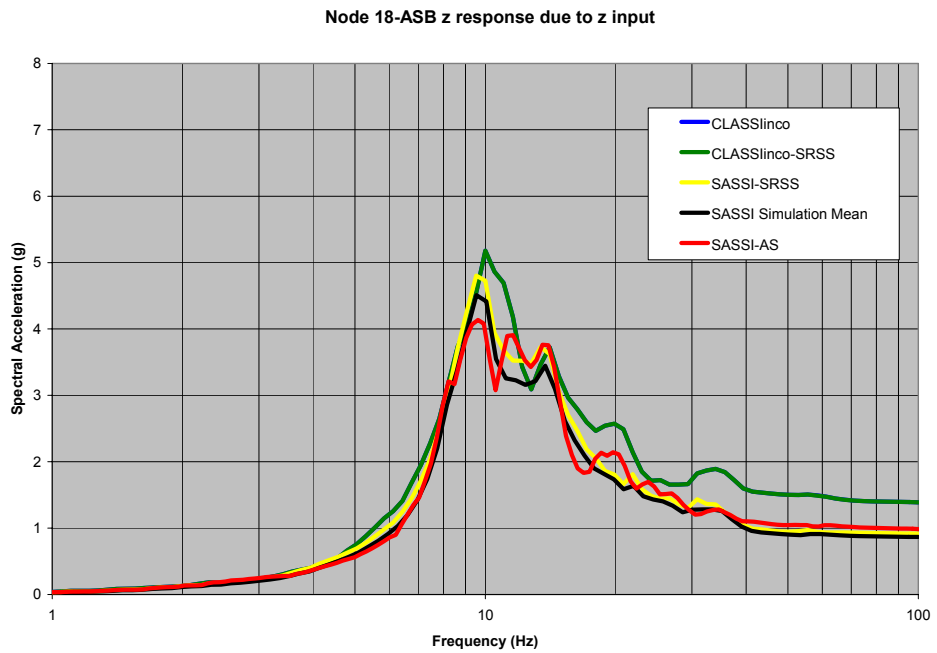

Figure A-64
Top of ASB Response Spectra – Z Direction Due to Z Input – CLASSlinco, CLASSlinco-SRSS, SASSI-SRSS, SASSI Simulation Mean, SASSI-AS (Node 18)

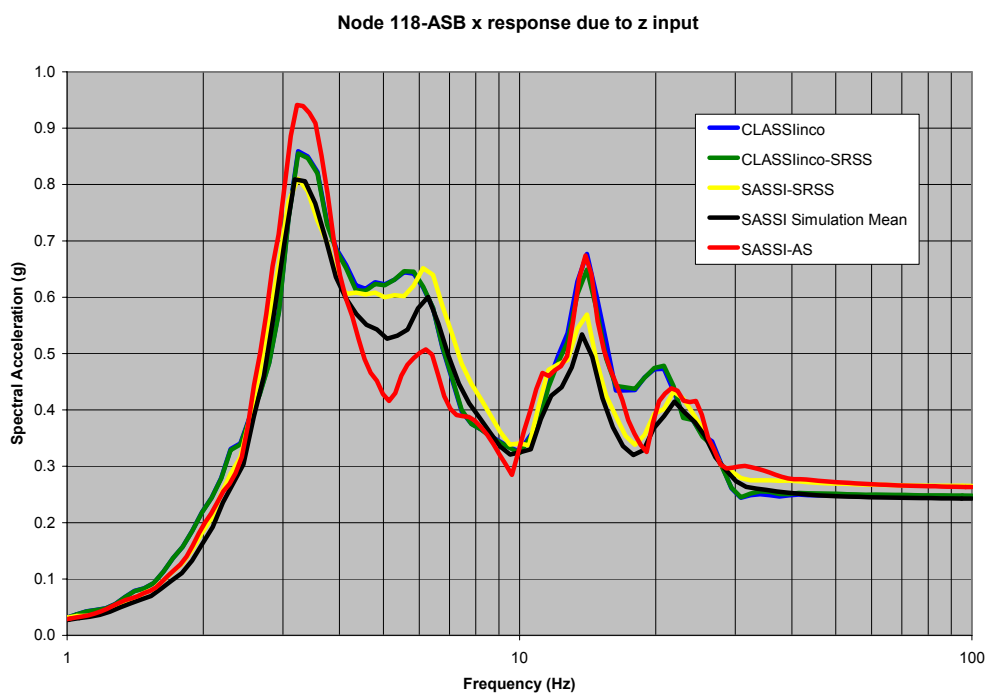

Figure A-65
ASB Outrigger Response Spectra – X Direction Due to Z Input – CLASSlinco, CLASSlinco-SRSS, SASSI-SRSS, SASSI Simulation Mean, SASSI-AS (Node 118)

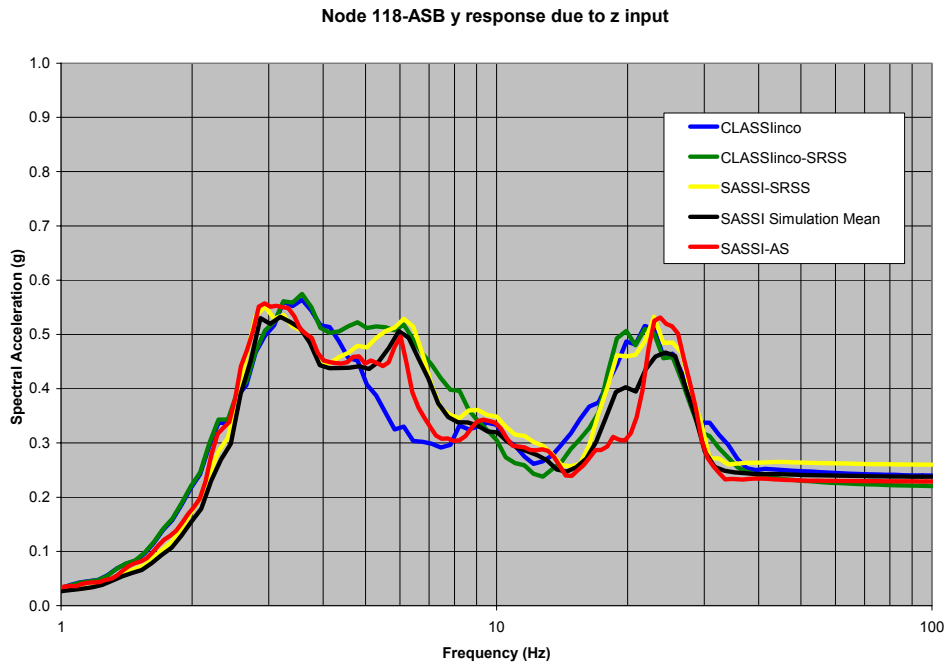

Figure A-66
ASB Outrigger Response Spectra – Y Direction Due to Z Input – CLASSlinco, CLASSlinco-SRSS, SASSI-SRSS, SASSI Simulation Mean, SASSI-AS (Node 118)

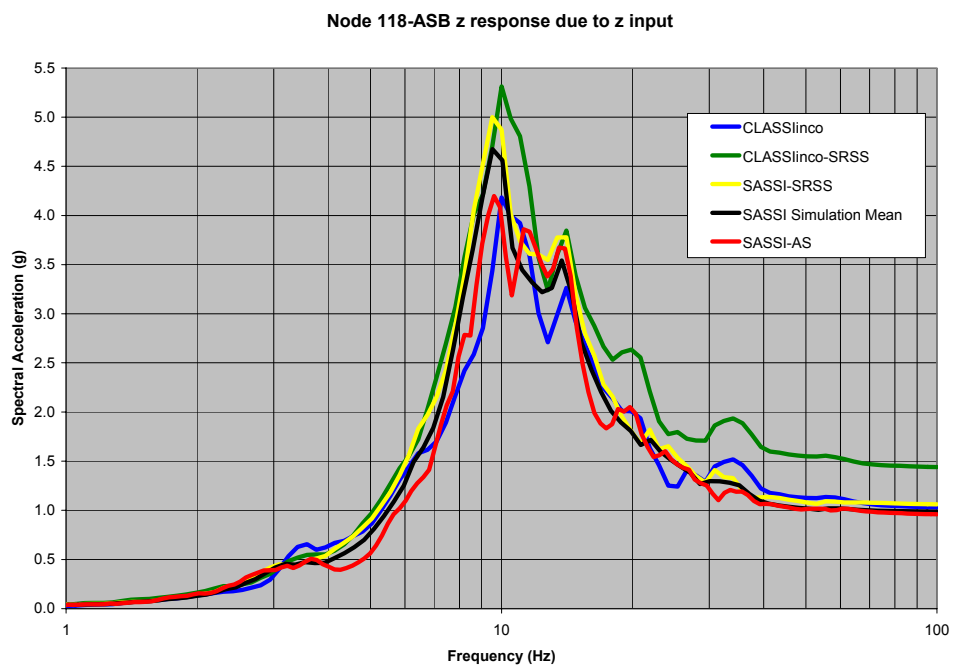

Figure A-67
ASB Outrigger Response Spectra – Z Direction Due to Z Input – CLASSlinco, CLASSlinco-SRSS, SASSI-SRSS, SASSI Simulation Mean, SASSI-AS (Node 118)

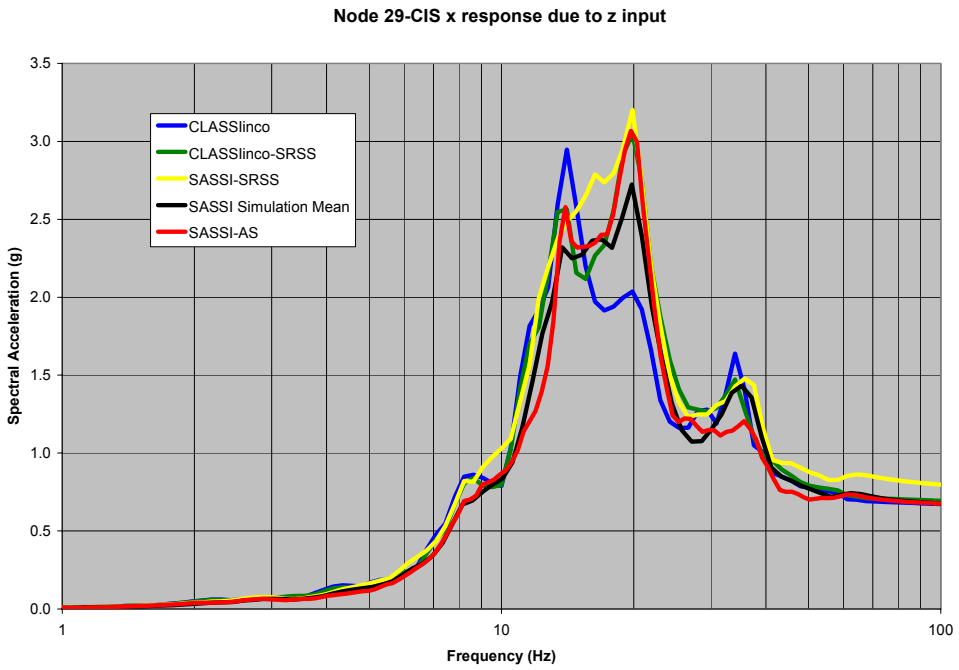

Figure A-68
Top of CIS Shear Center Response Spectra – X Direction Due to Z Input – CLASSlinco, CLASSlinco-SRSS, SASSI-SRSS, SASSI Simulation Mean, SASSI-AS (Node 29)

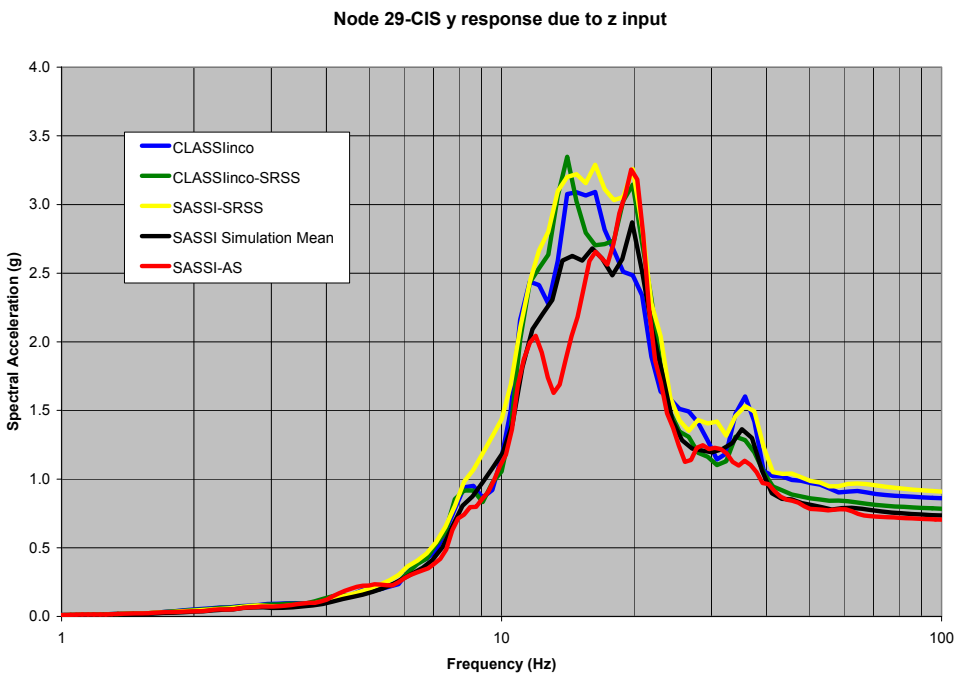

Figure A-69
Top of CIS Shear Center Response Spectra – Y Direction Due to Z Input – CLASSlinco, CLASSlinco-SRSS, SASSI-SRSS, SASSI Simulation Mean, SASSI-AS (Node 29)

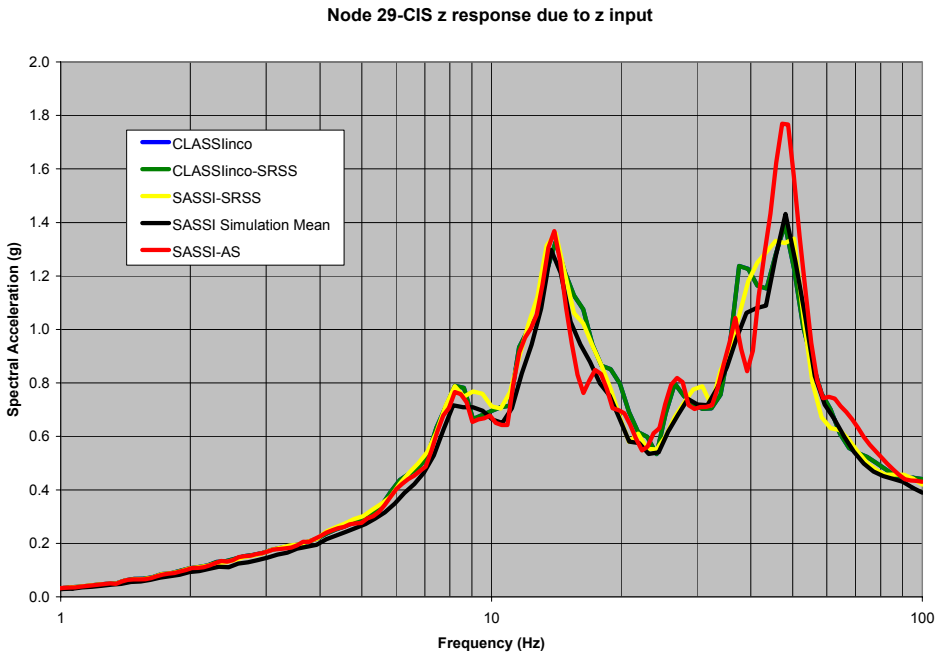

Figure A-70
Top of CIS Shear Center Response Spectra – Z Direction Due to Z Input – CLASSlinco, CLASSlinco-SRSS, SASSI-SRSS, SASSI Simulation Mean, SASSI-AS (Node 29)

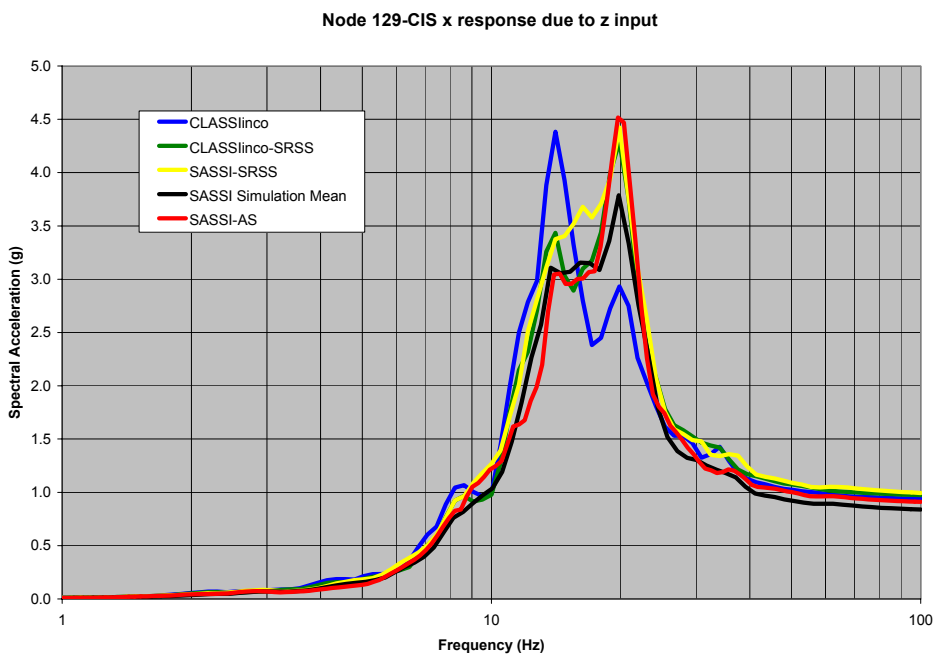

Figure A-71
Top of CIS Horizontal Mass Center Response Spectra – Z Direction Due to X Input – CLASSlinco, CLASSlinco-SRSS, SASSI-SRSS, SASSI Simulation Mean, SASSI-AS (Node 129)

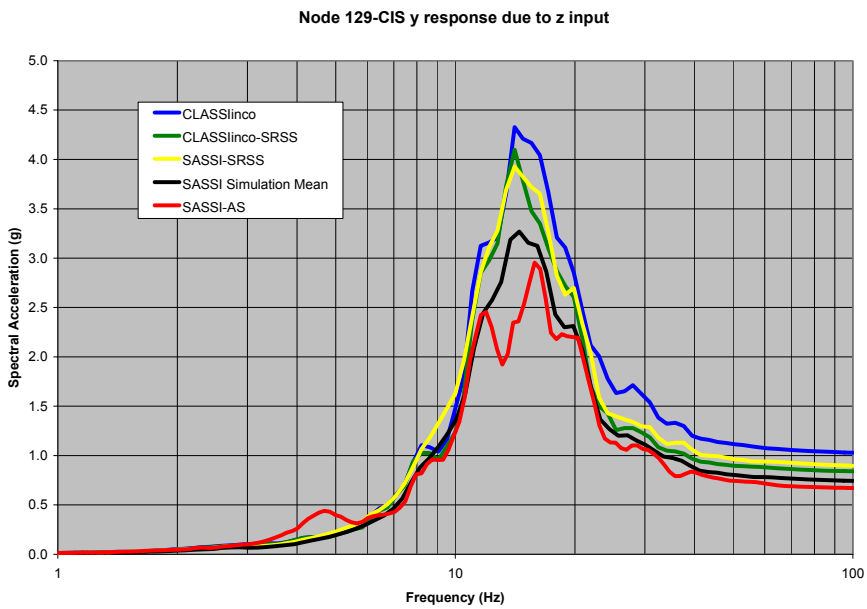

Figure A-72
Top of CIS Horizontal Mass Center Response Spectra – Y Direction Due to Z Input – CLASSlinco, CLASSlinco-SRSS, SASSI-SRSS, SASSI Simulation Mean, SASSI-AS (Node 129)

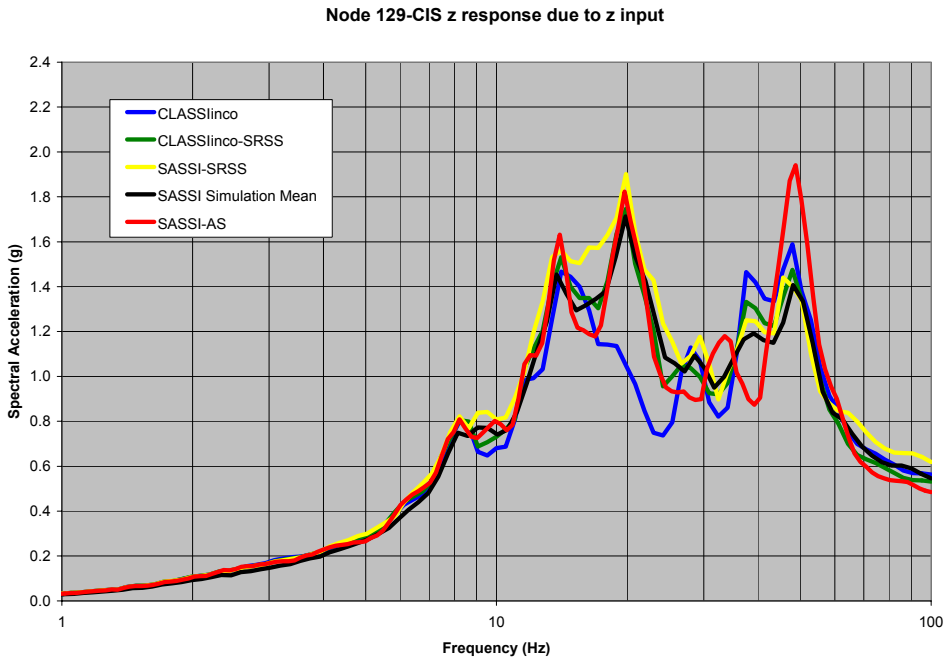

Figure A-73
Top of CIS Horizontal Mass Center Response Spectra – Z Direction Due to Z Input – CLASSlinco, CLASSlinco-SRSS, SASSI-SRSS, SASSI Simulation Mean, SASSI-AS (Node 129)

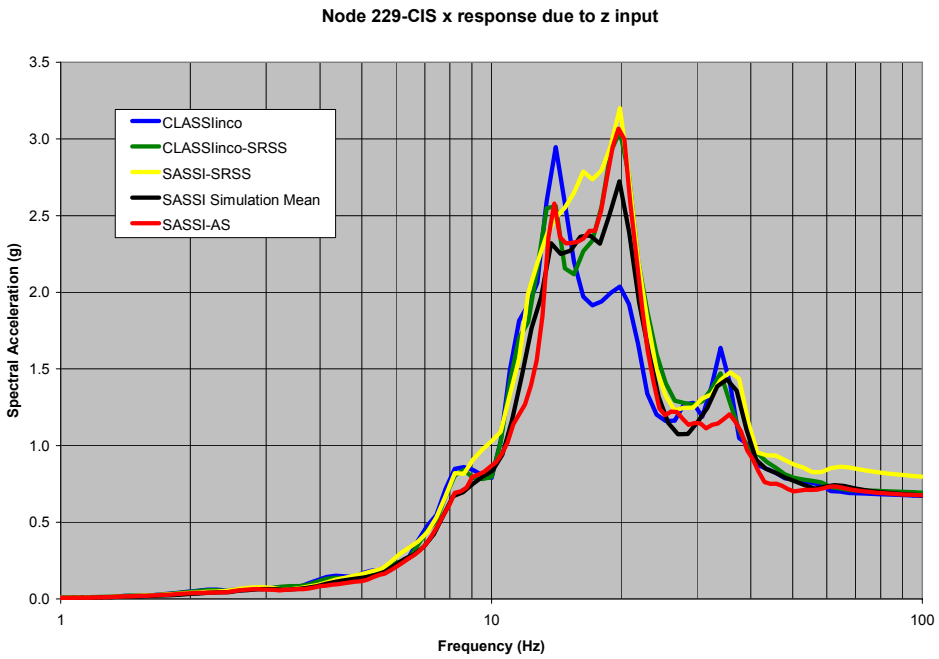

Figure A-74
CIS Outrigger Response Spectra – X Direction Due to Z Input – CLASSlinco, CLASSlinco-SRSS, SASSI-SRSS, SASSI Simulation Mean, SASSI-AS (Node 229)

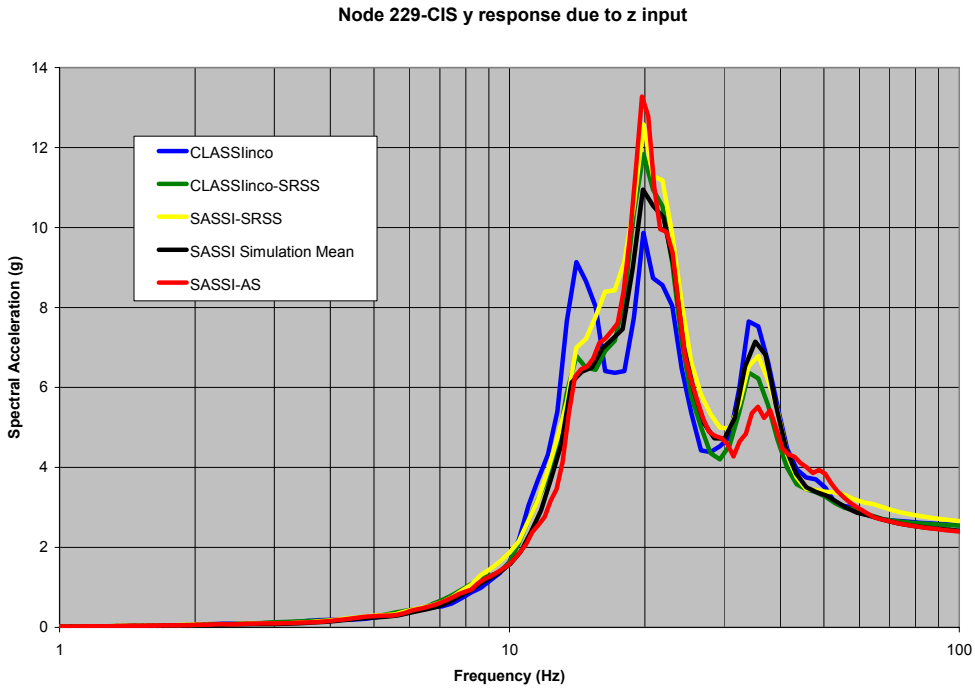

Figure A-75
CIS Outrigger Response Spectra – Y Direction Due to Z Input – CLASSlinco, CLASSlinco-SRSS, SASSI-SRSS, SASSI Simulation Mean, SASSI-AS (Node 229)

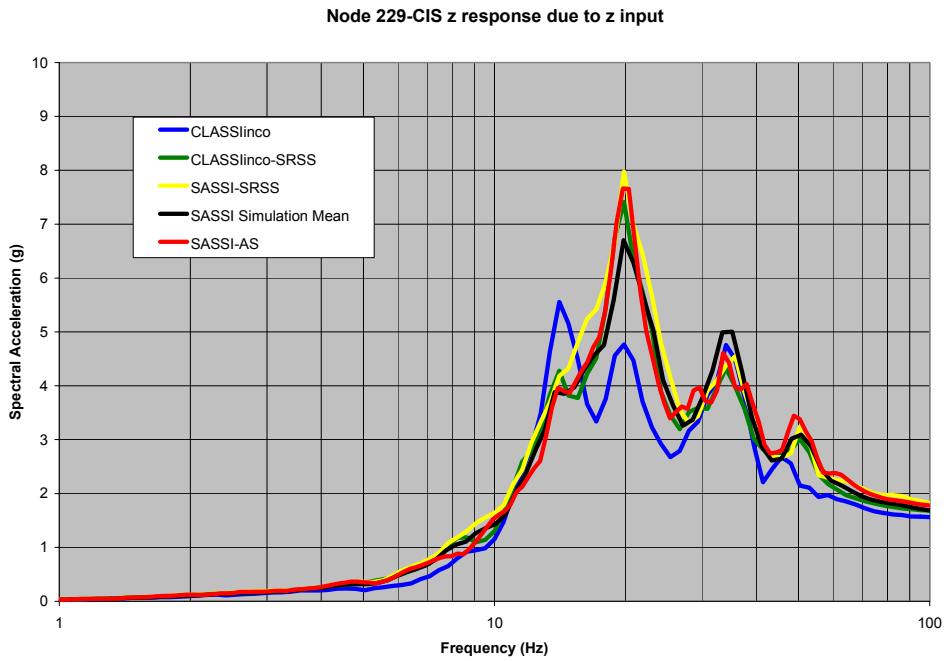

Figure A-76
CIS Outrigger Response Spectra – Z Direction Due to Z Input – CLASSlinco, CLASSlinco-SRSS, SASSI-SRSS, SASSI Simulation Mean, SASSI-AS (Node 229)

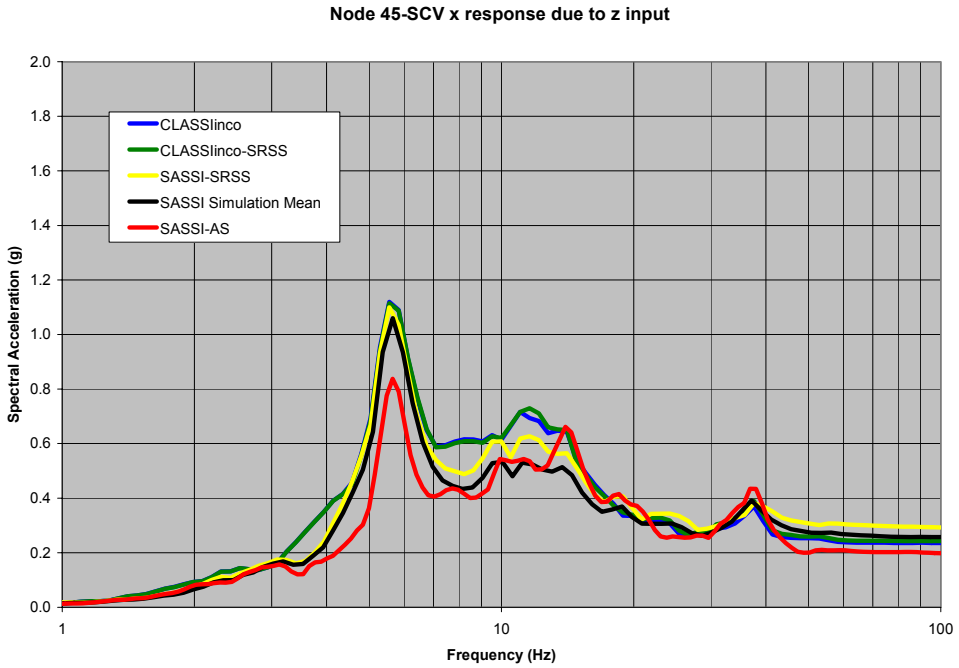

Figure A-77
Top of SCV Response Spectra – X Direction Due to Z Input – CLASSlinco, CLASSlinco-SRSS, SASSI-SRSS, SASSI Simulation Mean, SASSI-AS (Node 45)

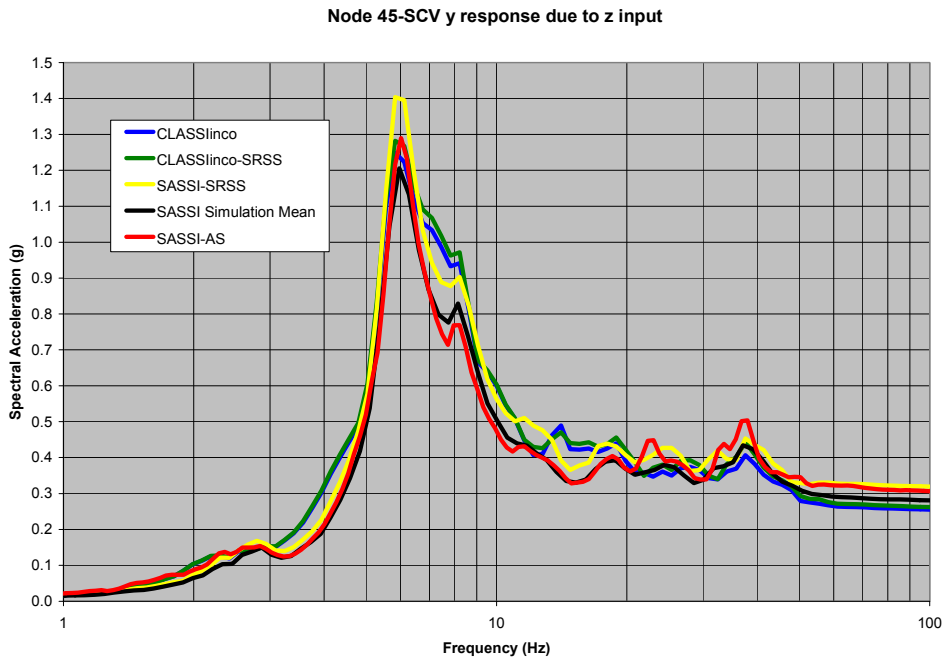

Figure A-78
Top of SCV Response Spectra – Y Direction Due to Z Input – CLASSlinco, CLASSlinco-SRSS, SASSI-SRSS, SASSI Simulation Mean, SASSI-AS (Node 45)

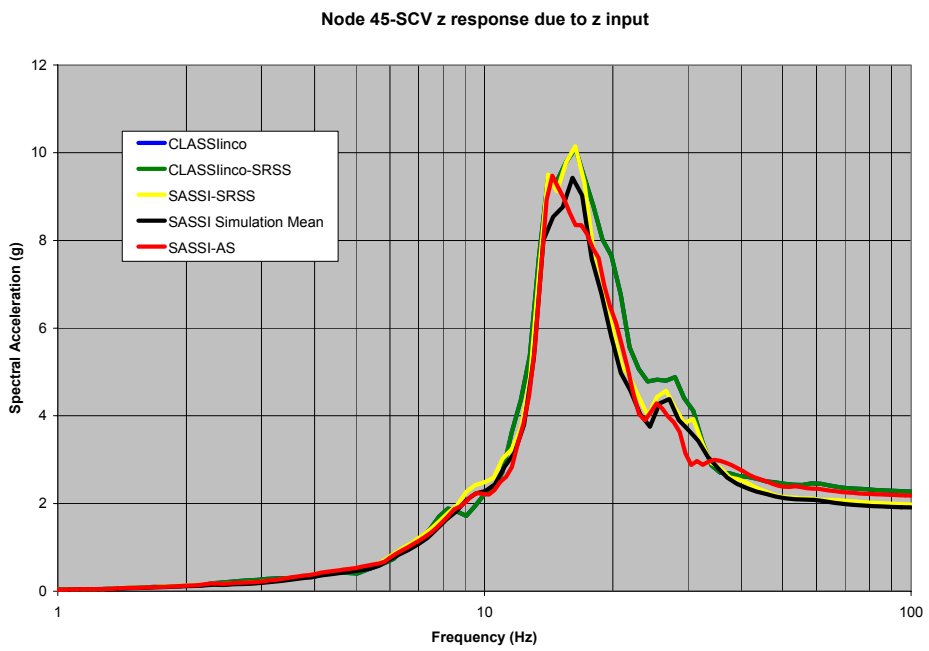

Figure A-79
Top of SCV Response Spectra – Z Direction Due to Z Input – CLASSlinco, CLASSlinco-SRSS, SASSI-SRSS, SASSI Simulation Mean, SASSI-AS (Node 45)

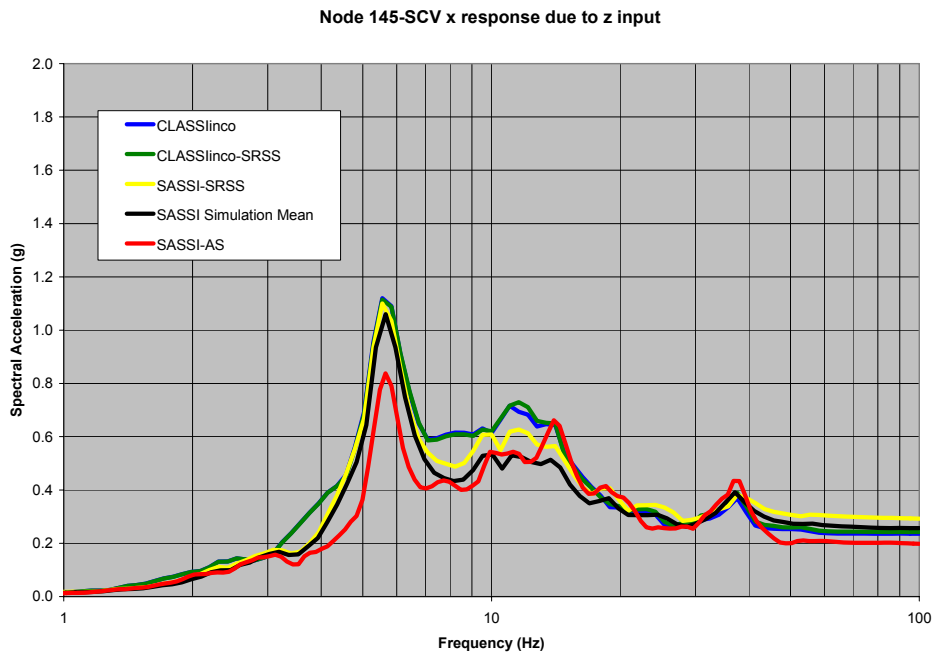

Figure A-80
SCV Outrigger Response Spectra – X Direction Due to Z Input – CLASSlinco, CLASSlinco-SRSS, SASSI-SRSS, SASSI Simulation Mean, SASSI-AS (Node 145)

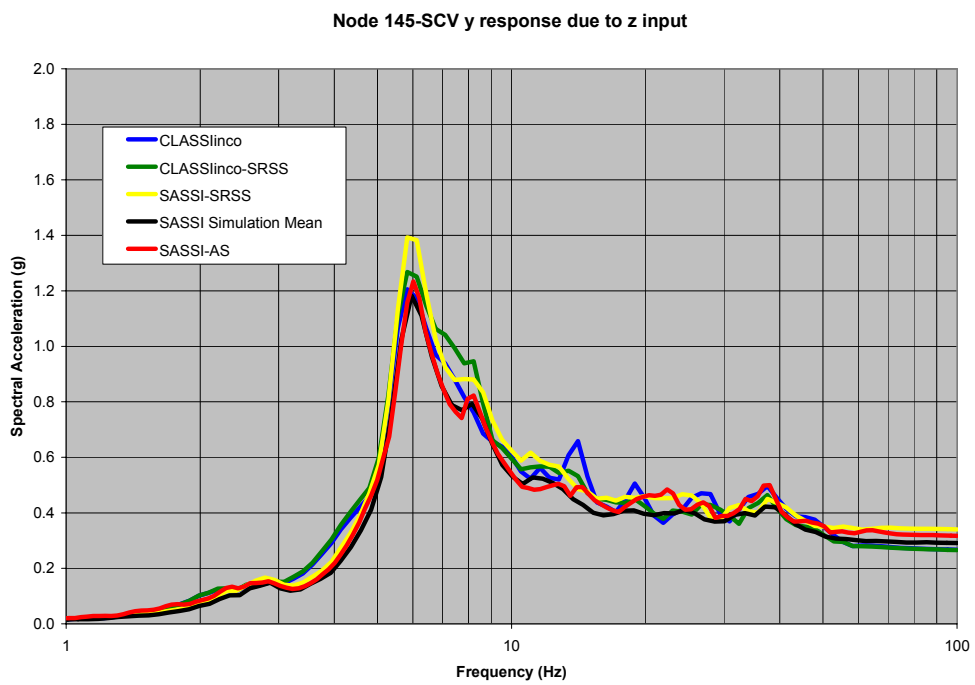

Figure A-81
SCV Outrigger Response Spectra – Y Direction Due to Z Input – CLASSlinco, CLASSlinco-SRSS, SASSI-SRSS, SASSI Simulation Mean, SASSI-AS (Node 145)

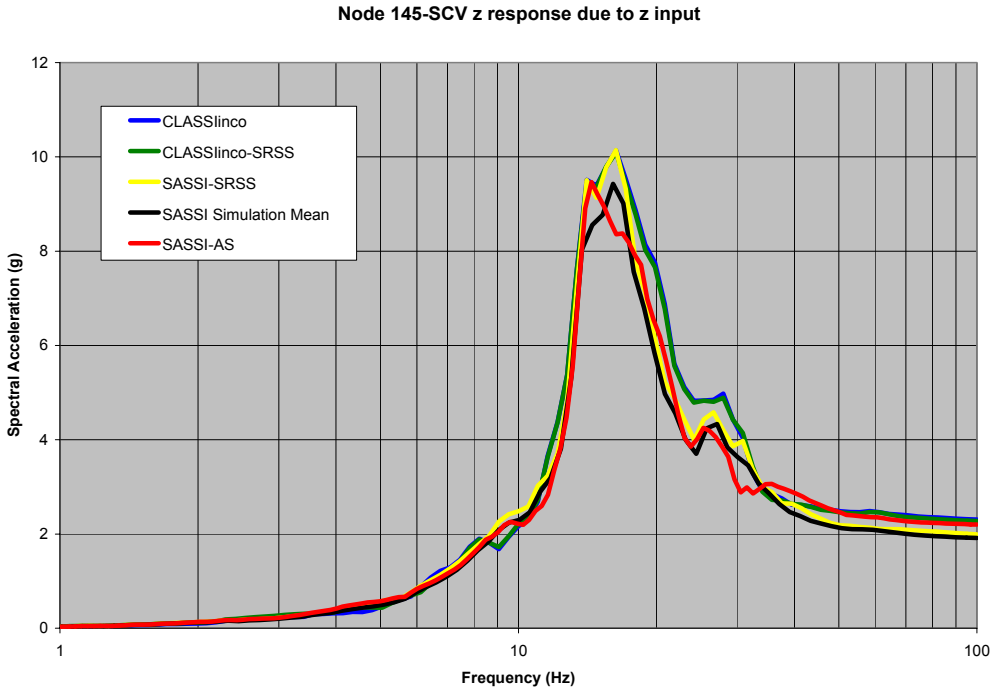

Figure A-82
SCV Outrigger Response Spectra – Z Direction Due to Z Input – CLASSlinco, CLASSlinco-SRSS, SASSI-SRSS, SASSI Simulation Mean, SASSI-AS (Node 145)

B
EFFECT OF ABRAHAMSON HARD ROCK COHERENCY FUNCTIONS

Effect of Abrahamson Ground Motion Coherency Functions for Hard Rock on Response of Simplified Representation of Nuclear Power Plant Structure: Summary

James J. Johnson
Stephen A. Short
May 11, 2007
July 27, 2007 (Rev)

General

An extensive study was performed on the effect of seismic wave incoherence on foundation and structure response (Short et al., 2006). The study evaluated the effects of incoherence on the response of rigid, massless foundations and for example structural models. The starting points for the study were the ground motion coherency functions developed by Dr. Abrahamson (Abrahamson, 2005, 2006). These coherency functions remain applicable to soil sites for surface foundations. Recently, these ground motion coherency functions were revised considering only ground motion data recorded at rock sites. The resulting revisions are applicable to rock sites (Abrahamson, 2007) for surface and embedded foundations. These "Hard Rock" coherency functions were implemented in CLASSIinco, the version of CLASSI used to calculate incoherency transfer functions (ITFs) of the rigid, massless foundation and in-structure response. The soil and hard rock coherency functions are compared in Figure B-1. The effects of changes to the coherency functions have been assessed and representative results are presented herein.

SSI and Structure Response

The subject of these analyses is the response of the representative nuclear power plant structure studied previously (Short et al., 2006). The relevant parameters of the analyses are described in detail in Chapter 2, Short et al. (2006): the rock site profile; the 15-ft thick, 150-ft square foundation; and the simplified structure model based on some of the AP1000 properties. The structure model is comprised of three sticks with limited inter-connectivity at upper elevations. The free-field ground motion of interest is that motion compatible with the rock site profile, i.e., exhibiting significant high-frequency motion. For all analyses, spectrum compatible time histories defined the free-field ground motion. All analyses considered three directions of simultaneous earthquake input motion. Figure B-2 shows a schematic of the structure model with response locations identified.

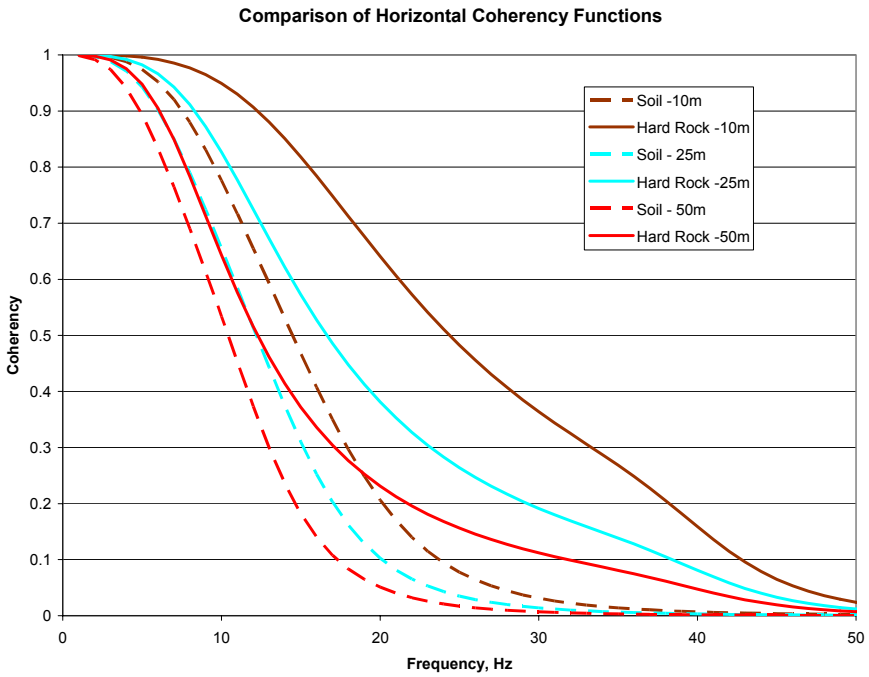

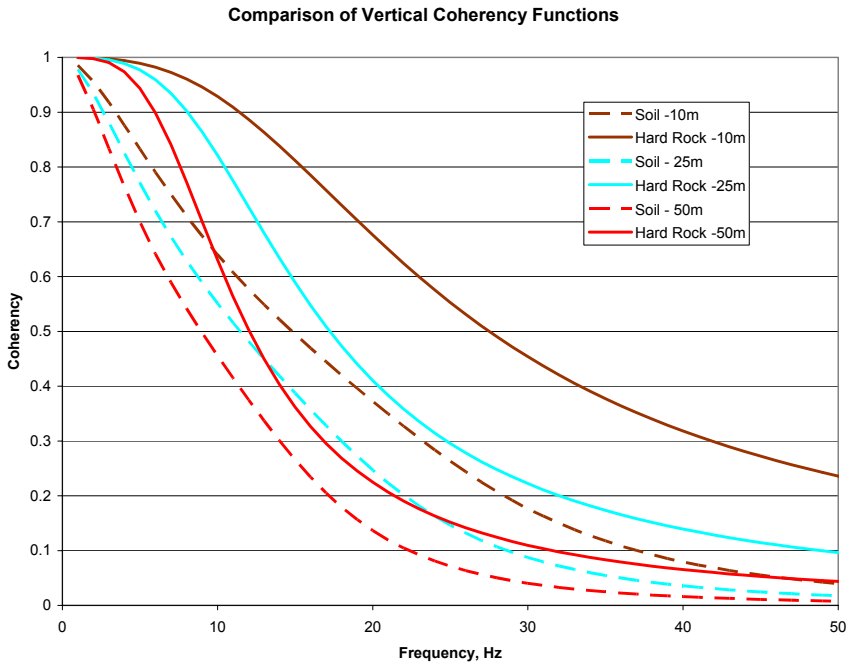

Figure B-1
Comparison of Hard Rock (Abrahamson, 2007) and Soil (Abrahamson, 2005, 2006) Coherency Functions

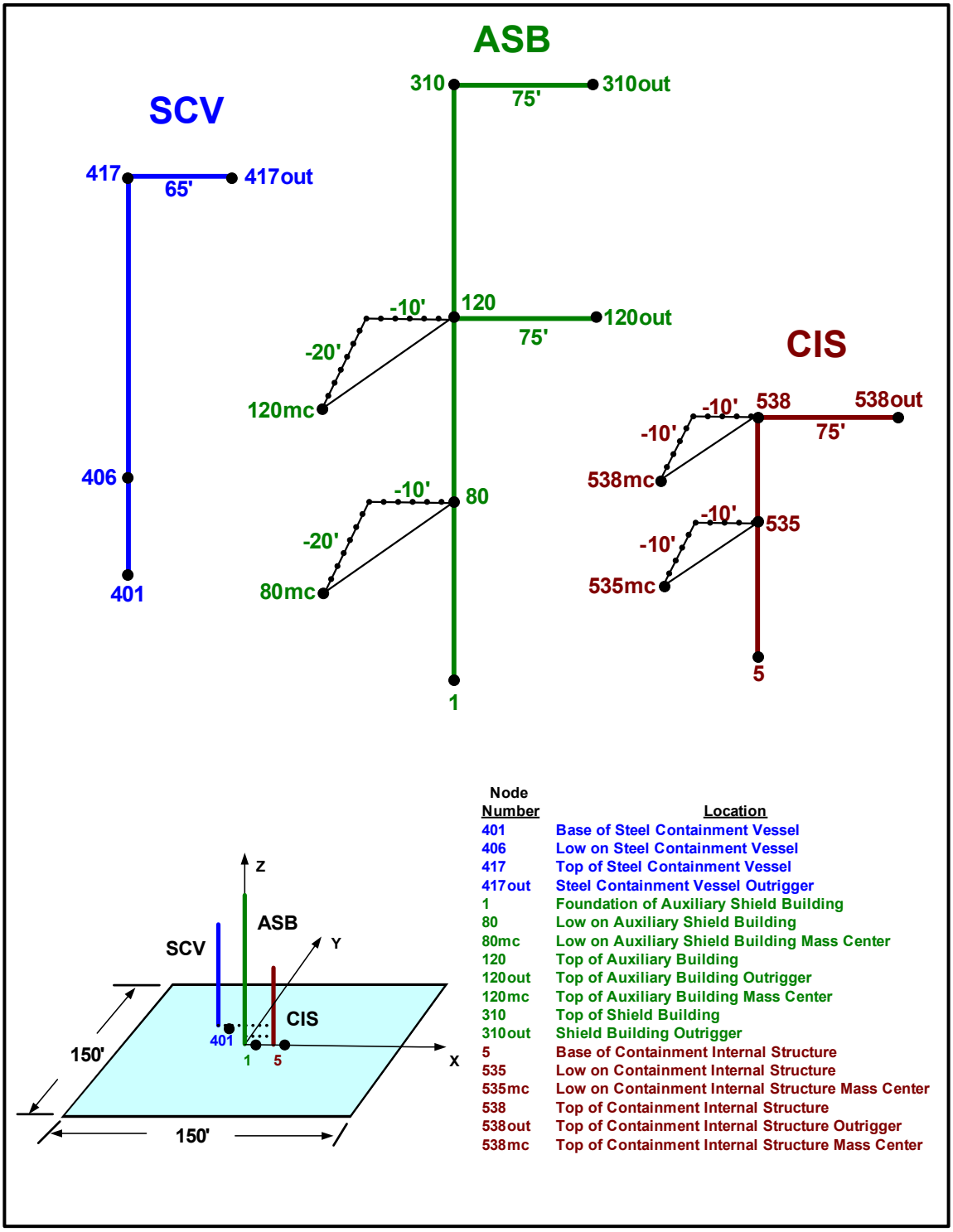

Figure B-2
Locations on the AP1000-Based Stick Model where In-Structure Response Spectra are Computed

Three sets of analyses have been performed for the example structural model:

1. SSI analysis with coherent input motion (dark blue curves in response spectra figures); identical results to those reported in Chapter 5, Short et al. (2006).
2. SSI analysis with incoherent input motion; ground motion coherency functions – soil, surface foundations (Abrahamson, 2005, 2006) (green curves in response spectra figures – denoted NAA 2005-2006); identical results to those reported in Chapter 5, Short et al. (2006).
3. SSI analysis with incoherent input motion; ground motion coherency functions – hard rock, surface and embedded foundations (Abrahamson, 2007) (red curves in response spectra figures – denoted NAA 2007).

To evaluate the effects of hard rock ground motion coherency functions on in-structure response, response spectra were calculated and compared for the various analyses at the tops of the structure sticks, at lower elevations on the structure sticks, and on outriggers extending 65 or 75-ft. from the top of each stick in the X direction (these dimensions were selected to approximately correspond to the AP1000 design dimensions).

SSI and Incoherence

As background, the fixed-base modes of the three structure sticks provide some insight into the dynamic behavior. The ASB has predominate modes with frequencies less than 10 Hz with fundamental modes in the horizontal directions of 3.2 Hz (X-direction) and 3.0 Hz (Y-direction); the fundamental mode in the vertical direction of frequency 9.9 Hz (Z-direction). Many modes participate in the response of the ASB. The predominate modes of the SCV in the horizontal directions also have frequencies less than 10 Hz – the lowest frequency of an important X-direction mode being 5.5 Hz; Y-direction mode being 6.14 Hz; the lowest frequency of an important vertical mode being 16 Hz. As with the ASB, many modes participate in the response of the SCV. The predominant modes of the CIS have frequencies greater than 10 Hz. Many modes also participate in the response of the CIS.

The total mass of the structures is apportioned approximately ASB – 86%, CIS – 11%, and SCV – 3%, i.e., ignoring the mass of the foundation. The dynamic behavior of the three stick model is coupled through the inter-connectivity of the sticks and natural torsion is induced throughout the three structures due to the eccentricities assumed in the ASB and CIS structures.

Results presented are in-structure response spectra (5% damping) at the foundation and at points on each of the three models (ASB, SCV, CIS) as shown in Figure B-2. Responses at the top of each model and at approximately mid-height (referred to as “low on” a particular structure within Figure B-2), are calculated and compared. The near mid-height locations were selected to investigate the potential effect of incoherence on points where higher modes more fully participate in the response. Note that the ASB stick represents both the auxiliary building and the shield building. The combined auxiliary and shield building extends up to the top of the auxiliary building at Node 120. Above this node and elevation, the ASB stick only represents the shield building. Hence, in addition to the top of the shield building and low in the combined ASB model, output was calculated and is presented at the top of the auxiliary building at the centerline (Z-direction), at the center of mass for the horizontal directions (X and Y), and at the outrigger (X, Y, Z).

In addition to foundation response, results are presented at Nodes 310, 310out, 120mc, 120out, and 80mc on the ASB, Nodes 417, 417out and 406 on the SCV, and Nodes 538mc, 538out, and 535mc on the CIS where node locations are illustrated in Figure B-2. The "mc" designation added to the node number indicates that the mass and shear centers are not coincident and response is given at the mass center. The "out" designation added to the node number indicates an outrigger location used to display torsional response at the periphery of the structure. In-structure response spectra at these twelve locations for two horizontal, X and Y, and the vertical direction, Z, of ground motion are presented in Figures B-3 through B-38. Again, all analyses considered 3 directions of simultaneous earthquake input motion.

General Observations

For the high frequency ground motion, rock site profile, foundation behavior essentially rigid, and sample nuclear power plant structure, in-structure response spectra are generally reduced in frequency ranges greater than about 12 Hz. as evidenced by comparing spectra including the effects of incoherency as represented by the "Hard Rock" ground motion coherency functions (Abrahamson, 2007) with spectra calculated assuming coherent ground motion. As expected, these reductions in response spectra are less than the reductions derived for the soil ground motion coherency functions (Abrahamson, 2005, 2006). In general, reductions in in-structure response spectra are greater in the vertical direction than in the horizontal directions. With limited exceptions, the reductions are significant at frequencies greater than about 12 Hz. where local peaks in the response spectra occur.

Although not shown here, it is extremely important to account for SSI in the calculation of structure response for ground motions dominated by high frequencies. This is the case for coherent and incoherent ground motion assumptions. Comparisons of fixed-base response with response calculate taking into account SSI show the latter cases to be very significantly reduced when compared to the former.

Foundation Response

Foundation response is presented in Figures B-3, B-4, and B-5. Comparing the foundation response spectra including the effects of incoherency (NAA-2007) with those of the coherent case generally shows significant reductions at frequencies greater than 15 Hz. Spectral accelerations are reduced by a factor of 1.1 to 2 over significant frequency ranges. The free-field ground motion response spectra are plotted in Figures B-3, B-4, and B-5. Comparing coherent and incoherent foundation response with the free-field motion demonstrates the importance of SSI and incoherency of ground motion on foundation response.

Auxiliary and Shield Building (ASB)

- **Top of Shield Building.** Responses at the top of the coupled auxiliary and shield building (ASB) are presented in Figures B-6, B-7, and B-8. Comparing the response spectra due to incoherency effects (Analysis 3) with those of Analysis 1, generally, shows reductions due to incoherency for frequencies greater than 12 Hz. For horizontal directions, the reductions are range from no reduction to a factor of about 2. For the vertical direction, reductions are observed in the frequency range above 10 Hz, including at the ZPA frequency.

At a frequency of peak amplification less than 10 Hz (X-direction 6.5 Hz; Y-direction 6 Hz), slight increases in spectral accelerations of the incoherent case above the coherent case are observed. As for Analysis Case 2, this is attributed to the effect of induced rotations of the foundation.

The responses of the outrigger, extending 75-ft. in the X-direction, are presented in Figures B-15, B-16, and B-17. The reductions in response spectral accelerations generally follow the trend of the values on the centerline, but the reductions are observed to be less. The effects of incoherence induced torsion are shown in Figure B-16 Y-direction response, where the responses calculated due to coherence and incoherence (blue and red curves) are relatively close for frequencies above 12 Hz. At frequencies of peak amplification less than 10 Hz (X- and Y-directions 6.5 Hz.), slight increases in spectral accelerations of the incoherent case above the coherent case are observed. This is attributed to the effect of induced rotations of the foundation.

- **Top of Auxiliary Building.** Responses at the top of the auxiliary building are presented in Figures B-9, B-10, and B-11. In the X-direction, spectral accelerations are reduced by a factor of 1 (no reduction) to about 1.4 due to incoherence for frequencies greater than about 14 Hz. In the Y-direction, reductions in the response are observed for frequencies greater than 10 Hz up to and including the ZPA. There are no observed low-frequency exceedances of the incoherent responses at this location.

  The responses of the outrigger, extending 75-ft. in the X-direction, are presented in Figures B-18, B-19, and B-20. The reductions in response spectral accelerations generally follow the trend of the values of the points at the mass centers, but the reductions are observed to be less. The X-direction response is close to the same as the response at the center of mass. The Y-direction response demonstrates the effects of induced torsion when compared to the response at the center of mass. The Y-direction response has significant reductions incoherent to coherent in the frequency range of 20 – 60 Hz. Vertical response spectra are significantly reduced for frequencies greater than about 12 Hz.

- **Low in ASB.** Responses at a lower elevation of the coupled auxiliary and shield building (ASB) are presented in Figures B-12, B-13, and B-14. Generally, these spectra in the horizontal directions demonstrate reductions in the spectral accelerations at frequencies greater than 20 Hz. Generally, the response reductions in the vertical direction are significant for frequencies greater than 12 Hz.

Steel Containment Vessel (SCV)

- **Top of SCV.** Response at the top of the steel containment vessel (SCV) at the centerline is presented in Figures B-21, B-22, and B-23. Comparing the response spectra due to incoherency effects (Analysis 3) with those of Analysis 1, generally, show significant reductions in response for frequencies greater than about 15 Hz with less reduction at the ZPA. In the vertical direction, significant reductions are observed for all frequencies greater than 12 Hz.

  The responses of the outrigger extending 65-ft in the X direction from the top of the steel containment vessel (SCV) are presented in Figures B-27, B-28, and B-29. Reductions in response spectral accelerations are observed for frequencies greater than about 15 Hz in the X-direction. The Y-direction response demonstrates the effect of induced torsion coupled

with a significant torsional mode at about 12 Hz. – the incoherent response exceeds the coherent response by about a factor of 1.15. At higher frequencies in the Y-direction response, the peak spectral accelerations are reduced when accounting for incoherency. Significant reductions in the vertical direction are observed for frequencies greater than about 12 Hz.

- **Low in the SCV.** Responses at lower elevations of the steel containment vessel (SCV) are presented in Figures B-24, B-25, and B-26. These spectra demonstrate similar behavior to that seen on the centerline at the top of the SCV.

Containment Internal Structure (CIS)

- **Top of CIS.** Responses at the top of the containment internal structure (CIS) at the center of mass are presented in Figures B-30, B-31, and B-32. Comparing the response spectra due to incoherency effects (Analysis 3) with those of Analysis 1, generally, shows significant reductions over those due to coherent SSI effects at frequencies greater than about 12 Hz. These reductions range from factors of 1.0 (no reduction) to 1.5. For vertical response, significant reductions occur for frequencies greater than about 15 Hz.

  Responses of the outrigger extending 75-ft in the X direction from the top of the containment internal structure (CIS) are presented in Figures B-36, B-37, and B-38. Reductions in response spectral accelerations are observed in all three directions at this location at frequencies greater than about 12 Hz. Reductions range from factors of 1.0 (no reduction) to about a factor of 2.

- **Low in the CIS.** Responses at lower elevations of the containment internal structure (CIS) are presented in Figures B-33, B-34, and B-35. Generally, responses in the horizontal directions show minimal reductions compared to the coherent case. For the vertical direction significant reductions occur for frequencies greater than about 11 Hz.

Conclusions

The fundamental conclusion is that there are significant reductions in high-frequency response due to seismic wave incoherence even for the “Hard Rock” ground motion coherency functions.

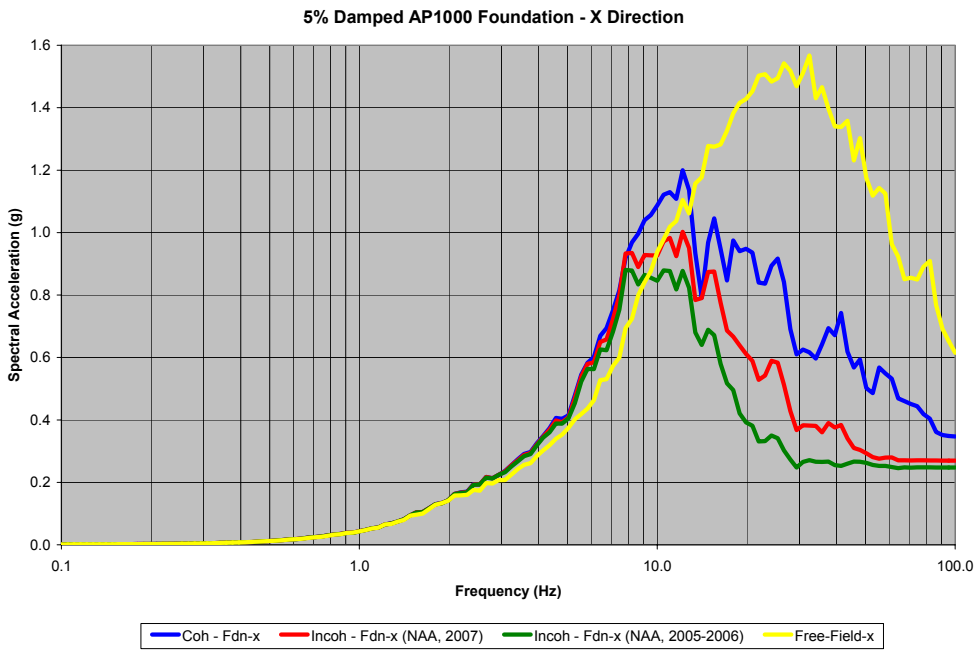

Figure B-3
Foundation Response Spectra – X Direction –SSI Coherent, SSI Incoherent NAA2005-2006, SSI Incoherent NAA2007, (Node 1) and Free-Field

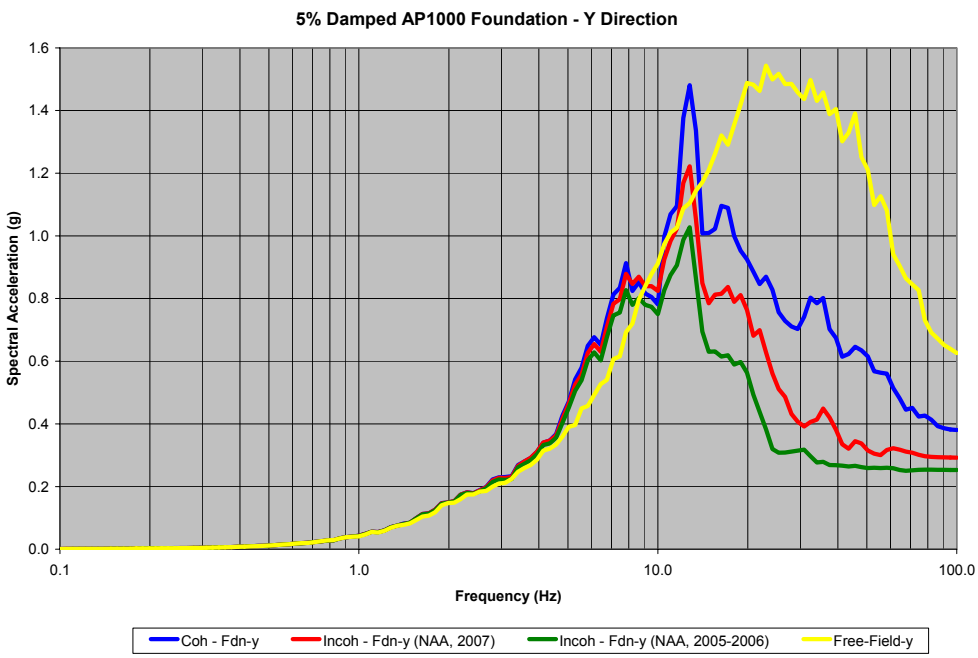

Figure B-4
Foundation Response Spectra – Y Direction –SSI Coherent, SSI Incoherent NAA2005-2006, SSI Incoherent NAA2007, (Node 1) and Free-Field

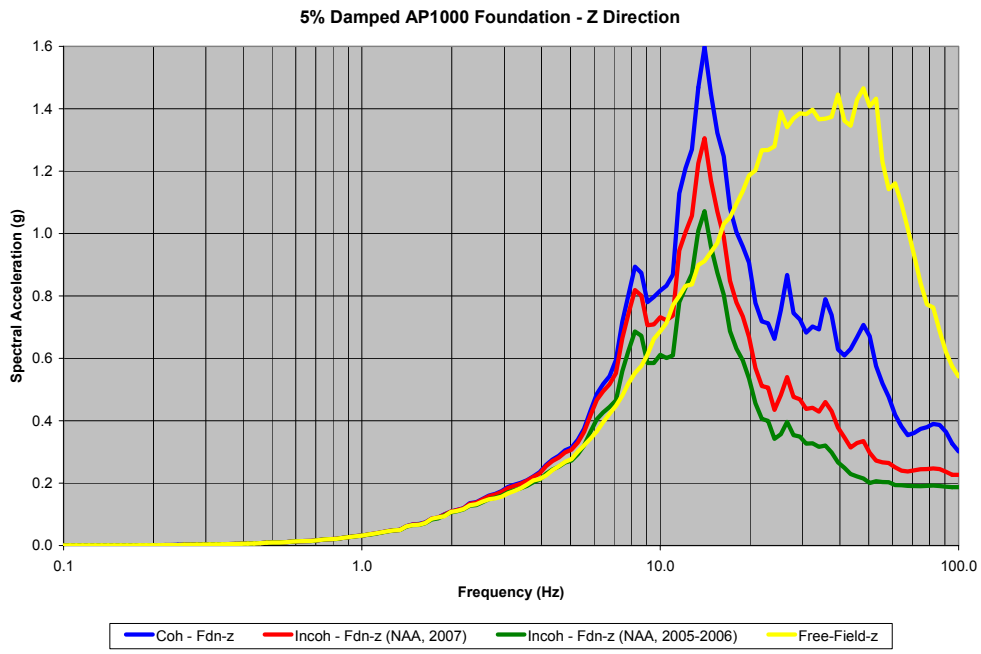

Figure B-5
Foundation Response Spectra – Z Direction –SSI Coherent, SSI Incoherent NAA2005-2006, SSI Incoherent NAA2007, (Node 1) and Free-Field

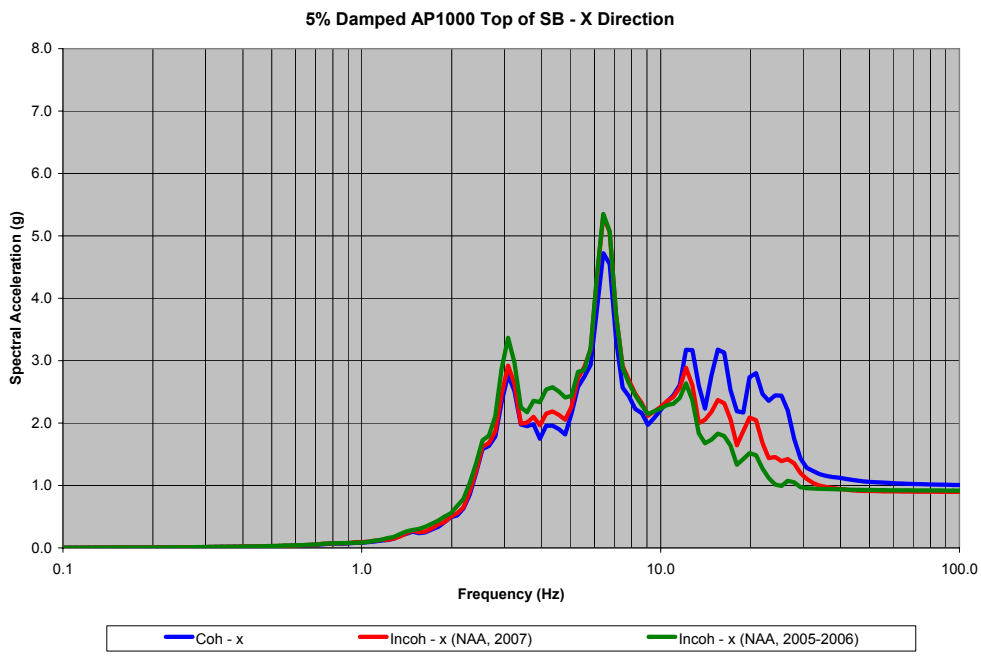

Figure B-6
Top of Shield Building Response Spectra – X Direction –SSI Coherent, SSI Incoherent NAA2005-2006, SSI Incoherent NAA2007 (Node 310)

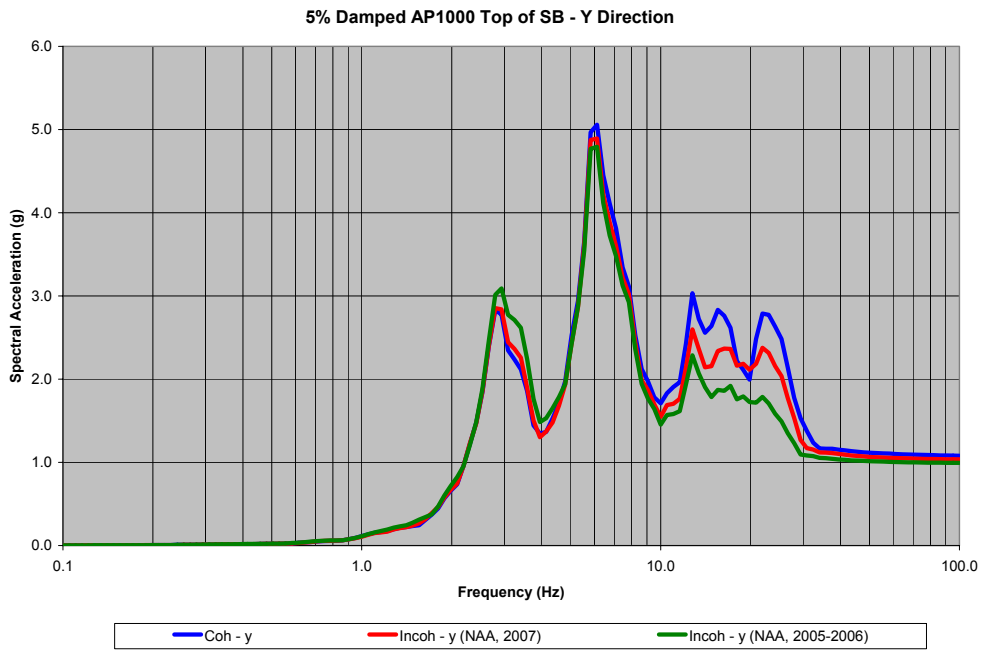

Figure B-7
Top of Shield Building Response Spectra – Y Direction –SSI Coherent, SSI Incoherent NAA2005-2006, SSI Incoherent NAA2007 (Node 310)

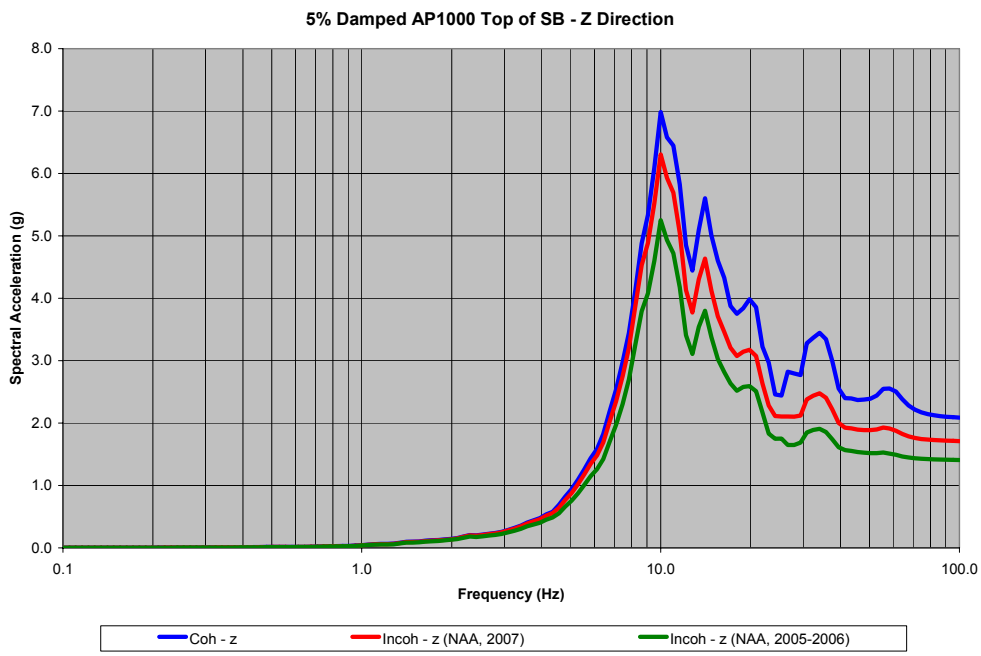

Figure B-8
Top of Shield Building Response Spectra – Z Direction –SSI Coherent, SSI Incoherent NAA2005-2006, SSI Incoherent NAA2007 (Node 310)

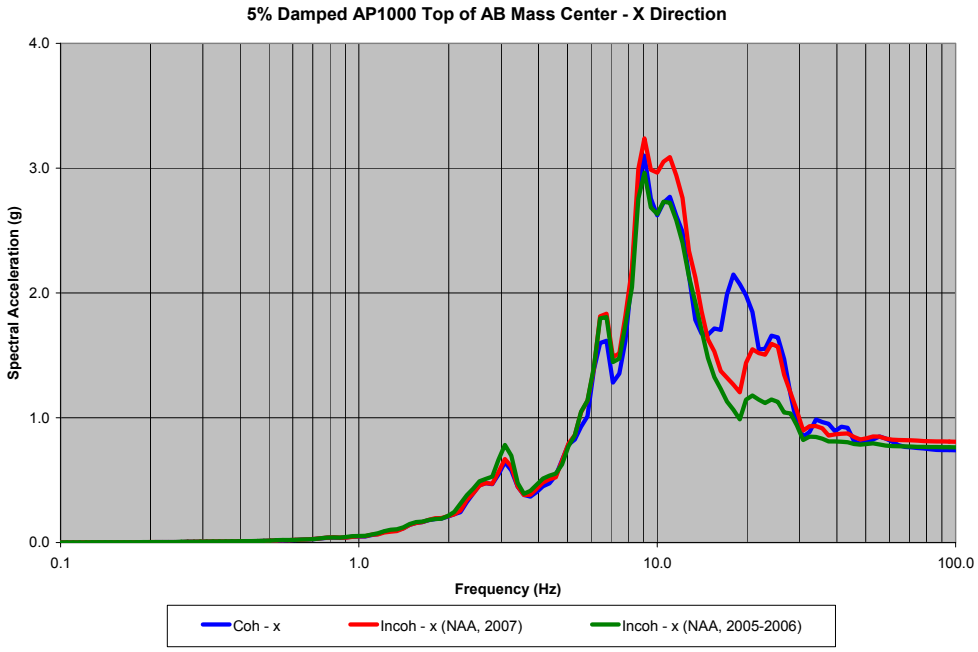

Figure B-9
Top of Auxiliary Building Response Spectra – X Direction –SSI Coherent, SSI Incoherent NAA2005-2006, SSI Incoherent NAA2007 (Node 120mc)

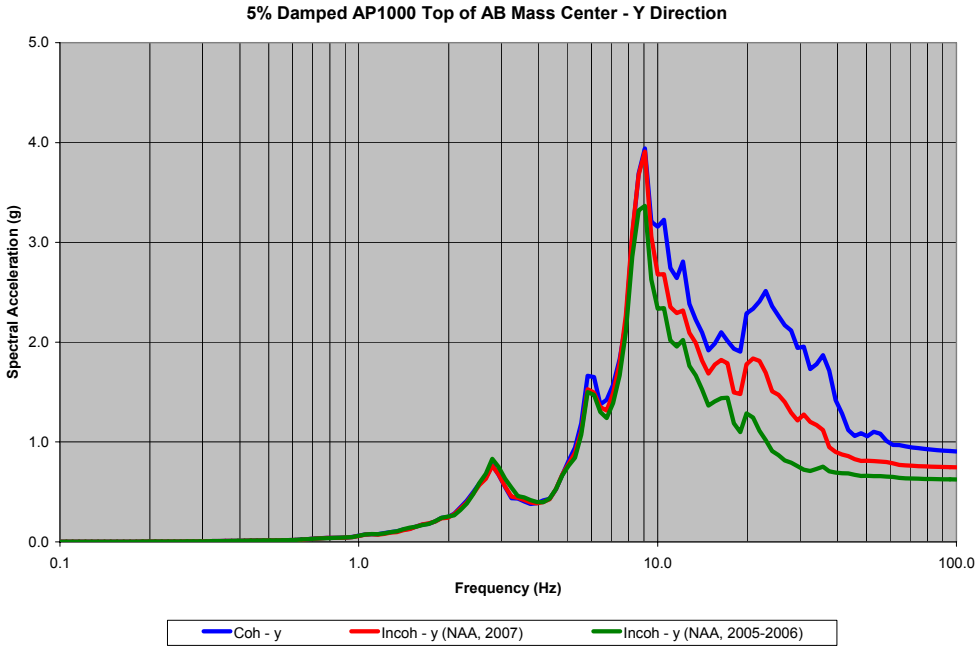

Figure B-10
Top of Auxiliary Building Response Spectra – Y Direction –SSI Coherent, SSI Incoherent NAA2005-2006, SSI Incoherent NAA2007 (Node 120mc)

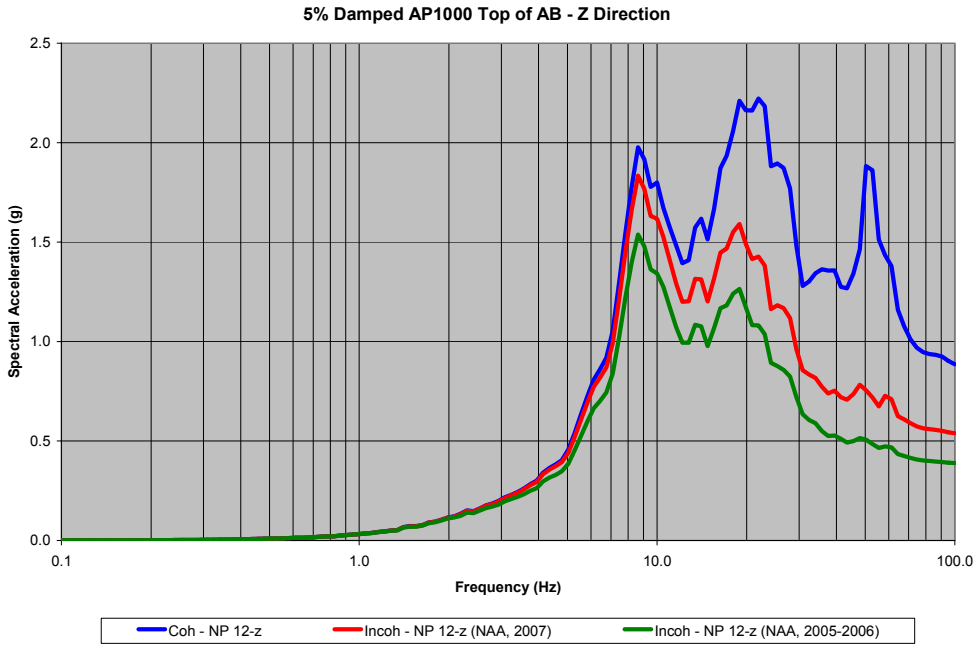

Figure B-11
Top of Auxiliary Building Response Spectra – Z Direction –SSI Coherent, SSI Incoherent NAA2005-2006, SSI Incoherent NAA2007 (Node 120)

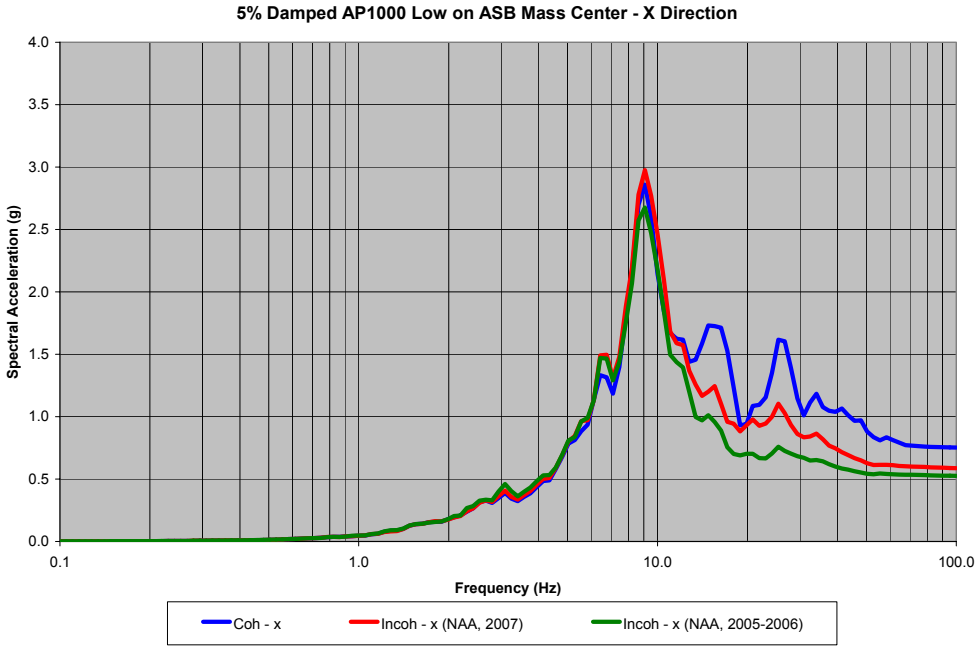

Figure B-12
Low on ASB Response Spectra – X Direction – SSI Coherent, SSI Incoherent NAA2005-2006, SSI Incoherent NAA2007 (Node 80mc)

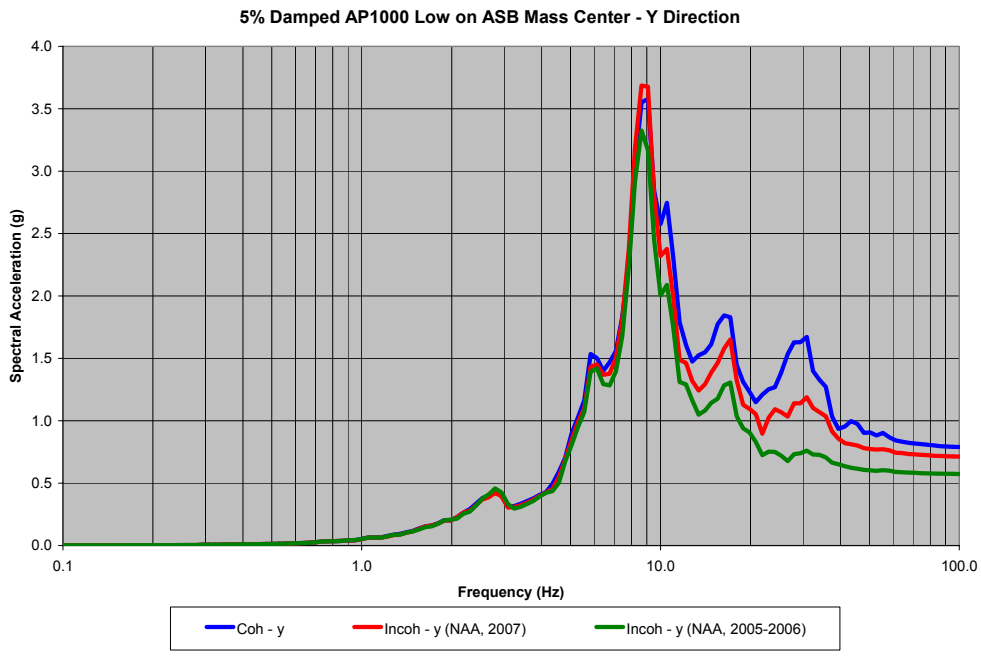

Figure B-13
Low on ASB Response Spectra – Y Direction – SSI Coherent, SSI Incoherent NAA2005-2006, SSI Incoherent NAA2007 (Node 80mc)

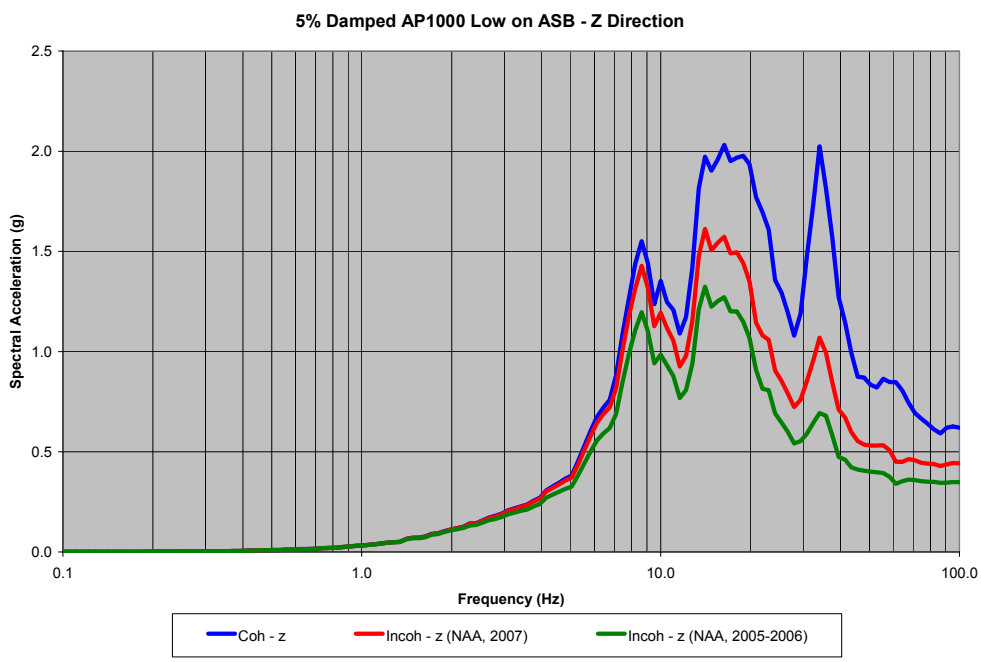

Figure B-14
Low on ASB Response Spectra – Z Direction – SSI Coherent, SSI Incoherent NAA2005-2006, SSI Incoherent NAA2007 (Node 80)

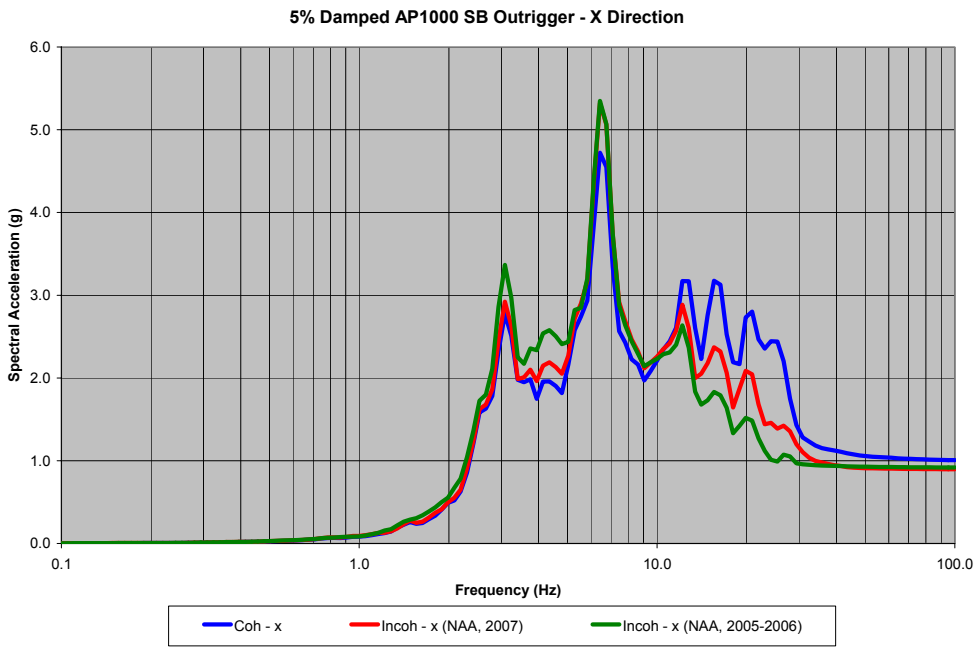

Figure B-15
Shield Building Outrigger Response Spectra – X Direction – SSI Coherent, SSI Incoherent NAA2005-2006, SSI Incoherent NAA2007 (Node 310out)

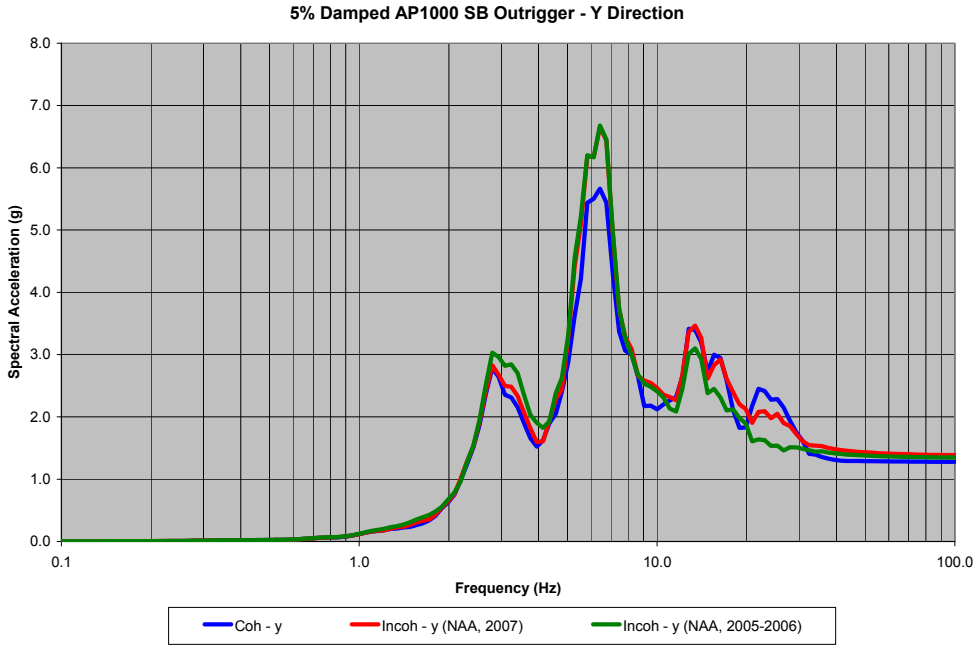

Figure B-16
Shield Building Outrigger Response Spectra – Y Direction – SSI Coherent, SSI Incoherent NAA2005-2006, SSI Incoherent NAA2007 (Node 310out)

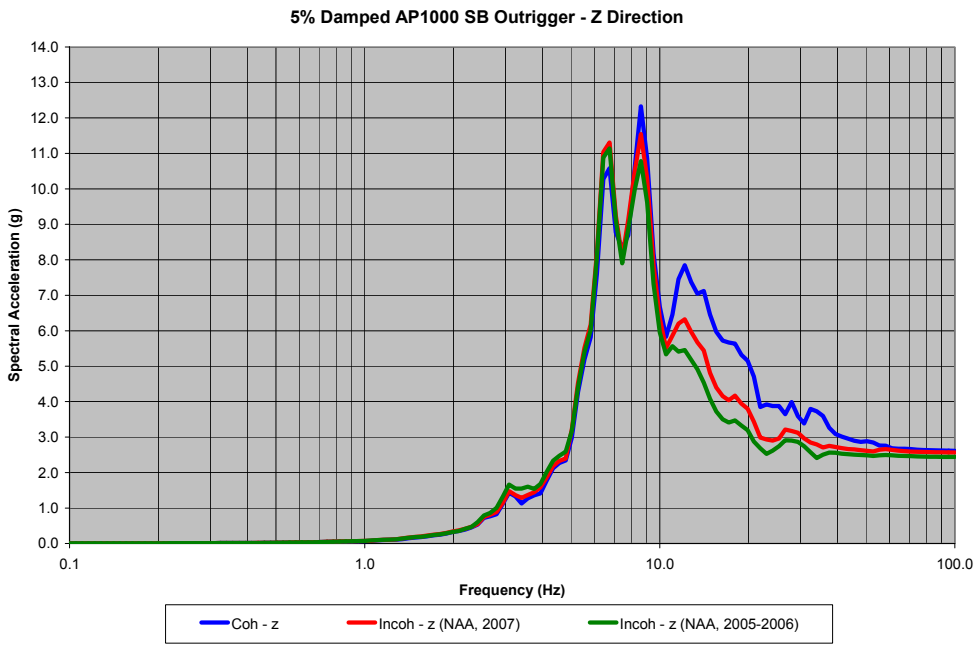

Figure B-17
Shield Building Outrigger Response Spectra – Z Direction – SSI Coherent, SSI Incoherent NAA2005-2006, SSI Incoherent NAA2007 (Node 310out)

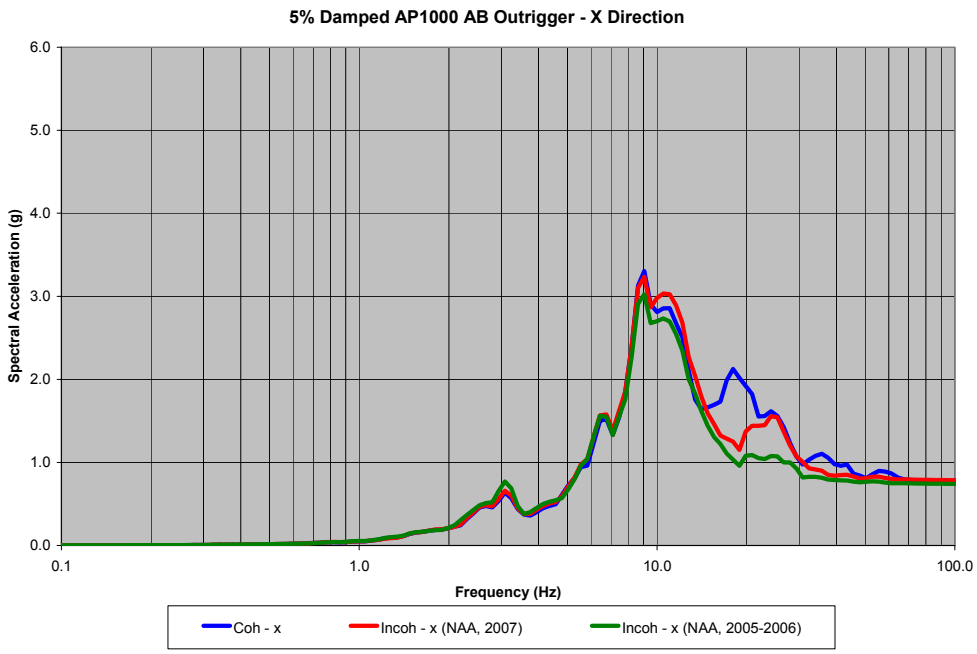

Figure B-18
Auxiliary Building Outrigger Response Spectra – X Direction – SSI Coherent, SSI Incoherent NAA2005-2006, SSI Incoherent NAA2007 (Node 120out)

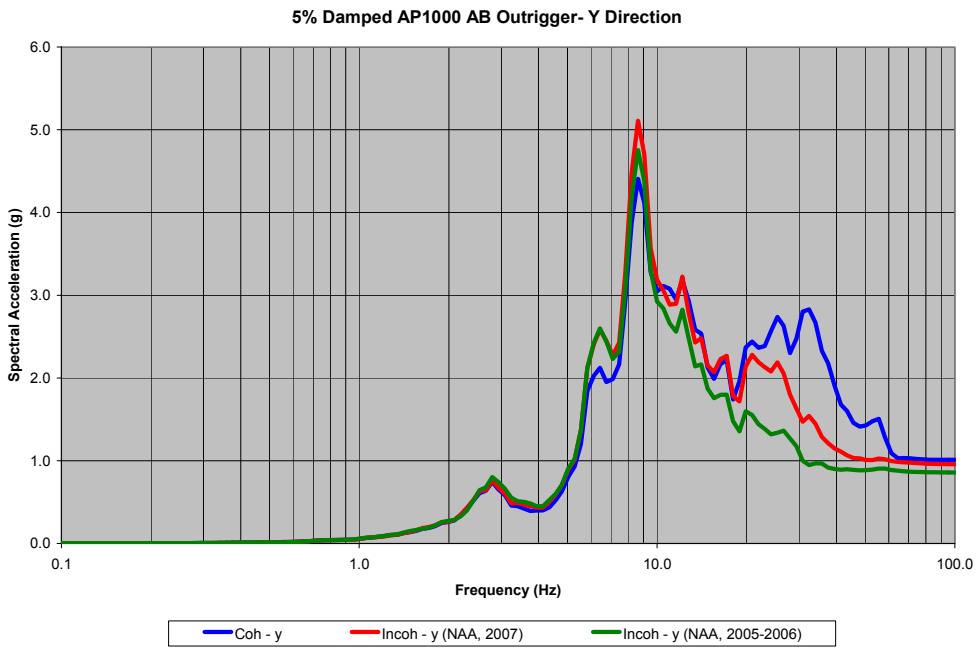

Figure B-19
Auxiliary Building Outrigger Response Spectra – Y Direction – SSI Coherent, SSI Incoherent NAA2005-2006, SSI Incoherent NAA2007 (Node 120out)

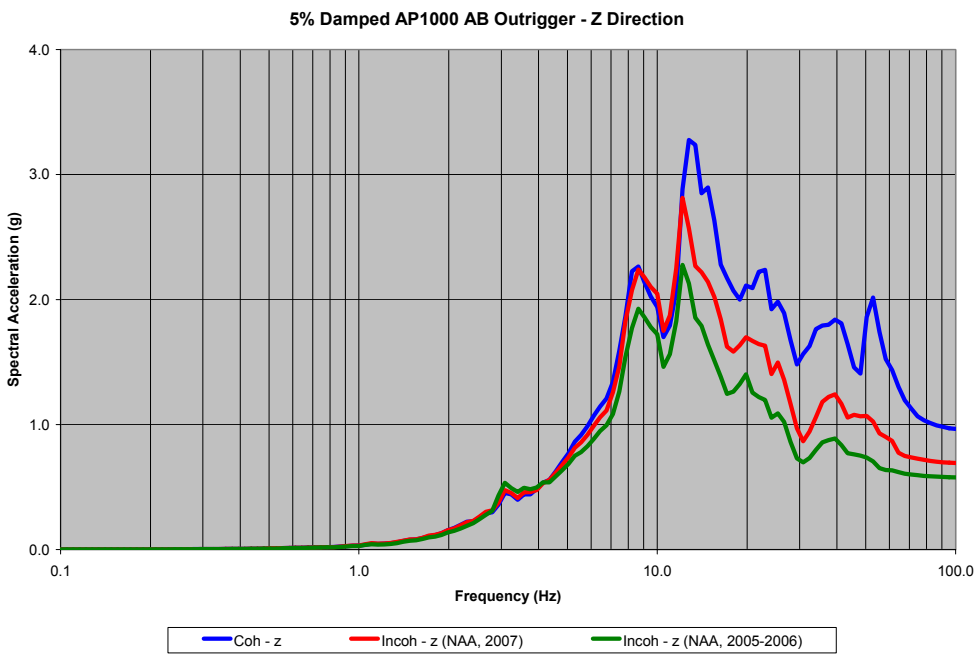

Figure B-20
Auxiliary Building Outrigger Response Spectra – Z Direction – SSI Coherent, SSI Incoherent NAA2005-2006, SSI Incoherent NAA2007 (Node 120out)

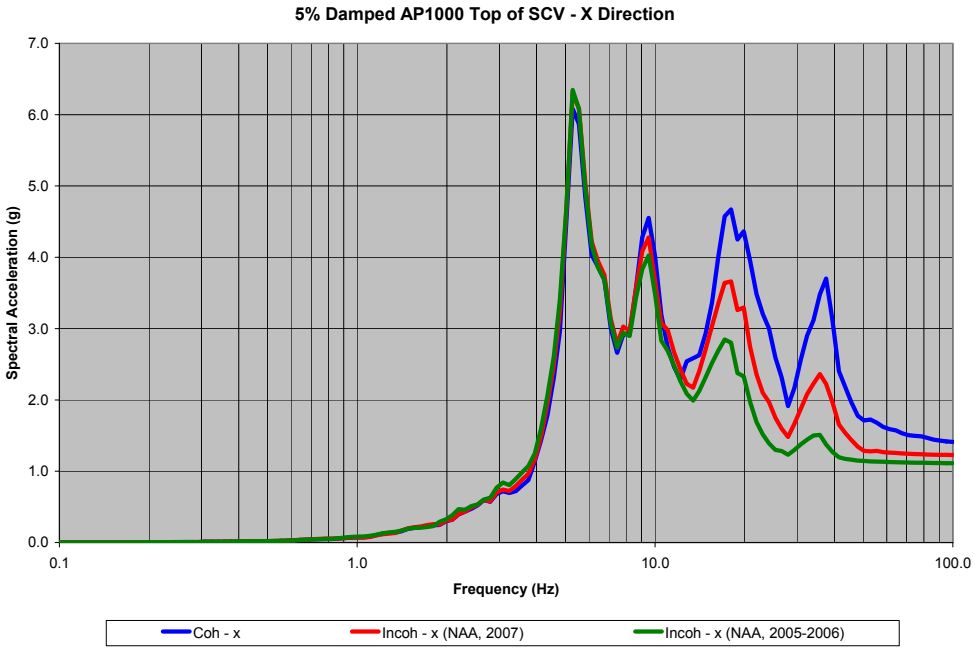

Figure B-21
Top of SCV Response Spectra – X Direction –SSI Coherent, SSI Incoherent NAA2005-2006, SSI Incoherent NAA2007 (Node 417)

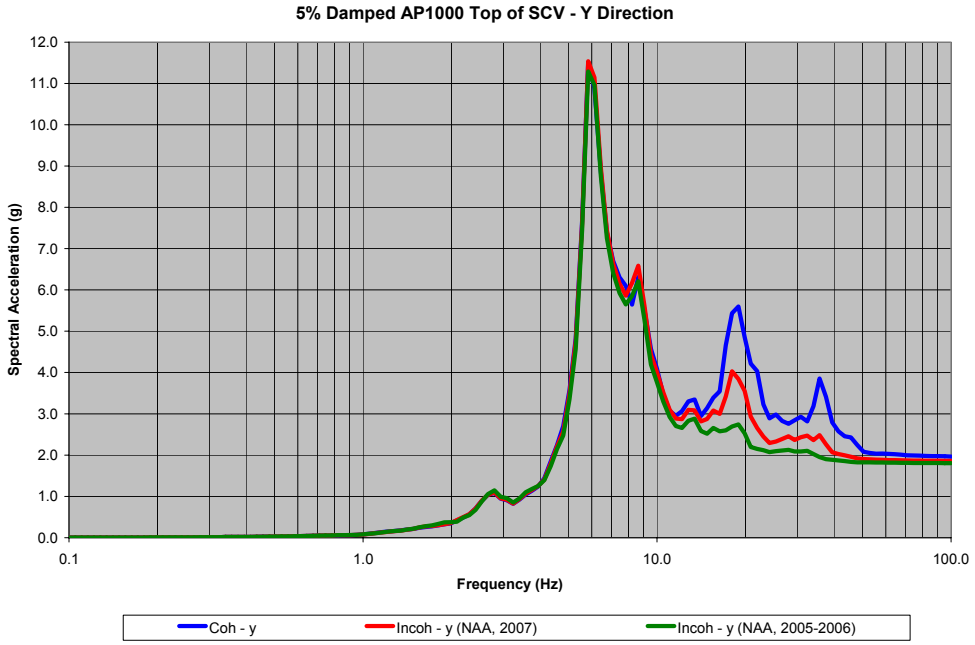

Figure B-22
Top of SCV Response Spectra – Y Direction –SSI Coherent, SSI Incoherent NAA2005-2006, SSI Incoherent NAA2007 (Node 417)

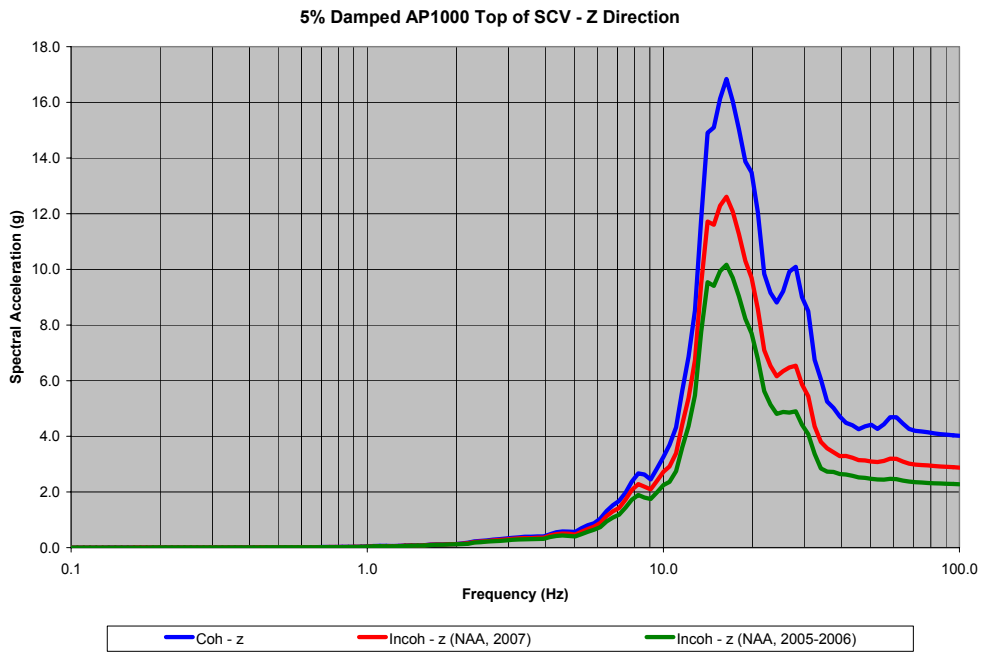

Figure B-23
Top of SCV Response Spectra – Z Direction –SSI Coherent, SSI Incoherent NAA2005-2006, SSI Incoherent NAA2007 (Node 417)

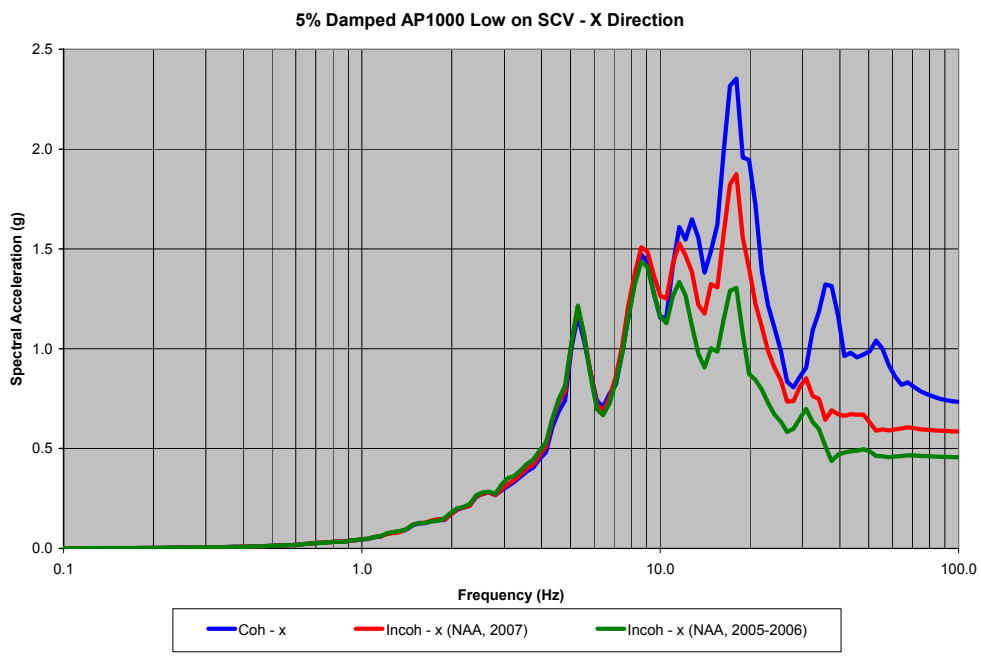

Figure B-24
Low on SCV Response Spectra – X Direction – SSI Coherent, SSI Incoherent NAA2005-2006, SSI Incoherent NAA2007 (Node 406)

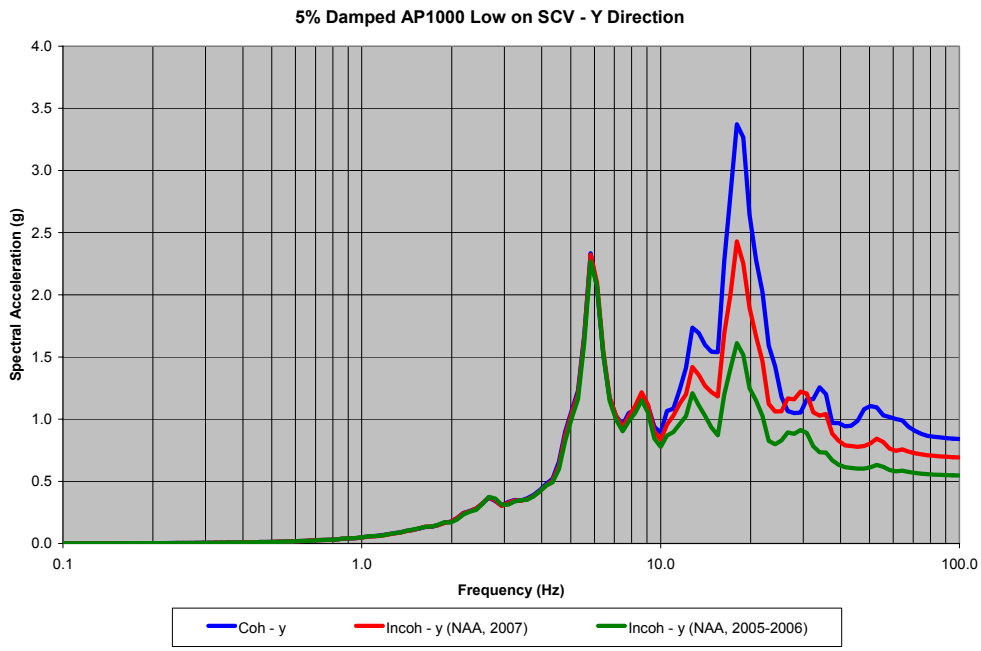

Figure B-25
Low on SCV Response Spectra – Y Direction – SSI Coherent, SSI Incoherent NAA2005-2006, SSI Incoherent NAA2007 (Node 406)

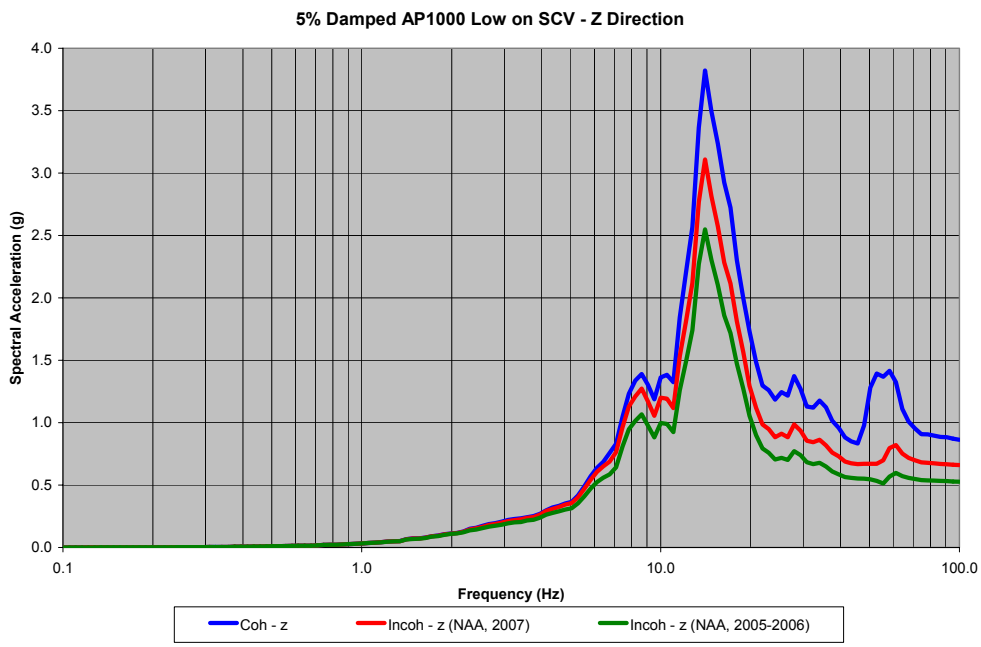

Figure B-26
Low on SCV Response Spectra – Z Direction – SSI Coherent, SSI Incoherent NAA2005-2006, SSI Incoherent NAA2007 (Node 406)

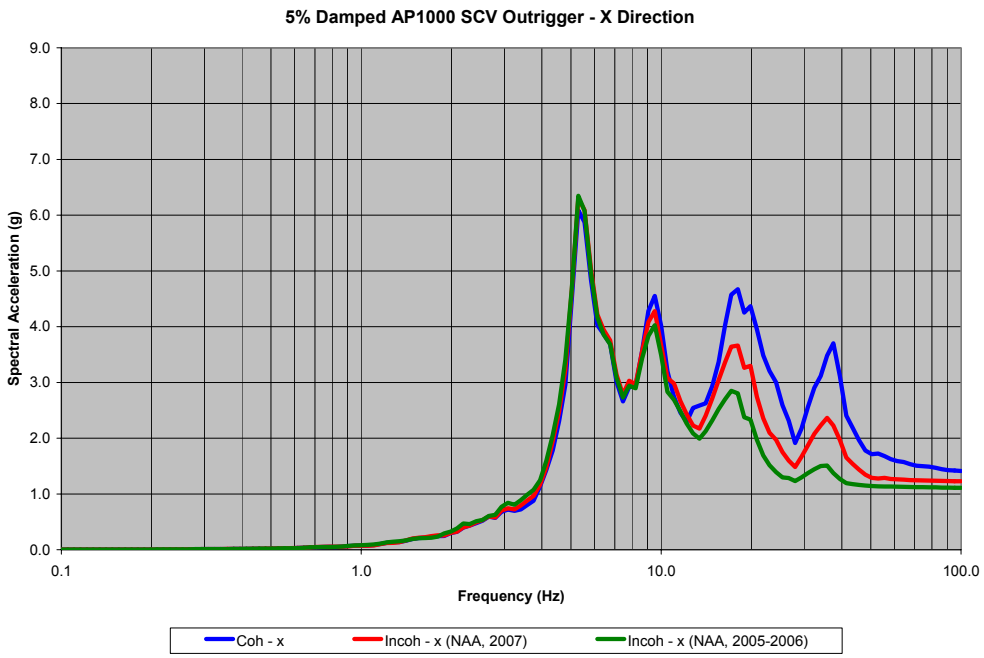

Figure B-27
SCV Outrigger Response Spectra – X Direction – SSI Coherent, SSI Incoherent NAA2005-2006, SSI Incoherent NAA2007 (Node 417out)

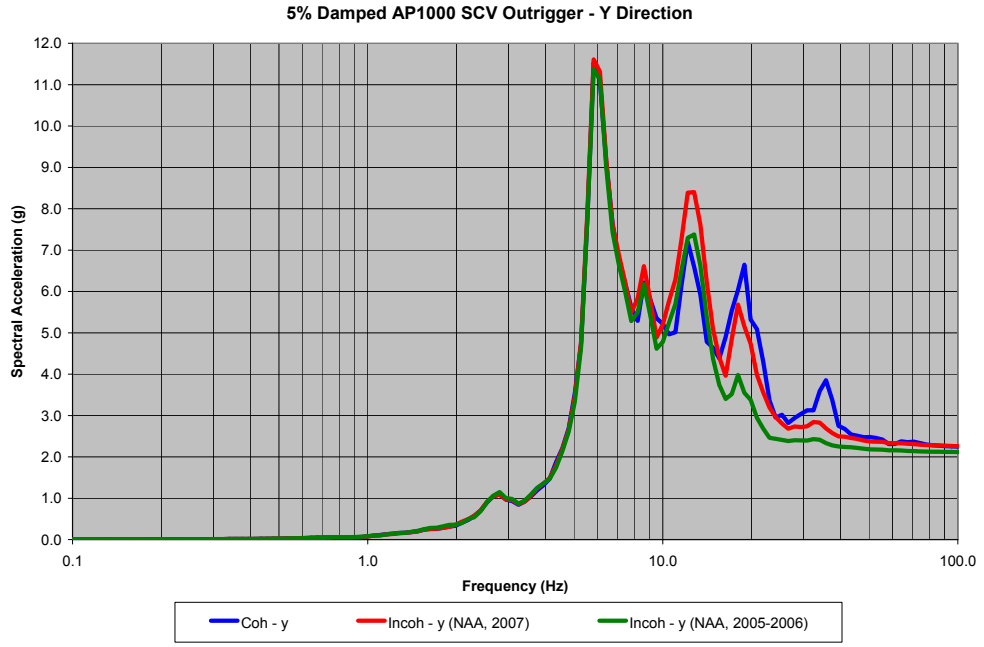

Figure B-28
SCV Outrigger Response Spectra – Y Direction – SSI Coherent, SSI Incoherent NAA2005-2006, SSI Incoherent NAA2007 (Node 417out)

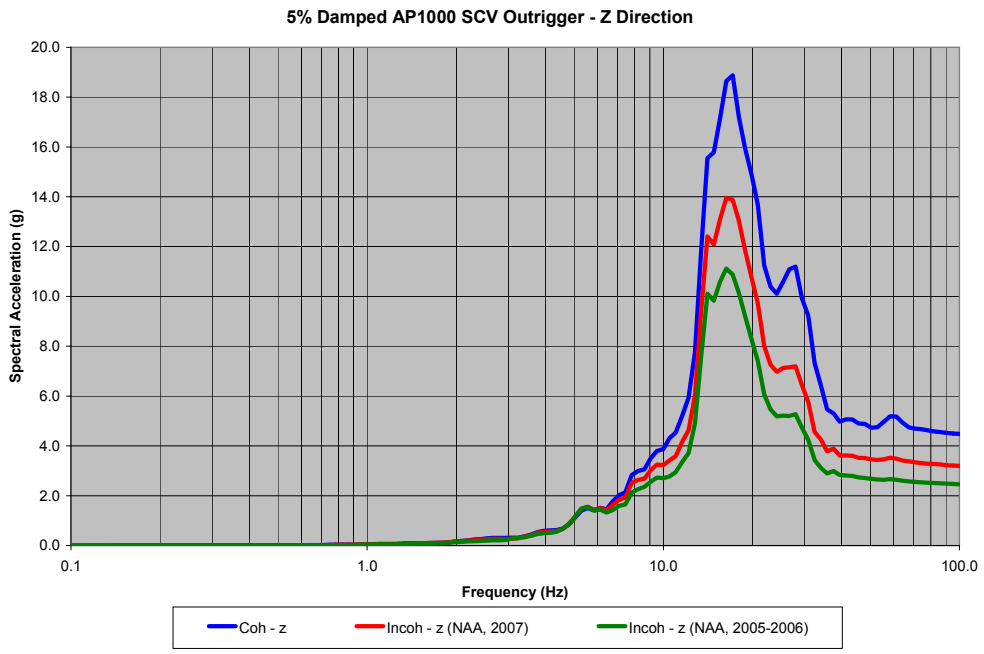

Figure B-29
SCV Outrigger Response Spectra – Z Direction – SSI Coherent, SSI Incoherent NAA2005-2006, SSI Incoherent NAA2007 (Node 417out)

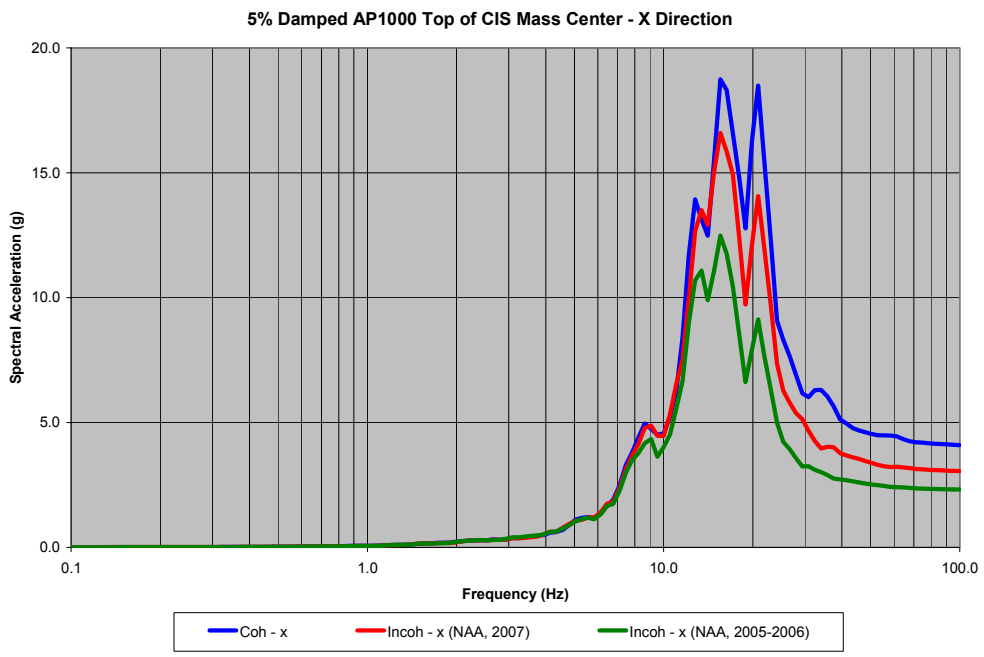

Figure B-30
Top of CIS Response Spectra – X Direction –SSI Coherent, SSI Incoherent NAA2005-2006, SSI Incoherent NAA2007 (Node 538mc)

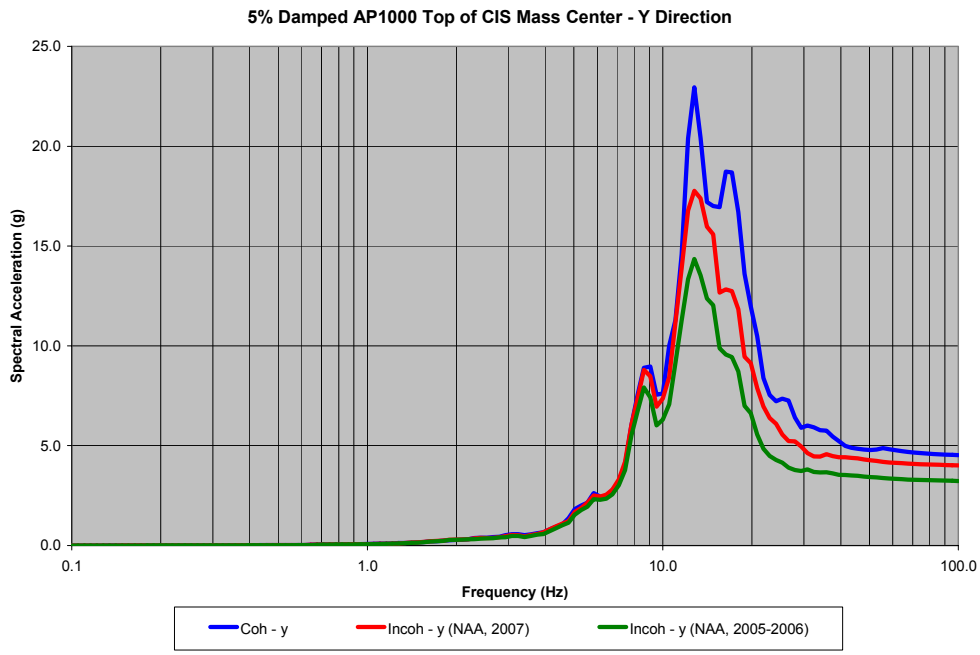

Figure B-31
Top of CIS Response Spectra – Y Direction –SSI Coherent, SSI Incoherent NAA2005-2006, SSI Incoherent NAA2007 (Node 538mc)

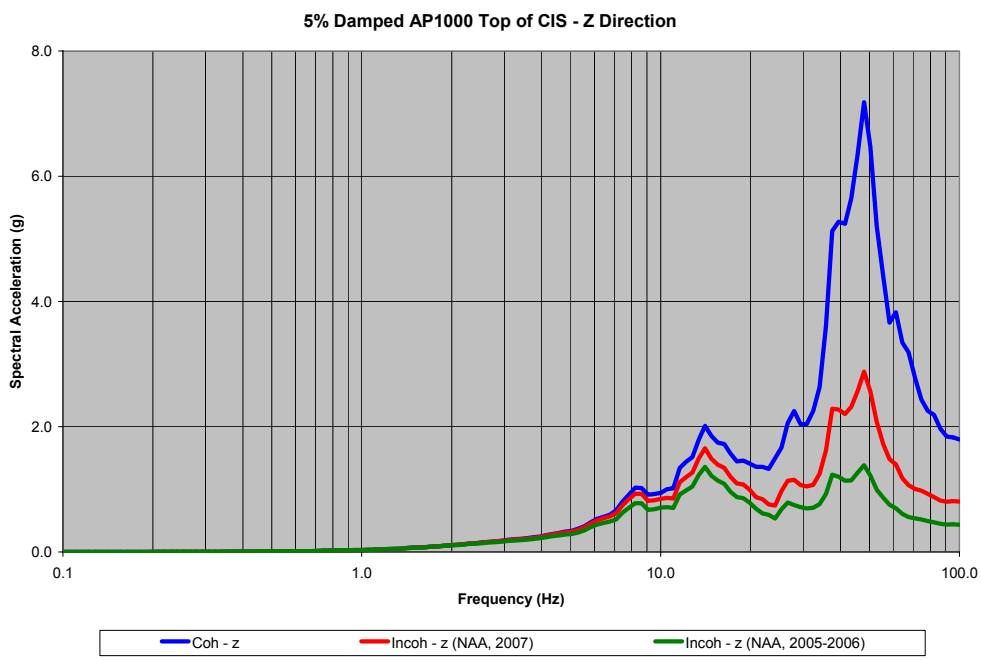

Figure B-32
Top of CIS Response Spectra – Z Direction –SSI Coherent, SSI Incoherent NAA2005-2006, SSI Incoherent NAA2007 (Node 538)

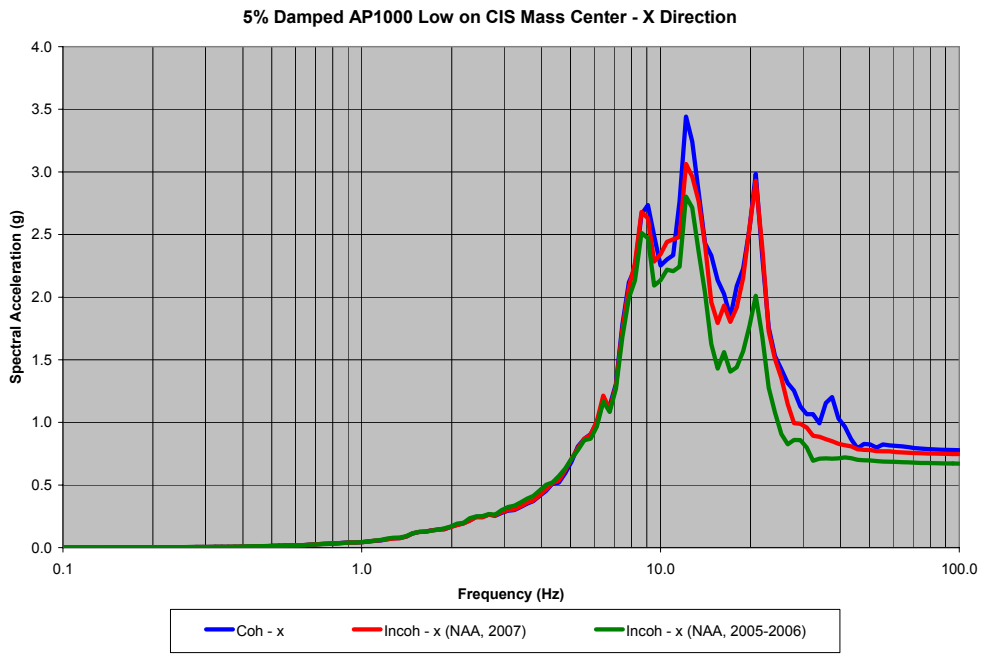

Figure B-33
Low on CIS Response Spectra – X Direction –SSI Coherent, SSI Incoherent NAA2005-2006, SSI Incoherent NAA2007 (Node 535mc)

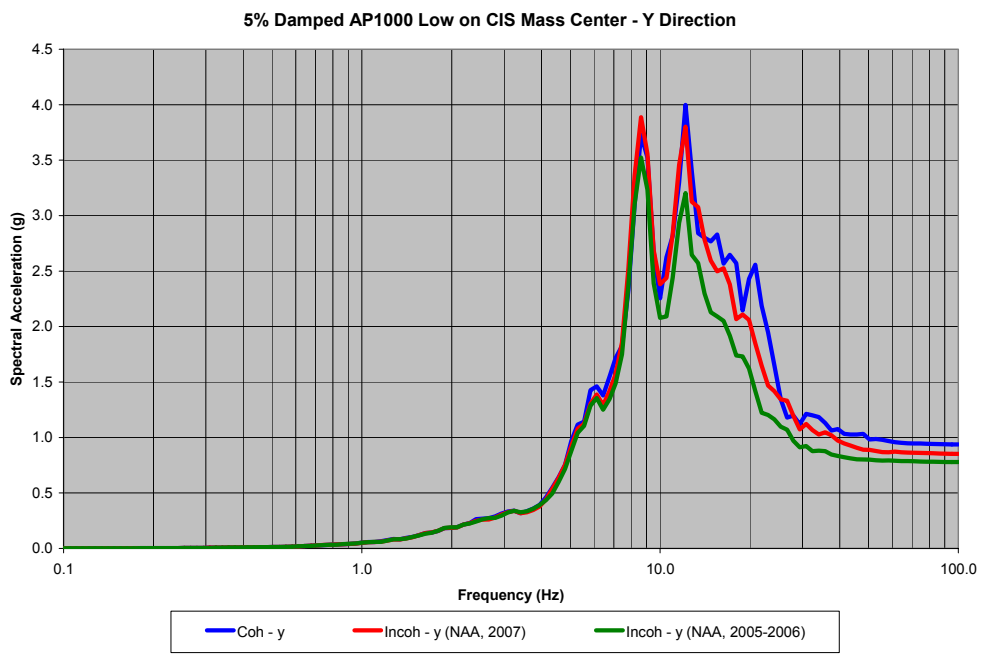

Figure B-34
Low on CIS Response Spectra – Y Direction –SSI Coherent, SSI Incoherent NAA2005-2006, SSI Incoherent NAA2007 (Node 535mc)

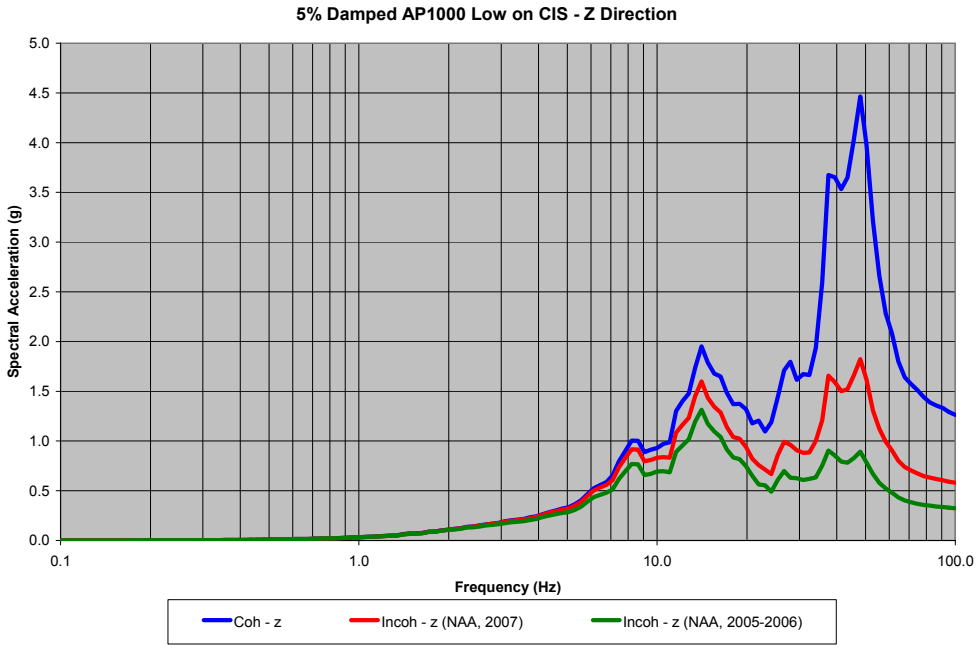

Figure B-35
Low on CIS Response Spectra – Z Direction –SSI Coherent, SSI Incoherent NAA2005-2006, SSI Incoherent NAA2007 (Node 535)

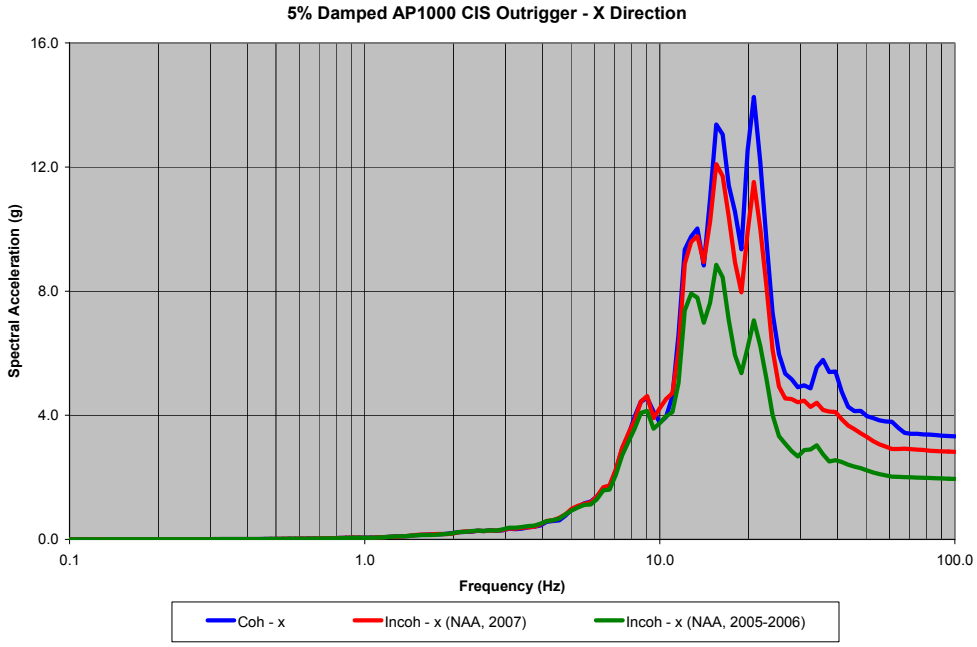

Figure B-36
CIS Outrigger Response Spectra – X Direction – SSI Coherent, SSI Incoherent NAA2005-2006, SSI Incoherent NAA2007 (Node 538out)

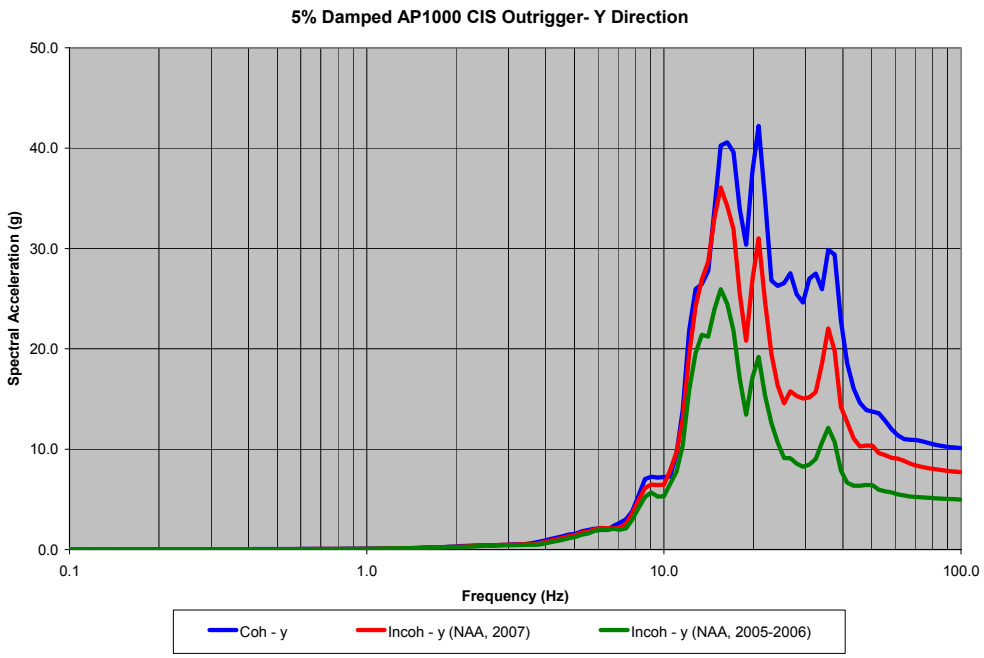

Figure B-37
CIS Outrigger Response Spectra – Y Direction – SSI Coherent, SSI Incoherent NAA2005-2006, SSI Incoherent NAA2007 (Node 538out)

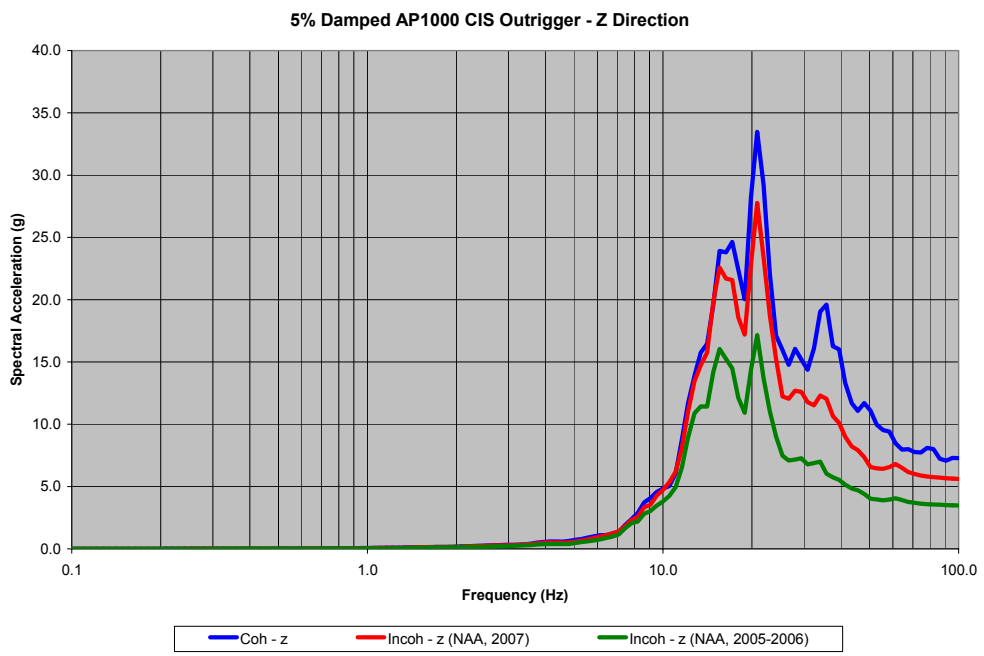

Figure B-38
CIS Outrigger Response Spectra – Z Direction – SSI Coherent, SSI Incoherent NAA2005-2006, SSI Incoherent NAA2007 (Node 538out)

References

Abrahamson, N. (2006). *Program on Technology Innovation: Spatial Coherency for Soil-Structure Interaction.* Electric Power Research Institute, Palo Alto, CA: December. Report 1014101.

Abrahamson, N. (2005). *Spatial Coherency for Soil-Structure Interaction*. Electric Power Research Institute, Technical Update Report 1012968, Palo Alto, CA. December.

Abrahamson, N. (2007). *Hard Rock Coherency Functions Based on the Pinyon Flat Data,* April 2.

Short, S.A., G.S. Hardy, K.L. Merz, and J.J. Johnson (2006), *Program on Technology Innovation: Effect of Seismic Wave Incoherence on Foundation and Building Response.* Electric Power Research Institute, Palo Alto, CA and U.S. Department of Energy, Germantown, MD: November. Final Report TR-1013504.

C
SASSI SIMULATION & SASSI-AS APPROACHES FOR SSI ANALYSIS WITH INCOHERENT GROUND MOTIONS

Stochastic and Deterministic Approaches for Incoherent Seismic SSI Analysis as Implemented in ACS SASSI

Dan M. Ghiocel
GP Technologies, Inc.
Rochester, NY
August 2007

This appendix describes the theoretical basis and specific implementation aspects related to the stochastic *Simulation Mean* (SASSI-Simulation Mean) and deterministic *Linear Algebraic Summation* (SASSI-AS) approaches that are used in this EPRI report. These two approaches are currently implemented in the ACS SASSI code for performing incoherent seismic SSI analyses.

Brief Introduction to Stochastic Modeling Terminology

Typically, the term "stochastic process" is used in conjunction with the time evolution of a dynamic random phenomenon, while the term "stochastic field" is used in conjunction with the spatial variation of a stochastic (hyper) surface. A space-time stochastic process is a stochastic function having time and space as independent arguments. The term "space-time stochastic process" is synonymous with the term "time-varying stochastic field." Stochastic field term fits well with stochastic boundary value problems, including the problem of the seismic free-field motion local spatial variation within dense arrays of recorders. Stochastic fields can be homogeneous or non-homogeneous, isotropic or anisotropic, depending on whether their statistics are invariant or variant to the axis translation and, respectively, invariant or variant to the axis rotation in space.

It should be noted that the stochastic field models proposed by Abrahamson (Abrahamson, 1993, 2005, 2006, 2007) for approximating the local spatial variation of seismic motions assume an isotropic stochastic field model that is invariant to translation and rotation in the horizontal ground surface plane.

Coherence Function

For a seismic wave stochastic field, with an amplitude denoted u(t) in time domain and $U(\omega)$ in frequency domain, the (pair) cross-spectral density (CSD) function for two separated locations on ground surface j and k, $S_{Uj,Uk}(\omega)$, can be expressed by

$$S_{Uj,Uk}(\omega) = [S_{Uj,Uj}(\omega)S_{Uj,Uj}(\omega)]^{1/2}\Gamma_{Uj,Uk}(\omega) \qquad \textbf{Equation C-1}$$

where $S_{Uj,Uj}(\omega)$ and $S_{Uk,Uk}(\omega)$ are the power spectral density (PSD) of the seismic motion at locations j and k, and $\Gamma_{Uj,Uk}(\omega)$ is the pair coherence function for locations j and k. More generally, the CSD function is a complex quantity. However, in many advanced engineering applications, since coherence function is assumed to be a real and positive quantity - this is used for quadrant symmetric and isotropic stochastic fields (Vanmarcke, 1983) - the CSD function is also real and positive. The coherence function, $\Gamma_{Uj,Uk}(\omega)$, is a measure of the similarity of the two location motions including both the amplitude spatial variation and the wave passage effects. Thus, more generally, the coherence function is a complex quantity, often called in earthquake engineering literature the "unlagged" coherence function (Abrahamson, 1993, 2005, 2006, 2007). However, often in earthquake engineering practice, we use isotropic, "lagged" coherence functions that are real and positive quantities that incorporate only the amplitude spatial randomness effects with no consideration of the wave-passage effects. The numerical investigations shown in this EPRI report are based on "lagged" coherency models that consider only amplitude randomness aspects and neglect wave-passage aspects.

Inversing Equation C-1, we get the definition of the coherence function between two arbitrary motions:

$$\Gamma_{Uj,Uk}(\omega) = \frac{S_{Uj,Uk}(\omega)}{[S_{Uj,Uj}(\omega)S_{Uk,Uk}(\omega]^{1/2}} = \frac{E[U_j(\omega)U_k(\omega)]}{\left\{E[U_j(\omega)U_j(\omega)]E[U_k(\omega)U_k(\omega)]\right\}^{1/2}} \qquad \textbf{Equation C-2}$$

In Equation C-2 using the statistical expectation operator, denoted by E[.], we highlight that the CSD function, $S_{Uj,Uk}(\omega)$, at each frequency is identical with the second-order statistical moment (scaled covariance) of the motion amplitudes $U_j(\omega)$ and $U_k(\omega)$ assumed to be two random variables. The last expression of coherence function in Equation C-2 (right-side term) at any given frequency is identical with the expression of a statistical correlation coefficient between two random variables that can be found in any statistical textbook. This observation suggests that a series of efficient engineering numerical tools developed for digital simulation of (static) stochastic spatial variation fields based on factorization of covariance kernels could be extended for simulation of seismic motion spatial variation fields using factorization of coherence kernels at each frequency.

Factorization of Coherency Kernels

Several factorization techniques can be used for simulating of complex pattern stochastic fields. A quite frequent approach in engineering research literature is to employ the Pearson differential equation for defining different types of stochastic series representations based on orthogonal Hermite, Legendre, Laguerre, and Cebyshev polynomials (Ghanem and Spanos, 1991, Ghiocel, 2004, Nair, 2004). These polynomial expansions are usually called Askey chaos series.

A major application of stochastic field decomposition theory is the representation of stochastic fields using the covariance kernel factorization. These covariance-based techniques have a large potential for practical engineering applications because they can be applied to any complex, static, or dynamic Gaussian or non-Gaussian stochastic field (Ghiocel, 2004). There are two competing stochastic simulation techniques using the covariance kernel factorization: (1) Choleski factorization and (2) Spectral factorization (called sometime Karhunen-Loeve expansion, or POD expansion) based on eigen-decomposition. Both techniques can be employed to simulate both static and dynamic stochastic fields including seismic incoherent motions. A notable property of these two simulation techniques is that they can handle both real-valued and complex-valued covariance kernels. For simulating space-time processes (or dynamic stochastic fields), both covariance-based techniques can be employed. A detailed presentation of these two simulation techniques is provided by Ghiocel (Ghiocel, 2004). It should be noted that spectral factorization has the advantage of providing useful engineering insights. The covariance eigenvectors, also called spatial modes, describe the "wavelength" component structure of the stochastic spatial variation field. It should be noted that for random spatial variations with large correlation-lengths, the number of (covariance) spatial modes required by the stochastic field eigen-series expansion convergence is reduced to only few modes. This provides often some practical advantages.

Incoherent Seismic SSI Analysis Methodology

The implementation of incoherent SSI analysis is based on the spectral factorization of the coherency kernel at each selected frequency as described in 1997 EPRI Report TR-102631 2225 on "Soil-Structure Interaction Analysis Incorporating Spatial Incoherence of Ground Motions" by Tseng and Lilhanand. The incoherent SSI analysis methodology is described in detail in the above referenced report.

In this section we review few key equations from the above referenced 1997 EPRI report that are the basis of the numerical implementations of the *Simulation Mean* and *Linear Algebraic Summation* approaches in ACS SASSI. To make reading easier, we used as much as possible the same notations as were used in the referenced 1997 EPRI report. The main differences in notations are that for structure dofs we use superscript s instead of subscript s, and for ground motion at interaction nodes we use superscript g instead of subscript g. The notations for coherent and incoherent motions by superscript c and i, respectively, are identical with the notations used in referenced EPRI report.

Let's consider first the free-field motion. The coherent free-field motion at any interaction node dof k, $U_k^{g,c}(\omega)$, is computed by (1997 EPRI report, Equation 3-32):

$$U_k^{g,c}(\omega) = H_k^{g,c}(\omega)U_0^g(\omega)$$ **Equation C-3**

where $H^{g,c}(\omega)$ is the (deterministic) complex coherent ground transfer function vector at interface nodes and $U_0^g(\omega)$ is the complex Fourier transform of the control motion.

Similarly, the incoherent free-field motion at any interaction node dof k, $U_k^{g,i}(\omega)$, is computed by (1997 EPRI report, Equation 3-24):

$$U_k^{g,i}(\omega) = \tilde{H}_k^{g,i}(\omega)U_0^g(\omega)$$ **Equation C-4**

where $\tilde{H}^{g,i}(\omega)$ is the (stochastic) incoherent ground transfer function vector at interaction node dofs and $U_0^g(\omega)$ is the complex Fourier transform of the control motion.

The main difference between coherent and incoherent free-field transfer function vectors is that the $H^{g,c}(\omega)$ is deterministic quantity while $\tilde{H}_k^{g,i}(\omega)$ is a stochastic quantity (tilda hat marks this) that includes deterministic effects due to the seismic plane-wave propagation, but also stochastic effects due to incoherent motion spatial variation in horizontal plane. Thus, the incoherent free-field transfer function at any interaction node can be defined by:

$$\tilde{H}_k^{g,i}(\omega) = S_k(\omega)H_k^{g,c}(\omega)$$ **Equation C-5**

where $S_k(\omega)$ is a frequency-dependent quantity that includes the effects of the stochastic spatial variation of free-field motion at any interaction node dof k due to incoherency. In fact, $S_k(\omega)$ represents the complex Fourier transform of relative spatial random variation of the motion amplitude at the interaction node dof k due to incoherency. Since these relative spatial variations are random, $S_k(\omega)$, is stochastic in nature. The stochastic $S_k(\omega)$ can be computed for each interaction node dof k using spectral factorization of coherency matrix computed for all SSI interaction nodes. Thus, for any interaction node dof k, the stochastic spatial motion variability transfer function $\tilde{H}_k^{g,i}(\omega)$ in complex frequency domain is described by the product of the stochastic eigen-series expansion of the spatial incoherent field times the deterministic complex coherent ground motion transfer function:

$$\tilde{H}_k^{g,i}(\omega) = [\sum_{j=1}^{M}\Phi_{j,k}(\omega)\lambda_j(\omega)\eta_{\theta j}(\omega)]H_k^{g,c}(\omega)$$ **Equation C-6**

where $\lambda_j(\omega)$ and $\Phi_{j,k}(\omega)$ are the j-th eigenvalue and the j-th eigenvector component at interaction node k. The factor $\eta_{\theta j}(\omega)$ in equation C-6 is the random phase component associated

with the j-th eigenvector that is given by $\eta_{\theta j}(\omega) = \exp(i\theta_j)$ in which the random phase angles are assumed to be uniformly distributed over the unit circle, $\theta_j(\omega) \sim U[-\pi, \pi]$ (1997 EPRI report, Equation 3-26). The number of coherency matrix eigenvectors, or incoherent spatial modes, could be either all modes or a reduced number of modes M depending on the eigen-series convergence.

Let's consider now the structural SSI response. For a coherent motion input, assuming a number of interaction nodes equal to N, the complex Fourier SSI response at any structural dof i, $U_i^{s,c}(\omega)$, is computed by the superposition of the effects produced by the application of the coherent motion input at each interaction node k (1997 EPRI report, Equation. 3-32):

$$U_i^{s,c}(\omega) = \sum_{k=1}^{N} H_{i,k}^{s}(\omega) U_k^{g,c}(\omega) = \sum_{k=1}^{N} H_{i,k}^{s}(\omega) H_k^{g,c}(\omega) U_0^{g}(\omega) \qquad \textbf{Equation C-7}$$

where the $H^s(\omega)$ matrix is the structural complex transfer function matrix given unit inputs at interaction node dofs. The component $H_{i,k}^{s}(\omega)$ denotes the complex transfer function for the i-th structural dof if a unit amplitude motion at the k-th interaction node dof is applied.

For incoherent motion input, the complex Fourier SSI response at any structural dof i, $U_i^{s,i}(\omega)$, is computed similarly by the superposition of the effects produced by the application of the incoherent motion input at each interaction node dof k (1997 EPRI report, Equation 3-32b is):

$$U_i^{s,i}(\omega) = \sum_{k=1}^{N} H_{i,k}^{s}(\omega) U_k^{g,i}(\omega) = \sum_{k=1}^{N} H_{i,k}^{s}(\omega) [\sum_{j=1}^{M} \Phi_{j,k}(\omega) \lambda_j(\omega) \eta_{\theta j}(\omega)]\, H_k^{g,c}(\omega) U_0^{g}(\omega) \qquad \textbf{Equation C-8}$$

Obviously that in Equation C-8, $H_{i,k}^{s}(\omega)$ is the same as in Equation C-7, since the structural transfer matrix does not depend on seismic input motion characteristics.

Incoherent SSI Analysis Implementation

Equations C-4, C-6 and C-8 are the theoretical basis of incoherent seismic SSI analysis in ACS SASSI. The differences between *Simulation Mean* (SASSI-Simulation Mean) and *Linear Algebraic Summation* (SASSI-AS) are due to the way in which the random phases are handled in Equation C-6, as described in next sections. Also, the Simulation Mean approach requires a set of random incoherent motions and SSI runs for computing the mean response, while the Linear Algebraic Summation approach uses only a single incoherent motion and a single SSI run.

Independently of the selected incoherent SSI approach to be used, the ACS SASSI incoherent SSI analysis includes the following computational steps (single analysis for SASSI-AS and multiple analyses for SASSI Simulation Mean):

1. Compute the free-field coherency matrix at interaction nodes

2. Perform spectral factorization of the coherency matrix (also check its accuracy)
3. Use linear superposition of scaled spatial modes at each selected frequency (assuming zero phases for SASSI-AS and random phases for SASSI-Simulation Mean)
4. Compute ITF including the smoothing of interpolation errors to avoid spurious peaks (select smoothing parameter based on comparisons between TFU and TFI files)
5. Adjust ITF phases to avoid canceling phase effects (default option)
6. Perform the convolution of complex ITF with input control motion FFT
7. Compute acceleration time histories at selected structural nodes by inverse FFT
8. Compute ISRS from acceleration time histories at selected structural nodes

Since the ACS SASSI implementations uses Equation C-6 that is derived in free-field before the SSI analysis is started, the number of extracted coherency matrix eigenvectors, or incoherent spatial modes, can be as large as is desired by the user with a very negligible impact on the SSI analysis run time. By default, all the incoherent spatial modes are included. Consideration of all incoherent spatial modes improves the incoherent SSI accuracy and produces a very accurate recovery of the free-field coherency matrix at interaction nodes; this can be checked by the user for each calculation frequency. Very importantly, since the incoherent spatial modes are combined at the level of the free-field incoherent input motion, and not at the level of the SSI response, the incoherent SSI analysis run time is practically equal to the coherent SSI analysis run time. This indicates the practicality of the ACS SASSI implementations.

Stochastic Approach or Randomization (SASSI-Simulation Mean)

The stochastic approach implemented in ACS SASSI is called either *Stochastic Approach or Randomization, or SASSI Simulation Mean* in this EPRI report. The incoherent mean in-structure response spectra (ISRS) results computed with the stochastic approach are denoted *Simulation Mean* in the legends of the ISRS figures of the report.

The Simulation Mean approach uses Equations C-4 and C-6 to generate random incoherent input free-field motions. Using Monte Carlo simulation, a set of random incoherent motion samples are generated at SSI interaction nodes. These incoherent motion random samples are obtained by simulating random phase angles in Equation C-6. For each incoherent motion random sample, an incoherent SSI analysis is performed. Finally, the mean SSI response is computed by statistical averaging of the response quantities of interest. Thus, Simulation Mean approach implies that a set of statistical incoherent SSI analyses are required.

To speed up the set of SSI simulations, a fast restart option for reanalysis was introduced. This restart option bases on the fact that for each incoherent motion SSI run only seismic load vector changes, while the soil impedance matrix and the structural transfer functions with respect to interaction node excitations remain the same. If the restart option is used the run time for each SSI analysis drops to only 1/3 to 1/5. Thus, it is possible to do up to 5 stochastic SSI simulations in the time of a single initiation run. This provides quite reasonable run times for the Simulation Mean approach.

Useful details on the computational steps of the stochastic approach are provided in the report at pages 4-3 and 4-4. Other implementation aspects are presented at pages 4-4 to 4-7. It should be noted that the stochastic approach (SASSI-Simulation Mean) is a repeated application of the Linear Algebraic Sum approach (SASSI-AS) - that is described in next section - assuming that the random phase angles associated to interaction node coherency matrix eigenvectors are uniformly distributed random variables at each frequency (Equation C-6) based on the Gaussianity assumption.

Deterministic Approach or Linear Algebraic Summation (SASSI-AS)

The basic idea of the Linear Algebraic Summation (SASSI-AS) approach is to develop a fast-accurate incoherent SSI analysis approach that is based on spectral factorization of coherency matrix and approximates closely the mean response in a *single* SSI analysis run. This deterministic approach is based on a simple, engineering practical rule that has been accepted in the past practice for NPP Seismic PRA reviews, namely that "Median Input produces Median Response".

To implement the "median input produces median output" rule for incoherent SSI analysis, SASSI-AS combines the incoherent spatial modes using a linear algebraic summation as described in Equation C-6 assuming zero random phase values (the zero phases are the statistical mean phase values). For SASSI-AS Equation C-6 simplifies to the following form:

$$\tilde{H}_k^{g,i}(\omega) = [\sum_{j=1}^{M} \Phi_{j,k}(\omega)\lambda_j(\omega)]H_k^{g,c}(\omega) \qquad \textbf{Equation C-9}$$

Equation C-9 shows that as the result of assuming zero phase angles, the incoherent spatial modes are scaled deterministically by the values of the square roots of the coherency matrix eigenvalues that are also equal to the standard deviations of the spatial modes that are measures of their contributions to the total motion spatial variability.

As a consequence of the zero phase assumption, the SASSI-AS approach is capable to reproduce exactly the free-field coherency matrix if all the spatial modes are employed (assuming that no numerical errors occur in the calculation of the eigenvectors of coherency matrix).

To further improve the accuracy of the incoherent complex response using SASSI-AS, smoothing and phase adjustment techniques are applied. These techniques are described in the next section.

Specific Numerical Techniques Implemented for Incoherent SSI Analyses

Since the incoherent SSI analysis calculations are done in the context of the complex Fourier transform representation of the input motion, it is assumed that the Fourier amplitudes of a two neighbor frequencies are statistically uncorrelated. No smoothing or correlation between neighbor frequency components in included (the power spectral content is represented by the Schuster periodogram). If this assumption is violated, then the inverse complex Fourier transformation results to time domain would be distorted. As a consequence of the

high-frequency resolution demanded by the complex Fourier representation of the stochastic incoherent motions, the incoherent transfer function amplitudes (obtained by convolution in frequency domain of the complex structural transfer functions with complex Fourier spatial free-field variation at interaction nodes, see equation C-8) are relatively unsmoothed, and because of this the original SASSI interpolation scheme could produce significant spurious spectral peaks and valleys. Also, the complex response phasing is partially deterministic due to SSI physics and partially random due to motion incoherency (equation C-6). Specific numerical techniques were implemented to address these aspects as discussed in the next two sections.

Improved Interpolation Scheme for Incoherent Transfer Function (ITF) Calculations

To avoid these spurious peaks and valleys in the interpolated transfer functions, an improved interpolation scheme that bases on the original SASSI interpolation scheme but includes an efficient spectral smoothing capability of the interpolation error was implemented. More specifically, first, the differences between the computed complex transfer functions from SSI solution (using a simple, smooth cubic spline interpolant) and the interpolated transfer functions using the original SASSI interpolation scheme are computed at all Fourier frequencies. Next, the differences between the two types of interpolated transfer functions are smoothed using the Parzen windowing technique with a user specified smoothing parameter (Parzen, 1962). The smoothing parameter represents the number of Fourier frequency steps that is used to define the bandwidth of the Parzen spectral window (equal to the standard deviation of the Gaussian function used). For small smoothing parameter values, say 1-5, the final smoothed complex transfer functions are closer to the interpolated transfer functions using original SASSI interpolation scheme and large deviations from the calculated transfer function values are reduced or eliminated when larger smoothing parameters are used. Depending on the selection of the frequency set for transfer function calculations, a smoothing parameter value from 10 to 100 is recommended. Before deciding the final smoothing parameter value to be used, the user should compare the original computed amplitude transfer functions with the interpolated amplitude transfer functions. If spurious spectral peaks or valleys are present in the interpolated transfer functions, then the smoothing parameter should be increased.

It should be noted that the spectral windowing is a smoothing or interpolation method that reconstructs the transfer functions. However, if the selected set of frequencies for incoherent SSI analysis is insufficient for capturing key features of the incoherent response spectral content, then spectral windowing will not help to improve results. The selection of an appropriate set of frequencies for response calculations still remains as an aspect of essence for the SSI analysis accuracy. Typically, a set of 100 to 200 frequencies appears to be sufficient for practical purposes.

As shown this EPRI report, pages 6-12 to 6-15, the effect of smoothing of the interpolated incoherent transfer function is highly beneficial for the accuracy of incoherent SSI analyses. Figure C-1 shows the effect of beneficial effect of smoothing on the computed incoherent transfer function (ITF) at the top of ASB using the AP1000-Based Stick Model (see report, page 5-2, Figure 5-1), at node 118 Y-dof for Z-shaking (118YZ). A set of 201 frequencies was used.

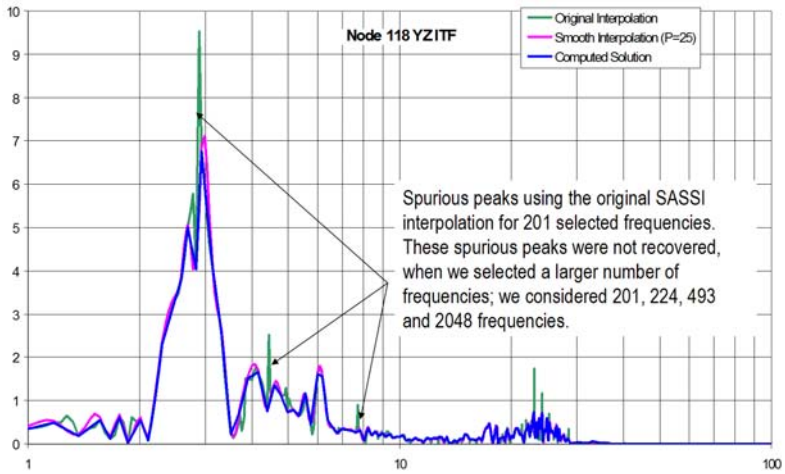

Figure C-1
Effects of Smoothing on the ITF Computed at Node 118, Y-Dof and Z-Shaking

Phase Adjustment for Incoherent Transfer Functions (ITF)

It should be noted that the stochastic nature of motion incoherency also is reflected on the complex response phasing. Figure C-2 shows the "rosette" of the complex plane representation of the computed ITFs computed at 20Hz for the node 229 for all six dofs and for 20 random simulations of incoherent Z-direction inputs (translations 229XZ, 229YZ, 229ZZ and rotations 229XX,Z, 229YY,Z and 229ZZ,Z). Each of the 229 node dof is plotted with another color and it is also marked at the tip of the rosette arrows with explanatory notations (for example, the mark 7zz indicates the random sample number 7 for the zz rotation). It should be noted that the phase angle of each dof component varies highly random from sample to sample. The differences in phase angles between each selected pair of components vary also stochastically, but with a smaller random scatter. This indicates that for 229 node, some of the dof components vary more random than others depending if the dof response is governed by the (deterministic) SSI physics or by the motion incoherency that is stochastic in nature. The phase angles of node 229 rotations under Z-shaking are governed by motion incoherency and because of this have larger random variations.

To include the random effects of input motion incoherency on the complex response phasing, the ACS SASSI implementations adjust the complex response phase angles to a variation range limit from –pi/2 to pi/2. This ensures that the phase angle cosines for all frequency components are positive. This phase angle variation limitation avoids the random occurrence of out-of-phase components due to motion incoherency, and by this generates higher energy response time histories for the same computed Fourier amplitude spectra (minimum phase delay wavelets).

The effect of phase adjustment on ISRS appears to be negligible for horizontal shakings, but it could produce an increase of ISRS for vertical shaking. Figure C-3 shows a typical effect of ITF phase adjustment for the SSI response acceleration history at the top of a RB internal structure.

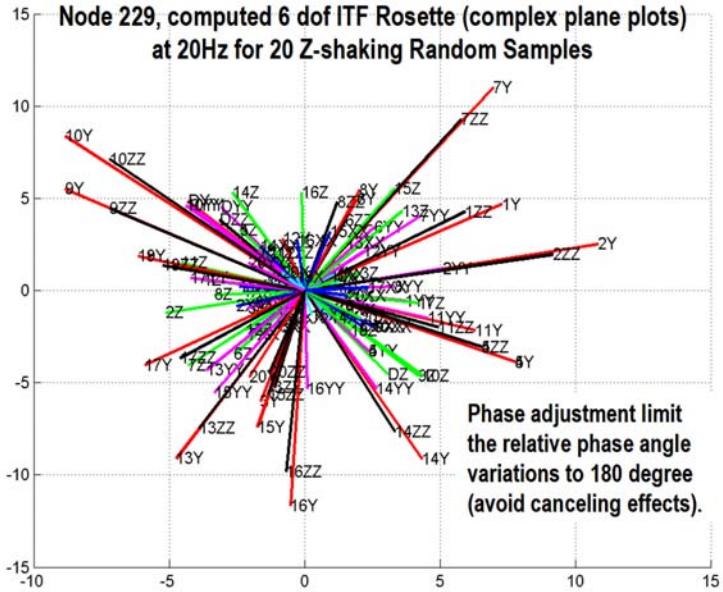

Figure C-2
Node 229 ITF Rosette at 20 Hz

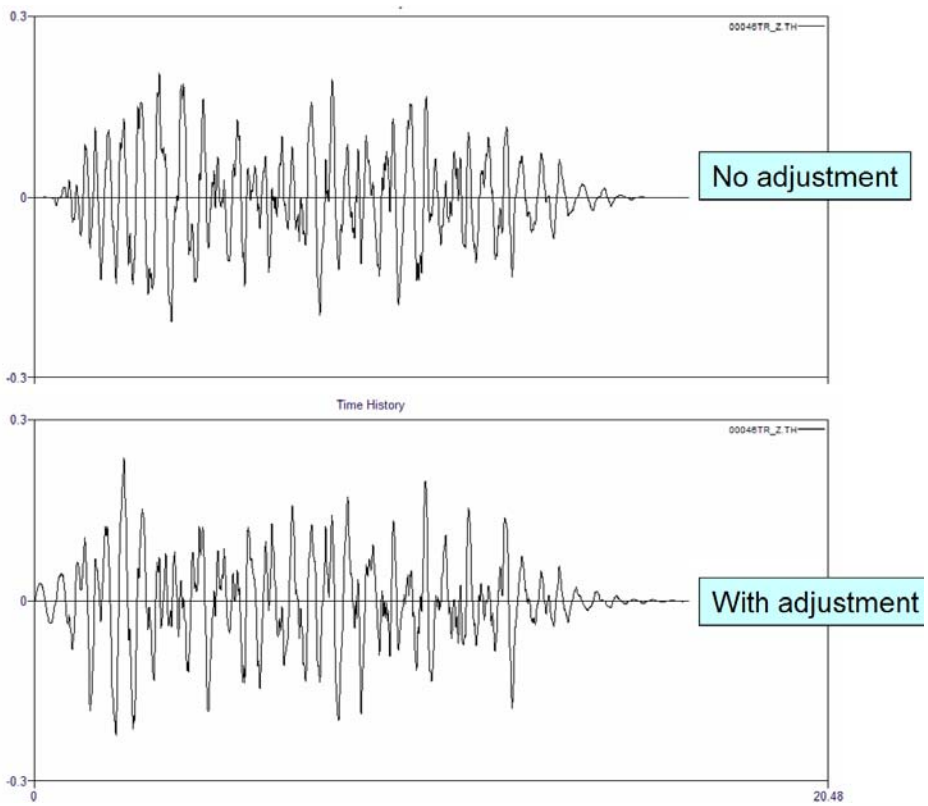

Figure C-3
Effect of ITF Phase Adjustment

During this EPRI project, we investigated the effect of ITF phase adjustment on the computed ISRS for the AP1000-based Stick Model subjected to both horizontal and vertical shakings in the Y direction and Z direction, respectively. There was no visible effect of phase adjustment on ISRS for the horizontal input, as shown in Figure C-4 for Node 145Y-dof for the X-shaking. For the vertical input, the phase adjustment effects produced a visible increase of ISRS as indicated in Figure C-5 for the same Node 145 Y-dof for the Z-shaking.

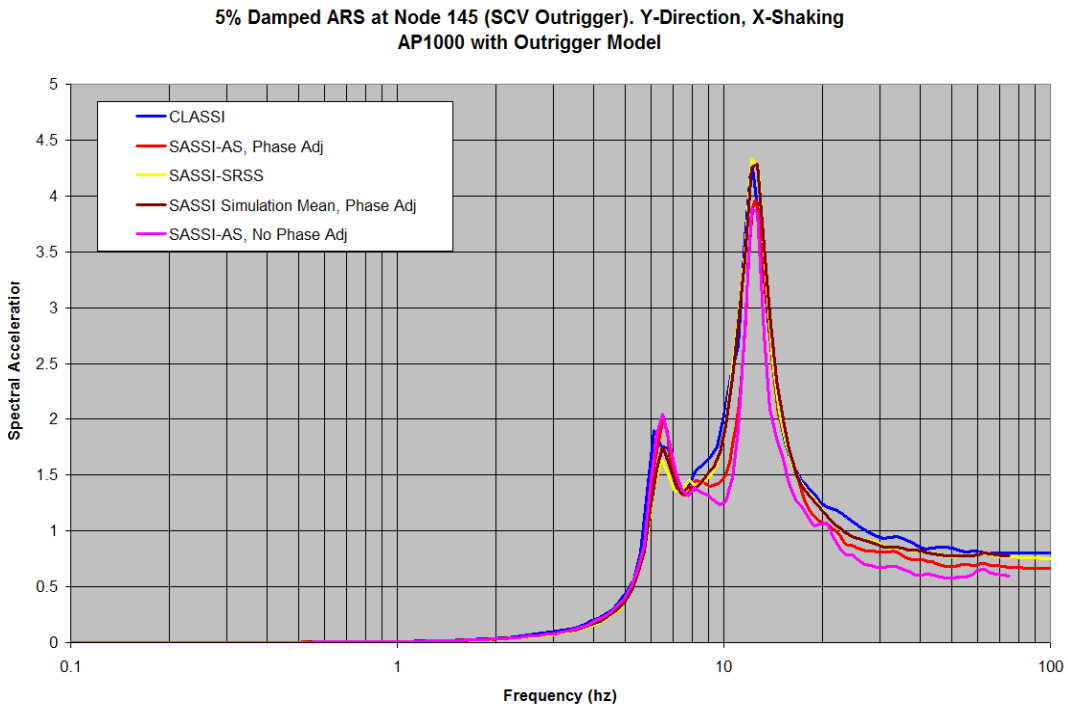

Figure C-4
Phase Adjustment Effect for Node 145Y for X-Shaking – Comparative ISRS Results

It should be noted that the introduction of phase adjustment effects closes the gap of numerical differences between the computed ISRS that were obtained by different technical teams at ARES, Bechtel Engineering and GP Technologies using different SSI codes (CLASSI and SASSI) and different incoherent SSI approaches (SRSS, AS and Simulation Mean). Since the application of the SASSI-AS and SASSI-Simulation Mean approaches with phase adjustment provided a closer matching of the ISRS results with the other industry approaches, and by this also built a stronger consensus among technical investigators, we included the phase adjustment as a default analysis option for the ACS SASSI incoherent analyses. However, the code has the capability to include no phase adjustment, if the user is interested to investigate and understand in more detail the complex response phasing aspects. The ISRS results presented in this EPRI report include only results obtained using SASSI-AS and SASSI-Simulation Mean applied with phase adjustment.

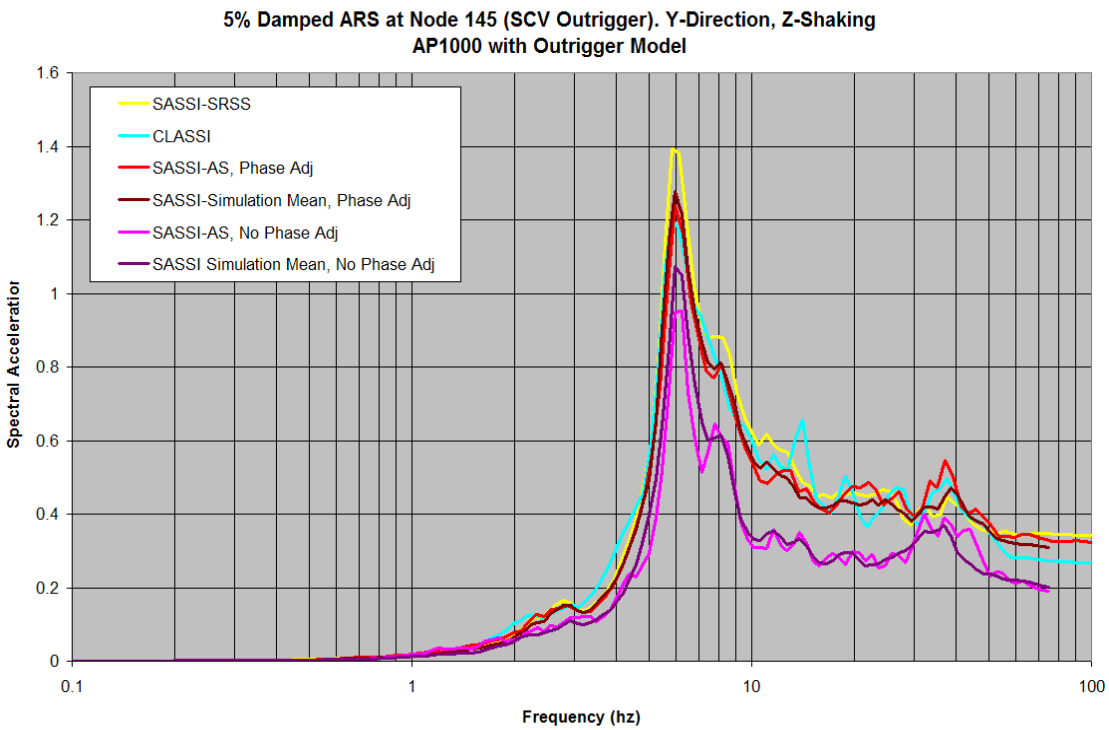

Figure C-5
Phase Adjustment Effect for Node 145Y for Z-Shaking – Comparative ISRS Results

Illustrative Example

During the EPRI project, we tested SASSI-AS and SASSI Simulation Mean for significant number problems in addition of the AP1000-based Stick Model SSI analyses presented in this report. Some of these tests are a part of the verification and validation problems used to test the computer ACS SASSI code for incoherent SSI analyses.

In this section we show a simple illustrative example based on the Luco-Mita cylinder structure on a viscous half-space subjected to incoherent, spatially random seismic excitation (Luco and Mita, 1987). This problem was also used to test the SASSI-SRSS approach in Ostadan & Deng, 2007. The motion coherency was simulated based on the Luco model with a coherence parameter varying from 0.1 to 0.5.

Figures C-6, C-7 and C-8 show the computed incoherent transfer functions (ITF) at the bottom-center and top-edge of the cylinder structure. The selected coherence parameter values were 0.1 and 03. Both horizontal and vertical excitations were applied. The ITF plots show a good agreement between SASSI-AS and SASSI Simulation Mean (with 20 random samples) and the analytically derived results.

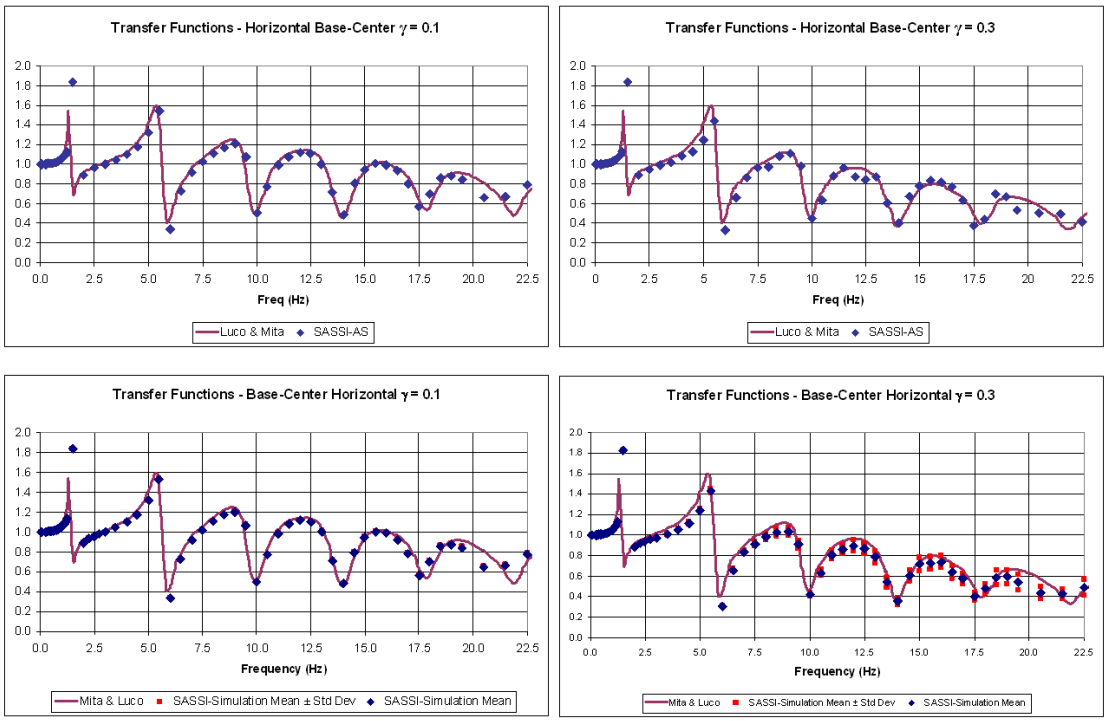

Figure C-6
Base-Center ITF Under Horizontal Shaking Using SASSI-AS and Simulation Mean

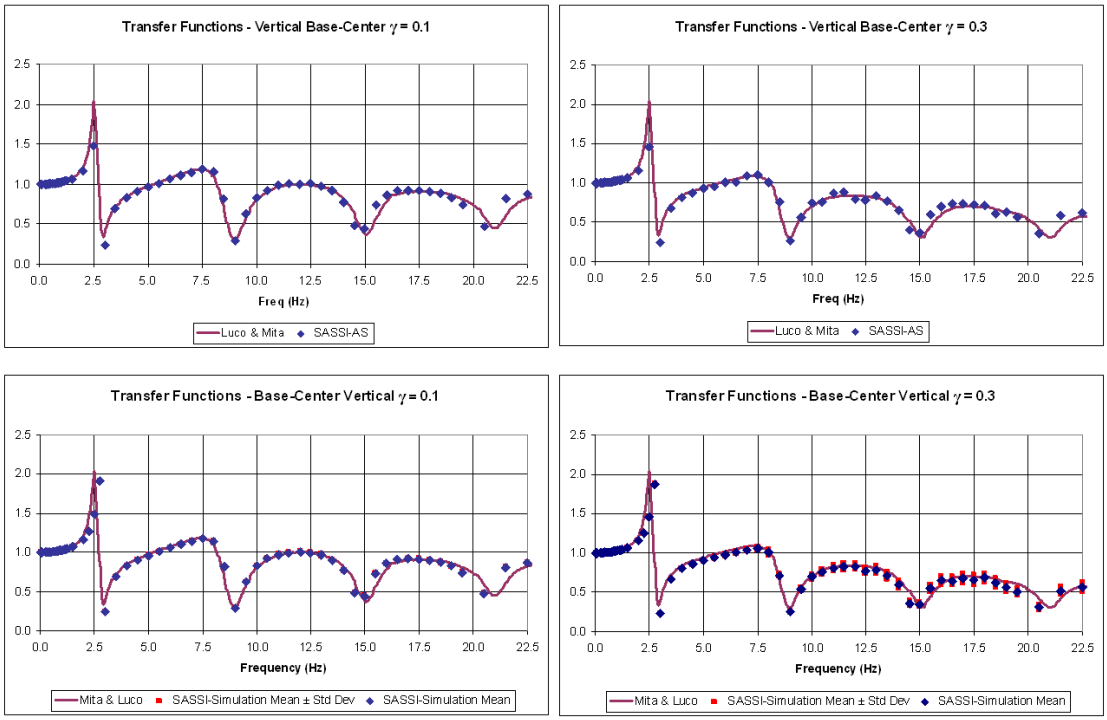

Figure C-7
Base-Center ITF Under Vertical Shaking Using SASSI-AS and Simulation Mean

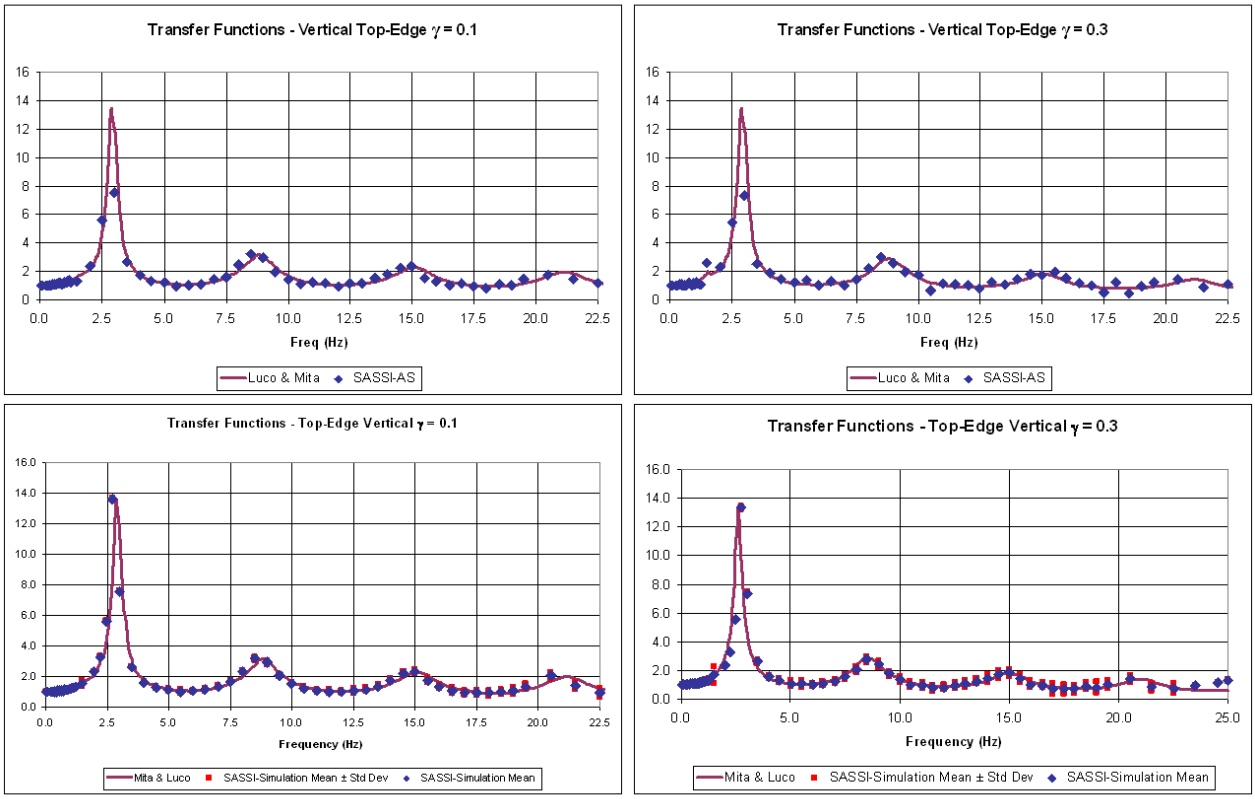

Figure C-8
Top-Edge ITF Under Vertical Shaking Using SASSI-AS and Simulation Mean

Summary and Conclusions

During this EPRI project, the SASSI-Simulation Mean and SASSI-AS approaches have been tested and validated for a number of incoherent seismic SSI problems with rigid foundations. For rigid foundations, both analytical results and CLASSI SSI results were available for comparisons. For the investigated problems, the two approaches produced results in close agreement with the other industry approaches implemented in SASSI and CLASSI as described in the report.

This appendix describes the underlying theory and key implementation details that state behind the two incoherent SSI approaches of ACS SASSI. This appendix also includes a comparison of the two approaches against analytical results published in engineering literature for a rigid cylinder structure subjected to horizontal and vertical incoherent seismic motions.

It should be noted that at this time there is no publication in engineering literature that discusses the effects of motion incoherency for flexible foundations. At the end of this appendix we provide few practical suggestions for the application of the two approaches to incoherent SSI analyses for both rigid and flexible foundations. However, we realize that at this time our accumulated experience on flexible foundations is more limited and in progress.

Rigid Foundations:

- Both SASSI-AS and SASSI-Simulation Mean could be used.
- If the number of selected frequencies is lower, it is expected that SASSI-Simulation Mean provides more robust results than SASSI-AS. Typically 100 to 200 frequencies should be sufficient. However, the user has to inspect the computed and interpolated ITF before deciding on the final number of frequencies to be used.
- The number of SSI simulations required by SASSI-Simulation Mean is relatively low; it could be as low as 5 simulations that could be sufficient for getting a good approximation of the mean ISRSs for the frequency range of interest. The inspection of the computed ISRS random scatter for the simulated samples provides substantial information on this.

Flexible Foundations:

- For flexible foundations the free-field motion local spatial variations, especially at higher frequencies, are no longer filtered by the kinematic SSI interaction as much as for rigid foundations. The incoherent free-field motion has to be thought as a multiple, differential support seismic excitation.
- A deterministic approach such as SASSI-AS limits the modeling of incoherent SSI response to a single variation pattern. Because of this, SASSI-Simulation Mean is suggested for flexible foundation NPP applications. Based on some in-house studies, we noticed that the statistical convergence of computed mean ISRS is slower for flexible foundations than for rigid foundations.
- The spatial non-uniformity of the distribution of interaction nodes has larger effect for incoherent SSI analyses than for coherent SSI analyses.

Selected References

Abrahamson, N., (1993) *Spatial Variation of Multiple Support Inputs*, the 1st U.S. Seminar on Seismic Evaluation and Retrofit of Steel Bridges, University of California at Berkeley, San Francisco, October.

Abrahamson, N. (2005). *Spatial Coherency for Soil-Structure Interaction*. Electric Power Research Institute, Palo Alto, CA: December. Technical Update Report 1012968.

Abrahamson, N. (2006). *Program on Technology Innovation: Spatial Coherency for Soil-Structure Interaction.* Electric Power Research Institute, Palo Alto, CA, and U.S. Department of Energy, Germantown, MD: December. Report 1014101.

Abrahamson, N. (2007). *Hard Rock Coherency Functions Based on Pinyon Flat Data*, April 2.

Ghanem, R.G. and Spanos, P.D., (1991), *Stochastic Finite Elements: A Spectral Approach,* Springer-Verlag, Heidelberg.

Ghiocel, D (2004). *Stochastic Simulation Methods for Engineering Predictions,* Chapter 20, CRC Engineering Design Reliability Handbook, Eds. Nikolaidis, Ghiocel and Singhal, Taylor & Francis-CRC Press, New York, NY.

Luco, J.E. and A. Mita (1987). *Response of Circular Foundation to Spatially Random Ground Motion,* Journal of Engineering Mechanics, American Society of Civil Engineers, Vol. 113, No. 1, January. 1987, pp. 1-15.

Nair, P. (2004). *Stochastic Finite Element Projection Techniques*, Chapter 21, CRC Engineering Design Reliability Handbook, Eds. Nikolaidis, Ghiocel and Singhal, Taylor & Francis-CRC Press, New York, NY.

Parzen E. (1962). "On Estimation of a Probability Density Function and Mode", Ann. Math. Stat. 33, pp. 1065-1076.

Vanmarcke, E. (1983). *Random Fields*, MIT Press.

Export Control Restrictions

Access to and use of EPRI Intellectual Property is granted with the specific understanding and requirement that responsibility for ensuring full compliance with all applicable U.S. and foreign export laws and regulations is being undertaken by you and your company. This includes an obligation to ensure that any individual receiving access hereunder who is not a U.S. citizen or permanent U.S. resident is permitted access under applicable U.S. and foreign export laws and regulations. In the event you are uncertain whether you or your company may lawfully obtain access to this EPRI Intellectual Property, you acknowledge that it is your obligation to consult with your company's legal counsel to determine whether this access is lawful. Although EPRI may make available on a case-by-case basis an informal assessment of the applicable U.S. export classification for specific EPRI Intellectual Property, you and your company acknowledge that this assessment is solely for informational purposes and not for reliance purposes. You and your company acknowledge that it is still the obligation of you and your company to make your own assessment of the applicable U.S. export classification and ensure compliance accordingly. You and your company understand and acknowledge your obligations to make a prompt report to EPRI and the appropriate authorities regarding any access to or use of EPRI Intellectual Property hereunder that may be in violation of applicable U.S. or foreign export laws or regulations.

The Electric Power Research Institute (EPRI), with major locations in Palo Alto, California; Charlotte, North Carolina; and Knoxville, Tennessee, was established in 1973 as an independent, nonprofit center for public interest energy and environmental research. EPRI brings together members, participants, the Institute's scientists and engineers, and other leading experts to work collaboratively on solutions to the challenges of electric power. These solutions span nearly every area of electricity generation, delivery, and use, including health, safety, and environment. EPRI's members represent over 90% of the electricity generated in the United States. International participation represents nearly 15% of EPRI's total research, development, and demonstration program.

Together...Shaping the Future of Electricity

Program:

Technology Innovation

© 2007 Electric Power Research Institute (EPRI), Inc. All rights reserved. Electric Power Research Institute, EPRI, and TOGETHER...SHAPING THE FUTURE OF ELECTRICITY are registered service marks of the Electric Power Research Institute, Inc.

Printed on recycled paper in the United States of America

1015111

Electric Power Research Institute
3420 Hillview Avenue, Palo Alto, California 94304-1338 • PO Box 10412, Palo Alto, California 94303-0813 USA
800.313.3774 • 650.855.2121 • askepri@epri.com • www.epri.com